Pre-Clinical Metabolism Studies with Fenretinide in Paediatric Cancer

Nicola Ann Illingworth

Thesis Submitted for the Degree of Doctor of Philosophy

August 2011

Northern Institute for Cancer Research

Faculty of Medical Sciences

The Medical School

Newcastle University

Abstract

Fenretinide (4-HPR) is a retinoic acid analogue used in clinical trials for the treatment of neuroblastoma and Ewing's sarcoma. The work described involves investigations into factors that may impact on 4-HPR drug disposition. Metabolism of 4-HPR is of particular interest due to production of the active metabolite 4'-oxo 4-HPR and the clinical challenge of obtaining consistent 4-HPR plasma concentrations. The enzymes involved in 4-HPR metabolism were characterised and the impact of metabolism on efficacy in neuroblastoma and Ewing's sarcoma cell lines assessed. In addition, the potential for 4-HPR to act as a substrate for common drug transporters was explored.

4-HPR was metabolised to 4'-oxo 4-HPR and 4'-OH 4-HPR primarily by CYPs 3A4, 3A5 and 2C8. Genetic variance in CYP2C8 affected oxidative metabolism, with much lower affinity for 2C8*4 (k_m of 59.8µM compared to 19.3µM for wild-type), and may be of clinical relevance. Both 4-HPR and 4'-oxo 4-HPR were glucuronidated. 4-HPR was glucuronidated by UGTs 1A1, 1A3 and 1A6, whilst 4'-oxo 4-HPR was glucuronidated by UGTs 1A1, 1A3, 1A8 and 1A9. However, very high K_m values were observed (ranging from 389µM to 716µM for 4-HPR). Methylation of 4-HPR to the major metabolite 4-methoxyphenyl retinamide (4-MPR) was determined to be carried out by amine N-methyltransferases.

Neuroblastoma and Ewing's sarcoma cell lines metabolised 4-HPR to 4'-oxo 4-HPR, 4'-OH 4-HPR and 4-MPR. Although upregulation of *CYP26A1* expression increased metabolism, inhibition of CYP26A1 had no effect on cell sensitivity. It is therefore unlikely that *CYP26A1* expression will have a significant impact on 4-HPR efficacy.

4-HPR appears to be a substrate for the drug transporters MDR1, MRP2 and BCRP. However evidence for the role of these transporters is weak with no difference in 4-HPR sensitivity observed in cell lines over-expressing individual transporters in the presence or absence of specific transporter inhibitors.

The major metabolites and metabolising enzymes of 4-HPR have been identified and characterised. This provides the potential to increase plasma concentrations of 4-HPR, and therefore optimise drug efficacy, through modulation of drug metabolism.

Acknowledgements

I would like to thank my supervisors, Prof. Alan Boddy and Dr. Gareth Veal, for the opportunity to work on this project, as well as their invaluable support and guidance throughout my experimental work and write-up.

I would also like to thank everyone at the NICR for their technical support, particularly the members of the pharmacology group for never tiring of answering ‘daft’ questions!

I am also especially grateful to my family for their ceaseless encouragement, my friends for their continued belief in me, and my husband for his never-ending support.

Table of Contents

List of Figures

List of Tables

List of Abbreviations

12-lox:	12-lipoxygenase
13-cis RA:	13-cis Retinoic Acid
4’-OH 4-HPR:	4’-hydroxy 4-hydroxyphenyl retinamide
4’-oxo 4-HPR:	4’-oxo 4-hydroxyphenyl retinamide
4-EPR:	4-ethoxyphenyl retinamide
4-HPR:	4-hydroxyphenyl retinamide
4-MPR:	4-methoxyphenyl retinamide
4-oxo 13-cis RA:	4-oxo 13-cis retinoic acid
9-cis RA:	9-cis retinoic acid
AA:	Arachidonic acid
ABC:	ATP-binding cassette
ADP:	Adenosine di-phosphate
δ-ALA:	δ-Aminolevulinic acid
ANOVA:	Analysis of variance
AML:	Acute myeloid leukaemia
APL:	Acute promyelocytic leukaemia
ATP:	Adenosine tri-phosphate
ATRA:	All-trans retinoic acid
AUC:	Area under the curve
BSA:	Bovine serum albumin
BCRP:	Breast cancer resistance protein
BMT:	Bone marrow transplantation
CAPS:	3-(Cyclohexylamino)-1-propanesulfonic acid
CC:	Chemotherapy
CHAPS:	3-[(3-Cholanidopropyl)Dimethylammonio]-1, Propanesulfonate
CO:	Carbon monoxide
C_{max}:	Maximum plasma concentration
COMT:	Catechol-O-methyltransferases
CT:	Computerised tomography
CYP:	Cytochrome P450
DNA:	Deoxyribose nucleic acid

ECL:	Enhanced chemiluminescence
EDTA:	Ethylenediaminetetraacetic acid
EFS:	Event free survival
ER:	Endoplasmic reticulum
ESFT:	Ewing's sarcoma family of tumours
FBS:	Foetal bovine serum
HCl:	Hydrogen chloride
HDACI:	Histone deacetylase inhibitor
HER2:	Hormone epidermal growth factor receptor 2
HIM:	Human intestinal microsomes
HLM:	Human liver microsomes
HPLC:	High performance liquid chromatography
HRP:	Horseradish peroxidase
H:	Hour
IC_{50}:	Half maximal inhibitory concentration
IgG:	Immunoglobulin G
INRC:	International neuroblastoma response criteria
INSS:	International neuroblastoma staging system
IPTG:	Isopropyl-beta-D-thiogalactopyranoside
K_m:	Substrate concentration at half maximal velocity
LB:	Lysogeny broth
LC/MS/MS:	Liquid chromatography/mass spectrometry/mass spectrometry
MDCK-II cells:	Madin-Darby Canine Kidney II cells
MDR:	Multidrug resistance
MIBG:	Metaiodobenzylguanidine
Min:	Minute
MRI:	Magnetic resonance imaging
MRM:	Multiple reaction monitoring
MRP:	Multidrug resistance-associated protein
MTD:	Maximum tolerated dose
MTS:	3-(4,5-dimethylthiazol-2-yl)-5-(3-carboxymethoxyphenyl)-2-(4-sulfophenyl)-2H-tetrazolium
NADPH:	Nicotinamide adenine dinucleotide phosphate (reduced)
OATP:	Organic anion-transporting polypeptide
OS:	Overall survival

PARP:	Poly ADP ribose polymerase
PBS:	Phosphate Buffered Saline
PCR:	Polymerase chain reaction
PDA:	Photodiode array
PLA2:	Phospholipase A2
PMSF:	Phenylmethanesulfonylfluoride fluoride
PMT:	Phenol methyltransferase
RAMBA:	Retinoic acid metabolism blocking agent
RAR:	Retinoic acid receptor
RARE:	Retinoic acid response element
RNA:	Ribose nucleic acid
ROS:	Reactive oxygen species
RPMI medium:	Roswell Park Memorial Institute medium
RT:	Retention time
RXR:	Retinoid X receptor
RXRE:	Retinoid X responsive element
S:	Second
SAM:	S-adenosyl methionine
SC:	Sub-cutaneous
SD:	Standard deviation
SDS:	Sodium dodecyl sulphate
SNP:	Single nucleotide polymorphism
SOC:	Super optimal broth with catabolite repression
TB:	Terrific broth
TBS:	Tris-buffered saline
TSE:	Tris/sucrose/EDTA
UDPGA:	Uridine diphosphate glucuronic acid
UGT:	Uridine 5'-diphospho-glucuronosyltransferase
UV:	Ultraviolet
VKORC1:	Vitamin K epoxide reductase
V_{max}:	Maximum reaction rate

Chapter 1 Introduction

1.1 Cancer

Malignant neoplasms (more frequently referred to as cancers), result from the unchecked growth of cells. They differ from benign neoplasms by their potential ability to migrate to other parts of the body and form additional metastatic tumour sites. There are six main biological features of cancerous cells, which are known as the 'hallmarks of cancer'. These features include the ability to sustain proliferative signaling, evade growth inhibitory signaling and resist apoptosis (resulting in replicative immortality), as well as possessing the ability to invade other tissues and to maintain their own blood supply by inducing angiogenesis (Hanahan and Weinberg, 2011).

Cancer is the second most common cause of death in developed countries (after heart disease), with 15 million cases a year predicted to be diagnosed by 2012 (Jemal et al., 2007). Up to 90% of cancers are thought to be caused by environmental factors such as tobacco use, obesity, alcohol, infections and sun exposure (Anand et al., 2008). The remaining cases are due to germline genetic mutations, although even these hereditary cases often result from a combination of a genetic pre-disposition to cancer as well as environmental triggers.

1.2 Chemotherapy

Cancer can be treated by surgery to physically remove the tumour, by radiotherapy to induce DNA damage and subsequent cell death, or chemotherapy, where natural or synthetic compounds are used to induce apoptosis or cell differentiation. The ability of certain chemicals to reduce cancerous growths was investigated from the early 1900's, although the field of cancer chemotherapeutics only became widely researched during the 1930s. The growth of this field followed the discovery during World War II that exposure to mustard gas (subsequently found to be an alkylating agent) resulted in myelosuppression, with potential utility as a haematopoietic cancer treatment (DeVita and Chu, 2008). This finding was rapidly followed by the discovery that antifolates such as methotrexate were able to produce remissions in children with leukaemia (Farber et al., 1948), as did the use of thiopurine compounds such as 6-mercaptopurine (Hitchings and Elion, 1954). Another decade of research revealed that some antibiotics,

including actinomycin D, could act as effective chemotherapeutic agents (Pinkel, 1959). Research during the 1950's also resulted in the discovery of the first chemotherapeutic agent to target solid tumours, 5-fluorouracil (Heidelberger et al., 1957). Following these early advances in the development of chemotherapeutics, research into the use of chemotherapy to treat a wide range of tumour types has continued, with hundreds of compounds now in use or in clinical trials. However, many of the initial agents discovered in the 1950s are also still in use, though their dosing regimens have been refined during the decades since they were first utilised. Combinations of chemotherapeutic agents are now often used, frequently in association with surgery and radiotherapy. Many forms of cancer are now curable, with survival rates greatly improved from the 1970s (as shown in Figure 1-1).

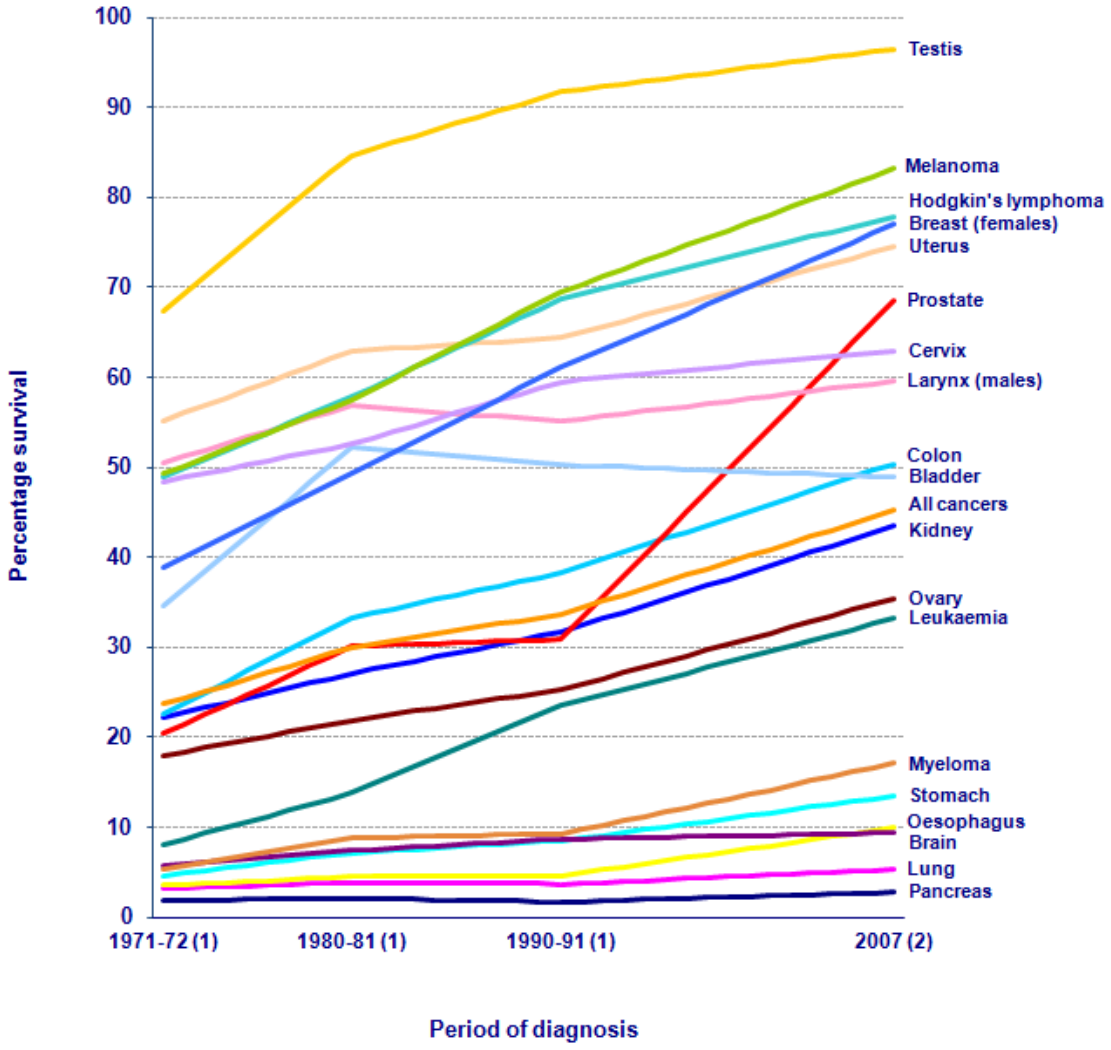

Figure 1-1. Ten year relative survival (%), adults (15-99 years), selected cancers, England and Wales: survival trends for selected cancers 1971-2007.

(1) 1971-1991 Cohort analysis - actual survival. (2) 2007 Hybrid analysis - predicted survival. Cancer Research UK 2010.

However, there are still cancer types, such as lung and pancreatic cancer, where little improvement in survival has been made (Cancer Research UK, 2010), and research is ongoing to try to improve survival rates for these cancers. Even for those cancers with relatively good 5-year survival rates there are subsets of patients who have a significantly worse prognosis. In order to improve curative rates in these patients, as well as to reduce side effects for all patients, there is currently a significant focus on individualizing cancer treatment. This means that patients are treated with the most appropriate agent to target the molecular or genetic 'signal' for their particular cancer, rather than a standard therapy for their type of tumour. For instance, patients with breast cancer are treated with trastuzamab (herceptin) only if their tumour expresses the target for that compound, hormone epidermal growth factor receptor-2 (HER2) (Cobleigh et al., 1999). Individualised therapy is also beginning to take account of genetic differences in drug metabolism (pharmacogenetics), as this can also have a significant effect on both drug efficacy and side effects suffered by the patient (Efferth and Volm, 2005). This means that in addition to improvements in cancer survival from the development of novel chemotherapeutic compounds, patients are also benefiting from increased knowledge about the mechanism of action, molecular target and metabolism of chemotherapeutic agents already in use.

1.3 Retinoids

Vitamin A (retinol) is a dietary vitamin essential for life. Vitamin A deficiency is a major health problem in many developing countries, and is the main cause of preventable blindness in children. It is thought the distribution of vitamin A supplements may have saved the lives of 1.25 million women and children over the past 15 years (World Health Organization, 2011). Vitamin A was initially found to be involved in cell differentiation almost a century ago (Wolbach and Howe, 1925). Decades of further research subsequently resulted in the mechanism of action of vitamin A being traced to regulation of gene transcription via activation of nuclear receptors specific to all-trans retinoic acid (ATRA), a metabolite of retinol (see Figure 1-2) (Giguere et al., 1987, Petkovich et al., 1987). There are also several stereoisomers of retinoic acid, including 13-cis retinoic acid (13-cis RA) and 9-cis retinoic acid (9-cis RA) as well as synthetic analogues including fenretinide (4-HPR) (McCaffery et al., 2002).

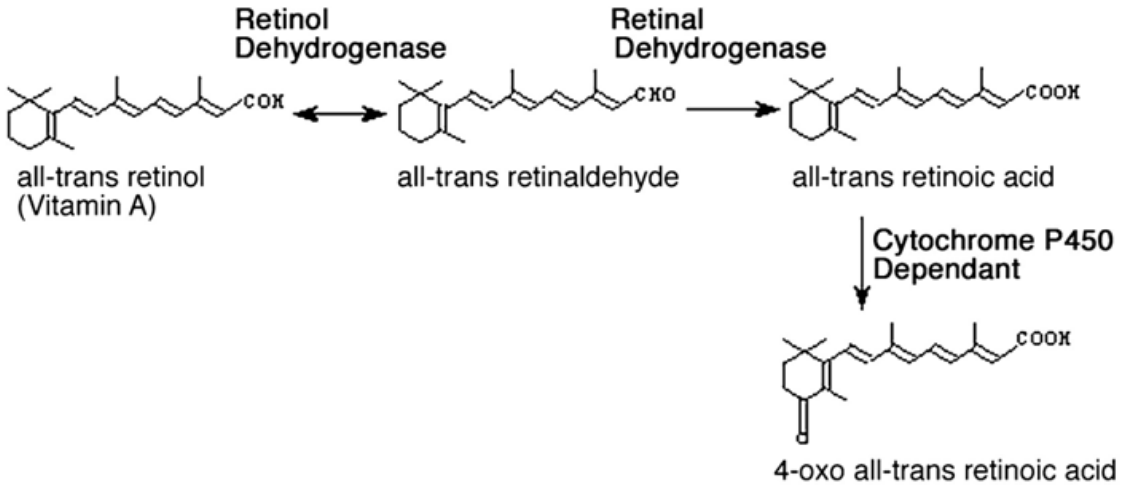

Figure 1-2. Retinoic acid metabolism.

McCaffery P et al. *J. Lipid Res*. 43:1143-1149; 2002

Further research led to the discovery that there are two types of retinoid receptors, known as retinoic acid receptors (RARs) and retinoid X receptors (RXRs). There are three subtypes of each of these receptors (α, β and γ), that bind as heterodimers to the retinoic acid response elements or retinoid X responsive elements (RAREs and RXREs) of target genes (Chambon, 1996). Both ATRA and its isomer, 13-cis RA are able to bind to all three subtypes of RARs, whilst 9-cis RA, an additional isomeric form of retinoic acid, is able to bind all three RXR subtypes (Idres et al., 2002). Isomerisation of retinoic acid has a significant effect on transcriptional regulation, as ATRA has a greater RAR binding affinity than 13-cis RA. It is therefore thought that 13-cis RA acts as a 'pro-drug', with the majority of its cellular effects resulting from isomerisation to ATRA (Allenby et al., 1993, Veal et al., 2002).

1.3.1 Retinoid Clinical Use

Retinoid treatment *in vitro* produced cellular differentiation and apoptosis, leading to one of the earliest clinical trials of 13-cis RA for the treatment of oral leukoplakia. This trial had limited success, as although a clinical response was seen in 67% of patients treated with 13-cis RA, compared to 10% of patients treated with a placebo, the majority of patients suffered relapses on cessation of treatment (Hong et al., 1986). Since then, trials of 13-cis RA and ATRA have shown them to be successful as chemopreventative agents in reducing the recurrence of skin carcinomas (Moon et al.,

1997) and low grade cervical cancers (Meyskens et al., 1994), as well as treating oesophageal (Han, 1993), head and neck (Hong et al., 1990, Benner et al., 1994) and early stage non-small cell lung cancers (Pastorino et al., 1993), amongst others (Evans and Kaye, 1999). The greatest initial success with retinoid chemotherapy was seen in the treatment of acute promyelocytic leukaemia (APL). Prior to the discovery of retinoids, APL was generally a fatal condition. However with ATRA treatment, and more recently the addition of arsenic trioxide to chemotherapy regimens, more than 70% of patients are now alive five years after diagnosis. Unfortunately relapse upon cessation of treatment is common and patients require follow-on therapy in order to maintain remission rates (Sanz et al., 2009). In addition to the success of ATRA in an APL setting, treatment of high-risk neuroblastoma patients with 13-cis RA, following high dose myeloablative therapy and radiotherapy, resulted in significant increases in survival (Matthay et al., 1999).

1.4 Fenretinide (4-HPR)

Fenretinide (4HPR) is a synthetic analogue of retinoic acid (structure shown in Figure 1-3) that has been used in clinical trials in children for the treatment of neuroblastoma and Ewing's sarcoma. 4-HPR was initially shown to be cytotoxic to Ewing's sarcoma and neuroblastoma cell lines *in vitro*, and to reduce tumour growth in mouse models, as shown in Figure 1-4 (Myatt et al., 2005, Di Vinci et al., 1994). 4-HPR was also better tolerated in children than other retinoid derivatives currently in clinical use, such as ATRA and 13-cis RA (Garaventa et al., 2003).

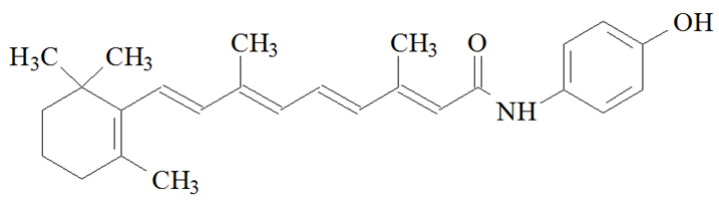

Figure 1-3. Structure of 4-HPR

Currently there are two fenretinide clinical trials recruiting neuroblastoma patients and one trial recruiting Ewing's sarcoma patients. Both trials in neuroblastoma patients are phase I trials, with one aiming to determine the maximum tolerated dose (MTD), toxicities and pharmacokinetics of an intravenous dosing regimen (US National Institutes of Health, 2010b), and the second trial aiming to determine the same

parameters for a novel oral formulation of 4-HPR, either alone or in combination with ketoconazole (a CYP3A4 inhibitor) (US National Institutes of Health, 2010a). The trial in Ewing's sarcoma patients is a phase III trial, to investigate the inclusion of 4-HPR as an additional treatment in standard risk patients after induction and maintenance chemotherapy, either alone or in combination with zoledronic acid (a bisphosphonate) (US National Institutes of Health, 2009).

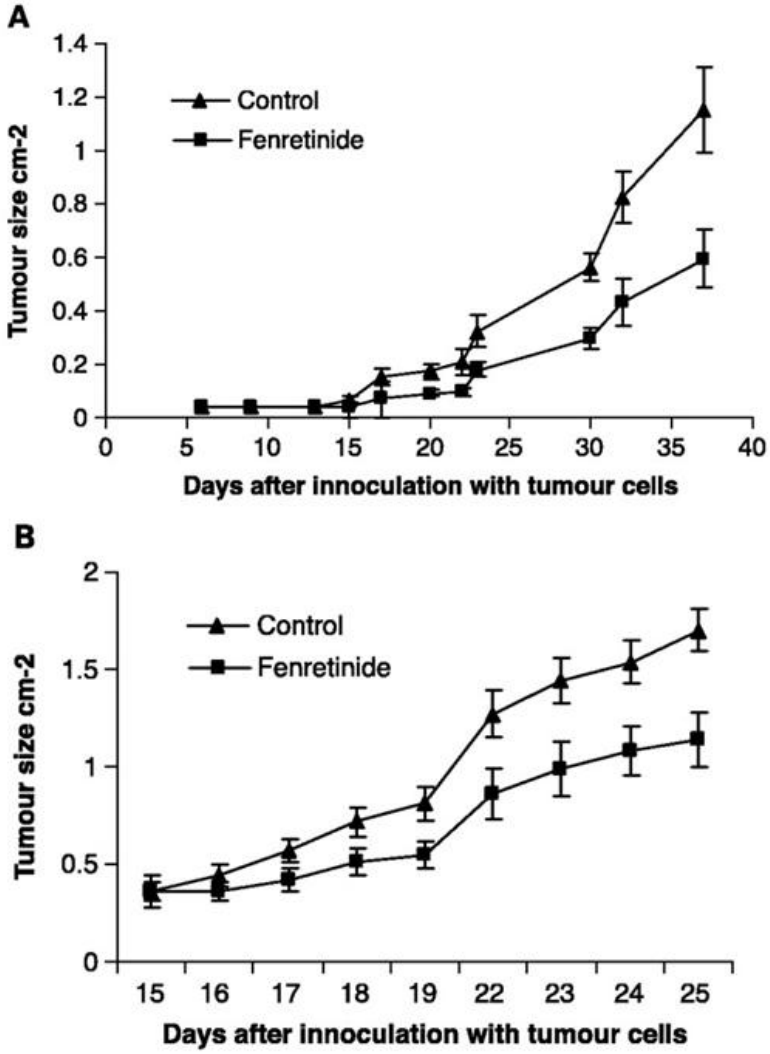

Figure 1-4. Effect of 4-HPR on s.c. growth of ESFT in nude mice.

Mice (n = 10) were injected s.c. in one flank with RD-ES cells (2.5×10^6 per mouse). From day 15, when a tumor mass was measurable, the mice were treated by A) s.c. injection daily with either 4-HPR (100 mg/kg) or vehicle control or B) oral gavage with 4-HPR (100 mg/kg) in corn oil and cremaphor. Adapted from Myatt et al. *Clinical Cancer Research* 11(8): 3136-3148; 2005

The main clinical obstacle in the use of 4-HPR as a chemotherapeutic agent is its relatively low bioavailability, coupled with high inter-patient variability in maximum

plasma concentrations achieved (Villablanca et al., 2006). Novel formulations of 4-HPR currently in development should help to overcome these issues. Improving bioavailability should also reduce the problem of patient non-compliance. This is often seen, especially in younger patients, in high dose 4-HPR trials, that currently involve taking several dozen large capsules, or alternatively removing the capsule contents and mixing with food. However, using the latter approach not only lowers peak 4-HPR plasma concentrations, it is also impractical at high doses due to the unpleasant taste of the capsule oil and may further increase inter-patient variation in peak 4-HPR plasma concentrations (Garaventa et al., 2003). Overcoming these problems is therefore particularly important for the treatment of paediatric patients.

1.5 Neuroblastoma

1.5.1 Epidemiology

Neuroblastoma is a cancer derived from neuronal crest cells (Hoehner et al., 1996). It is the most common extracranial solid tumour of paediatric patients, accounting for 9% of total paediatric cancer cases, with 90% of cases occurring in children under 5 years of age (Schwab et al., 2003). However, despite the relatively low incidence rate, neuroblastoma accounts for approximately 15% of all childhood cancer deaths (Cancer Research UK, 2005). The majority of primary tumours occur in the abdomen, mainly in the adrenal glands, although the neck, chest and pelvis are also common sites of primary tumours (Maris et al., 2007). The genetic basis for the cause of neuroblastoma has yet to be completely elucidated, though amplification of the *MYCN* gene was discovered as an indicator of aggressive disease nearly 30 years ago (Schwab et al., 1983), as shown in Figure 1-5 (Vandesompele et al., 2003). More recently deletion of chromosome 1p or alteration has also been associated with a worse prognosis (Schwab et al., 2003, Maris and Matthay, 1999).

There is also limited evidence that external factors may influence the occurrence of neuroblastoma, as factors such as birth weight and maternal vitamin, alcohol and medication intake have all been associated with an impact on neuroblastoma incidence rates (Olshan et al., 2002, Bjorge et al., 2008, Bluhm et al., 2008, Cook et al., 2004, Goh et al., 2007, McLaughlin et al., 2009, Urayama et al., 2007). However, due to the relatively low incidence rate of neuroblastoma and the use of retrospective

questionnaires for most studies it is difficult to determine the overall impact of prenatal risk factors for neuroblastoma.

1.5.2 Diagnosis and Staging

Neuroblastoma is often difficult to diagnose as the primary tumour can occur anywhere along the sympathetic ganglia or within the adrenal medulla. This means that patients usually present with symptoms caused by local effects of the primary tumour (Hildebrandt and Traunecker, 2005). Generally these are non-specific symptoms including localized pain, fatigue, weight-loss and fever. Neuroblastoma is often only diagnosed once a tumour mass is palpable, for example causing abdominal distension, or once there are more specific symptoms such as paralysis caused by the tumour compressing the spinal cord. An indication of favourable-prognosis neuroblastoma is 'blueberry muffin syndrome', where patients present with painless, bluish subcutaneous nodules (Ishola and Chung, 2007). Suspected neuroblastoma cases can initially be diagnosed via urine catecholamine levels, with confirmation obtained by imaging studies, that may include CT, MRI or bone scan or MIBG scintigraphy, as well as using bone marrow histochemical examinations (Kushner, 2004).

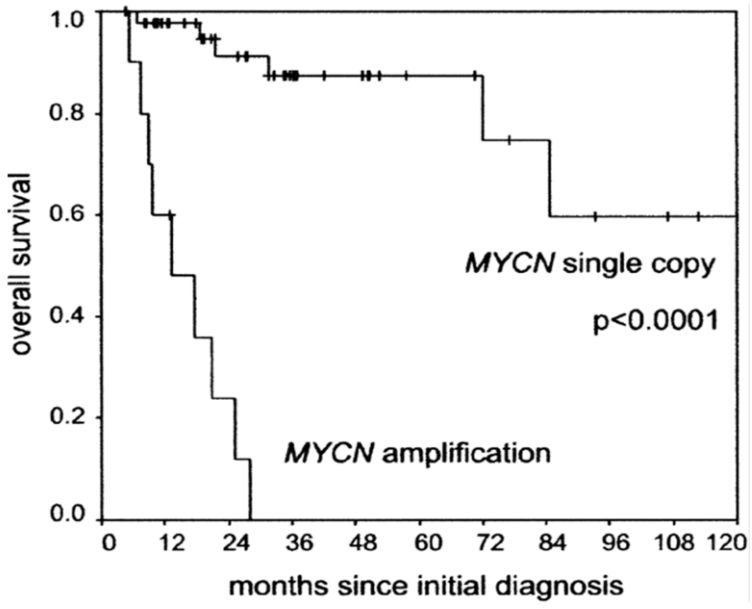

Figure 1-5. Kaplan-Meier overall survival analysis of 59 patients with or without *MYCN* amplification.

Adapted from Vandesompele, J. et al. *Oncogene*, 22, 456-460; 2003.

Staging of neuroblastoma is determined by the International Neuroblastoma Staging System (INSS) and the International Neuroblastoma Response Criteria (INRC), that were established in 1988. There are 6 distinct stages of neuroblastoma, as shown in Table 1-1 (Schwab et al., 2003), with stage, age at diagnosis and *MYCN* amplification being the main prognostic factors. Tumours are staged depending on regional lymph node status, whether the tumour infiltrates across the midline of the body and whether the tumour is rescectable (Kushner, 2004).

Stage 1	Localized tumour with complete gross excision, with or without microscopic residual disease; representative ipsilateral lymph nodes negative for tumour microscopically (nodes attached to and removed with the primary tumour may be positive).
Stage 2A	Localized tumour with incomplete gross excision; representative ipsilateral nonadherent lymph nodes negative for tumour microscopically.
Stage 2B	Localized tumour with or without complete gross excision, with ipsilateral nonadherent lymph nodes positive for tumour. Enlarged contralateral lymph nodes must be negative microscopically.
Stage 3	Unresectable unilateral tumour infiltrating across the midline (vertebral column) with or without regional lymph node involvement; or localized unilateral tumour with contralateral regional lymph node involvement; or midline tumour with bilateral extension by infiltration (unresectable) or by lymph node involvement.
Stage 4	Any primary tumour with dissemination to distant lymph nodes, bone, bone marrow, liver, skin and/or other organs (except as defined for stage 4S).
Stage 4S	Localized primary tumour (as defined for stage 1, 2A or 2B), with dissemination

Table 1-1. International Staging System for Neuroblastoma.
Schwab, M. et al. *The Lancet Oncology*, 4, 472-480; 2003.

1.5.3 Treatment

The treatment strategy used depends on neuroblastoma risk stratification, with risk factors primarily being age at diagnosis, stage of disease and *MYCN* status, as well as whether residual tumour remains after surgical resection. Figure 1-6 shows the impact of age and disease stage on neuroblastoma patient survival (Schleiermacher et al., 2007). This allows patients to be grouped into 3 categories for treatment: low risk, intermediate risk or high risk. Treatment methods include surgery, chemotherapy and

radiotherapy, though observation without treatment is an additional strategy for some 4S tumours, as many undergo spontaneous regression without treatment (Maris et al., 2007). Spontaneous regression is the main reason why screening programmes for neuroblastoma have largely been unsuccessful in terms of improving survival rates (Hiyama et al., 2008, Schilling et al., 2003, Tajiri et al., 2009), whereas improvements in diagnosis have reduced the average age of diagnosis and been associated with improvements in survival (Davis et al., 1987, Schroeder et al., 2009). However, it is difficult to dissociate the benefits of improved diagnosis from concurrent improvements in therapy.

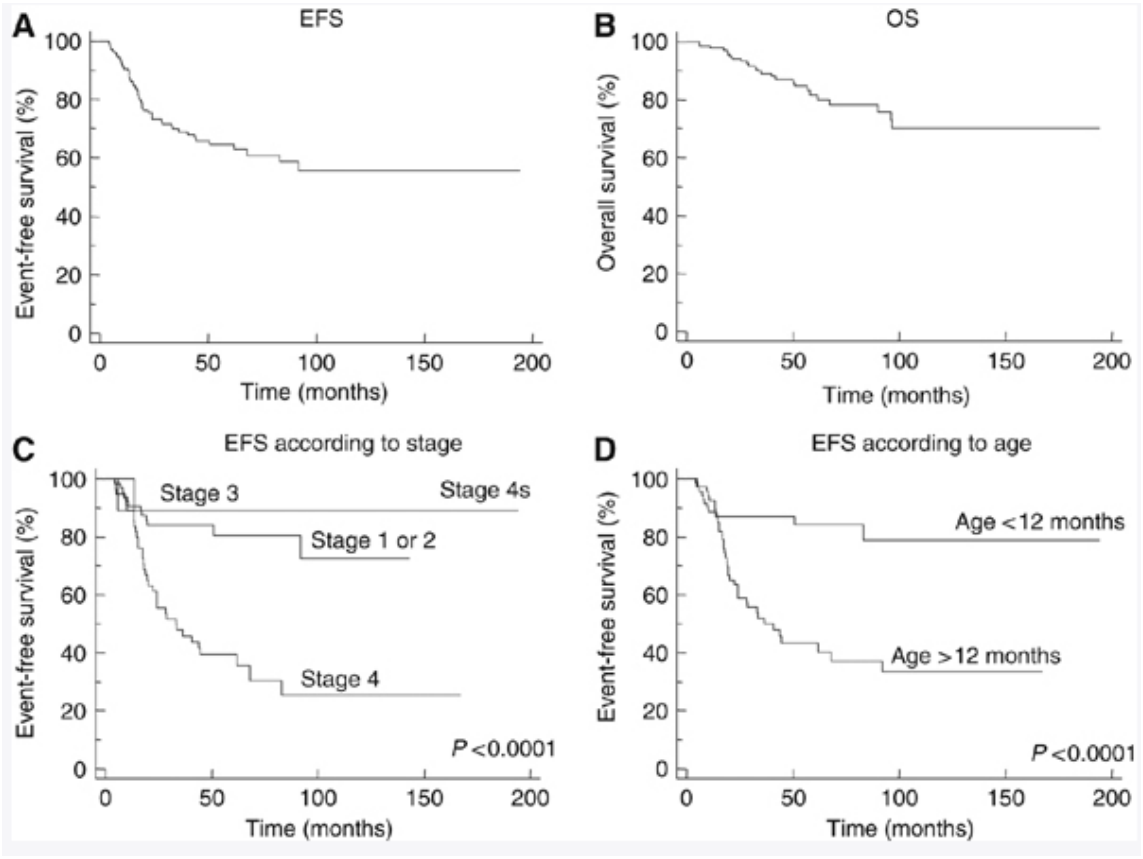

Figure 1-6. Survival curves of 139 neuroblastoma patients. (A) Event-free survival of all patients. (B) Overall survival of all patients. (C) Event-free survival according to stage at diagnosis. (D) Event-free survival according to age at diagnosis.

Schleiermacher, G. et al. *British Journal of Cancer,* 97**,** 238-246; 2007.

For low risk tumours, surgery remains the primary treatment and may be the only intervention required. High risk patients require surgery, radiotherapy and intensive chemotherapy, involving a combination of several cytotoxic drugs. Even with this

intense therapy, high risk patients still have a 30% chance of recurrence within 5 years after treatment, compared to only 10% in low risk groups (Berthold et al., 1996).

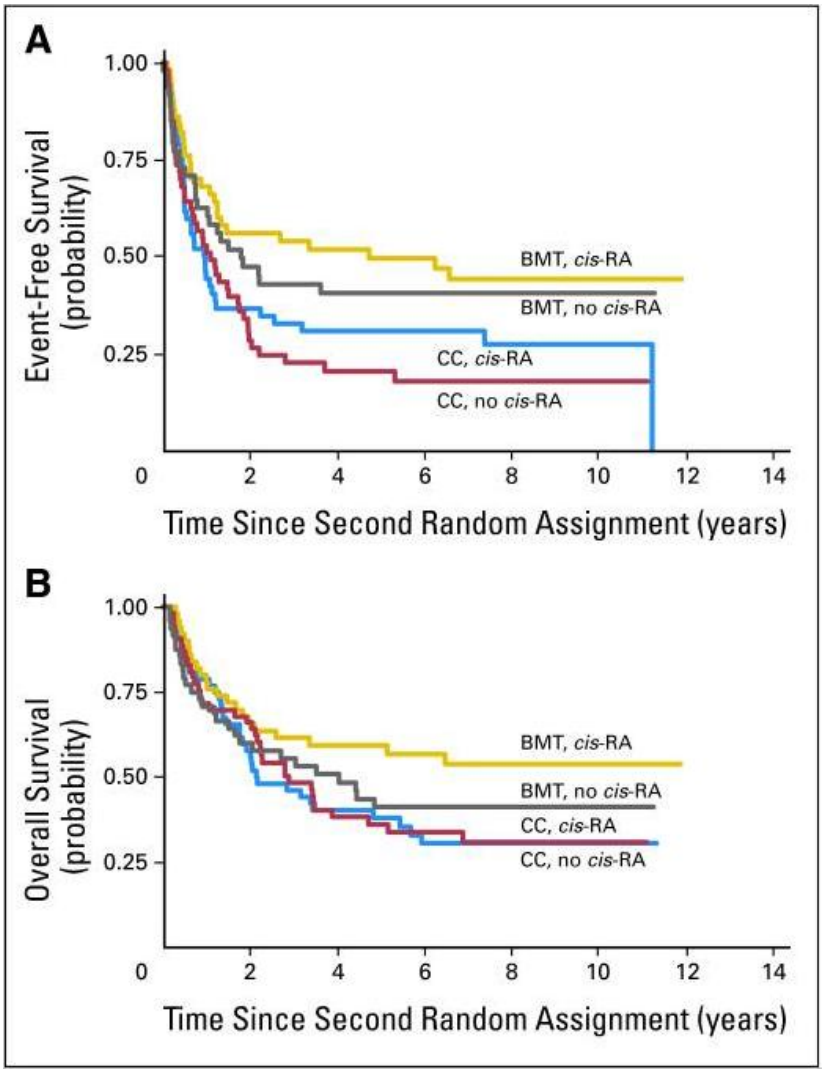

Figure 1-7. Long-term results for children with high-risk neuroblastoma treated on a randomized trial of myeloablative therapy followed by 13-cis RA.

CC = chemotherapy, BMT = bone marrow transplantation. Matthay, K.K. et al. *Journal of Clinical Oncology*, 27, 1007-1013; 2009.

Chemotherapy agents used for the treatment of neuroblastoma include alkylating agents (cyclophosphamide or ifosfamide), platinum compounds (cisplatin or carboplatin), topoisomerase inhibitors (topotecan or irinotecan as topoisomerase I inhibitors, etoposide or doxorubicin as toposiomerase II inhibitors) and vincristine (Kushner, 2004). Survival rates have been further improved in the last 10 years by the addition of 13-cis RA as a maintenance treatment after high dose chemotherapy. This addition to the treatment regimen was found to improve 3-year survival in a clinical trial in neuroblastoma patients from 29% to 40% (Matthay et al., 1999). Longer term follow up

of these patients ascertained that the greatest increase in overall survival was achieved by treating patients with autologous bone marrow transplantation followed by 13-cis RA maintenance therapy, as shown in Figure 1-7 (Matthay et al., 2009), with the treatment protocol shown in Figure 1-8 (International Society of Paediatric Oncology, 2009). This therapy regimen is now included in the standard treatment of high risk neuroblastoma and it is hoped the pre-clinical success seen with 4-HPR treatment *in vitro* and *in vivo* will result in further improvements in neuroblastoma therapy.

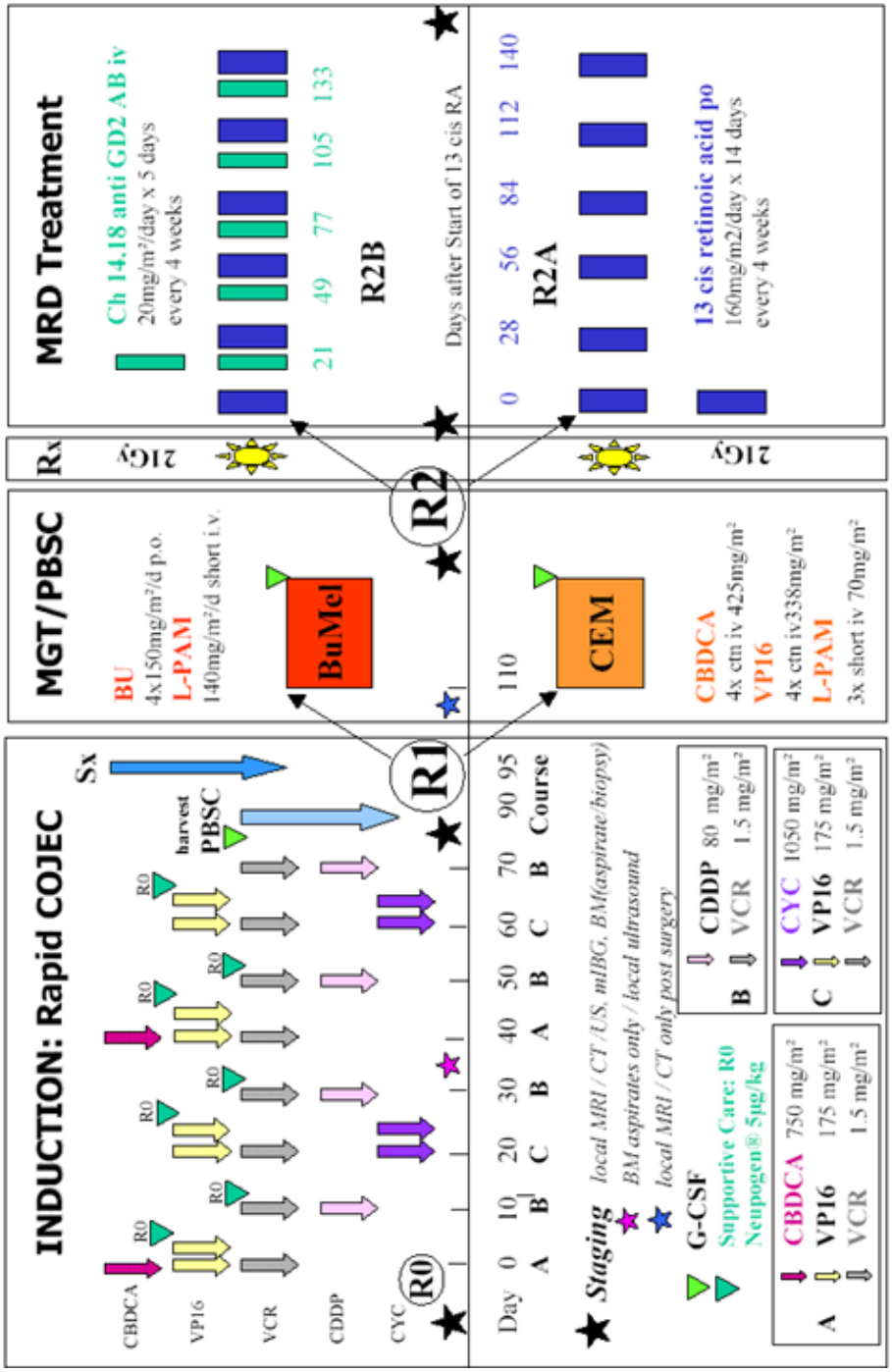

Figure 1-8. Treatment protocol for high-risk neuroblastoma patients.

High risk neuroblastoma study 1 of SIOP-Europe; 2009.

1.6 Ewing's Sarcoma

1.6.1 Epidemiology

Ewing's Sarcoma is one of a family of sarcomas, known collectively as the Ewing's Sarcoma Family of Tumours (ESFT), as they were first characterised by James Ewing in 1920 (Ewing, 1984). ESFT are believed to develop from poorly differentiated mesenchymal cells, with ESFT tumours including 'classical' Ewing's, peripheral Primitive Neuroectodermal Tumours (pPNET) and Askin's Tumours (Riggi and Stamenkovic, 2007). Similar tumours had been described in the literature as early as 1866 but James Ewing was the first to show that ESFT tumours were different to lymphoma and neuroblastoma, and that they were separate from other osteosarcomas in that ESFT are responsive to radiotherapy (CancerIndex, 1999). ESFT account for approximately 30% of all bone cancers diagnosed under the age of 24 and affects approximately 1 in 100,000 children (Buckley et al., 1998). The peak age for diagnosis is during the mid-teens (as shown in Figure 1-9) (Cotterill et al., 2000).

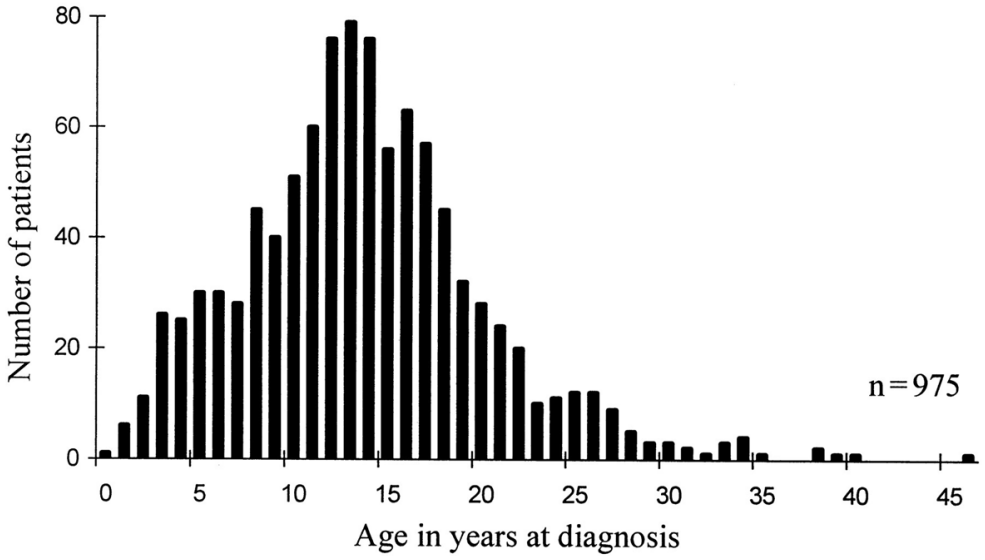

Figure 1-9. Age distribution of patients with Ewing's sarcoma of bone registered with clinical trial groups in Germany and the UK.

Cotterill S et al. *Journal of Clinical Oncology*;18:3108-3114; 2000

Approximately 85% of Ewing's sarcomas occur in bones (most commonly the long bones, the chest wall or the pelvis) though tumours can also occur in the kidneys, bladder, lung or limb tissues (Riggi and Stamenkovic, 2007). Ewing's sarcoma is rarely seen in Black or Asian populations, however no specific risk factors (such as parental

occupation or medication use, or exposure to therapeutic radiation) have so far been identified (Buckley et al., 1998).

1.6.2 Molecular and Cytogenetic Characteristics

ESFT have several well characterised chromosomal rearrangements, that can be used as diagnostic features. More than 90% of Ewing's sarcoma tumours exhibit a chromosomal rearrangement between the *EWS* gene on chromosome 22 and the genes of the *ETS* family on chromosome 11, generally referred to as the EWS-ETS fusion gene (Aurias et al., 1984). The most common of these rearrangements (seen in over 85% of cases) is between *EWS* and the *FLI1* gene. The exact functions of the products of these fusion genes are not yet known, however several studies have suggested they play a role as dominant oncogenes that exert their influence via regulation of mRNA transcriptional activation or repression (Arvand and Denny, 2001, Sandberg and Bridge, 2000, de Alava and Gerald, 2000). It has been demonstrated that the *EWS-FLI1* fusion gene is responsible for the phenotype of ESFT cells, most likely by inhibiting the myogenic differentiation of the cells (Eliazer et al., 2003, Hu-Lieskovan et al., 2005). There are also many other cytogenetic variants of the *EWS-FLI1* fusion gene, usually involving a third and occasionally even a fourth chromosome (Sandberg and Bridge, 2000), with genetic events such as trisomy 8 and 12 also seen in 46% and 33% of cases respectively (Maurici et al., 1998). Other genetic markers of Ewing's sarcoma include activation of the *Trk* family of tyrosine kinase proteins, with over-expression of *TrkA* receptors characteristic of neuronally differentiated tumours, whereas *TrkB* and *C* receptors are over-expressed in undifferentiated tumours (Sandberg and Bridge, 2000).

1.6.3 Diagnostic and Prognostic Factors

The main symptoms of ESFT are localised pain and swelling at the site of the tumour, sometimes accompanied by breaks or fractures resulting from bone weakness caused by the tumour itself. There may also be more general symptoms of tiredness, weakness, fever and anaemia (CancerIndex, 2003).

Diagnosis of sarcoma is initially by X-ray, MRI or CT scan, with a specific diagnosis of ESFT requiring histological staining of a biopsy sample to identify the differentiation

lineage. However, due to the shared characteristics of ESFT and several other tumours, confirmation of a diagnosis of ESFT generally requires cytogenetic analysis, for example to identify the presence of the *EWS-FLI1* fusion gene. Once diagnosed, ESFT cases are then staged according to tumour grade and size, the depth of invasion and, most importantly, the presence of metastases. Tumour grades are defined as high or low grade, with high grade tumours being those with high mitotic activity and necrosis within the tumour (Mackall et al., 2002).

A 15 year study of almost 1,000 Ewing's sarcoma patients identified prognostic factors correlating to overall and event free survival. The greatest prognostic factor was the presence of metastases, with only 27% of patients presenting with metastases surviving 6 years after diagnosis, whereas 61% of patients without metastases were still alive after this period, as shown in Figure 1-10. It was found that tumour volume became an indicator of prognosis above 100ml. Time to relapse has also been shown to be important, with almost all patients who relapse within 2 years subsequently dying from the disease (Cotterill et al., 2000). In addition, age at diagnosis has been found to be a prognostic marker, with those over age 14 at greater risk of relapse, as has the presence of lung metastases (Ladenstein et al., 2010).

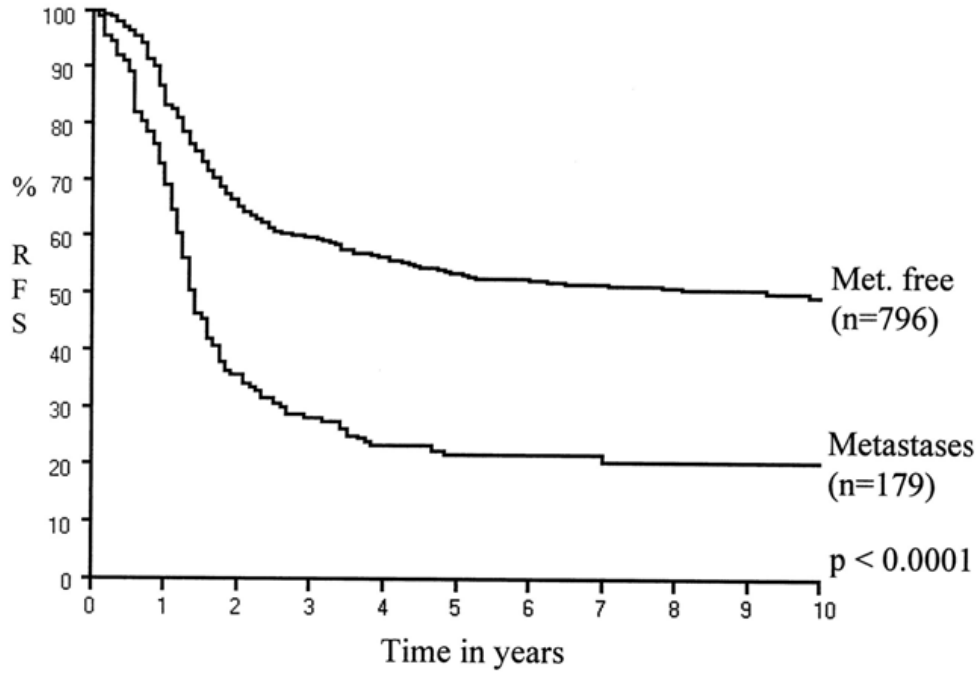

Figure 1-10. ESFT relapse-free survival according to detectable metastases at diagnosis. Cotterill, S.J. et al. *J Clin Oncol*, 18**,** 3108-3114.

Although several studies have attempted to examine a link between cytogenetic markers and disease prognosis, there have so far been few definitive correlations found. While deletion of chromosome 1p has been found to be associated with an unfavourable outcome, this deletion is relatively uncommon in ESFT (Hattinger et al., 1999). The type of *EWS-FLI1* fusion has also been shown to be important. Fusion of *EWS* exon 7 to *FLI1* exon 6 is known as type 1 and is associated with rapid tumour progression and death (Sandberg and Bridge, 2000). Race and ethnicity also affect prognosis, with overall survival significantly lower for Black, Asian, and white Hispanic patients, compared with white non-Hispanic patients (Lee et al., 2010, Worch et al., 2010). This distribution suggests there may be genetic markers of poor prognosis that are yet to be found, and work is ongoing to elucidate these.

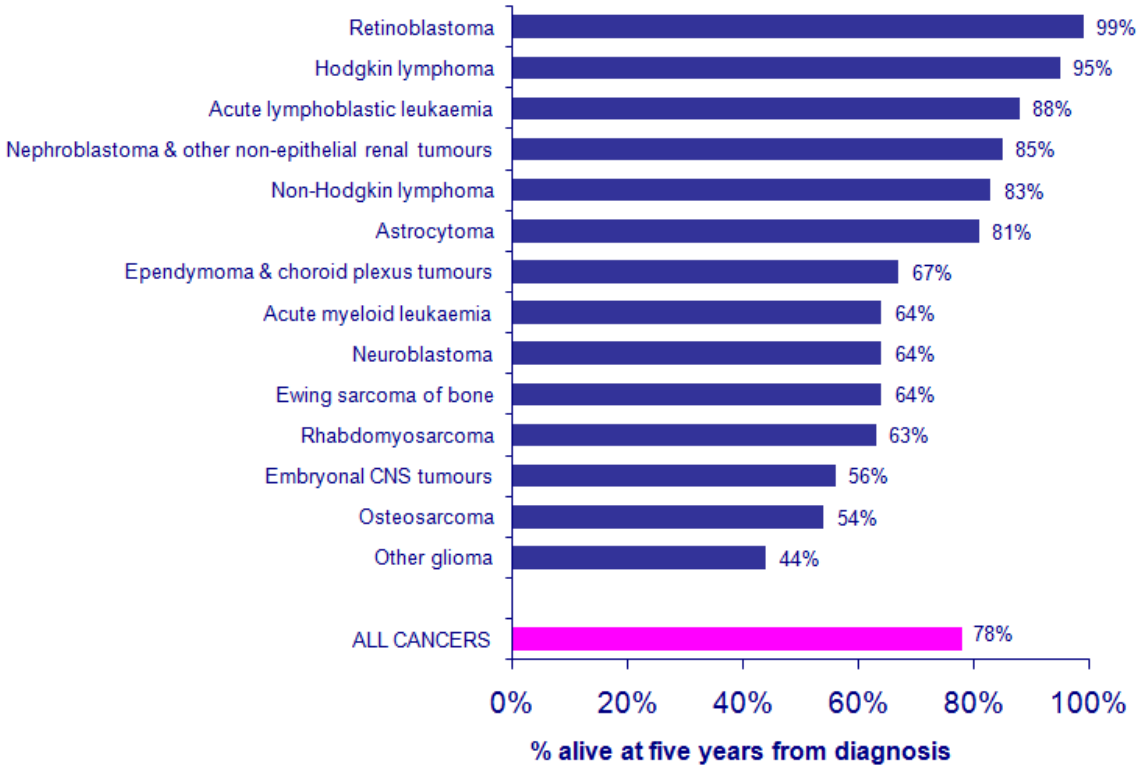

Figure 1-11. Percentage of patients still alive 5 years after diagnosis, childhood cancers, Great Britain, 2001 - 2005.

Cancer Research UK, 2005.

During the past 30 years more information has become available on the molecular basis and prognostic factors of ESFT. This information has enabled better classification of high risk patients and has resulted in a significant increase in survival rates. However, patients with metastatic disease or those who relapse early still have a very poor

prognosis, with lower five-year survival rates than for many other childhood cancers (see Figure 1-11) (Cancer Research UK, 2005). There is still considerable scope to improve our understanding of the molecular basis of ESFT, as well as factors affecting the progression and relapse of the disease and to improve treatment regimens to further boost overall survival rates in the future.

1.6.4 Treatment

The current treatment approach to ESFT is multimodal, consisting of a combination of surgery, radiotherapy and chemotherapy, as shown in Figure 1-12, although low grade, localised tumours, may be treated with surgery alone (Dunst et al., 1991, Rodriguez-Galindo et al., 2003). This approach has resulted in an increase in survival rates over the last 30 years, with almost 80% of patients without metastases currently progression free after 5 years (Grier et al., 2003), compared to less than 50% of patients in the 1980s (Nesbit Jr et al., 1990). There have been contradictory suggestions as to why this increase in survival has been seen. Some studies have suggested it was associated with a change in chemotherapy regimen, as after 1986 ifosfamide was substituted for cyclophosphamide treatment (Grier et al., 1994) (Meyer et al., 1992). Other trials did not find any evidence to show that ifosfamide was more beneficial than cyclophosphamide (Oberlin et al., 1992, Bacci et al., 1989). A more recent trial found that ifosfamide was just as effective as cyclophosphamide for treating standard risk patients, with cyclophosphamide treatment associated with increased toxicity. The same trial also found that high risk patients benefited from the addition of etoposide to a treatment regimen of vincristine, dactinomycin, ifosfamide, and doxorubicin (Paulussen et al., 2008). In addition, there have been significant improvements in the use of radiation to gain local tumour control, either with or without surgery (La et al., 2006). Improvements in imaging techniques and the development of cytogenetic testing have also contributed to earlier diagnosis and therefore increased survival. The use of retinoid therapy has also been investigated as ESFT-derived cell signs have shown considerable sensitivity *in vitro* to 4-HPR, resulting in its inclusion as a maintenance therapy in a current clinical trial in ESFT patients.

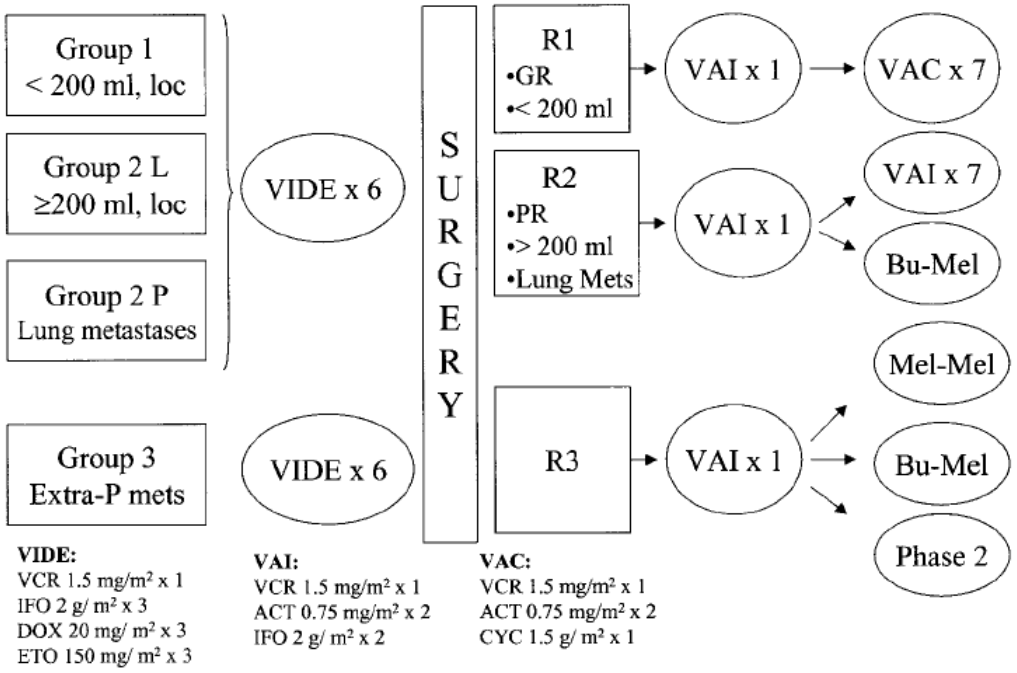

Figure 1-12. Risk stratification and treatment outline of the EURO-EWING-99 study.
VCR: Vincristine, IFO: Ifosfamide, DOX: Doxorubicin, ETO: Etoposide, ACT: Actinomycin D, CYC: Cyclophosphamide, Bu-Mel: Busulphan and mephalan. Rodriguez-Galindo, C. et al. *Medical and Pediatric Oncology*, 40, 276-287; 2003.

1.7 Xenobiotic Metabolism and Disposition

The vast majority of xenobiotic compounds require biotransformation in order to reduce toxic effects on the body, and to enable excretion of toxic compounds and their metabolites. These detoxification pathways occur in three phases: phase I, phase II and phase III. Phase I metabolism involves modification of xenobiotics, most commonly oxidation by CYPs, but also includes alcohol or aldehyde dehydrogenation (Lewis, 2003). Phase II metabolism involves methylation or conjugation reactions. These are generally glucuronidation, sulphation or acetylation, though they can also include the incorporation of a glutathione or glycine molecule. All of these reactions have the function of increasing the polarity, and therefore solubility, of toxic compounds, in order to facilitate excretion from the body (Back and Rogers, 1987). Phase III metabolism involves further modification of xenobiotic conjugates, for example the removal of glycine or glutamate residues by peptidases, resulting in acetylation of the compound. Again, phase III metabolism occurs to aid the removal of toxic compounds from cells in order to assist excretion (Xu et al., 2005).

1.7.1 Human Liver and Intestine Microsomal Enzymes

The liver is the major organ in the human body responsible for the detoxification of toxic xenobiotic compounds, as well as environmental and dietary toxins. Blood is supplied to the liver via both the hepatic portal vein and the hepatic arteries, meaning that most chemotherapeutic compounds will pass through the liver and be subjected to both phase I and phase II metabolism by hepatic enzymes (He, 2005). It is therefore of paramount importance that the effect of liver metabolism on chemotherapeutic compounds is investigated, in order to understand the likely pharmacokinetics of a particular compound. This can be investigated by the use of human liver microsomes (HLM), that are generally prepared from the livers of brain dead organ donors whose organs are unsuitable for transplantation (Pearce et al., 1996). A section of homogenized human liver is centrifuged at a relatively low speed (less than 12,000g) to pellet out cell debris, nuclei, peroxisomes, lysosomes, and mitochondria. Membrane bound liver enzymes are contained in the supernatant fraction, and this is then centrifuged at a much higher speed (typically greater than 100,000g) to precipitate the microsomes (Nelson et al., 2001). Pooled liver samples from several donors are used in order to reduce effects due to genetic variance.

Chemotherapeutic compounds given orally additionally undergo significant metabolism in the intestine, as many of the same metabolising enzymes found in the liver are also present in the intestine. It can therefore be of particular importance to investigate intestinal metabolism of orally dosed compounds, using human intestinal microsomes (HIM). These can be prepared by differential centrifugation in the same way as HLM.

In order to further elucidate the specific enzymes responsible for metabolism of individual xenobiotics, and in order to assess the possible impact of genetic variants of these enzymes on drug metabolism, studies can also be carried out using enzyme expression systems. Such approaches generally involve either a bacterial expression system, such as *E. coli*, or a baculovirus-infected insect cell system, transfected to over-express individual human enzymes. Transfection with genetic variants of a particular enzyme can also be carried out, enabling research into the potential effects of genetic variation on clinical metabolism (Terpe, 2006).

1.7.2 Cytochrome P450s (CYPs)

The main phase I metabolising enzymes present in the liver and intestine are the cytochrome P450 enzymes (CYPs). These enzymes are part of a superfamily of haem-containing mono-oxygenases, that were first purified over 50 years ago (Greenwood, 1963, Levin et al., 1972, Beaune et al., 1979). More than 1,200 CYPs have so far been identified, and these are divided into 70 families, based on enzyme identity. CYP enzymes are named by an Arabic numeral for the family number, then by a letter for the subfamily, followed by another Arabic numeral to identify the individual enzyme, for example CYP1A1, CYP3A4 etc. Families require sequence identity of at least 40%, with at least 55% identity between members of the same sub-family. An enzyme with a difference in identity of 3% or more will be designated as a new member of a particular family (Nelson et al., 1996). Approximately 60 CYPs are found in humans, where they are involved in the biosynthesis and detoxification of many exogenous and endogenous compounds, such as xenobiotic drugs (including retinoid derivatives), steroids, prostaglandins, and fatty acid derivatives (Ortiz de Motellano, 1995). The oxidation reaction is carried out by the insertion of one atom of molecular oxygen into the substrate (forming the hydroxylated product) while the other oxygen atom present is reduced to water, as shown in Figure 1-13. Almost all human CYPs are polymorphic (i.e. they have more than one possible allele, with the variant alleles occurring at a frequency too great to be considered a mutation), that can result in either defective or enhanced enzyme activity (Anzenbacher and Anzenbacherová, 2001).

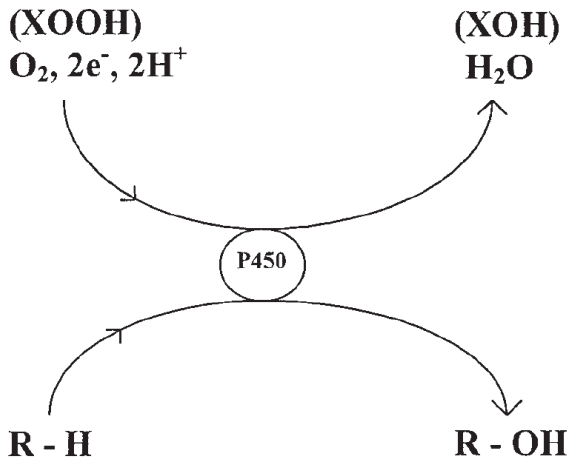

Figure 1-13. Scheme of P450 reactions.

R–H, substrate; R–OH, hydroxylated product; XOOH, peroxide (X = H or organic residue); XOH, hydroxylated by-product. Anzenbacher and Anzenbacherova *Cellular and Molecular Life Sciences*, 58, 737-747; 2001.

CYP polymorphisms are known to have an impact on drug metabolism. In particular, CYP2C8 and CYP2D6 polymorphisms play a role in determining the effectiveness of several chemotherapeutic drugs. Approximately 10% of Caucasians are 'poor metabolisers' of substrates of CYP2D6, as polymorphisms in this enzyme result in a loss of activity (Bosch et al., 2006, Cholerton et al., 1992, Daly et al., 1998). CYP2C8 polymorphisms *2 and *3 both result in significantly lower clearance of paclitaxel and arachidonic acid, resulting in clinical implications for patients homozygous for these alleles (Bahadur et al., 2002, Dai et al., 2001, Daly et al., 2007).

Similarly, polymorphisms of CYP3A4 have been associated with decreased survival in breast cancer patients treated with cyclophosphamide, as shown in Figure 1-14. It is thought this is due to reduced metabolism of cyclophosphamide to its active form (4-hydroxy cyclophosphamide), as higher plasma levels of the inactive parent molecule are found in patients expressing variant alleles (Petros et al., 2005). However, other studies found no such association (Ekhart et al., 2008). In addition, some studies have also found that CYP3A4 polymorphisms are associated with poor prognosis for both breast cancer and prostate cancer (Keshava et al., 2004). These conflicting results demonstrate the difficulties that can be faced in differentiating the prognostic effects of genetic polymorphisms from those that are predictive of response to particular treatments.

Treatment of breast cancer patients with tamoxifen results in markedly variable plasma concentrations of tamoxifen metabolites. This is of particular importance as tamoxifen efficacy relies on metabolism to a series of active metabolites. Metabolism of tamoxifen is relatively complex, involving several CYPs and UGT enzymes, many of that are polymorphic, that result in the formation of more than 20 metabolites. As shown in Figure 1-15, *CYP2D6* genotype is a major determinant of estrogen receptor inhibition by the tamoxifen metabolite endoxifen. This study demonstrated that most patients with at least 1 'poor metaboliser' allele were unable to reach the target of 90% estrogen receptor inhibition. However, *CYP2D6* genotype still only accounted for approximately 38% of the variation seen in endoxifen plasma concentrations (Murdter et al., 2011). The remainder of the variation is likely to be due to the combined effects of other polymorphic genes, as patients with variant allele for CYP2C9 had significantly lower plasma concentrations of endoxifen and another tamoxifen metabolite, 4-hydroxytamoxifen. This unexplained variation demonstrates the difficulty in clarifying the genetic factors involved in patient response to chemotherapy in cases where multiple

genes are involved in complex drug metabolism pathways. Elucidation of the impact of polymorphic P450 enzymes on drug metabolism is further complicated by the fact that the expression of several of these enzymes can be up- or down-regulated by xenobiotic compounds. For example, concomitant administration of grapefruit juice increases the oral availability of CYP3A4 substrates by down-regulating enzyme expression (Schmiedlin-Ren et al., 1997). The opposite effect is seen in an additional CYP family, CYP26. This family of enzymes is involved in the metabolism of retinoic acid and its derivatives, with enzyme expression up-regulated by the presence of retinoids. Auto-induction of metabolism by CYP26 can therefore be a significant issue for retinoid-based drugs, limiting maximum plasma concentrations of these compounds that can be achieved (Ray et al., 1997).

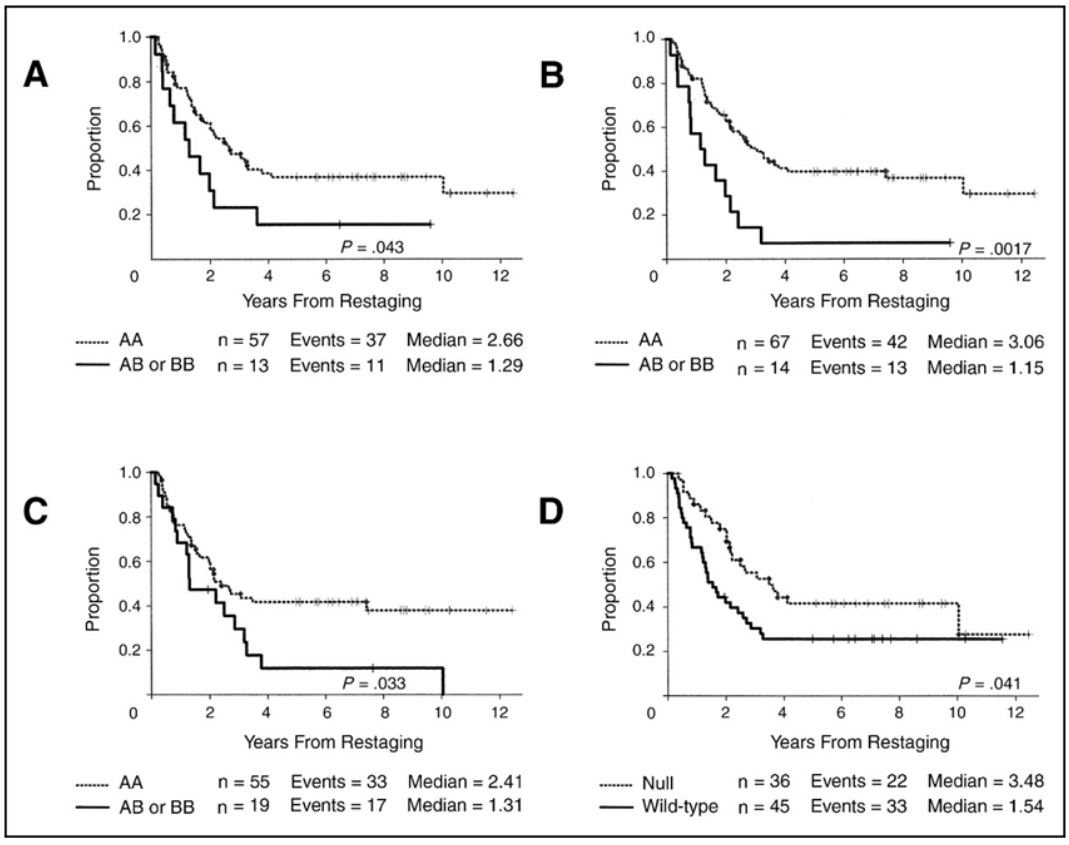

Figure 1-14. Kaplan-Meier analyses of overall survival following cyclophosphamide chemotherapy with patients segregated based on the presence of genetic polymorphisms (A) CYP 3A4*1B, (B) CYP3A5*1, (C) MET1F G-7T and (D) glutathione-S-transferase M1. Dotted lines indicate patients with no variant copies of the respective genes (AA) whereas patients represented by the solid lines have at least one variant copy (AA or BB). Petros, W. P. et al. *Journal of Clinical Oncology* 23:6117-6125; 2005

Another example of a commonly prescribed drug where inter-patient variation has a major impact on clinicians' ability to standardise dosing is warfarin, an anti-coagulant drug. Haemorrhage is a major risk factor for patients taking warfarin and means that patients are monitored for their initial few days of treatment, with doses being altered on a case-by-case basis depending on the intensity of anti-coagulation for each patient. However, this approach is still only successful in predicting the correct maintenance dose in 69% of patients. The most potent enantiomeric form of warfarin (s-warfarin) is metabolised to inactive hydroxylated metabolites by CYP2C9 and this metabolism is significantly reduced *in vitro* in the presence of variant isoforms of CYP2C9 (Rettie et al., 1994, Haining et al., 1996). A further study found that patients expressing a variant CYP2C9 allele were 6 times more likely to require a reduction in their warfarin dose, and that these patients were also more likely to suffer bleeding complications during the initial monitoring period (Aithal et al., 1999).

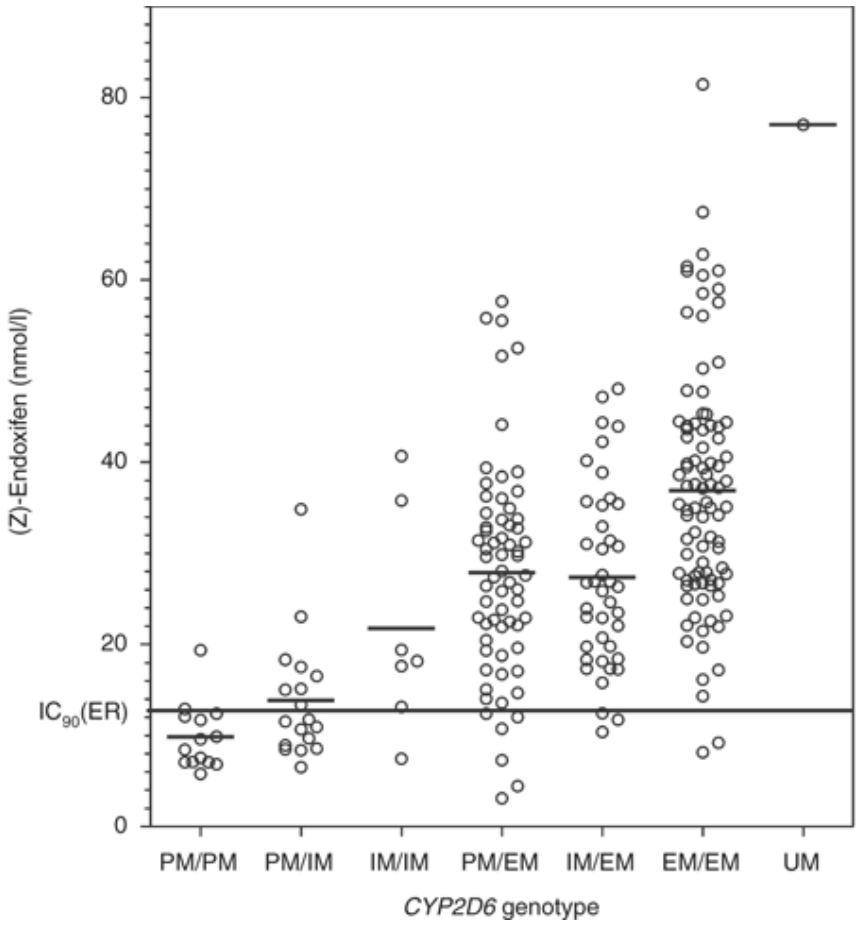

Figure 1-15. CYP2D6 genotype-associated (Z)-endoxifen levels in plasma and estrogen receptor (ER)-inhibiting activity.

EM, allele with normal activity; IM, allele with decreased activity; PM, allele with no activity; UM, duplication of functional alleles. Murdter, T.E. et al. *Clin Pharm Ther*, 89, 708-717; 2011.

Additional polymorphic genes have also been found to influence warfarin dosing requirements, for example vitamin K epoxide reductase (VKORC1). VKORC1 polymorphisms affect warfarin-associated coagulation in both African American and European American patients, whereas CYP2C9 polymorphisms have a much greater effect on European Americans than in African Americans. This ethnic genetic differences result in CYP2C9 and VKORC1 polymorphisms accounting for up to 30% variability in warfarin dose among European Americans compared to only 10% among African Americans (Limdi et al., 2008). It is therefore important to have an understanding of all polymorphic genes involved in the metabolism of a particular type of drug and their interaction in a particular patient population in order for patients to benefit from genotyping prior to initiation of therapy.

1.7.3 Uridine 5'-Diphospho-glucuronosyltransferase Enzymes (UGTs)

The products from phase I metabolism generally acquire functional groups that render them substrates for phase II conjugation reactions such as glucuronidation. This reaction is carried out by UGT (uridine 5'-diphospho-glucuronosyltransferase) enzymes and involves the conjugation of toxic compounds with glucuronic acid (derived from the co-factor uridine diphosphate glucuronic acid (UDPGA)) in order to increase their polarity and solubility. Glucuronidated metabolites can then be excreted through the kidneys. UGT enzymes are able to glucuronidate endogenous compounds (e.g. steroids and bilirubin) and xenobiotics, containing hydroxyl, amine or carboxylic acid functional groups (Nagar and Remmel, 2006).

There are nineteen human UGTs currently known, and these are primarily expressed in the liver. UGTs are divided into families in much the same way as CYPs, and similarly are named by an Arabic numeral for the family number, then by a letter for the subfamily, followed by another Arabic numeral to identify the individual enzyme, for example UGT1A1, UGT2B17 etc. There are five UGT1 isoforms substantially expressed in human liver microsomes (UGTs 1A1, 1A3, 1A4, 1A6 and 1A9) along with five UGT2 isoforms (2B4, 2B7, 2B10, 2B15 and 2B17) (Izukawa et al., 2009). There is also substantial extra-hepatic expression of UGTs, particularly in the intestinal epithelium, with expression also observed in the kidney, brain and skin (Radominska-

Pandya et al., 1998, Ohno and Nakajin, 2009). Indeed UGT's 1A7 and 1A10 have been found to be expressed only in extra-hepatic tissue (Strassburg et al., 1997).

Another similarity between UGT and CYP enzymes is that polymorphisms of UGTs have also been shown to have a major effect on drug metabolism. Irinotecan toxicity particularly is known to be associated with polymorphisms of UGT1A1. Patients who express the UGT1A1*28 allele have significantly decreased metabolism of SN-38, the active metabolite of irinotecan. This increase in SN-38 can result in a much higher risk of treatment related toxicity, and has led to dose-reduction advice for patients homozygous for the risk-allele being included on the product label (Ando et al., 2000, O'Dwyer and Catalano, 2006, United States Food and Drug Administration, 2010, Gagné et al., 2002). Several other UGTs have also been associated with inter-patient variation in toxicity or drug clearance and accumulation. Exposure to mycophenolic acid (an immunosuppressive drug) was found to be significantly lower in patients with UGT1A9-275/-2152 polymorphisms, while carriers of UGT1A9*3 had significantly higher maximum plasma levels of the drug, as did patients homozygous for UGT2B7*2 (Levesque et al., 2007, Miura et al., 2008). Patients homozygous for UGT2B15*2 have also been shown to have significantly lower clearance of lorazepam than those expressing the wild-type *1 allele (Chung et al., 2005).

The major UGTs responsible for the glucuronidation of retinoid-based drugs including ATRA have previously been investigated (Little et al., 1997, Czernik et al., 2000, Samokyszyn et al., 2000, Radominska et al., 1997). These studies showed that both hepatic and intestinal UGTs were able to metabolise ATRA, though significantly more metabolism occurred with hepatic UGTs than with intestinal UGTs. An additional glucuronide metabolite was also seen, that was likely to be a glucuronide resulting from isomerisation of ATRA to 13-cis RA. However glucuronidation of other retinoids has not yet been investigated.

1.7.4 ATP-Binding Cassette (ABC) Transporters

The mammalian ATP-binding cassette (ABC) transporters are a super-family of proteins responsible for the efflux of many endogenous compounds, as well as xenobiotic drugs and metabolites. They are transmembrane proteins that utilise the hydrolysis of ATP to transport substrates across the cell membrane (Higgins, 1992).

Forty-eight ABC transporter genes have so far been identified in humans, with MDR1 (also known as ABCB1 or p-glycoprotein), MRP2 (ABCC2) and BCRP (ABCG2) being among the best characterised (Fletcher et al., 2010).

The expression of ATP transporters has been associated with tumour resistance to chemotherapy, as it can result in decreased intracellular drug concentrations in tumour cells (Gottesman et al., 2002). Since the commonly-expressed transporters, such as MDR1, have a broad substrate profile, tumours expressing these transporters are resistant to a wide range of agents, with the only criterion for resistance being that a molecule is a substrate for the ABC transporter. This is known as multi drug resistance (MDR) and has been observed in resistance to vincristine, doxorubicin and paclitaxel (Ambudkar et al., 1999).

Although MDR can result from initial tumour exposure to a drug, some tumours show intrinsic expression of the transporters. A trial in breast cancer patients found that a lack of expression of MDR1 at the time of diagnosis was a prognostic marker for complete response to therapy with doxorubicin, cyclophosphamide, vincristine, and prednisone. In addition, matched biopsy samples taken before and after chemotherapy showed no increase in MDR1 expression during the course of treatment (Ro et al., 1990). It should be noted that, for some drugs, resistance can also be due to decreased drug uptake, as seen in resistance to methotrexate, 5-flurouracil and cisplatin (Shen et al., 2000, Shen et al., 1998).

As well as impacting on tumour sensitivity to drugs, the physiological expression of drug transporters in normal tissues influences drug disposition, for example by modulating uptake into the liver and kidneys, and subsequently altering either drug metabolism or excretion (Yamazaki et al., 1996). In an attempt to reverse the MDR phenomenon, inhibitors of MDR1, such as verapamil, were administered in combination with substrates such as doxorubicin (also known as adriamycin). Increased peak plasma concentrations of adriamycin were observed in a trial of patients with small cell lung cancer when given concurrently with verapamil. There was also a longer half-life and larger volume of distribution. The decreased drug clearance observed suggested that inhibition of drug efflux from cells has a significant impact on drug disposition and pharmacokinetics (Kerr et al., 1986). Significant differences in the pharmacokinetics of many drugs have also been observed in knockout mice, adding further weight to the

importance of drug transporter expression. Knockout of *MDR1* genes in a mouse model resulted in hypersensitivity to xenobiotics (including the chemotherapeutic agents vinblastine, paclitaxel and doxorubicin), as well as increased bioavailability. In addition, drug accumulation was seen in the liver, brain and gall bladder, that are all tissues that normally express MDR1 (Brinkmann and Eichelbaum, 2001).

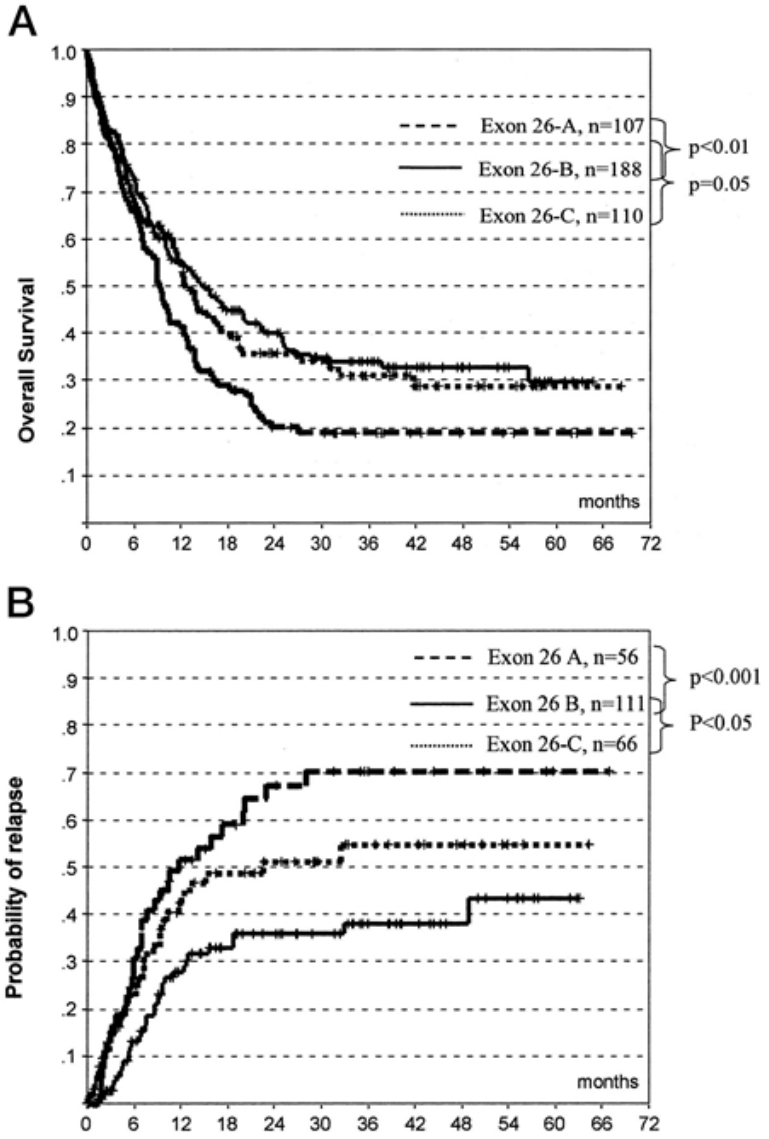

Figure 1-16. Survival of AML patients according to their genetic variants in exon 26 of MDR1. A) Kaplan-Meier analysis for overall survival of AML patients. B) Kaplan-Meier analysis for probability of relapse of AML patients.

Study distinguished between homozygous Ex-26-A, heterozygous Ex-26-B, and homozygous Ex-26-C polymorphisms. Modified from Illmer, T. et al. *Cancer Research*, 62, 4955-4962; 2002.

Investigations into polymorphisms of ABC transporters have given further insight into the role they play in resistance to chemotherapeutic compounds and subsequent effects on relapse and survival. A trial in patients with acute myeloid leukaemia treated with daunorubicin and cytosine arabinoside found that polymorphisms in MDR1 were associated with a higher probability of relapse and lower overall survival, as shown in Figure 1-16. However, the pharmacokinetic effect of MDR1 polymorphisms was not investigated in this trial (Illmer et al., 2002).

1.8 Retinoid Metabolism

Retinoids are known to be involved in a diverse range of biological functions, including vision, embryonic development and cell differentiation. The latter of which has resulted in considerable interest in the use of retinoic acid analogues in the treatment of cancer (Evans and Kaye, 1999). Due to their wide range of functions, metabolism of retinoids has also been extensively investigated. The main metabolising enzymes of retinoids are alcohol dehydrogenases, aldehyde dehydrogenases and CYPs, as shown in Figure 1-17 (Perlmann, 2002, Blomhoff and Blomhoff, 2006, Roos et al., 1998).

Clinical trials have demonstrated that plasma concentrations of ATRA are much lower following repeated doses than during the initial course of therapy (Muindi et al., 1992, Smith et al., 1992). Various CYP enzymes are known to metabolise retinol and ATRA, as well as 9-cis RA and 13-cis-RA. These retinoids are also able to upregulate the expression of some CYPs, and are therefore able to induce their own metabolism (Ray et al., 1997, White et al., 1997, Marill et al., 2002). It is thought that increasing metabolism resulting from auto-induction of *CYP26* expression may be the reason that whilst initial chemotherapy with ATRA is generally successful, almost all patients prescribed ATRA as maintenance chemotherapy ultimately develop resistance to the treatment, resulting in relapse (Delva et al., 1993). Auto-induction of *CYP26* expression by 13-cis RA may be less problematic, as although isomerisation of 13-cis RA to ATRA is likely to result in up-regulation of *CYP26*, a recent clinical trial of 13-cis RA in neuroblastoma patients found that plasma concentrations remained relatively consistent over successive treatment courses. However, there was still significant metabolism of 13-cis RA, as well as considerable inter-patient variation in 13-cis RA peak plasma concentrations (Veal et al., 2007). This may be due to differences in dosing regimen between 13-cis RA and ATRA, as 13-cis RA is given as a four week cycle involving two weeks of treatment followed by a two week break, whereas there is

no treatment break in the ATRA treatment regimen. *CYP26* expression induced by 13-cis RA consequently has time to return to base levels before the next cycle of treatment.

Oxidative metabolism of ATRA and 13-cis RA by CYPs has been extensively researched. The major metabolite observed following *in vivo* treatment with 13-cis RA is 4-oxo 13-cis RA, with 4-hydroxy 13-cis RA also seen in patient samples (Vane and Buggé, 1981, Khan et al., 1996). Studies relating to retinoic acid metabolism have mainly focused on oxidation by CYP26 isoforms, as these are induced by retinoic acid (White et al., 1997). *CYP26A1* has been shown to be induced by ATRA, with inhibition of *CYP26A1* by retinoic acid metabolism blocking agents (RAMBAs) significantly increasing plasma concentrations of ATRA both *in vitro* and in mouse models of neuroblastoma and prostate cancer (Armstrong et al., 2005, Huynh et al., 2006).

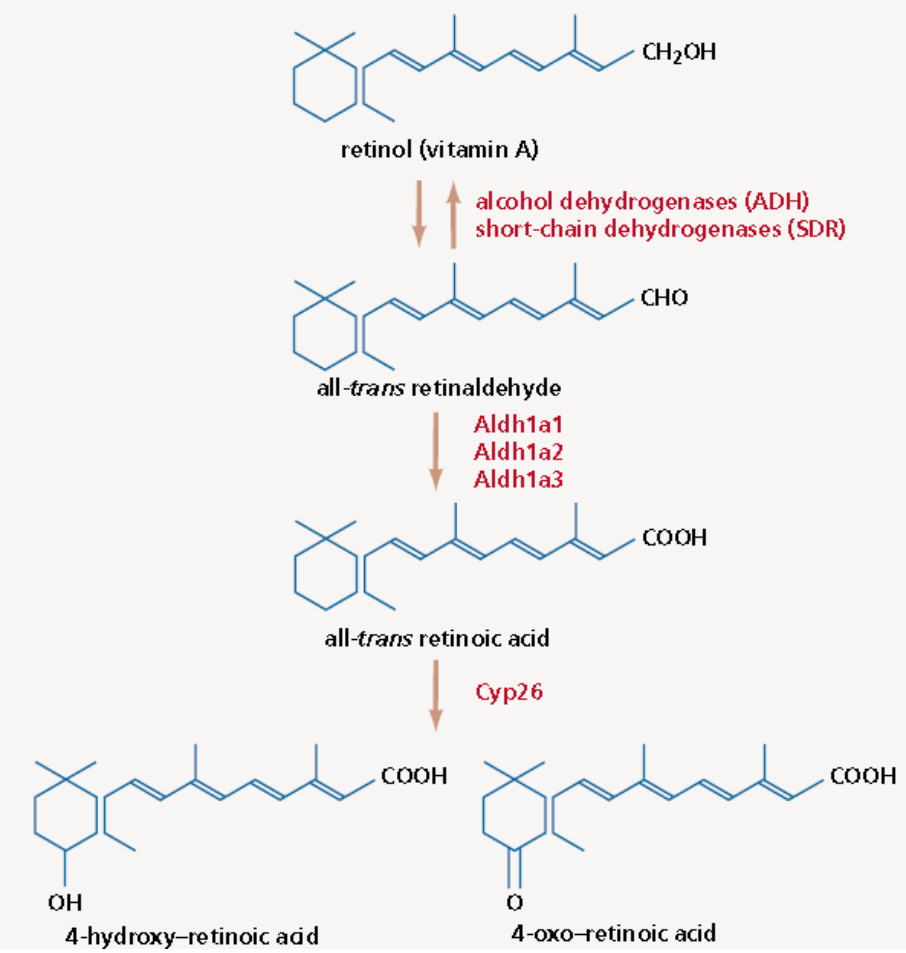

Figure 1-17. Biosynthetic pathway for the metabolism of retinol.

Perlmann, T. *Nature Genetics*, 31**,** 7 – 8; 2002.

As retinoids are metabolised by CYPs, it possible that CYP polymorphisms may play a role in determining the extent of metabolism. However, relatively little is currently known about the impact of CYP polymorphisms on retinoid metabolism, although CYP2C8 isoform has been shown not to affect 13-cis RA metabolism (Rowbotham et al., 2010a).

1.8.1 4-HPR Metabolism

Metabolism of 4-HPR occurs by methylation, oxidation or esterification. An early study of 4-HPR biotransformation in rats identified the major metabolite produced *in vivo* as N-(4-methoxyphenyl) retinamide (4-MPR) (Swanson et al., 1981). The presence of 4-MPR and a 4-HPR-ester were subsequently confirmed by further studies in female rats and mice in 1986, when a cis isomer of 4-HPR as well as an additional unidentified metabolite were also discovered (Hultin et al., 1986). This additional major metabolite was not identified until 2004, when it was characterised as 4'-oxo 4-HPR, resulting from an oxidation in the cyclohexene ring, as shown in Figure 1-18. 4-MPR and 4'-oxo 4-HPR were also the major metabolites detected in breast cancer patients (Mehta et al., 1991, Mehta et al., 1998) as well as in cell lines (Appierto et al., 2001). 4'-oxo 4-HPR was subsequently found to be an active metabolite that inhibits cell proliferation. The active metabolite was identified following formation of the metabolite by *CYP26A1* induction (Villani et al., 2004). Further analysis of the growth-inhibitory properties of 4'-oxo 4-HPR determined that the metabolite is more effective at inhibiting growth in several cell lines than its parent molecule, 4-HPR. 4'-oxo 4-HPR is also able to inhibit growth in cell lines that are resistant to 4-HPR itself and has been shown to exert a synergistic effect with 4-HPR (Villani et al., 2006). Although 4-MPR has been shown to have modest growth inhibitory effects in some cell lines, overall it is now generally thought to be inactive (Sabichi et al., 2003, Mehta et al., 1998).

As CYP26 isoforms are major metabolisers of retinoids, inhibitors of CYP26 metabolism have been developed that are able to significantly increase plasma concentrations of ATRA and 13-cis-RA in mice (Armstrong et al., 2005, Armstrong et al., 2007b, Huynh et al., 2006, Njar et al., 2006). 4-HPR is metabolised to its 4'-oxo metabolite by CYP26A1, and is also able to upregulate the expression of this enzyme. Unlike ATRA, the auto-induction of 4-HPR metabolism does not result in a decrease in

plasma concentrations of the drug during long-term treatment (Formelli et al., 1993). However there is some evidence that continuous treatment of an ovarian carcinoma cell line with 4-HPR up-regulated *CYP26*, resulting in increased metabolism of 4-HPR to its 4'-oxo 4-HPR metabolite (Villani et al., 2004). In contrast to the detrimental effect of ATRA metabolism on drug efficacy, oxidative metabolism of 4-HPR may result in an increase in efficacy due to 4'-oxo 4-HPR being an active metabolite (Villani et al., 2006).

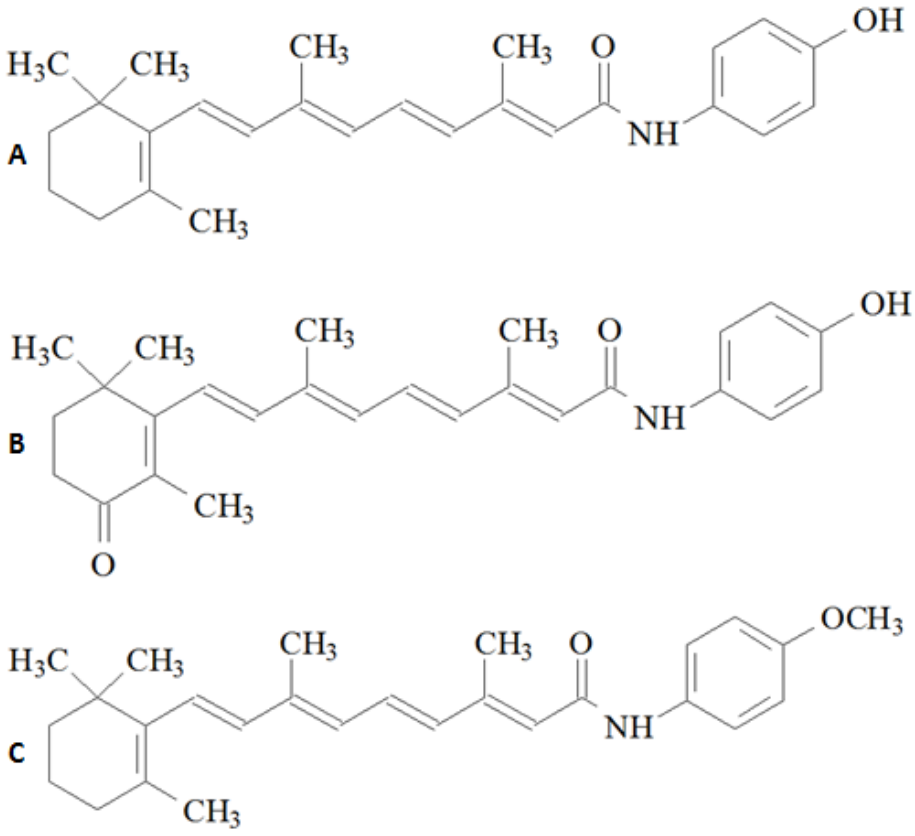

Figure 1-18. Structures of A) 4-HPR, B) 4'-oxo 4-HPR and C) 4-MPR.

1.9 4-HPR Mechanism of Action

4-HPR is able to cause caspase-dependent apoptosis in human neuroblastoma cells. It has been demonstrated that treatment of cells with 4-HPR causes poly ADP ribose polymerase (PARP) cleavage by caspase 3 and that 4-HPR-induced apoptosis is inhibited by DEVD, (a caspase 3 specific inhibitor) (Lovat et al., 2000). However, these data contrast with those obtained from subsequent studies, in different cell lines, that found DEVD only partially inhibited apoptosis, and therefore suggested that 4-HPR-induced apoptosis is partially caspase-independent (Vene et al., 2007).

Most retinoids act via retinoid receptor dependent pathways, requiring direct interaction with either RARs or RXRs. 4-HPR is unusual as it has been shown to induce apoptosis by both retinoid receptor dependent and independent pathways (Dmitrovsky, 2004). It has been demonstrated that 4-HPR is able to selectively activate retinoid receptors in breast cancer cell lines. 4-HPR is a potent activator of RARγ, exhibits moderate activity with RARβ and no activity with RARα or RXRα (Fanjul et al., 1996). Similar results were obtained in neuroblastoma cell lines, demonstrating that 4-HPR-induced apoptosis is blocked by RARβ and RARγ inhibitors, but not by RARα inhibitors (Lovat et al., 2000). However, in epithelial cells RAR antagonists had no effect on 4-HPR-induced apoptosis (Kitareewan et al., 1999). The use of wild-type and retinoid receptor knock-out F9 murine embryonal carcinoma cells showed two distinct effects of 4-HPR. At high concentrations of 4-HPR (>10μM) there was a rapid induction of apoptosis in both the wild-type and knock-out cell lines, suggesting that apoptosis was induced by retinoid independent pathways. At lower 4-HPR concentrations (<1μM) there was a slow induction of differentiation and an accumulation of cells in G_1. This second effect was only seen in the wild-type cells, indicating that this effect was via retinoid dependent pathways (Sabichi et al., 2003).

The differences seen in retinoid receptor effects between cell lines may also be due to differences in 4-HPR metabolism, as the effects of the 4'-oxo 4-HPR metabolite are retinoid receptor independent (Villani et al., 2006). Therefore, it is possible that cell lines that efficiently metabolise 4-HPR may utilise the retinoid receptor dependent mechanisms of action of 4-HPR itself, as well as the retinoid receptor independent mechanisms of action of the 4-oxo metabolite.

Unlike other retinoids, 4-HPR is able to induce apoptosis by induction of reactive oxygen species (ROS) (Delia et al., 1997, Myatt and Burchill, 2008), as shown in Figure 1-19. Experiments in Ewing's sarcoma cell lines showed that free radicals increased within 2 hours of 4-HPR treatment, while addition of antioxidants inhibited this increase in free radicals and also inhibited apoptosis. The generation of free radicals was not affected by the addition of inhibitors of caspase 3 or RARs, showing that generation of free radicals is via a separate pathway (Lovat et al., 2000).

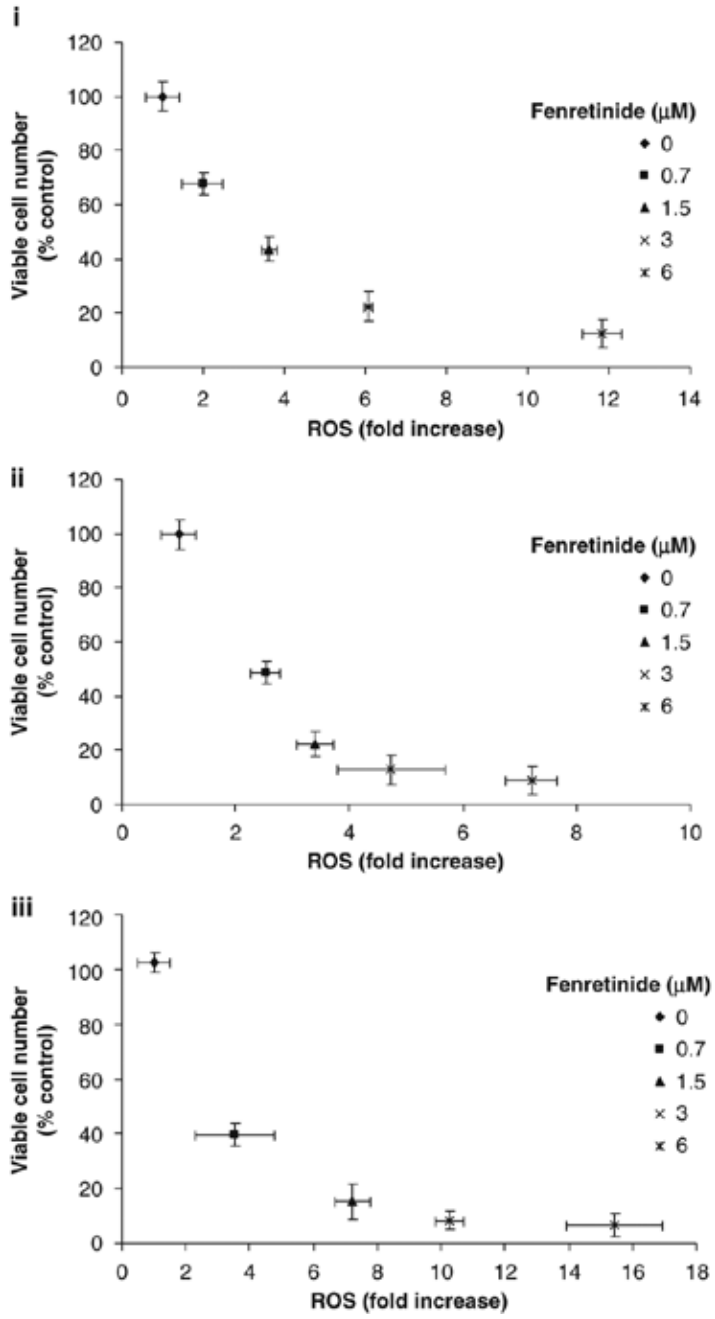

Figure 1-19. Level of reactive oxygen species (ROS) produced in Ewing's sarcoma cell lines after exposure to Fenretinide.

(i) A673, (ii) TC-32 and (iii) TTC-466 cells were treated with fenretinide (0.7–6μM) for 1h or 24h and ROS and viable cell number determined respectively. Modified from Myatt and Burchill *Oncogene* 27(7): 985-996; 2008.

It has been established that lipid oxygenases are the primary source of ROS, as inhibitors of the nitric oxide, CYP and NADPH oxidase pathways all had negligible effects on 4-HPR induced ROS (Lovat et al., 2003c). It was subsequently demonstrated that phospholipase A2 (PLA2) and 12-lipoxygenase (12-Lox) are the only enzymes

involved in ROS generation in response to 4-HPR. PLA2 is able to release arachidonic acid (AA), that then acts as a substrate for 12-Lox. The pro-apoptotic factors Gadd153 and Bak are then upregulated, resulting in cytochrome C release and apoptosis (Lovat et al., 2003a, Corazzari et al., 2005). Bak and Gadd153 are both major components in the endoplasmic reticulum (ER) stress pathway, and may also be acting through this to induce apoptosis, as shown in Figure 1-20. However, as Gadd153 inhibition only partly inhibits Bak, it is likely there is also a Gadd153-independent mechanism contributing to Bak induction (Lovat et al., 2003b).

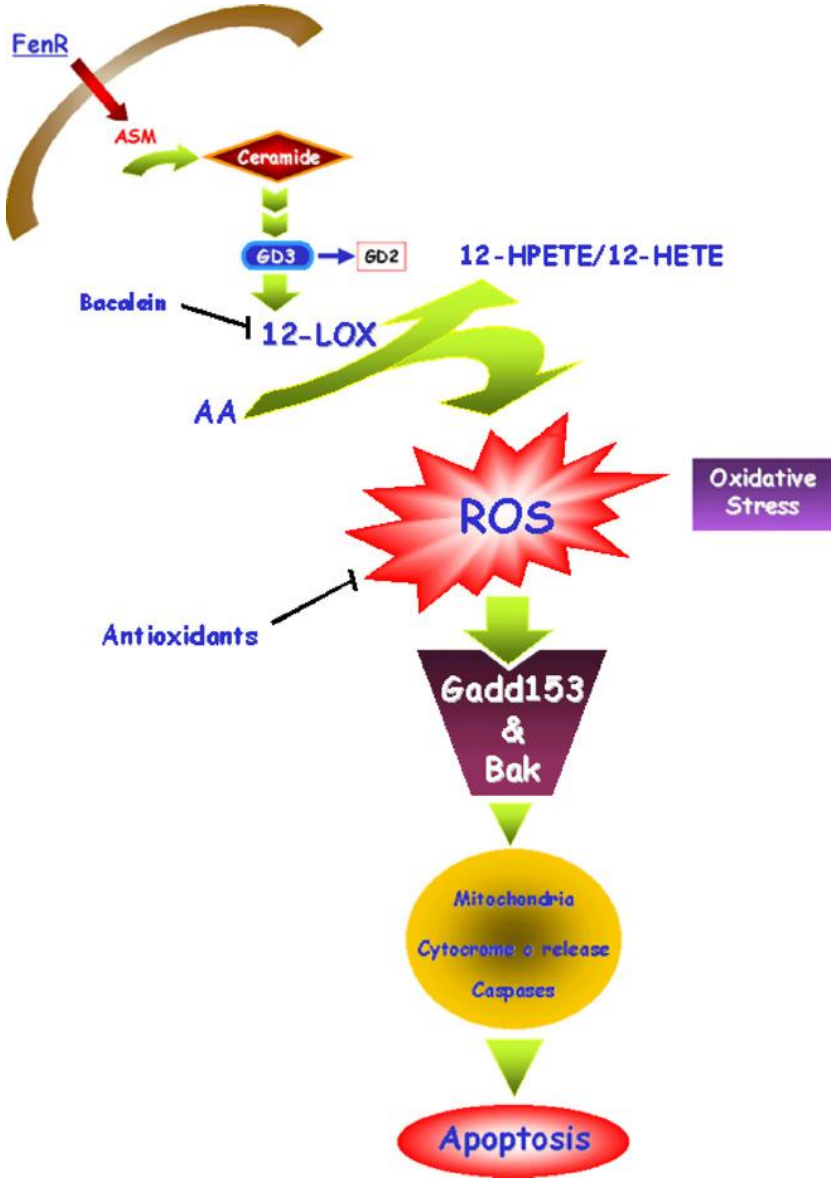

Figure 1-20. Schematic of 4-HPR induced apoptotic pathway

Corazzari et al. *Biochem & Biophys Res Com* 331(3): 810-815; 2005.

4-HPR treatment also results in the induction of ceramide, an intracellular lipid messenger able to cause apoptosis via several p53-independent pathways. Ceramide can work either directly as a lipid-signaling molecule or by metabolism to lipid mediators, e.g. gangliosides. Ceramide is also able to function in hypoxic conditions, causing activation of the JNK/SAPK cascade, via activation of caspase 3 (Maurer et al., 1999). Ceramide induction can be a result of either *de novo* synthesis by ceramide synthase, or from hydrolysis of membrane sphingomyelin. There is some debate over which of these methods of ceramide induction is activated by 4-HPR. Ceramide-induced apoptosis in neuroblastoma cells is inhibited by sphingomyelinase inhibitors, but not by fumosin B1, that is an inhibitor of ceramide synthase (Lovat et al., 2005), whereas the opposite effect was found in endothelial cells, suggesting that ceramide synthases (not sphingomyelinases) were responsible for apoptosis (Erdreich-Epstein et al., 2002). The different effects of these inhibitors suggests that the method of ceramide induction by 4-HPR is dependent on the cell line, as well as the concentration of 4-HPR used (high concentrations may activate both pathways together) and also whether or not conditions are hypoxic (Lovat et al., 2005).

An additional route of 4-HPR induced apoptosis is through Noxa, a p53-independent BH3 domain only protein. Noxa is able to activate Bak to induce apoptosis by the displacement of Bak from its pro-survival partners. Noxa itself is also able to induce ER stress and activate mitochondrial dysfunction by increasing membrane permeabilisation, thereby further inducing apoptosis (Armstrong et al., 2007a).

1.10 4-HPR Pre-Clinical Animal Studies

The first pharmacokinetic study of 4-HPR was carried out in male rats in 1980. It was found that with an intravenous dose of 5mg/kg, or an oral dose of 10mg/kg, 4-HPR had a half-life of approximately 12h. When given orally, 4-HPR plasma concentration peaked after 4h (Swanson et al., 1980). Importantly, it was also shown that 4-HPR does not accumulate in the liver, as development of liver disease has been associated with the long-term use of retinol (Muenter et al., 1971). Similar results were obtained from a pharmacokinetic study carried out in female rats, and it was ascertained that the metabolism of 4-HPR was markedly different in rats compared to mice (Hultin et al., 1986). These studies also showed that oral dosing of 4-HPR resulted in an area under

the curve (AUC) plasma concentration approximately one third of the AUC observed with intravenous dosing, suggesting that the bioavailability of 4-HPR is relatively low.

Due to the low bioavailability of 4-HPR, there have been several investigations into ways to increase 4-HPR uptake in cells using *in vivo* murine models, including encapsulating 4-HPR in stabilised immunoliposomes. These are coupled to an antibody to G2, a disialoganglioside that is abundantly expressed in neuroectoderm-derived tumours. It was established that uptake of 4-HPR into neuroblastoma cells was 10- to 20-fold higher than if non-targeted liposomes were used (Raffaghello et al., 2003). In addition, there have been investigations into ways to improve 4-HPR delivery by the use of the Lym-X-Sorb matrix, as shown in Figure 1-21.

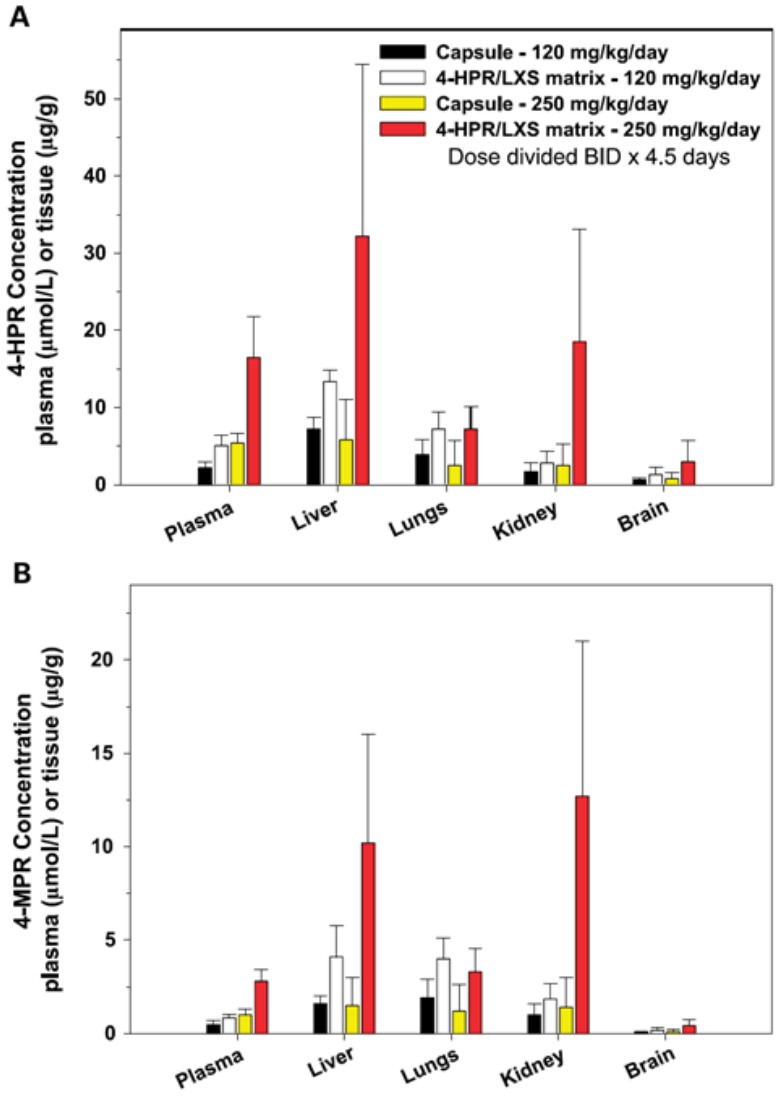

Figure 1-21. A) 4-HPR and B) 4-MPR levels obtained in mouse plasma and tissues using 4-HPR administered in 4-HPR/LYM-X-SORB (LXS) organized lipid matrix or as the contents of NCI corn oil capsules.

Modified from Maurer et al. *Clinical Cancer Research* 13(10): 3079-3086.

Lym-X-Sorb is a matrix of organized lipids and free fatty acids, designed to improve the solubility and bioavailability of drugs by forming chylomicron-like particles in the stomach, and therefore enhancing drug absorption via the lymphatic system. In a murine neuroblastoma model, significantly higher plasma levels of 4-HPR were achieved than when using the traditional corn oil capsule dosing (Maurer et al., 2007), although there was still significant metabolism to the inactive metabolite, 4-MPR.

1.11 4-HPR Clinical Pharmacology

There have been several clinical trials in adults investigating the pharmacokinetics of 4-HPR, both on a short-term chemotherapeutic schedule, as well as longer-term studies relating to its use as a chemopreventative agent.

A 1 year chemoprevention trial in breast cancer patients found that 4-HPR treatment caused an initial reduction in plasma retinol levels, that was reversible on cessation of treatment (Formelli et al., 1989). A subsequent phase III five year chemoprevention trial showed similar results, with stable drug plasma levels and a constant (reduced) level of retinol. 4-HPR concentrations were at the limit of detection within six months of cessation of treatment, and retinol concentrations returned to normal levels within one month (Formelli et al., 1993). Long-term 4-HPR administration was tolerated well, with the main side effects being decreased night-vision and dermatological disorders (Camerini et al., 2001).

More recently, there have been several studies on the pharmacokinetics of 4-HPR in children, particularly in neuroblastoma patients. The first such study, carried out in 2003, was designed to determine the MTD, toxicity and pharmacokinetics of 4-HPR in children with neuroblastoma (Garaventa et al., 2003). An MTD was not reached, as no significant side effects were observed at up to 4,000mg/m^2/day, and doses higher than this were not practical due to capsule numbers (up to 40 capsules per day for the highest doses used). The drug was administered daily for 28 days, with peak plasma concentrations being approximately 2-fold higher at the end of the cycle than at the start (as shown in Figure 1-22). This is very different to other retinoids; with ATRA and 9-cis RA, plasma levels decrease with chronic administration (Muindi et al., 1992, Smith et al., 1992). The plasma concentrations of 4-HPR observed were comparable to those

required for cell growth inhibition *in vitro*. 4-HPR half-life was also significantly longer at the end of the cycle than at the start (Garaventa et al., 2003).

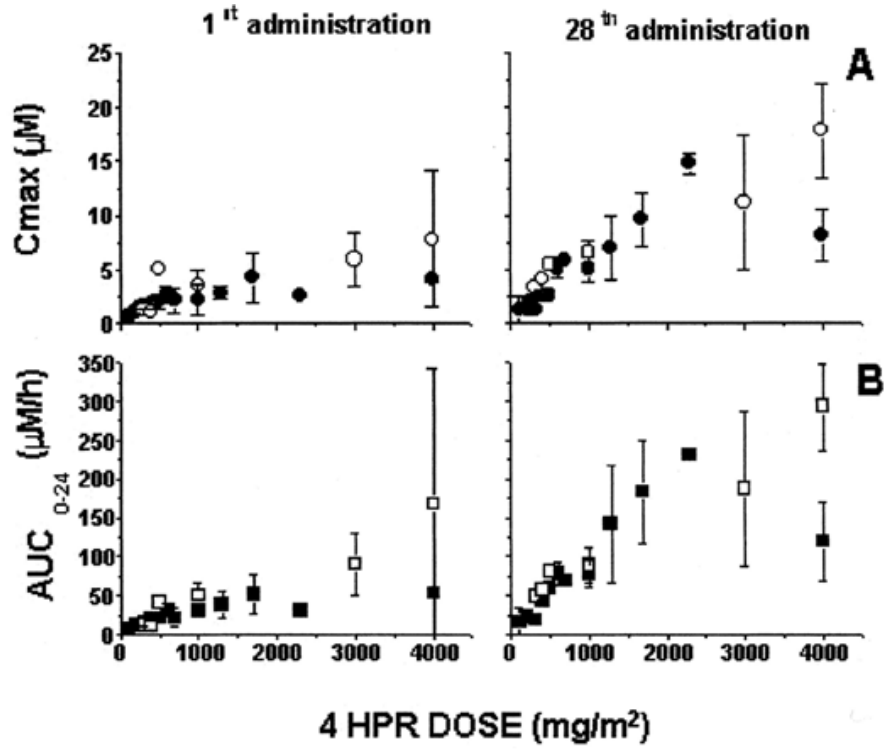

Figure 1-22. A) 4HPR peak concentrations (C_{max}) and B) $AUC_{0–24h}$ after the first and 28th administration of the first course of 4-HPR.

Patients with grade 2–3 toxicity (open symbols) and patients with grade 1 or without toxicity (closed symbols). Garaventa et al. *Clinical Cancer Research* 9: 2032 – 2039; 2003

A separate phase I trial of 4-HPR in children with high-risk solid tumours also found 4-HPR was well tolerated but found an increased incidence of toxicity, resulting in an MTD of 2,475mg/m^2/day. However this lower MTD still produced 4-HPR plasma concentrations equivalent to those found to be effective *in vitro* (approximately 5µM to 10µM), although there was considerable inter-patient variation, as shown in Figure 1-23 (Villablanca et al., 2006).

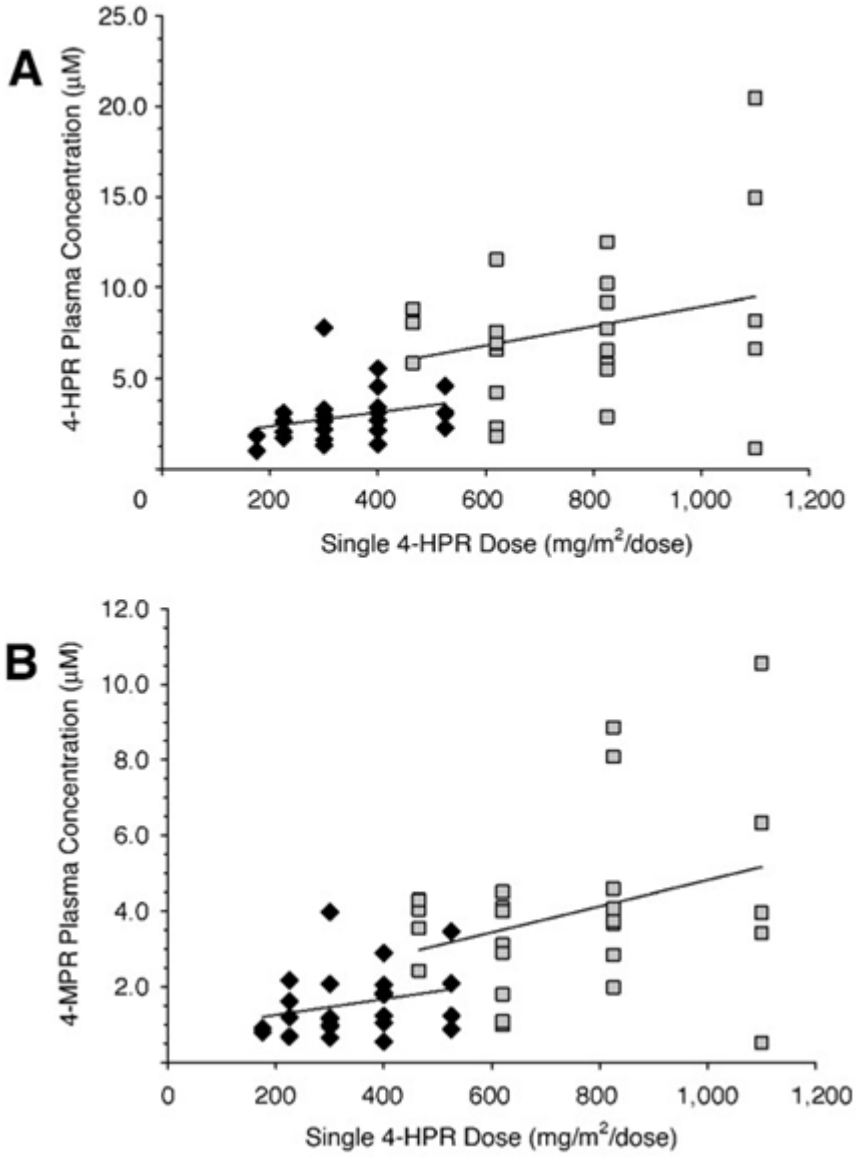

Figure 1-23. Graph of A) 4-HPR and B) 4-MPR steady-state trough plasma concentrations in a phase I paediatric trial.

Values were measured on day 7 of the first course of treatment with total daily dosage divided into two (diamonds) or three (squares) doses. Villablanca et al. *J Clin Oncol* 24(21): 3423-3430.

1.12 Summary and Aims

4-HPR is a promising chemotherapeutic compound for the treatment of several types of cancer, particularly the paediatric tumours neuroblastoma and Ewing's sarcoma. There has already been a significant increase in five year survival in neuroblastoma patients following the introduction of another retinoic acid analogue, 13-cis RA, in a minimal residual disease setting. 4-HPR is effective at reducing the growth of neuroblastoma and Ewing's sarcoma tumour cells both *in vitro* and *in vivo*, and has shown some effectiveness in clinical trials. 4-HPR has several potential benefits over treatment with ATRA or 13-cis RA, including:

- The ability to induce apoptosis rather than differentiation.
- Production of an active metabolite, 4'-oxo 4-HPR, that acts synergistically with 4-HPR itself.
- A mechanism of action involving both retinoid receptor-dependent and receptor-independent pathways.
- Auto-induction of metabolism does not result in a decrease in plasma concentrations during long-term treatment.
- Improved tolerability compared to other retinoids.

Despite these potential benefits, clinical trials in paediatric patients have also demonstrated limitations in the use of 4-HPR. The main issue has been an inability to achieve and maintain consistent 4-HPR plasma concentrations following oral administration. However another limitation preventing optimum efficacy of 4-HPR is the fact that it is significantly metabolised *in vivo*. Some of this metabolism is to an active metabolite, 4'-oxo 4-HPR, and is likely to be of benefit to 4-HPR efficacy rather than a hindrance, in contrast to the metabolism of other retinoid drugs. Conversely, 4-MPR, the other major metabolite of 4-HPR, is inactive. Factors affecting metabolism of 4-HPR may therefore have a significant impact on the overall efficacy of 4-HPR treatment. Elucidation of the enzymes of 4-HPR metabolism may become even more important if novel formulations of 4-HPR are successful at increasing 4-HPR bioavailability and improving compliance in dosing regimens.

The main aims of the work incorporated in this thesis were to:

- Characterise the oxidative metabolism of 4-HPR by CYP enzymes.
- Characterise the methylation of 4-HPR to the major metabolite 4-MPR.
- Characterise the glucuronidation of 4-HPR by UGT enzymes.
- Characterise the membrane-transport of 4-HPR using cell lines over-expressing common drug transporters.
- Assess the contribution of 4-HPR metabolism to its effectiveness in neuroblastoma and Ewing's sarcoma cell lines.

It is anticipated that the information gained in meeting these aims may be beneficial in guiding the treatment of patients with 4-HPR, particularly children with neuroblastoma or Ewing's sarcoma.

Chapter 2 4-HPR Microsomal Metabolism

2.1 Introduction

Unlike other retinoid derivatives currently in clinical use, such as ATRA and 13-cis RA, 4-HPR induces apoptosis as well as differentiation (Kitareewan et al., 1999) and is also better tolerated than other retinoid drugs (Garaventa et al., 2003). The metabolism of both ATRA and 13-cis RA has previously been characterized. The main CYPs responsible for the metabolism of both compounds are CYPs 2C8, 2C9, 3A4 and 3A5 (Marill et al., 2002, Marill et al., 2000, McSorley and Daly, 2000).

Whilst 4-HPR metabolism is similar to that of ATRA and 13-cis RA in many respects, 4-HPR produces an active metabolite, 4'-oxo 4-HPR, that is able to act synergistically with 4-HPR and is also active against some 4-HPR-resistant cell lines (Villani et al., 2006). 4-HPR is also metabolized to an inactive metabolite in the form of 4-methoxy 4-HPR (4-MPR) (Mehta et al., 1998), with significant metabolism to both of these metabolites observed in clinical trials (Villani et al., 2004, Villablanca et al., 2006, Formelli et al., 2008).

As one of the main limitations to the clinical development of orally administered 4-HPR is the achievement of effective and consistent plasma concentrations in patients (Maurer et al., 2007), metabolism of the parent drug is clearly an important issue. In addition, many CYPs are polymorphic and this impacts on drug metabolism (Bosch et al., 2006, Cholerton et al., 1992, Daly et al., 1998). Although CYP2C8 polymorphism plays a role in determining the effectiveness of several chemotherapeutic drugs (Bahadur et al., 2002, Dai et al., 2001, Daly et al., 2007), there were no differences reported in 13-cis RA metabolism by the major CYP2C8 isoforms (Rowbotham et al., 2010a).

The current study was designed to characterise the *in vitro* metabolism of 4-HPR in human liver microsomes (HLM), Supersomes over-expressing individual human CYPs and CYP2C8 variants expressed in *E. coli*. In addition, studies were performed to determine the effect of CYP2C8 polymorphisms on 4-HPR metabolism, where any effect on the formation of the active 4'-oxo metabolite may be important (Illingworth et al., 2011).

2.2 4-HPR Oxidative Metabolism

2.2.1 Materials and methods

2.2.2 Chemicals

CYP2C8 clones were kindly provided by Dr Frank J Gonzalez of the National Cancer Institute, Bethesda, USA. The human P450 reductase clone was kindly provided by Dr Thomas Friedberg of the University of Dundee. 4-HPR and 4-MPR were generously provided by the Drug Development Office, Cancer Research UK and 4'-oxo 4-HPR was provided by High Force Research Ltd. (Durham, UK). Anti-cytochrome P450 reductase, anti-cytochrome P450 2C8 and horseradish peroxidase-linked donkey anti-rabbit IgG antibodies were purchased from Millipore (Watford, UK). HLM and 2C8 Supersomes were supplied by BD Biosciences (Oxford, UK). Bactopeptone, bactotryptone, yeast extract and bactoagar were purchased from Difco Laboratories (East Molesey, UK). ECL Plus Western blotting detection reagents were obtained from G E Healthcare (Buckinghamshire). Tris-glycine gels and Magic Mark^{TM} molecular weight protein standard were supplied by Invitrogen (Paisley, UK). JM109 competent cells were purchased from Promega (Southampton, UK). Carbon monoxide was supplied by BOC gases (Guildford, UK). HPLC-grade solvents were from Fisher Scientific (Loughborough, UK). All other chemicals and reagents were purchased from Sigma-Aldrich (Poole, UK). SpectraMax® 250 Microplate Spectrophotometer System was from Molecular Devices Corporation (Reading, UK).

2.2.3 LC/MS analysis of 4-HPR and metabolites

Separation of 4-HPR and its metabolites was achieved using a Perkin Elmer LC (Beaconsfield, UK) system, consisting of a vacuum degasser, two series 200 pumps, a thermostatically controlled series 200 autosampler and a Waters 2487 UV absorbance detector. Reverse-phase chromatography was performed using a Luna 3µm C_{18} (50 x 2mm) column with a flow rate of 250µl/min and an injection volume of 10µl. Mobile phases consisted of (A) 40% acetonitrile / 60% (0.2%) acetic acid and (B) acetonitrile / 0.2% acetic acid. A linear gradient ran from 100% A at 0min to 100% B at 3min, at which it was maintained for 2.5min before returning to 100% A to re-equilibrate the column. An Applied Biosystems (Warrington, UK) API-2000 LC/MS/MS triple Q (quadrupole) mass spectrometer with electrospray ionisation source, controlled by

Analyst software, was operated in triple quadrupole negative mode for the detection of 4-HPR (multiple reaction monitoring (MRM) 392/283), 4'-OH 4-HPR (MRM 407/283) and 4'-oxo 4-HPR (MRM 406/283).

2.2.4 HPLC analysis of 4-HPR and metabolites

Separation of 4-HPR and its metabolites by HPLC analysis was achieved using a Waters 2690 Separations Module and 996 Photodiode array (PDA) detector (Waters Ltd., Elstree, UK), with Waters Millennium software for data acquisition. A Waters Symmetry C_{18} 3.5µm (4.6 x 150mm) column was used with mobile phases (A) 70% acetonitrile / 30% (0.2%) acetic acid and (B) acetonitrile / 0.2% acetic acid. A linear gradient ran at 1ml/min from 100% A at 0min to 100% B at 20min, returning to 100% A for 10min to re-equilibrate the column. A sample volume of 50µl was injected onto the column for analysis.

2.2.5 Incubation of 4-HPR with human liver microsomes (HLM), human intestinal microsomes (HIM) and CYPs

To determine optimum experimental conditions, HLM (0.5mg/ml) were incubated with varying concentrations of 4-HPR (0-100µM) for 3h, or 4-HPR (50µM) was incubated with varying concentrations of HLM (0-1.5mg/ml) for 3h. In addition, 4-HPR (50µM) was incubated with HLM (0.5mg/ml) for varying times (0-3h). Following optimisation of incubation parameters, HLM or a panel of CYP Supersomes (up to 1mg/ml protein) over-expressing individual human CYPs were incubated with 4-HPR (50µM) in phosphate buffer (100mM, pH 7.4), containing $MgCl_2$ (1mM) and NADPH (2mM) in a final volume of 200µl for 3h. CYPs 1A6, 2B6, 2E1, 3A4, 3A5, 2C8, 2C9 and 2C19 were used. The reaction was stopped by addition of acetonitrile (400µl) and samples were centrifuged at 10,000g for 5min to remove all protein. Supernatant was then retained for HPLC analysis. Experiments were carried out in parallel, with all comparative samples for a defined experiment being analysed within a single assay.

2.2.6 Inhibition of CYP metabolism

Known inhibitors or competitive substrates of CYP metabolism were added to HLM incubations. Compounds used were omeprazole (an inhibitor of CYP2C8 and 2C9) and ketoconazole (an inhibitor of CYP3A4), either alone or in combination. HLM (0.5mg/ml) were incubated with 4-HPR (50µM) and inhibitor (0-100µM) in phosphate buffer, (100mM, pH 7.4), containing $MgCl_2$ (1mM) and NADPH (2mM) in a final volume of 200µl for 3h. The reaction was stopped by addition of acetonitrile (400µl) and samples were centrifuged at 10,000g for 5min to remove all protein. Supernatant was then retained for HPLC analysis.

2.2.7 Determination of kinetic parameters for 4'-OH 4-HPR and 4'-oxo 4-HPR formation

Kinetic parameters for the formation of 4'-OH 4-HPR and 4'-oxo 4-HPR were determined following incubations of HLM or CYP 3A4, 3A5 or 2C8 Supersomes (0-1mg/ml protein) with 4-HPR (50µM), or 4-HPR (0-100µM) with 0.25mg/ml protein. Metabolism to 4'-OH 4-HPR and 4'-oxo 4-HPR by each CYP was then compared by ANOVA, with $P \leq 0.05$ used to determine significance. Calculations were performed with GraphPad Prism version 4.0 software (GraphPad Software Inc., San Diego, CA, USA). Due to the lack of an authentic standard for 4'-OH 4-HPR, V_{max} results were calculated in peak area units/min. Experiments were carried out in parallel, with all comparative samples for a defined experiment being analysed within a single assay.

2.2.8 Transformation of E. coli cells to express CYP2C8 variants

JM109 high competency *E. coli* cells were transfected with plasmids for CYP2C8 variants *1 (wild-type), *3, *3A, *3B, *4 or an empty plasmid (control), and co-transfected with cytochrome P450 reductase in order to assess the impact of CYP2C8 genotype on 4-HPR metabolism. CYP2C8 and P450 reductase expression plasmids were constructed by Dr. S Rowbotham (Rowbotham et al., 2010a).

2.2.8.1 Transformation of E. coli cells

JM109 high competency cells were transformed by mixing competent cells (100µl) with CYP2C8 plasmid DNA (50ng) (isoforms *1, *3, *3A, *3B, *4 or an empty plasmid) and P450 reductase plasmid DNA (50ng). Cells were kept on ice for 10min before being heat shocked at 42°C for 45-50s and returned to ice for 2min prior to addition of ice-cold SOC medium (900µl) (20g/L Bacto-tryptone, 5g/L yeast extract, 0.5g/L NaCl, 2.5mM KCl). Samples were incubated for 1h at 37°C in a shaking incubator (200rpm) and then diluted 1:10 and 1:100 in SOC medium. A 100µl aliquot of each suspension was plated on LB agar plates (10g/l NaCl, 10g/l bactopeptone, 5g/l yeast extract and 15g/l bactoagar), in addition to ampicillin (50µg/ml) and chloramphenicol (25µg/ml). Plates were incubated overnight at 37°C. Individual colonies were picked and grown in LB medium (5ml) containing ampicillin (50µg/ml) and chloramphenicol (25µg/ml) overnight at 37ºC with shaking (200rpm). The cultures were then diluted 1:100 in TB medium (100ml) (12g/l bactotryptone, 24g/l yeast extract, 2g/l bactopeptone, 0.4% (v/v) glycerol, 17mM KH_2PO_4, 72mM K_2HPO_4) with ampicillin (50µg/ml) and chloramphenicol (25µg/ml). These were incubated at 37°C with shaking (200rpm) until an optical density of 0.7-1 at 600nm was reached. Isopropyl β-D-1-thiogalactopyranoside (IPTG) (1mM) and δ-aminolevulinic acid (δ-ALA) (0.5mM) were added and expression allowed to proceed overnight (for 19-22h). Cultures were chilled on ice for 10min and centrifuged at 2,800g for 20min at 4ºC. Pellets were resuspended in ice-cold 2 x TSE buffer (5ml) (100mM Tris-acetate, 500mM sucrose, 0.5mM EDTA, pH 7.6) and diluted with ice-cold water (5ml). Lysozyme (0.25mg/ml) was added and stirred gently at 4ºC for 60min. Spheroplast pellets were generated by centrifugation at 2,800g at 4°C for 25min. Spheroplasts were then resuspended in ice-cold spheroplast resuspension buffer (4ml) (100mM potassium phosphate, 6mM magnesium acetate, 20% (v/v) glycerol, 0.1mM dithiothreitol; pH 7.6). Aprotinin (1µg/ml), leupeptin (1µg/ml) and PMSF (1mM) were added and spheroplasts were sonicated on ice (3 x 30s) and centrifuged at 12,000g for 12min at 4°C. The resulting supernatant was transferred to ultracentrifuge tubes and centrifuged at 180,000g for 60min at 4°C. The membrane pellet was resuspended in 1 x TSE buffer (1ml).

2.2.8.2 Protein analysis

Protein content was measured using the Bradford assay. A 10µl aliquot of membrane fraction was diluted 1:10 with dH_20 and 10µl of the diluted fraction was then added to Bradford reagent (200µl) in a 96 well plate, in quadruplicate. Protein concentration was determined from a standard curve of bovine serum albumin (0, 0.2, 0.4, 0.6, 0.8, 1 and 1.2mg/ml protein) against A_{595} using SOFTmax PRO analysis software version 3.0.

2.2.8.3 Western Blot analysis

Co-expression of CYP2C8 and P450 reductase was confirmed by Western Blot analysis. CYP2C8 variant membrane fractions or CYP2C8, 3A4 and reductase-only Supersomes were diluted to 1mg/ml in dH_2O. A 0.5µl aliquot was added to Laemelli sample buffer (19.5µl) (0.25M Tris-HCl, pH 8.0, 8% SDS, 40% glycerol, 0.008% bromophenol blue and 10% β-mercaptoethanol) and heated at 95ºC for 5min. An aliquot (10µl) was then loaded onto a 4-20% tris-glycine gel with 1x running buffer (25mM Tris-Base, 0.19M glycine, 0.1% (w/v) SDS, pH 8.5), as well as Magic Mark™ molecular weight protein standard (4µl). Gels were run in an Invitrogen XCell *SureLock*™ Novex Mini-Cell using a Bio-Rad PowerPac 300 (Hemel Hempstead, UK) at a constant 130V for approximately 1h until the dye reached the bottom of the gel. Separated proteins were then transferred to a polyvinylidine difluoride (PVDF) membrane. The membrane was soaked in methanol for 5min, rinsed several times in dH_2O and equilibrated in transfer buffer (10mM CAPS, 10% (v/v) methanol) for 10min. Transfer to the membrane was carried out in a Bio-Rad Mini-PROTEAN 2-D Electrophoresis Cell, using a Bio-Rad PowerPac 300 at a constant 100V for 1.5h. The membrane was then incubated in blocking buffer (50mM Tris-Base, 140mM NaCl, 0.1% (v/v) Tween-20, 5% (w/v) non-fat milk, pH 7.6) for 1h at room temperature to prevent antibody binding to non-specific binding sites, followed by 4 x 10min washes in TBS-Tween (50mM Tris-Base, 140mM NaCl, 0.1% (v/v) Tween-20, pH 7.6). The primary antibodies (anti-cytochrome P450 enzyme CYP2C8/9/10 and anti-cytochrome P450 reductase) were diluted 1:50,000 in blocking buffer and incubated with the membrane at 4ºC overnight. This was followed by a further 4 x 10min washes in TBS-Tween. The secondary antibody (donkey anti-rabbit IgG, HRP conjugate) was then diluted 1:5,000 in blocking buffer and incubated with the membrane for 1h at room

temperature and again followed by a final 4 x 10min washes in TBS-Tween. Bound antibodies were detected by enhanced chemiluminescence (ECL).

2.2.8.4 P450 CO difference spectral assay

Cytochrome P450 content was measured using Fe^{2+} -CO vs. Fe^{2+} difference spectra. P450 buffer (1.875ml) (100mM Tris-HCL, 10mM CHAPS, 20% glycerol, 1mM EDTA, pH 7.4) was added to membrane fraction (125µl) and fresh sodium dithionite powder (10mg). An aliquot (300µl) was removed into one well of a 96-well plate (reference well) and CO (1 bubble/sec for 60s) was bubbled through the remaining solution. A second aliquot (300µl) was then transferred into a second well of the 96-well plate (sample well). Absorbance at 400-500nm was measured on a SpectraMax® 250 Microplate Spectrophotometer. The absorbance of the reference well was subtracted from the absorbance of the sample well to generate a P450 absorbance spectrum.

2.2.8.5 Cytochrome C reductase assay

P450 reductase content was measured using the cytochrome C reductase assay. Reaction buffer (296µl) (0.3M potassium phosphate, 50µM cytochrome C, pH 7.7) was added to membrane fraction (1µl) in 2 wells of a 96 well plate (one sample well and one reference well). NADPH (3µl) was added to the sample well and H_2O (3µl) was added to the reference well. The change in absorbance at 550nm was measured for 15min on a SpectraMax® 250 Microplate Spectrophotometer.

2.2.9 Determination of kinetic parameters for 4'-OH 4-HPR and 4'-oxo 4-HPR formation by CYP2C8 variants

Kinetic parameters for the formation of 4'-OH 4-HPR and 4'-oxo 4-HPR were determined following incubations of CYP2C8 isoform membrane fractions (0-1mg/ml protein) with 4-HPR (50µM), or 4-HPR (0-100µM) with 0.25mg/ml protein. Due to the lack of an authentic standard for 4'-OH 4-HPR, V_{max} results are given in peak area units/min. One-way ANOVA followed by Bonferroni's post test was used to compare K_m and V_{max} data, with $P \leq 0.05$ used to determine significance. All calculations were performed with GraphPad Prism version 4.0 software (GraphPad Software Inc., San

Diego, CA, USA). Due to the lack of an authentic standard for 4'-OH 4-HPR, V_{max} results were calculated in peak area units/min. Experiments were carried out in parallel, with all comparative samples for a defined experiment being analysed within a single assay.

2.3 4-HPR Methyltransferase Metabolism

2.3.1 Materials and methods

2.3.2 Incubation of 4-HPR with HLM and S-adenosyl methionine (SAM)

Initial incubation of 4-HPR with HLM did not produce any 4-MPR metabolite. A methylating co-factor, S-adenosyl methionine (SAM) was therefore added to the incubations. To determine the optimum concentration of co-factor, SAM (0-1mM) was incubated with 4-HPR (50µM) and HLM (0.5mg/ml) for 3h, in a final volume of 100µl. The reaction was stopped by addition of acetonitrile (200µl) and samples were centrifuged at 10,000g for 5min to remove all protein. Supernatant was then retained for HPLC analysis.

2.3.3 Determination of kinetic parameters for 4-MPR formation

Kinetic parameters for the formation of 4-MPR were determined following incubations of HLM (0-1mg/ml protein) with 4-HPR (50µM) and SAM (0.2mM), or 4-HPR (0-100µM) with HLM (0.25mg/ml) and SAM (0.2mM). Calculations were performed with GraphPad Prism version 4.0 software (GraphPad Software Inc., San Diego, CA, USA). Due to the lack of an authentic standard for 4'-OH 4-HPR, V_{max} results for all kinetic parameters were calculated in peak area units/min.

2.3.4 Inhibition of methyltransferases

Known inhibitors or competitive substrates of several methylating enzymes were added to HLM incubations. Compounds used were 4-nitrocatechol, nialamide, pargyline (inhibitors of catechol-O-methyltransferases (COMT)), acetaminophen (inhibitor of phenol methyltransferase (PMT)) and imidazole (competitive substrate for amino-N-methyltransferase). HLM (0.5mg/ml) were incubated with 4-HPR (50µM), SAM (0.2mM) and inhibitor (0-5mM) in phosphate buffer (100mM, pH 7.4), containing

$MgCl_2$ (1mM) and NADPH (2mM) in a final volume of 100µl for 3h. The reaction was stopped by addition of acetonitrile (200µl) and samples were centrifuged at 10,000g for 5min to remove all protein. Supernatant was then retained for HPLC analysis.

2.4 Results – 4-HPR Oxidative Metabolism

2.4.1 Analytical assays

Following incubation of 4-HPR (20μM) with HLM (0.25mg/ml), the metabolites produced were separated by LC/MS/MS and HPLC analysis, as shown in Figure 2-1. Peaks were identified for 4-HPR, its methylated metabolite 4-MPR and its two main polar metabolites, 4'OH-4-HPR and 4'-oxo 4-HPR. 4-HPR, 4-MPR and 4'-oxo 4-HPR were identified by co-elution with authentic standards and by their MS/MS profiles. 4'-OH 4-HPR was identified by its MS/MS profile alone, as no authentic standard was available. Retention times (RT) for the HPLC assay were 3.5min, 3.9min and 13.5min for 4'-OH 4-HPR, 4'-oxo 4-HPR and 4-HPR respectively. Additional peaks seen at similar retention times to 4-HPR were isomers of 4-HPR. LC/MS/MS analysis identified 4-HPR with an MRM of 392/283 (RT 6.4min), 4'-OH 4-HPR with an MRM of 407/298 (RT 4.3min), 4'-oxo 4-HPR with an MRM of 406/297 (RT 5.1min) and 4-MPR with an MRM of 406/283 (RT 8.4min). Peak areas for 4'-oxo 4-HPR, 4'-OH 4-HPR and 4-MPR were approximately 5%, 10% and 5% respectively of the peak area for 4-HPR.

2.4.2 Incubation of 4-HPR with HLM

In order to determine the time course of metabolite formation, 4-HPR (50μM) was incubated with HLM (0.5mg/ml) for up to 3h, with metabolite formation measured every 10min. As shown in Figure 2-2, initially only 4'-OH 4-HPR was formed, with production of the metabolite increasing for approximately 1h before concentrations plateau and remain stable. Formation of 4'-oxo 4-HPR increased rapidly after an initial 10min lag, and continued to increase until approximately 3h. All future incubations were therefore carried out for 3h.

Incubation of increasing concentrations of HLM (0-1.5mg/ml) with 4-HPR (50μM) for 3h, as shown in Figure 2-3, demonstrated that production of 4'-oxo 4-HPR and 4'-OH 4-HPR is linear up to 0.5mg/ml HLM. This concentration of protein was used for all future incubations.

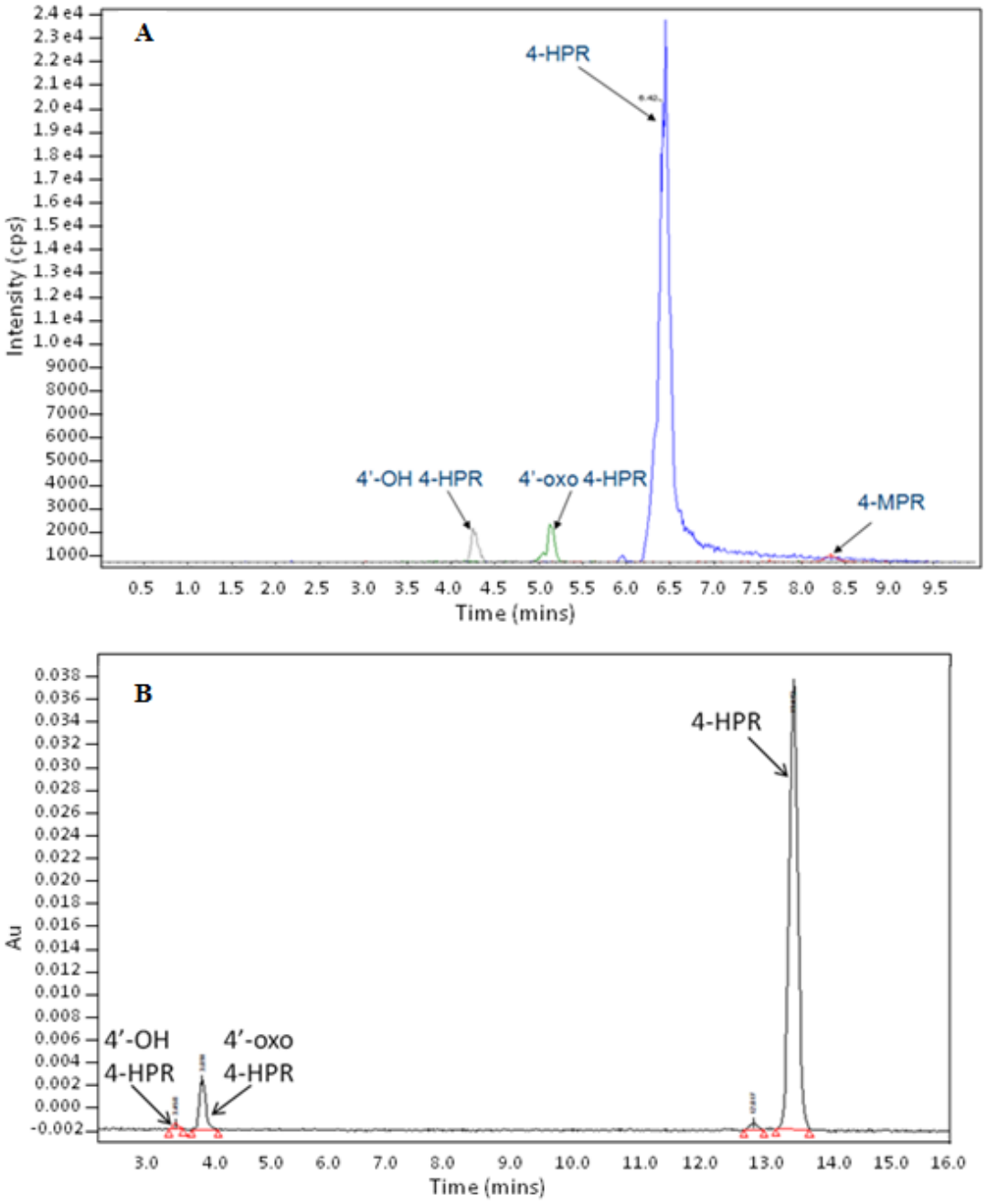

Figure 2-1. Representative chromatograms showing separation of 4-HPR and metabolites by A) LC/MS/MS and B) reversed phase HPLC.

Metabolites were generated following a 3h incubation of 4-HPR (50µM) with HLM (0.5mg/ml).

Incubation of increasing concentrations of 4-HPR (0-100µM) with HLM (0.5mg/ml) for 3h, as shown in Figure 2-4, demonstrated that production of 4'-oxo 4-HPR is dependent on 4-HPR concentration up to 50µM HPR. Formation of 4'-OH 4-HPR was dependent on 4-HPR concentration up to 15µM 4-HPR. This is likely to be due to conversion of 4'-OH 4-HPR to 4'-oxo 4-HPR and therefore the highest concentration at which

production of 4'-oxo 4-HPR was still dependent on 4-HPR concentration was used for all future incubations (50µM).

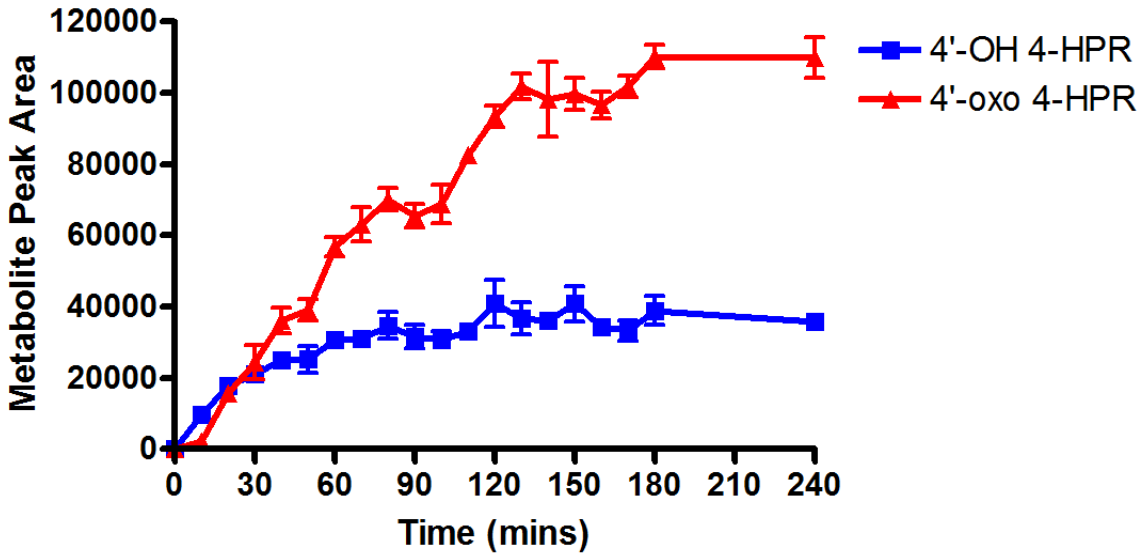

Figure 2-2. Formation of 4'-OH 4-HPR and 4'-oxo 4-HPR by HLM over time.
Metabolites were generated by incubation of 4-HPR (50µM) with HLM (0.5mg/ml) for up to 4h. Metabolite formation was determined by HPLC analysis. Results are the mean of 3 independent determinations (error bars are standard deviation).

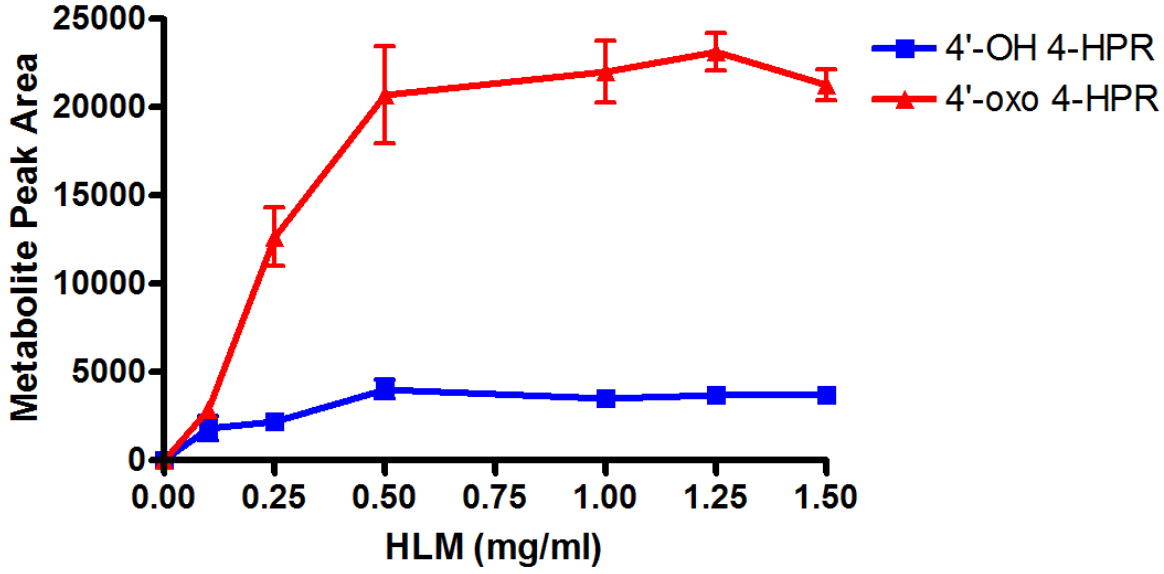

Figure 2-3. Formation of 4'-OH 4-HPR and 4'-oxo 4-HPR with increasing HLM.
Metabolites were generated by incubation of 4-HPR (50µM) with HLM (0-1.5mg/ml) for 3h. Metabolite formation was determined by HPLC analysis. Results are the mean of 3 independent determinations (error bars are standard deviation).

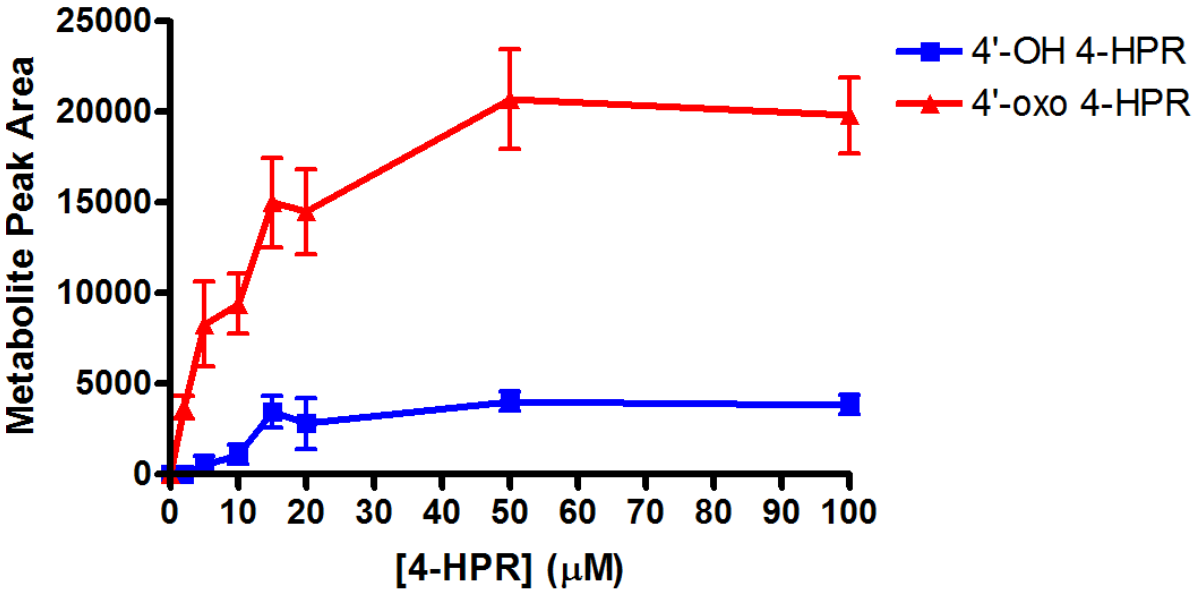

Figure 2-4. Formation of 4'-OH 4-HPR and 4'-oxo 4-HPR with increasing 4-HPR.
Metabolites were generated by incubation of 4-HPR (0-100μM) with HLM (0.5mg/ml) for 3h. Metabolite formation was determined by HPLC analysis. Results are the mean of 3 independent determinations (error bars are standard deviation).

2.4.3 Identification and characterization of 4-HPR metabolism by individual CYP isoforms

4-HPR (50μM) was incubated with a panel of Supersomes over-expressing individual human CYPs, to identify the enzymes responsible for the oxidation and hydroxylation of 4-HPR. While all CYPs tested were able to generate 4'-OH 4-HPR, as shown in Figure 2-5, CYPs 3A4, 3A5 and 2C8 clearly produced the highest levels. Only CYPs 3A4 and 2C8 were able to generate 4'-oxo 4-HPR, the known active metabolite of 4-HPR.

4-HPR (0-100μM) was incubated with HLM or Supersomes over-expressing individual human CYPs (0.5mg/ml) for 3h, to determine enzyme kinetic parameters. CYPs 3A4, 3A5 and 2C8 were used, as these had been shown to metabolise 4-HPR to 4'-OH 4-HPR and 4'-oxo 4-HPR.

Metabolite production was related to 4-HPR concentration as shown in Figure 2-6, with kinetic parameters for all three CYPs and HLM provided in Table 2-1. HLM were the

most effective at metabolising 4-HPR to the known active metabolite 4'-oxo 4-HPR, with a V_{max} of 131 peak area units/min, compared to V_{max} values of 30 and 25 peak area units/min for of the individual CYPs 2C8 and 3A4 respectively. In terms of 4'-OH 4-HPR production, HLM exhibited a V_{max} of 28 peak area units/min, compared to V_{max} values of 115-282 peak area units/min for Supersomes expressing individual CYPs.

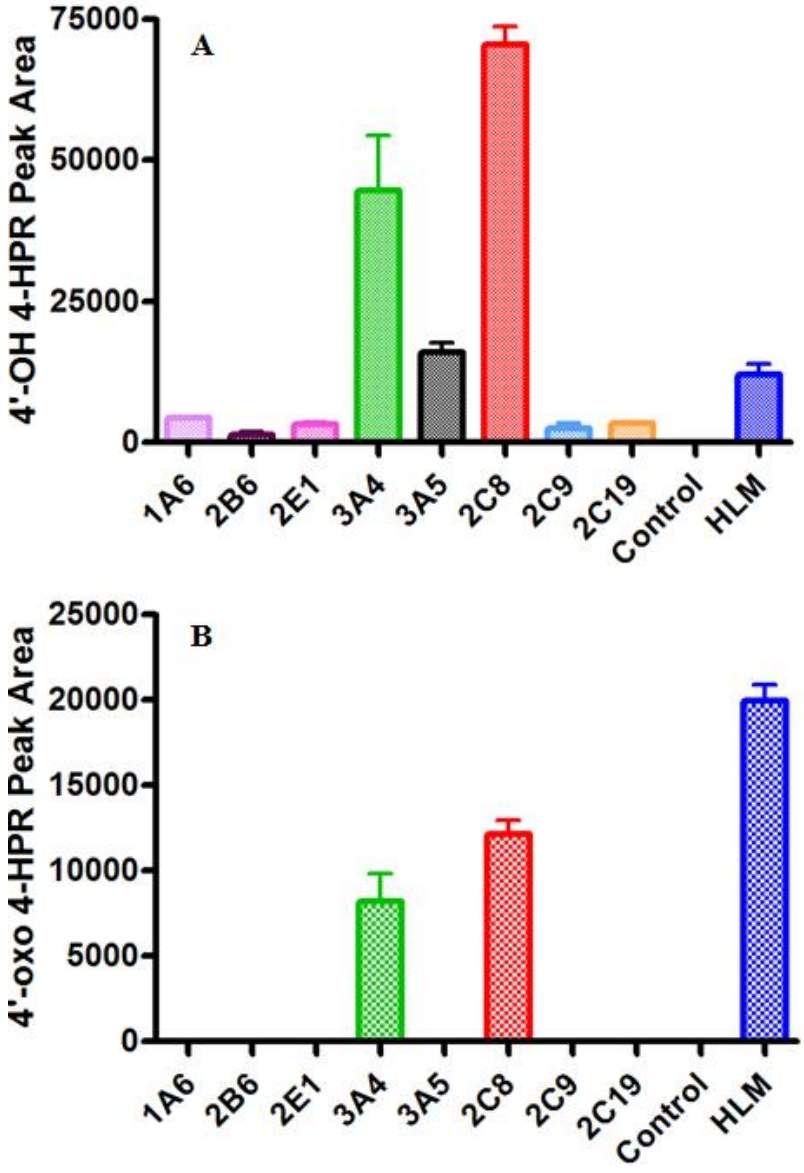

Figure 2-5. Formation of A) 4'-OH 4-HPR and B) 4'-oxo 4-HPR metabolites of 4-HPR by a panel of Supersomes over-expressing individual human CYPs.

Metabolite formation was determined by HPLC analysis. Control Supersomes were from *E. coli* cells transfected with an empty vector. Metabolites were generated by incubation of 4-HPR (20µM) with Supersomes over-expressing individual CYPs (0.5mg/ml) for 3h. Results are the mean of 3 independent determinations (error bars are standard deviation).

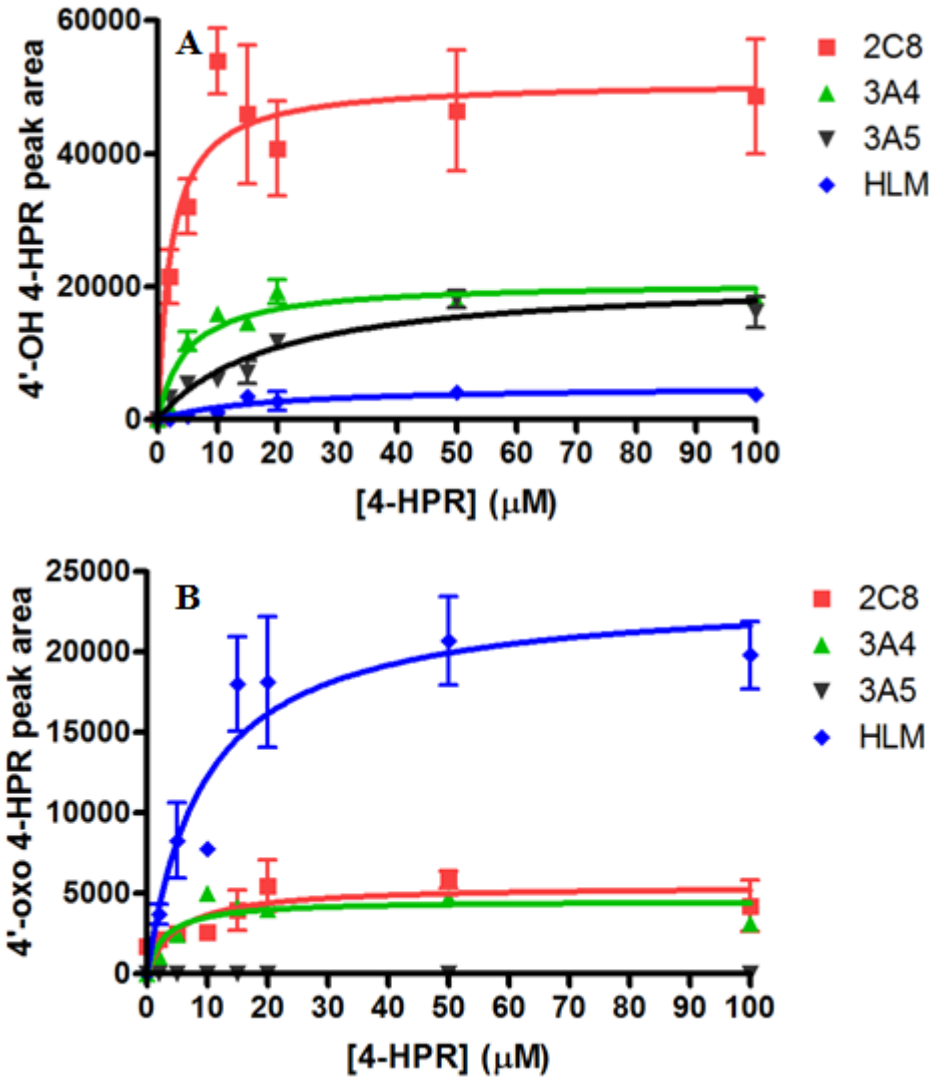

Figure 2-6. Effect of increasing 4-HPR concentration on the formation of A) 4'-OH 4-HPR and B) 4'-oxo 4-HPR by a panel of Supersomes over-expressing individual human CYPs. Metabolite formation was determined by HPLC analysis. Control Supersomes were from *E. coli* cells transfected with an empty vector. Metabolites were generated by incubation of 4-HPR (0-100μM) with individual Supersomes (0.5mg/ml) for 3h. Results are the mean of 3 independent determinations (error bars are standard deviation).

Results expressed as values normalized for CYP content are also shown for the individual human CYPs in Table 2-1. Significant differences were observed in V_{max} values between CYP2C8 and CYP3A4 for both 4'-oxo and 4'-OH metabolite formation ($p=0.0368$ and $p=0.0004$ respectively) by one way ANOVA followed by Bonferroni's post test. Significant differences in Km values were also observed for 4'-OH 4-HPR

($p<0.0001$), but not for 4'-oxo 4-HPR ($p=0.0598$). Due to the level of metabolism seen with CYP2C8, and as 2C8 is known to be polymorphic, the effect of CYP2C8 variants on metabolism was subsequently investigated.

	4'-oxo 4-HPR			4'-OH 4-HPR		
	K_m (μM)	V_{max}		K_m (μM)	V_{max}	
		(peak area units/min)	(peak area units/min/pmol CYP		(peak area units/min)	(peak area units/min/pmol CYP
HLM	9 ± 3	131 ± 14	N/A	18 ± 9	28 ± 6	N/A
3A4	3 ± 1	25 ± 2	0.5 ± 0.1	5 ± 1	115 ± 7	2 ± 0.1
3A5	N/D	N/D	N/D	19 ± 5	118 ± 6	2 ± 0.1
2C8	5 ± 3	30 ± 5	0.2 ± 0.1	2 ± 1	282 ± 24	1 ± 0.1

Table 2-1. Kinetic parameters for the formation of 4'-OH 4-HPR and 4'-oxo 4-HPR by HLM and a panel of Supersomes over-expressing individual human CYPs.

The major CYPs found to metabolise 4-HPR (CYPs 3A4, 3A5 and 2C8) were incubated with 4-HPR (0-100μM) for 3h. Metabolite formation was determined by HPLC analysis. Results are expressed as mean ± SD from n≥3 experiments. N/A – no data available; N/D – not detected.

2.4.4 Transformation of E. coli cells to express CYP2C8 variants

E. coli cells were transfected with plasmids for CYP2C8 variants *1 (wild-type), *3, *3A, *3B, *4 or an empty plasmid (control), and co-transfected with cytochrome P450 reductase. Co-transfection of CYP2C8 and P450 reductase was confirmed by Western Blot, as shown in Figure 2-7. Bands were clearly visible for CYP2C8 and P450 reductase in all CYP2C8 variant samples, at the same molecular weight as those seen in CYP2C8 Supersomes (56kDa and 78kDa respectively). There appeared to be some cross-reactivity with other CYPs, as a band also appeared for CYP3A4 (lane 2), however this band had a distinctively different appearance to the CYP 2C8 band. There was no CYP band visible in the samples only expressing P450 reductase (lanes 3 and 4).

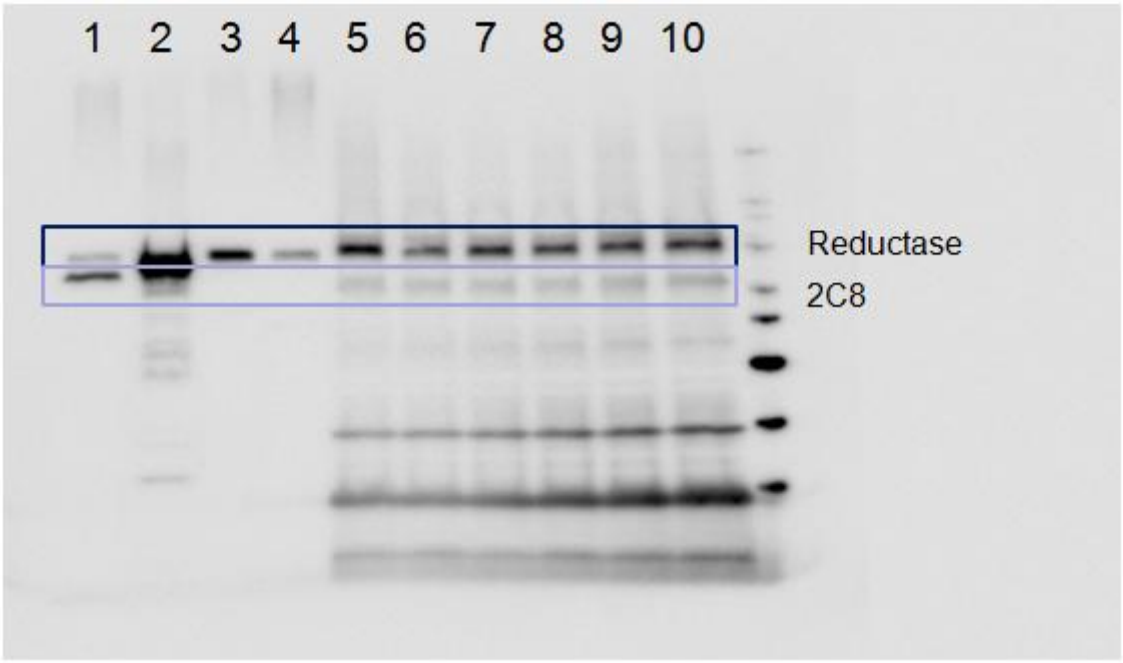

Figure 2-7. Western Blot for CYP Supersomes and *E. coli* membrane fractions transfected to over-express CYP2C8 variants and P450 reductase.

Lane 1= 2C8 Supersomes; 2= 3A4 Supersomes, 3= Reductase only supersome; 4= Reductase only variant; 5=*1, 6=*3; 7=*3A; 8=*3B; 9=*4; 10=*3, *3A *3B combined. Blots were probed with anti-cytochrome P450 enzyme CYP2C8/9/10 and anti-cytochrome P450 reductase diluted 1:50,000 in blocking buffer and incubated with the membrane at 4ºC overnight, followed by secondary antibody (donkey anti-rabbit IgG, HRP conjugate) diluted 1:5,000 in blocking buffer and incubated with the membrane for 1h at room temperature. Typical blot from 3 independent preparations of membrane fractions shown.

Following confirmation of the co-transfection of P450 reductase and CYP2C8, expression was quantified using the Fe^{2+} -CO vs. Fe^{2+} difference spectra (as shown in Figure 2-8) and the cytochrome C reductase assay (as shown in Figure 2-9). The Fe^{2+} -CO vs. Fe^{2+} difference spectra show a clear peak at 450nm, representing absorbance by cytochrome P450, as well as a peak at approximately 420nm due to the presence of denatured P450. There was no peak at 450nm for the reductase only control.

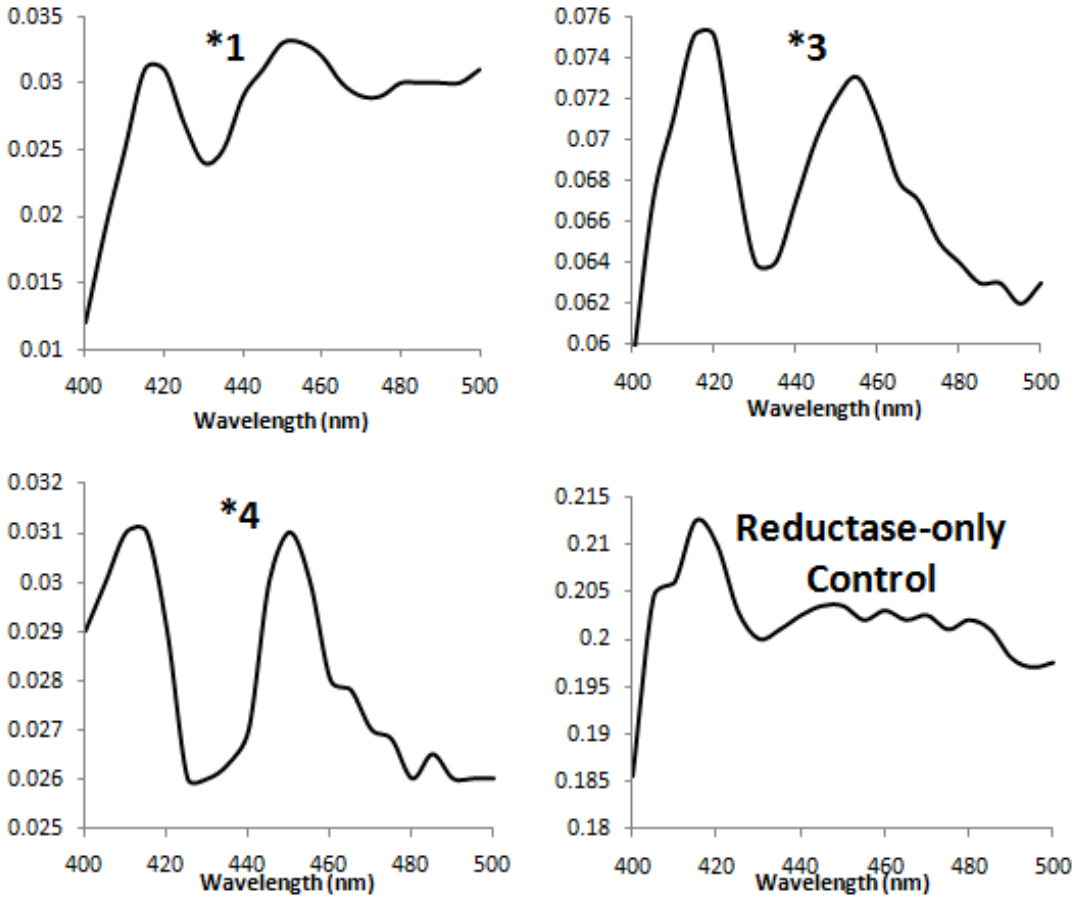

Figure 2-8. Graphs showing Fe^{2+} -CO vs. Fe^{2+} difference spectra for *E. coli* membrane fractions transfected to over-express CYP2C8 variants *1, *3 or *4, as compared to reductase-only control.

Cytochrome P450 content was measured using Fe^{2+} -CO vs. Fe^{2+} difference spectra. P450 buffer was added to membrane fraction (125µl) and fresh sodium dithionite powder (10mg). Absorbance at 400-500nm was subtracted from absorbance of the sample in the presence of CO (1 bubble/s for 60s). Typical spectra from 3 independent preparations of membrane fractions shown.

The cytochrome C reductase assay (Figure 2-9) shows an increase in absorbance at 550nm due to the reduction of cytochrome C in the presence of transfected membrane fractions. No reduction of cytochrome C was seen in control samples (without NADPH).

CYP content of *E. coli* transfectants varied from 175 - 295pmol/mg of protein, and was comparable to CYP2C8 Supersomes, that contained 293pmol of CYP/mg protein. Cytochrome P450 reductase concentrations ranged from 180 – 213nmol/mg/min, again comparable to CYP2C8 Supersomes (176nmol/mg/min), as shown in Table 2-2.

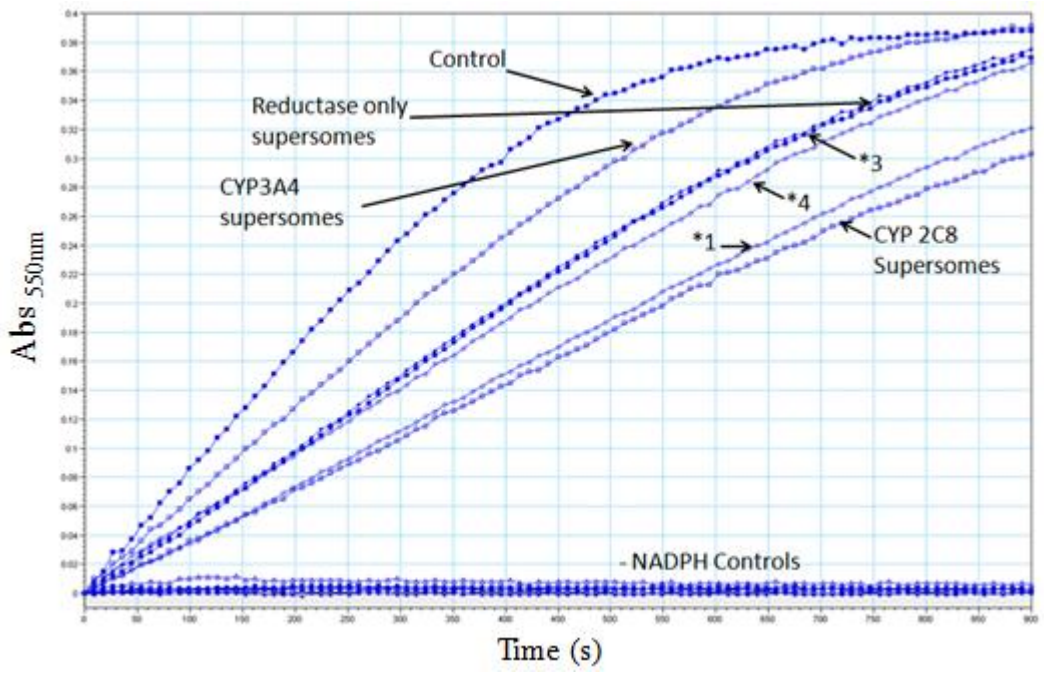

Figure 2-9. Graph showing P450 reductase activity for Supersomes and *E. coli* membrane fractions transfected to over-express CYP2C8 variants.

Reaction buffer (296µl) was added to membrane fraction (1µl), with NADPH (3µl) added to the sample well and H_2O (3µl) added to the reference well. The change in absorbance at 550nm was measured for 15min. Typical spectra from 3 preparations of membrane fractions shown.

2.4.5 Kinetic parameters for 4'-OH 4-HPR and 4'-oxo 4-HPR formation by CYP2C8 variants

4-HPR (0-100µM) was incubated with each CYP2C8 variant to determine enzymatic kinetic parameters. Metabolite production with increasing 4-HPR concentration is shown in Figure 2-10, with kinetic parameters provided in Table 2-3. Differences in metabolism to 4'-OH 4-HPR and 4'-oxo 4-HPR were observed with the 2C8 variants, most notably with CYP2C8*4. In terms of 4'-OH 4-HPR production, although there were no significant differences in K_m values for *1, *3 and *4 (6, 9 and 4µM respectively), V_{max} values for *1 and *3 (both 0.2 peak area units/min/pmol CYP) were significantly different from *4, that had a V_{max} of 0.1 peak area units/min/pmol CYP (P= 0.0025). V_{max}/K_m ratios for 4'-OH 4-HPR were 0.028 and 0.026 for *3 and *4, respectively, compared to 0.036 for *1. Formation of 4'-oxo 4-HPR by CYP2C8*1 was characterised by a V_{max} of 0.04 peak area units/min/pmol CYP and a K_m of 19µM. These results were comparable to V_{max} and K_m values of 0.05 and 19µM, respectively,

for CYP2C8*3. For CYP2C8*4, the V_{max} was 0.1 peak area units/min/pmol CYP and the K_m was 60µM, that was significantly different from CYP2C8 *1 (p=0.004).

	P450 (pmol/mg protein)	**P450 Reductase (nm/mg/min)**
2C8*1	295 ± 14	180 ± 15
2C8*3	192 ± 12	192 ± 22
2C8*4	175 ± 5	189 ± 12
Control	0	213 ± 12
2C8 Supersomes	293 ± 6	176± 10
3A4 Supersomes	284	203
Reductase-only Supersomes	0	192

Table 2-2. P450 content and P450 reductase activity in Supersomes and *E. coli* membrane fractions transfected to over-express CYP2C8 variants.

Cytochrome P450 content was measured using Fe^{2+} -CO vs. Fe^{2+} difference spectra. P450 buffer was added to membrane fraction (125µl) and fresh sodium dithionite powder (10mg). Absorbance at 400-500nm was subtracted from absorbance of the sample in the presence of CO (1 bubble/sec for 60s). P450 reductase activity was measured using the cytochrome C assay. Reaction buffer (296µl) was added to membrane fraction (1µl), with NADPH (3µl) added to the sample well and H_2O (3µl) added to the reference well. The change in absorbance at 550nm was measured for 15min. Results are mean ± SD from 3 independent preparations of membrane fractions.

	4'-oxo 4-HPR			4'-OH 4-HPR		
	K_m (µM)	**V_{max} (peak area units/min)/pmol CYP**	**V_{max} / K_m**	**K_m (µM)**	**V_{max} (peak area units/min)/pmol CYP**	**V_{max} / K_m**
2C8 *1	19 ± 6	0.04 ± 0.01	0.002	6 ± 2	0.2 ± 0.1	0.036
2C8 *3	19 ± 8	0.05 ± 0.01	0.003	9 ± 3	0.2 ± 0.1	0.028
2C8 *4	60 ± 23	0.13 ± 0.01	0.002	4 ± 2	0.1 ± 0.1	0.026

Table 2-3. Kinetic parameters for the formation of 4'-OH 4-HPR and 4'-oxo 4-HPR by CYP2C8 variants.

Individual CYP2C8 variants co-expressing P450 reductase, were incubated with 4-HPR (0-100µM) for 3h. Metabolite formation was determined by HPLC analysis. Results are expressed as mean ± SD from n≥3 experiments. V_{max} for 4'-oxo 4-HPR was significantly different for *1 and *4 (P=0.0037); K_m for 4'-oxo 4-HPR was significantly different for *1 and *4 (P=0.0035); V_{max} for 4'-OH 4-HPR was significantly different for *1 and *4.

2.4.6 Inhibition of CYP metabolism

4-HPR (50µM) was incubated with HLM (0.5mg/ml) and CYP inhibitors omeprazole (inhibitor of CYP2C8 and 2C9) and ketoconazole (inhibitor of CYP3A4), either alone or in combination (0-100µM), as shown in Figure 2-11. Ketoconazole (100µM) considerably inhibited the production of both metabolites, with 75% inhibition of 4'-OH 4-HPR and 85% inhibition of 4'-oxo 4-HPR. Omeprazole alone at a concentration of 100µM had very little effect on the production of either metabolite, but in combination with 100µM ketoconazole resulted in complete inhibition of the production of 4'-OH 4-HPR. The addition of omeprazole did not have any effect on the inhibition of 4'-oxo 4-HPR production seen with ketoconazole.

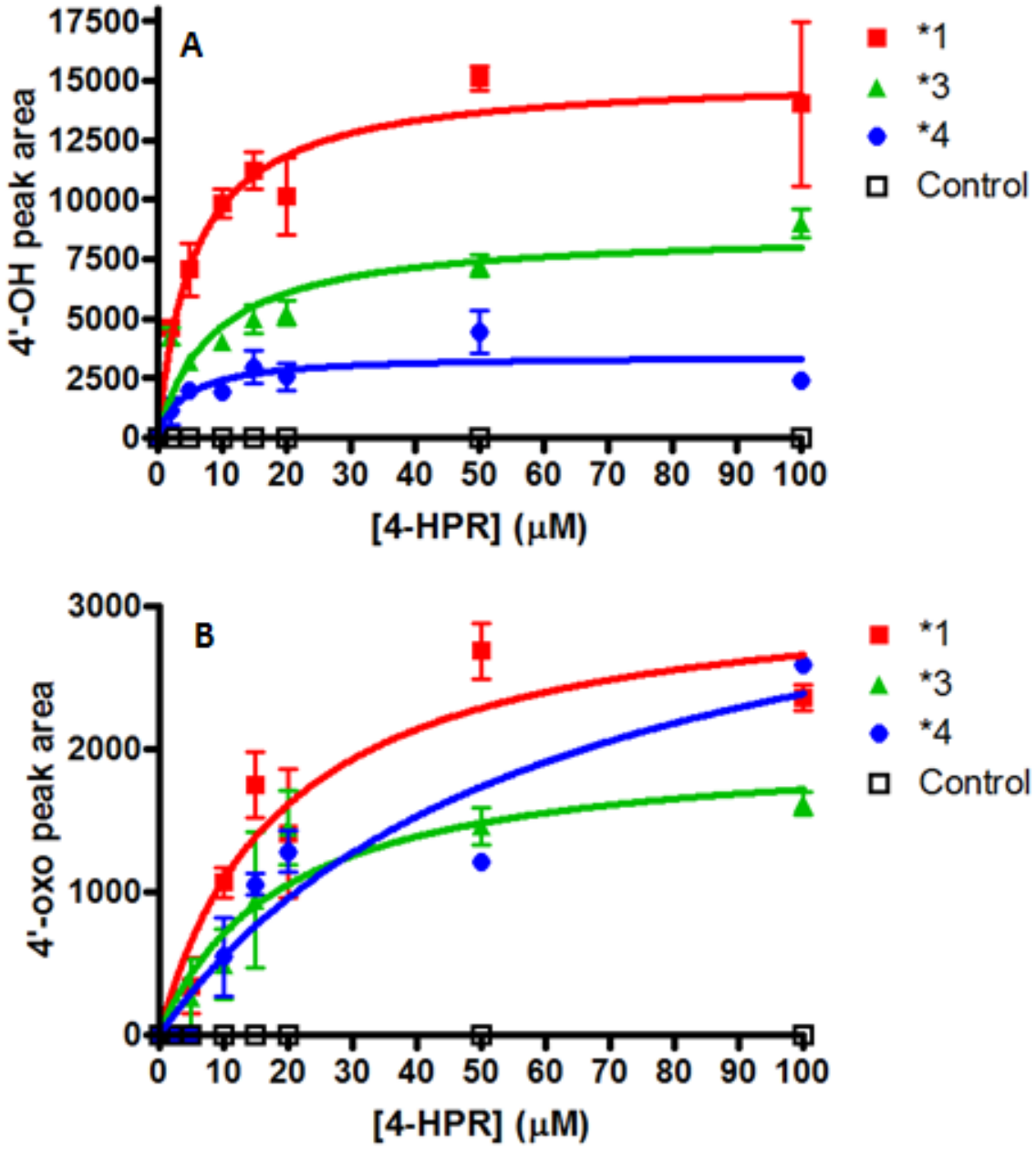

Figure 2-10. Effect of increasing 4-HPR concentration on the formation of A) 4'-OH 4-HPR and B) 4'-oxo 4-HPR by CYP2C8 variants.

E. coli membrane fractions (0.5mg/ml) co-expressing CYP2C8 variants and P450 reductase were incubated with 4-HPR (0-100μM) for 3h. Metabolite formation was determined by HPLC analysis. Results are mean ± SD from 3 independent experiments.

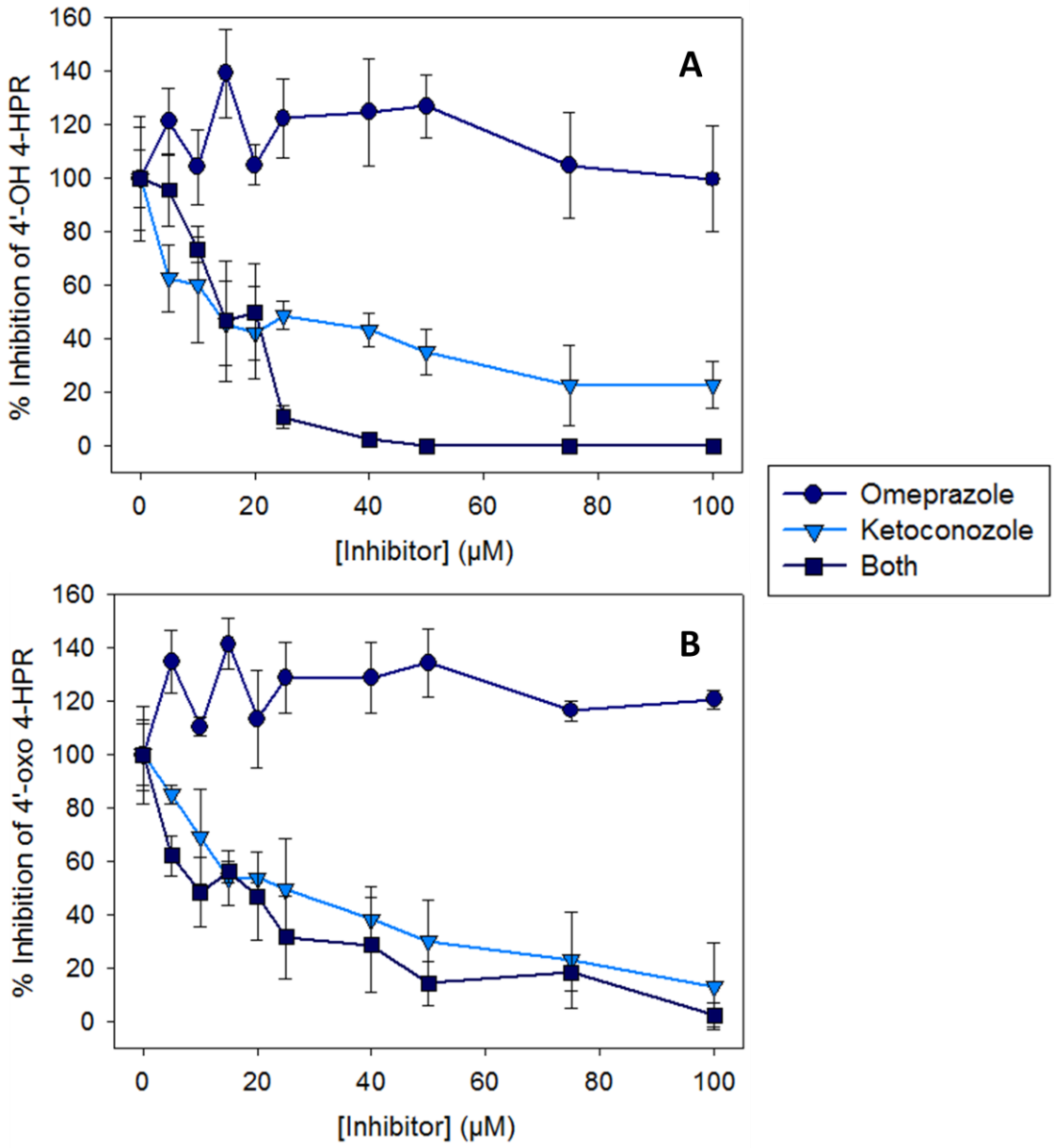

Figure 2-11. Inhibition of A) 4'-OH 4-HPR and B) 4'-oxo 4-HPR formation in HLM by CYP inhibitors.

4-HPR (50μM) was incubated with HLM (0.5mg/ml) and omeprazole, ketoconazole or both in combination (0-100μM) for 3h. Results are mean ± SD from 3 independent experiments.

2.5 Results – 4-HPR Methyltransferase Metabolism

2.5.1 Incubation of 4-HPR with HLM and SAM

Addition of the methylation co-factor SAM to incubations of HLM and 4-HPR resulted in production of 4-MPR (as shown in Figure 2-12), with 4-MPR peak area increasing with increasing SAM concentrations up to 0.2mM (Figure 2-13). This concentration of

SAM was subsequently added to all microsomal reactions investigating the production of 4-MPR.

The extent of formation of 4-MPR following incubations of 4-HPR (0-100µM) is shown in Figure 2-14. A K_m value of 236µM was determined for 4-MPR formation, markedly higher than those observed for 4'-OH and 4'-oxo 4-HPR. Similarly, a calculated V_{max} value of 823 peak area units/min for 4-MPR was higher than those observed for the 4'-OH and 4'-oxo metabolites, however kinetic parameters for the methylation of 4-HPR were difficult to obtain due to limitations of substrate solubility as it was not possible to use concentrations of 4-HPR greater than 100µM.

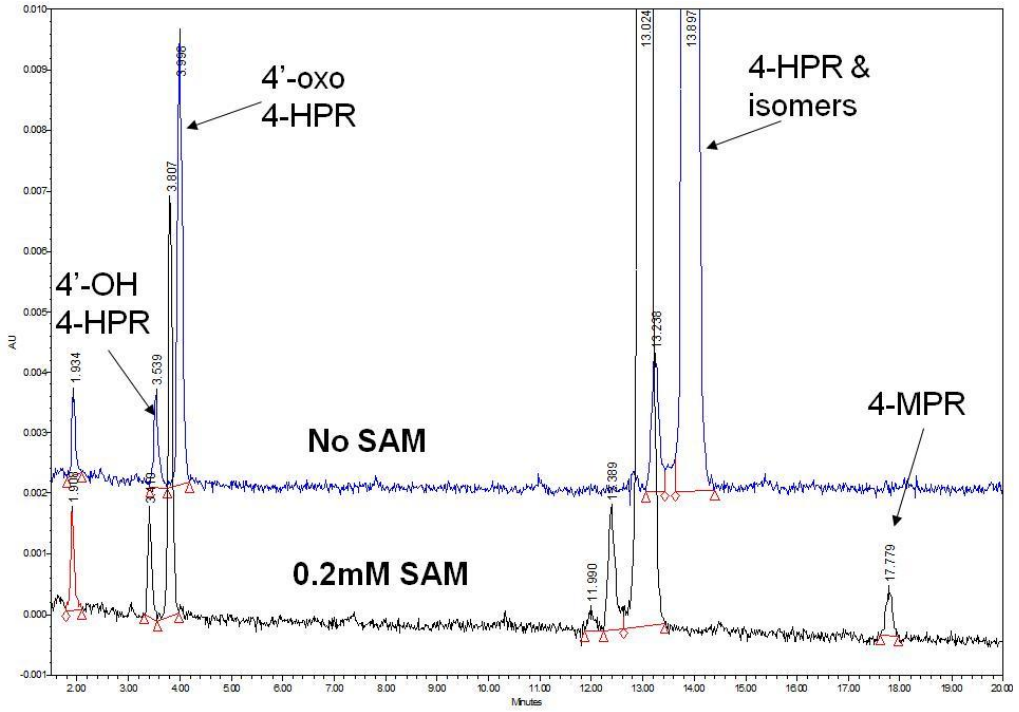

Figure 2-12. Representative chromatograms showing separation of 4-HPR and metabolites by reversed phase HPLC.

Metabolites were generated following a 3h incubation of 4-HPR (50µM) with HLM (0.5mg/ml) (top chromatogram) and in the presence of SAM (0.2mM) (bottom chromatogram).

2.5.2 Inhibition of methyltransferases

Known inhibitors or competitive substrates of several methylating enzymes were added to HLM incubations. While inhibitors of COMT and PMT had no effect on 4-MPR production, imidazole (a competitive substrate for amine-N-methyltransferase) inhibited 80% of 4-MPR production at a concentration of 5mM, as shown in Figure 2-15.

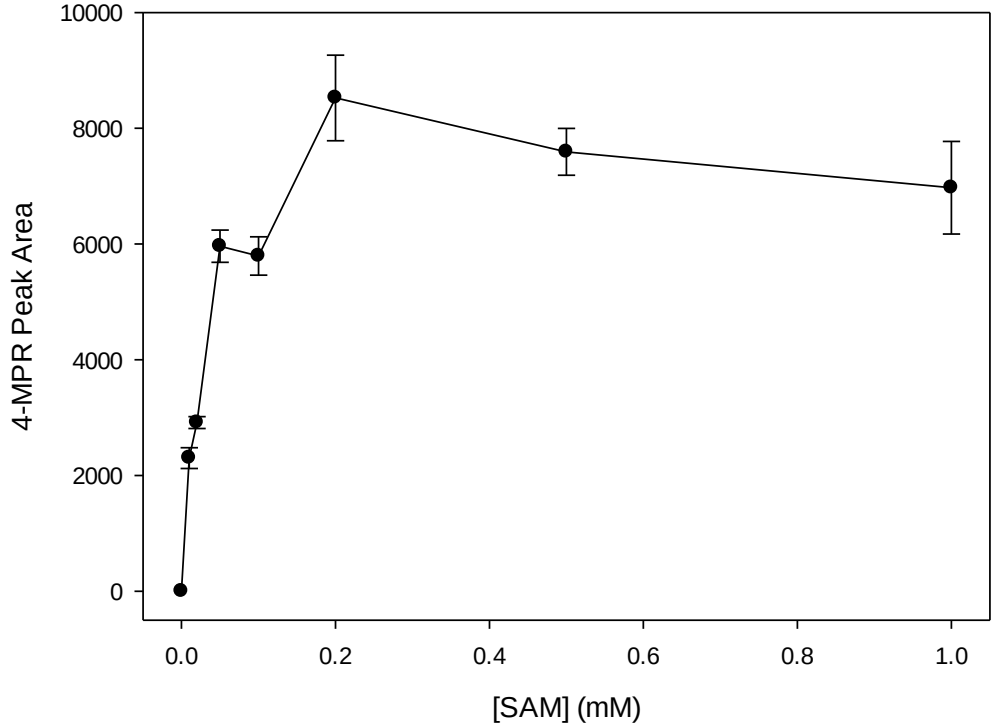

Figure 2-13. Formation of 4-MPR in the presence of SAM.

4-MPR was generated following a 3h incubation of 4-HPR (50µM) with HLM (0.5mg/ml) and SAM (0-1mM). Results are mean ± SD from 3 independent experiments.

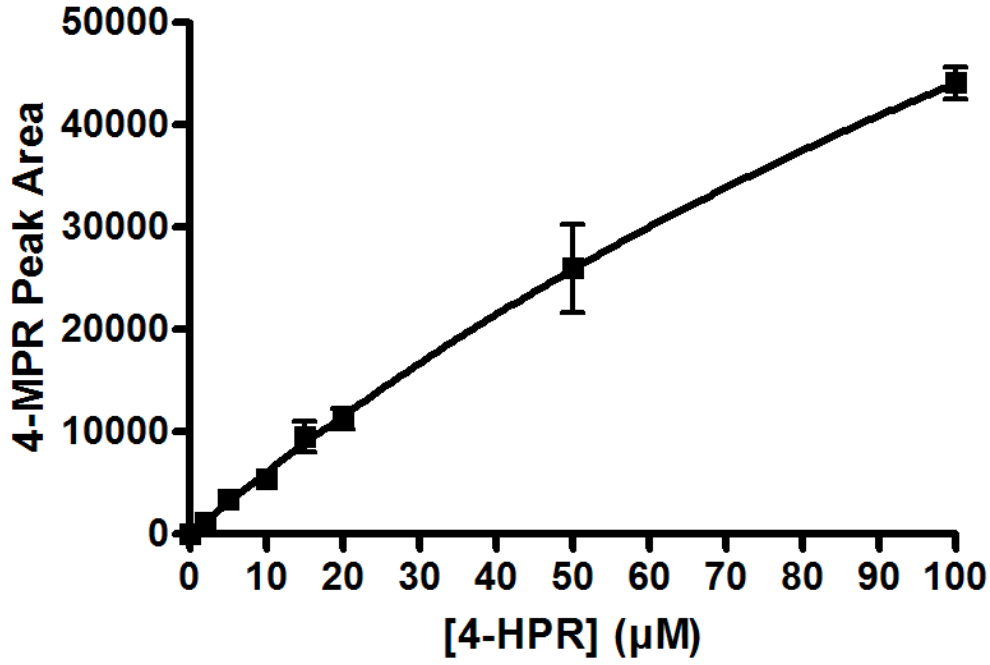

Figure 2-14. Kinetic parameters for the formation of 4-MPR.

4-HPR (0-100µM) was incubated with HLM (0.5mg/ml) for 3h. Results are mean ± SD from 3 independent experiments.

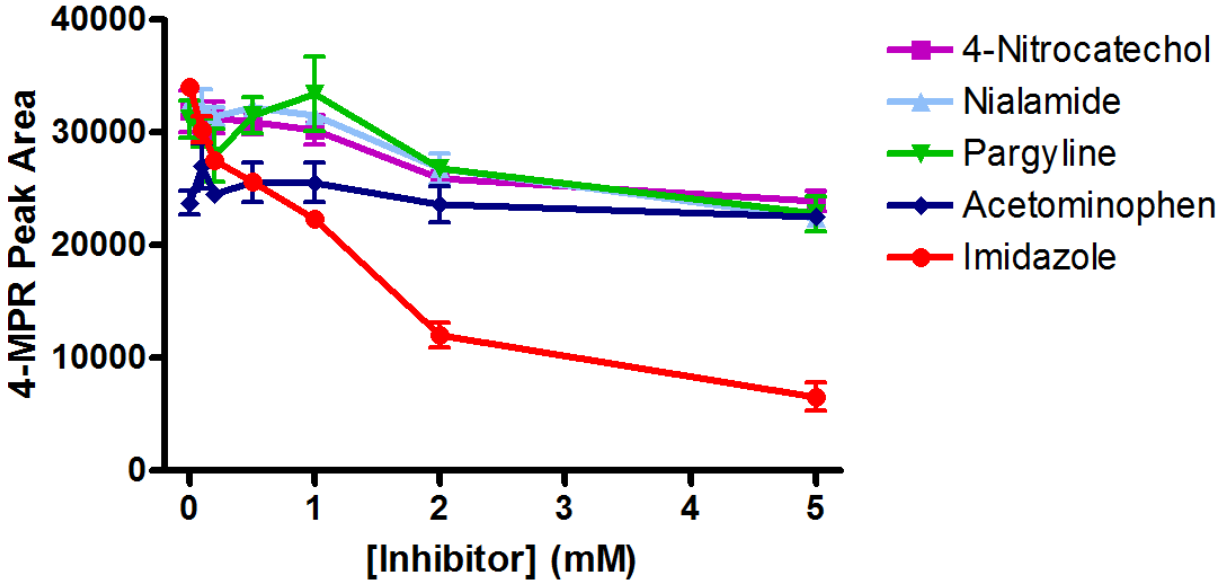

Figure 2-15. Inhibition of 4-HPR methylation.

4-HPR (50μM) was incubated with HLM (0.5mg/ml) for 3h in the presence of SAM (0.2mM) and methylation inhibitors (0-5mM). Results are mean ± SD from 3 independent experiments.

2.6 Discussion

The *in vitro* metabolism of 4-HPR was investigated to characterise the key metabolic pathways and enzymes involved. Elucidation of these enzymes is particularly important as 4-HPR is significantly metabolized *in vivo* to both active and inactive moieties, in the form of 4'-oxo 4-HPR and 4-MPR, respectively (Villani et al., 2004, Villablanca et al., 2006, Formelli et al., 2008). This study has also identified 4'-OH 4-HPR as an additional polar metabolite of 4-HPR formed *in vitro* (predicted structure shown in Figure 2-16). This metabolite is likely to be one of several additional unidentified polar metabolites previously observed by Formelli et al in breast cancer patients treated with 4-HPR (Formelli et al., 1989). 4-HPR metabolism is of particular relevance to its clinical utility as the achievement of effective and consistent plasma concentrations of parent drug in patients has been a key limitation to its clinical development (Maurer et al., 2007). It is expected that 4'-OH 4-HPR may be an intermediate in the metabolism of 4-HPR to 4'-oxo 4-HPR, as 4'-OH 4-HPR is formed before 4'-oxo 4-HPR. The formation of 4'-OH 4-HPR then remains stable as concentrations of 4'-oxo 4-HPR increase. As the same enzymes are responsible for the formation of both metabolites, the levelling off of 4'-OH 4-HPR formation is unlikely to be due to substrate or enzyme saturation, and it is probable that this is due to 4'-oxo 4-HPR being formed from 4'-OH 4-HPR.

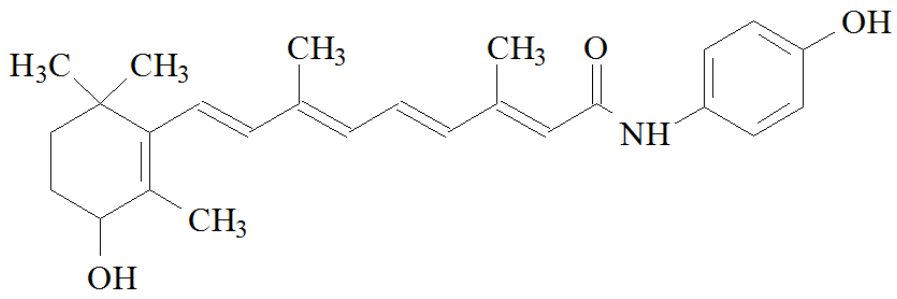

Figure 2-16. Predicted structure of 4'-OH 4-HPR.

Initial experiments were carried out to identify the metabolites produced from incubations of 4-HPR with HLM. The individual enzymes responsible for production of these metabolites were then investigated by incubation of 4-HPR with Supersomes over-expressing individual human CYP enzymes. The panel of CYPs tested contained those known to be involved in drug metabolism, including CYP3A4, as well as those

known to metabolize other retinoids (Marill et al., 2000, McSorley and Daly, 2000, Marill et al., 2002, Zhang et al., 2000). Metabolism to the newly identified metabolite, 4'-OH 4-HPR, was catalysed by all CYPs tested, but to the greatest extent by CYPs 3A4, 3A5 and 2C8. Due to the unavailability of authentic standards for the oxidative metabolites of 4-HPR, it was not possible to apply corrections for microsomal binding and therefore calculations were based on the assumption that all drug present was free and unbound. This error could have been reduced by minimising the concentration of protein used as quite high protein concentrations were used in order to maintain a reasonable rate of reaction. Metabolism to the active metabolite 4'-oxo 4-HPR was only achieved following incubations with CYPs 2C8 and 3A4. This is a similar profile of CYP isoforms to those previously identified as being involved in the metabolism of 9-cis RA, 13-cis RA and ATRA to their corresponding 4-oxo metabolites (Marill et al., 2000, McSorley and Daly, 2000, Marill et al., 2002). Metabolism by CYP2C8 was further investigated, as it is known to be highly polymorphic in the general population (Bahadur et al., 2002). CYP2C8 has previously been shown to play a role in the metabolism of cancer drugs, particularly paclitaxel, where metabolism by CYP2C8*3 was reduced by 85% compared to the wild-type protein, CYP2C8*1 (Dai et al., 2001).

Analysis of kinetic parameters of CYP2C8 isoforms demonstrated differences in the metabolism of 4-HPR in terms of metabolism to 4'-oxo 4-HPR and 4'-OH 4-HPR. Most notably, the V_{max} for the formation of 4'-OH 4-HPR was higher for wild-type CYP2C8*1 (V_{max} 0.2 peak area units/min/pmol CYP) as compared to CYP2C8*4 (V_{max} 0.11 peak area units/min/pmol CYP), with V_{max}/K_m ratios of 0.028 and 0.026 determined for *3 and *4, respectively, as compared to 0.036 for *1. Conversely, the V_{max} for the formation of 4'-oxo 4-HPR was lower for wild-type CYP2C8*1 (V_{max} 0.04 peak area peak area units/min/pmol CYP) as compared to CYP2C8*4 (V_{max} 0.128 peak area peak area units/min/pmol CYP). In fact, the V_{max} for the production of 4'-oxo 4-HPR by CYP2C8*4 may be even higher than this, as drug solubility issues limited the maximum concentration of substrate that could be used. These data suggest that CYP2C8 genotype may have a considerable impact on the metabolism of 4-HPR, and consequently on the clinical effects of this drug. This pathway of metabolism may be particularly important in tumour cells that are resistant to 4-HPR, but sensitive to the 4'-oxo metabolite (Villani et al., 2006). Of interest, lower activity for CYP2C8*3 and *4, as compared to wild-type, has previously been reported *in vitro* for the metabolism of arachidonic acid to epoxyeicosatrienoic acids, with a greater risk of renal toxicity

associated with CYP2C8*3 genotype in patients treated with calcineurin inhibitors (Smith et al., 2008). As different expression systems were used, it was not possible to directly compare kinetic parameters obtained from CYP2C8 variants expressed in *E. coli* with those obtained from Supersomes over-expressing CYP2C8. However, it is reassuring that V_{max}/K_m ratios of comparable magnitude were generated from experiments using the two different approaches.

The effect of known CYP inhibitors was also investigated to further corroborate the involvement of CYPs 3A4 and 2C8 in 4-HPR metabolism. 4-HPR was incubated with HLM in the presence and absence of ketoconazole and/or omeprazole. Ketoconazole considerably inhibited the production of both metabolites, with 75% inhibition of 4'-OH 4-HPR and 85% inhibition of 4'-oxo 4-HPR at 100μM. Omeprazole alone at a concentration of 100μM had very little effect on either metabolite, but in combination with 100μM ketoconazole resulted in complete inhibition of 4'-OH 4-HPR, whereas no additional effect was seen on inhibition of 4'-oxo 4-HPR. No effect was seen with omeprazole in the absence of ketoconazole as HLM have approximately 25 times more CYP3A4 activity than CYP2C8. Any inhibition of CYP2C8 alone may be masked by the greater activity of CYP3A4 in this system. It should be noted that these CYP inhibitors may be relatively non-selective at the concentrations used in these experiments. For example, ketoconazole has been shown to markedly inhibit CYP2C8, as well as CYP3A4, at concentrations >10μM (Ong et al., 2000). Similarly omeprazole has been shown to inhibit CYPs 2C9 and 2C19 (Li et al., 2004), although the role played by these two enzymes in the metabolism of 4-HPR would appear to be minimal. The results obtained in the current study are comparable to the effect of CYP inhibitors on other retinoids. ATRA metabolism, for example, has previously been shown to be inhibited approximately 90% by ketoconazole (Schwartz et al., 1995).

Retinoids are also known to be significantly metabolized by CYP26 isoforms. The contribution of CYP26 cannot be determined by the same methods as the other CYPs investigated, as Supersomes over-expressing CYP26 are not currently available.

In addition to 4'-OH 4-HPR and 4'-oxo 4-HPR, 4-MPR has previously been identified as a major metabolite of 4-HPR (Swanson et al., 1980) and its pharmacokinetic properties have subsequently been investigated (Hultin et al., 1990, Mehta et al., 1998, Vratilova et al., 2004). However, the enzymes responsible for this methylation reaction

have not previously been characterized. The identification of SAM as a necessary cofactor for 4-HPR methylation enabled investigations into the formation of all three major 4-HPR metabolites in a single *in vitro* system. Out of several candidate methylation enzymes that require SAM as a cofactor, only a limited number are microsomal. The current study showed that 4-MPR production was not affected by inhibitors of COMT or PMT but was inhibited up to 80% by imidazole (5mM), a competitive substrate for amine-N-methyltransferases, that are known to be microsomal and are involved in the metabolism of many drugs and carcinogens (Ansher and Jakoby, 1986). It was not possible to definitively identify the enzyme involved in this important pathway of 4-HPR metabolism. Kinetic parameters for the methylation of 4-HPR were difficult to obtain due to limitations of substrate solubility. It was not possible to use concentrations of 4-HPR greater than 100μM and comparison of the slope of the plot with derived values for K_m/V_{max} suggest that the calculated V_{max} may have been underestimated by up to two-fold.

The achievement of effective and consistent plasma concentrations in patients has been a major limitation to the clinical development of 4-HPR. Clinical trials in neuroblastoma patients have shown marked variability in peak plasma concentrations of 4-HPR, varying from 1- 20μM at higher doses (Villablanca et al., 2006). Differences in CYP expression in human tissues may have a substantial impact on the metabolism of 4-HPR in patients, as demonstrated by the CYP inhibition experiments described above, where formation of 4'-oxo 4-HPR was not reduced by inhibition of CYP2C8 unless CYP3A4 activity was additionally inhibited. As CYP expression varies greatly in different tissues and particularly in tumours, and even differs between foetal and adult tissues (Choudhary et al., 2005), the contribution of CYP isoforms to 4-HPR metabolism and efficacy is likely to vary between tissues as well as between patients. For example, CYP2C9 activity in human liver microsomes is more than 5-fold greater than in human intestinal microsomes, whereas CYP3A4 activity only differs by 25% between the same two tissue types. In addition, CYP expression has also been linked to expression of inflammatory cytokines, with a down-regulation in expression of hepatic CYPs in the presence of cytokines (Abdel-Razzak et al., 1993). This has been shown to alter the metabolism of epoxyeicosatrienoic and dihydroxyeicosatrienoic acids *in vivo* (Theken et al., 2011). Concurrent medications may also have an effect on CYP expression (Zhou, 2008), as can co-morbidities such as diabetes, that is associated with

a significant decrease in both CYP3A4 protein and mRNA expression (Dostalek et al., 2011).

Inhibition of CYP3A4 with ketoconazole has been investigated as a possible means of increasing 4-HPR concentrations. Co-administration of 4-HPR and ketoconazole is currently being investigated in clinical trials following a 2- to 3-fold increase in peak 4-HPR plasma concentrations observed in an animal model. However treatment with ketoconozole also resulted in a 2-fold increase in 4'-oxo 4-HPR plasma concentrations, rather than the expected decrease in this metabolite. This is possibly due to inhibition of other 4-HPR and 4'-oxo 4-HPR metabolites, or due to the contribution of other CYPs to 4-HPR metabolism (Cooper et al., 2011). Therefore due to the fact that the major metabolite of 4-HPR is 4-MPR, an inactive compound, it may be more beneficial to modulate 4-HPR metabolism by inhibiting or blocking methylation of 4-HPR. This has the potential to further increase plasma concentrations of 4-HPR and subsequently increase metabolism to the active metabolite, 4'-oxo 4-HPR.

In addition to variations in peak plasma concentrations of 4-HPR due to inter patient differences in metabolism, considerable variation due to bioavailability may also be an issue. 4-HPR is currently given orally in capsule form, with 4-HPR (typically 100mg) dissolved in a corn oil mixture. In a phase I trial of 4-HPR in neuroblastoma patients, dosing with the corn oil capsules resulted in huge variability in maximum plasma concentrations reached, with variation of up to 74% at the highest dose (4,000mg/m^2) (Formelli et al., 2008). Reformulation of 4-HPR from the currently used oil-based capsules to a lipid matrix has been shown to increase plasma concentrations up to 7-fold in a mouse model (Maurer et al., 2007). In a phase I trial in neuroblastoma patients, dosing with the lipid matrix reduced inter-patient variation and increased maximum 4-HPR concentrations 2- to 5-fold higher than with corn oil dosing. The improved formulation was also well tolerated, with no MTD reached at the highest doses used, (2,210mg/m^2/day), despite the higher 4-HPR concentrations achieved (Marachelian et al., 2009). While this largely represents a formulation and bioavailability issue, it is clearly not advantageous for a significant percentage of 4-HPR to be metabolized to inactive metabolites. Indeed as 4-HPR bioavailability is improved, the level of metabolism to its active, synergistic 4'-oxo 4-HPR metabolite, as compared to the inactive 4-MPR metabolite, may become a more significant factor in determining its overall effectiveness.

Identification of the enzymes responsible for 4-HPR metabolism in the current study provides a stepping stone for future studies to determine the potential role of these enzymes in determining the efficacy of 4-HPR.

Chapter 3 Glucuronidation

3.1 Introduction

Glucuronidation is one of the major phase II detoxification pathways. UGTs (Uridine 5'-diphospho-glucuronosyltransferases) conjugate toxic compounds with glucuronic acid in order to increase their polarity and make them more soluble. This enables excretion of toxic compounds and their metabolites through the kidneys. Nineteen human UGTs are currently known, and these are primarily expressed in the liver. There are five UGT1 isoforms substantially expressed in human liver microsomes (1A1, 1A3, 1A4, 1A6 and 1A9) along with five UGT2 isoforms (2B4, 2B7, 2B10, 2B15 and 2B17) (Izukawa et al., 2009). There is also substantial extra-hepatic expression of UGTs, particularly in the intestinal epithelium, with expression also observed in the kidney, brain and skin (Radominska-Pandya et al., 1998, Ohno and Nakajin, 2009). UGTs 1A7, 1A8 and 1A10 have been found to be expressed only in extra-hepatic (gastric) tissue (Strassburg et al., 1997). Polymorphisms of UGTs have been shown to have a major effect on drug metabolism. Irinotecan toxicity, particularly, is known to be associated with polymorphisms of UGT1A1 due to significantly lower metabolism of SN-38, the active metabolite of irinotecan (Ando et al., 2000, O'Dwyer and Catalano, 2006, United States Food and Drug Administration, 2010, Gagné et al., 2002). Several other UGTs have also been associated with inter-patient variation in toxicity or drug clearance and accumulation, including UGTs 1A9 and 2B15. Polymorphisms in UGT1A9 can either significantly increase or significantly decrease exposure to mycophenolic acid depending on the polymorphism present (Levesque et al., 2007, Miura et al., 2008), whilst significantly lower clearance of lorazepam has been observed in patients who express a variant allele of UGT2B15 (Chung et al., 2005).

Several studies have investigated the major UGTs responsible for the glucuronidation of retinoid-based drugs, including ATRA (Czernik et al., 2000, Samokyszyn et al., 2000). These studies showed that both hepatic and intestinal UGTs are able to metabolise ATRA, with 50-80% more metabolism by hepatic UGTs than with intestinal UGTs.

Variable expression of UGTs in different tissues means it is important to have an understanding of both hepatic and intestinal glucuronidation and the likely impact on overall metabolism, particularly for orally administered drugs. Due to the wide

variability in 4-HPR plasma concentrations in patients (Garaventa et al., 2003, Formelli et al., 2008), the contribution of UGTs to 4-HPR metabolism was investigated. In addition, as 13-cis RA is currently used during the maintenance chemotherapy regimen of treatment for high risk neuroblastoma, and as it shares many structural similarities with 4-HPR, the glucuronidation of 13-cis RA was also investigated (Rowbotham et al., 2010b, Illingworth et al., 2011). In common with 4-HPR, 13-cis RA also exhibits variable plasma concentrations following oral administration for children with cancer (Veal et al., 2007).

3.2 Materials and Methods

3.2.1 Chemicals

13-cis RA and β-glucuronidase (from *Helix pomatia*) were purchased from Sigma-Aldrich (Poole, UK). 4-oxo 13-cis RA was generously provided by Hoffmann-La Roche (Basel, Switzerland). 4-HPR, 4-MPR and 4-EPR (4-ethoxy retinamide) were generously provided by Cancer Research UK and 4'-oxo 4-HPR was provided by High Force Research Ltd. (Durham, UK). UGT Reaction Mix Solution A (25mM uridine 5`-diphosphoglucuronic acid) and UGT Reaction Mix Solution B (250mM Tris-HCl, 40mM $MgCl_2$, 0.125mg/ml alamethicin) were purchased from BD Gentest (Oxford, UK). Pooled human liver and intestinal microsomes as well as Supersomes expressing the recombinant human UGT1A1, UGT1A3, UGT1A4, UGT1A6, UGT1A7, UGT1A8, UGT1A9, UGT1A10, UGT2B4, UGT2B7, UGT2B15 and UGT2B17 enzymes as well as control microsomes with wild-type baculovirus were also purchased from BD Gentest. HPLC-grade solvents were from Fisher Scientific (Loughborough, UK). All other chemicals and reagents were purchased from Sigma-Aldrich (Poole, UK).

3.2.2 Incubation of 13-cis RA and 4-oxo 13-cis RA with UGTs, HLM and HIM

Glucuronidation activity was determined in pooled human liver microsomes (HLM), human intestinal microsomes (HIM) and Supersomes over-expressing individual UGT isoforms (UGT1A1, UGT1A3, UGT1A4, UGT1A6, UGT1A7, UGT1A8, UGT1A9, UGT1A10, UGT2B4, UGT2B7, UGT2B15, UGT2B17 and control). The incubation mixture consisted of Supersomes (0.5mg/ml), 13-cis RA (100µM) or 4-oxo 13-cis RA (100µM), 0.25% methanol and UGT solution mixes A and B (consisting of alamethecin (25µg/ml), $MgCl_2$ (8mM) and UDPGA (2mM)), made up to a final volume of 200µl with Tris-HCl buffer (50mM, pH 7.5). Incubations were carried out at 37°C for 1h. Reactions were initiated by the addition of enzyme and terminated with ice-cold acetonitrile (400µl). Samples were vortex mixed and centrifuged at 10,000g for 5min. Supernatant (200µl) was removed and evaporated to dryness and the residue reconstituted in 0.1% glacial acetic acid pH 5.0 (200µl), prior to HPLC analysis. All incubations were performed in triplicate.

3.2.3 HPLC analysis of 13-cis RA glucuronide and 4-oxo 13-cis RA glucuronide

Separation of 13-cis RA, 4-oxo 13-cis RA and glucuronide metabolites by HPLC analysis was carried out using a Waters 2690 Separations Module and 996 Photodiode array (PDA) detector (Waters Ltd., Elstree, UK), with Waters Millennium software for data acquisition. Separation of 13-cis RA and its glucuronide metabolites was achieved using a Luna C_{18} (2) column (50 x 2.0mm, 3µm) (Phenomenex, Torrance, CA, USA) with mobile phases (A) 0.1% acetic acid, pH 5.0 and (B) 100% acetonitrile. The gradient ran as shown in Table 3-1. Separation of 4-oxo 13-cis RA and its glucuronide metabolites was achieved as for 13-cis RA, except that after returning to 60% A by 5min, it remained at 60% A until 20min to re-equilibrate for the next sample. Sample volumes of 20µl were injected onto the column for analysis.

Time (min)	%A	%B
0	60	40
2	40	60
4	40	60
5	60	40
15	60	40
16	0	100
26	0	100
30	60	40
40	60	40

Table 3-1. Chromatographic conditions for the separation of 13-cis RA, 4-oxo 13-cis RA and glucuronide metabolites by HPLC.
Mobile phase (A) 0.1% acetic acid, pH 5.0 and (B) 100% acetonitrile.

3.2.4 Determination of kinetic parameters for 13-cis RA glucuronide and 4-oxo 13-cis RA glucuronide formation

Kinetic parameters for 13-cis RA and 4-oxo 13-cis RA glucuronide formation were determined for Supersomes that had been shown to generate the glucuronide metabolite (UGTs 1A1, 1A3, 1A7, 1A8 and 1A9), as well as HIM and HLM. All incubations were carried out as described above with 4-oxo 13-cis RA and 13-cis RA concentrations ranging from 0 – 100µM. Metabolism to 13-cis RA glucuronide and 4-oxo 13-cis RA

glucuronide by each UGT was then compared by ANOVA followed by Bonferroni's post test, with $P \leq 0.05$ used to determine significance. All calculations were performed with GraphPad Prism version 4.0 software.

3.2.5 Incubation of 4-HPR and 4'-oxo 4-HPR with UGTs, HLM and HIM

HLM, HIM or a panel of UGT Supersomes over-expressing individual UGTs were incubated with 4-HPR or 4'-oxo 4-HPR (200μM) in an incubation mixture consisting of alamethecin (25μg/ml), $MgCl_2$ (8mM), UDPGA (2mM) and methanol (0.25%), made up to a final volume of 50μl with Tris-HCl buffer (50mM, pH 7.5). UGTs 1A1, 1A3, 1A4, 1A6, 1A7, 1A8, 1A9, 1A10, 2B4, 2B7, 2B15 and 2B17 were used. Incubations were carried out at 37°C for 3h, at which point the reaction was still linear. Incubations were also carried out with 4-MPR (200μM) and 4-EPR (200μM) with HLM (0.5mg/ml). Reactions were initiated by the addition of enzyme and terminated with ice-cold acetonitrile (100μl). To confirm the metabolite produced was a glucuronide, β-glucuronidase (800U) in potassium phosphate buffer (75mM, pH 6.8) was added to samples prepared from the incubations as described above and the mixture was incubated at 37°C for an additional 30min. All reactions were terminated by the addition of ice-cold acetonitrile (100μl) and samples were centrifuged at 10,000g for 5min to remove all protein. Supernatant was then retained for HPLC analysis. Due to the lack of authentic standard of 4'-oxo 4-HPR for standard curves, experiments were carried out in parallel, with all comparative samples for a defined experiment being analysed within a single assay.

3.2.6 HPLC analysis of 4-HPR glucuronide and 4'-oxo 4-HPR glucuronide

Separation of 4-HPR, 4'-oxo 4-HPR and glucuronide metabolites by HPLC was carried out using a Luna C_{18} (2) column (50 x 2.0mm, 3μm) (Phenomenex, Torrance, CA, USA) with mobile phases (A) 0.1% acetic acid, pH 5.0 and (B) 100% acetonitrile. A linear gradient ran at 0.2ml/min from 60% A at 0min to 100% B at 6min, maintaining at 100% B for 4min and returning to 60% A for 10min to re-equilibrate the column, as shown in Table 3-2. A sample volume of 20μl was injected onto the column for analysis. The limit of quantification of the assay was 0.01μg/ml and the inter-assay coefficients of variation were 4.3 – 6.5% for 4-HPR and metabolites.

Time (min)	%A	%B
0	60	40
6	0	100
10	0	100
11	60	40
21	60	40

Table 3-2. Chromatographic conditions for the separation of 4-HPR, 4'-oxo 4-HPR and glucuronide metabolites by HPLC.

Mobile phase (A) 0.1% acetic acid, pH 5.0 and (B) 100% acetonitrile.

3.2.7 Determination of kinetic parameters for 4-HPR glucuronide and 4'-oxo 4-HPR glucuronide formation

Kinetic parameters for the formation of the glucuronide metabolite of 4-HPR were determined following incubations of HLM, HIM or UGTs 1A1, 1A3 or 1A6 (0-1.5mg/ml protein) with 4-HPR (200µM), or 0-2,000µM 4-HPR with 1mg/ml protein. Kinetic parameters for the formation of the glucuronide metabolite of 4'-oxo 4-HPR were determined following incubations of HLM, HIM or UGTs 1A1, 1A3, 1A8 and 1A9 (0-1.5mg/ml protein) with a fixed concentration of 4-HPR or 4'-oxo 4-HPR (200µM) or alternatively at a fixed protein concentration (1mg/ml) over a range of 4-HPR concentrations (0-2,000µM) or 4'-oxo 4-HPR concentrations (0-500µM). 4'-oxo 4-HPR could not be used at concentrations above 500µM as the highest stock solution concentration available was 10mM, dissolved in ethanol. Use of concentrations higher than 500µM resulted in enzyme inhibition due to the presence of ethanol quantities >5%. Metabolism to 4-HPR glucuronide and 4'-oxo 4-HPR glucuronide by each UGT was then compared by ANOVA, with $P \leq 0.05$ used to determine significance. Calculations were performed with GraphPad Prism version 4.0 software. Due to the lack of authentic standards for 4'-oxo 4-HPR and 4-HPR glucuronides, V_{max} results were expressed as peak area units/min.

3.3 Results

3.3.1 Incubation of 13-cis RA and 4-oxo 13-cis RA with UGTs, HLM and HIM

13-cis RA or 4-oxo 13-cis RA (100μM) were incubated with a panel of Supersomes expressing individual UGT enzymes, as well as HIM and HLM (1mg/ml), to identify the enzymes responsible for the production of the glucuronide metabolite (Figure 3-1). Of the UGTs included in the screen only UGTs 1A1, 1A3, 1A7, 1A8 and 1A9, in addition to HIM and HLM, produced 13-cis RA glucuronide or 4-oxo 13-cis RA glucuronide.

3.3.2 Kinetic parameters for 13-cis RA glucuronide and 4-oxo 13-cis RA glucuronide formation

13-cis RA or 4-oxo 13-cis RA (0-100μM) were incubated with HLM, HIM or individual UGT enzymes (0.5mg/ml) for 1h to determine enzyme kinetic parameters. UGTs 1A1, 1A3, 1A7, 1A8 and 1A9 were used, as well as HLM and HIM, as these had been shown to metabolize 13-cis RA and 4-oxo 13-cis RA to their glucuronide metabolites (as shown in Figure 3-1). Glucuronide production was related to substrate concentration, as shown in Figure 3-2, with kinetic parameters provided in Table 3-3 and Table 3-4. V_{max} values for formation of 13-cis RA glucuronide were highest for UGT1A3 (26 ± 5 peak area units/min/pmol UGT) and lowest for UGT1A9 (0.04 ± 0.01 peak area units/min/pmol UGT). K_m values ranged from 3μM for UGT1A9 to 170μM for UGT1A7. V_{max}/K_m ratios ranged from 0.006 for UGT1A7 to 0.25 for UGT1A3.

V_{max} values for the formation of 4-oxo 13-cis RA glucuronide were also highest for UGT1A3 and lowest for UGT1A9 (89 ± 20 peak area units/min/pmol UGT for UGT1A3 and 0.2 ± 0.01 peak area units/min/pmol UGT for UGT1A9). K_m values ranged from 18μM for UGT1A9 to 266μM for UGT1A3. V_{max}/K_m ratios for production of 13-cis RA glucuronide were identical to those for the formation of 4-oxo 13-cis RA for UGTs 1A1, 1A7 and 1A9 (0.01 for both UGT1A1 and UGT1A9 and 0.006 for UGT1A7). V_{max}/K_m ratios were higher for 4'-oxo 13-cis RA glucuronide than 13-cis RA glucuronide for UGT1A3 (2.98 compared to 0.25) and UGT1A8 (0.09 compared to 0.03).

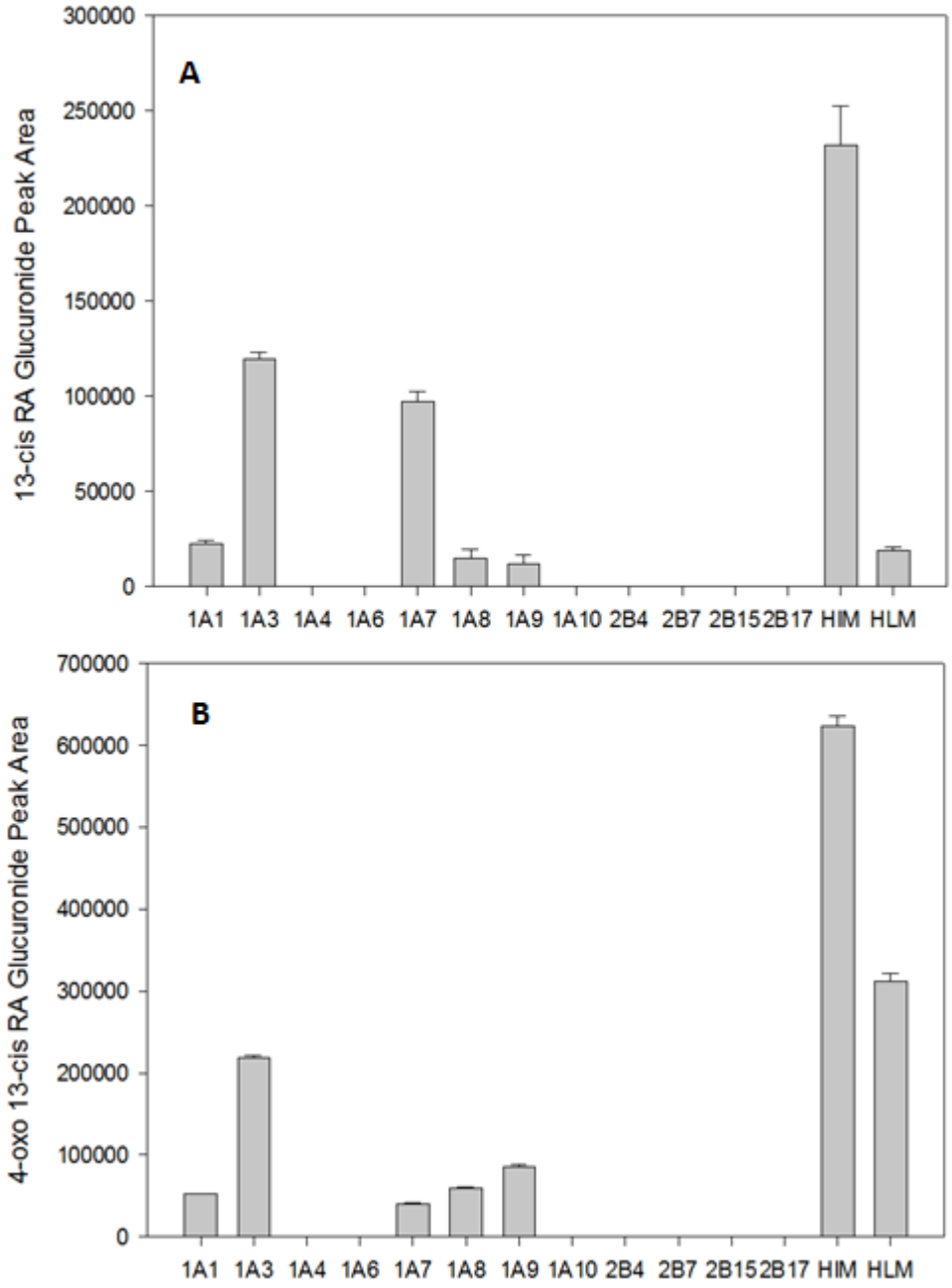

Figure 3-1. Formation of glucuronide metabolites of A) 13-cis RA and B) 4-oxo 13-cis RA by a panel of Supersomes over-expressing individual human UGTs.

Metabolite formation was determined by HPLC analysis. Metabolites were generated following a 1h incubation of 4-oxo 13-cis RA or 13-cis RA (100µM) with 1mg/ml protein. Results are the mean of 3 independent determinations (error bars are standard deviation).

Maximum rates of metabolism to 13-cis RA glucuronide and 4-oxo 13-cis RA glucuronide per pmol of each UGT were compared by ANOVA followed by Bonferroni's post test, with $P \leq 0.05$ used to determine significance. Statistically

significant differences were seen in metabolism to 13-cis RA glucuronide and 4-oxo 13-cis RA glucuronide ($p<0.0001$ for both).

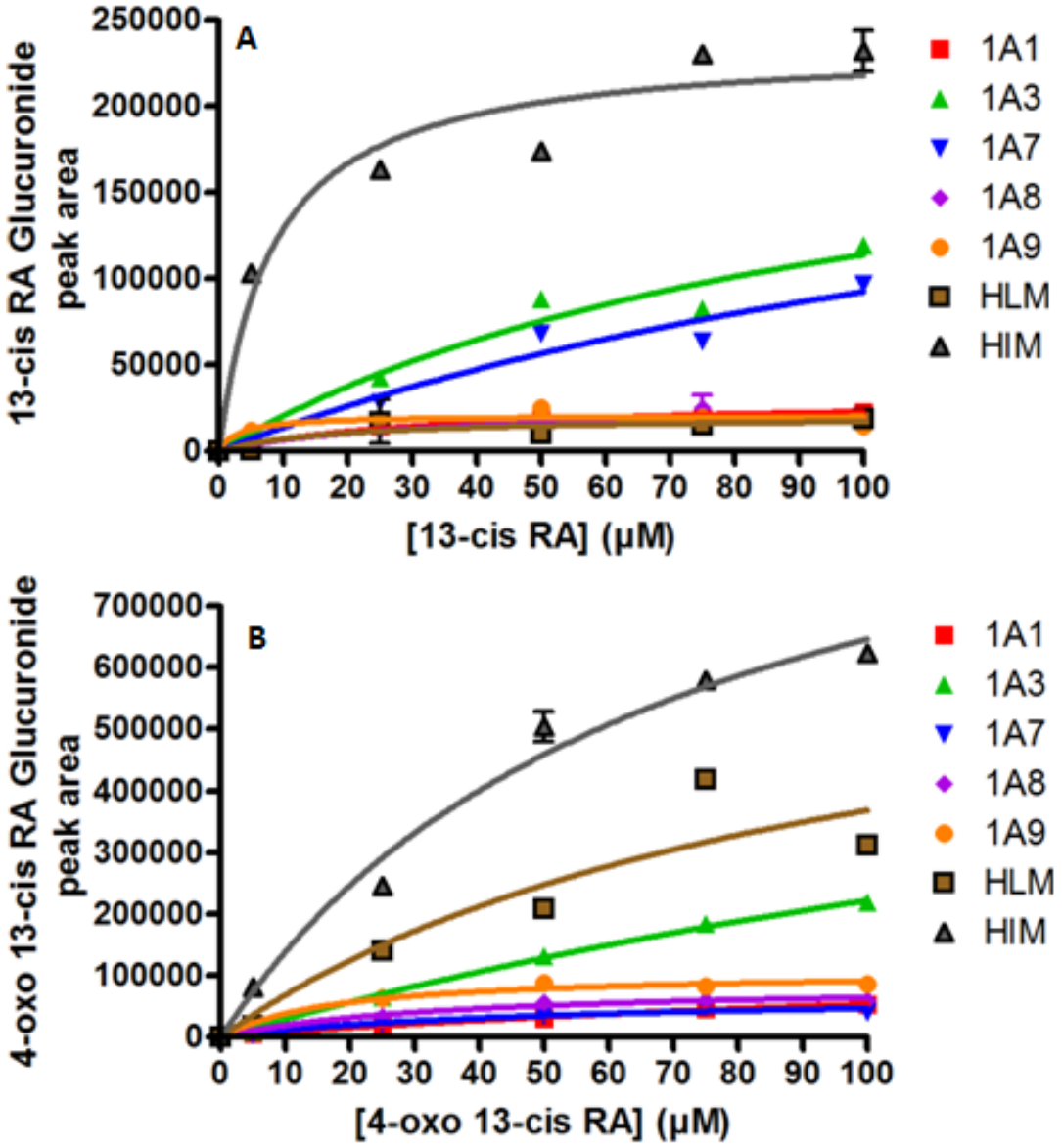

Figure 3-2. Effect of increasing substrate on the formation of A) 13-cis RA glucuronide and B) 4-oxo 13-cis RA glucuronide by a panel of Supersomes over-expressing individual human UGTs.

UGTs found to metabolise 4-oxo 13-cis RA or 13-cis RA, as well as HIM and HLM (0.5mg/ml), were incubated with 13-cis RA or 4'-oxo 13-cis RA (0-100µM) for 1h. Metabolite formation was determined by HPLC analysis. Results are mean ± SD from 3 independent experiments.

	K_m (μM)	V_{max} (peak area units/min)	V_{max} (peak area units/min/pmol UGT	V_{max}/K_m
UGT1A1	33 ± 15	503 ± 81	0.5 ± 0.1	0.015
UGT1A3	103 ± 36	3852 ± 784	26 ± 5	0.250
UGT1A7	170 ± 89	4153 ± 1499	1 ± 0.3	0.006
UGT1A8	28 ± 26	416 ± 132	1 ± 0.3	0.035
UGT1A9	3 ± 1	340 ± 27	0.1 ± 0.1	0.013
HIM	4.8 ± 1.2	3926 ± 174	N/A	N/A
HLM	8 ± 2	335 ± 131	N/A	N/A

Table 3-3. Kinetic parameters for the formation of the glucuronide metabolite of 13-cis RA by a panel of UGT enzymes, HIM and HLM.

The major UGTs found to metabolize 13-cis RA (1A1, 1A3, 1A7, 1A8 and 1A9 as well as HIM and HLM) were incubated with 0-100μM 13-cis RA for 1h. Metabolite formation was determined by HPLC analysis. Results are expressed as mean ± SD from n≥3 experiments. (N/A = not applicable as data on the individual UGT activities of HIM and HLM were not available).

3.3.3 Incubation of 4-HPR and 4'-oxo 4-HPR with UGTs, HLM and HIM

Incubation of 4-HPR or 4'-oxo 4-HPR (200μM) with HLM (0.5mg/ml) resulted in the formation of metabolites that were not present in control samples incubated without UGT cofactors (UDPGA). Subsequent incubation of 4-HPR and 4'-oxo 4-HPR (200μM) with β-glucuronidase (800U) and HLM (0.5mg/ml) resulted in complete removal of the metabolite peak, confirming it as a glucuronide, as shown in Figure 3-3. Incubations of HLM or HIM with 4-MPR and 4-EPR (4-ethoxyphenyl retinamide) did not result in formation of a glucuronide metabolite. 4-HPR or 4'-oxo 4-HPR (200μM) were incubated with a panel of Supersomes expressing individual UGT enzymes, as well as HIM and HLM, to identify the enzymes responsible for the production of the glucuronide metabolite (Figure 3-4). Of the UGTs included in the screen, only UGTs

1A1, 1A3 and 1A6, in addition to HIM and HLM, were able to produce 4-HPR glucuronide.

	K_m (μM)	V_{max} (peak area units/min)	V_{max} (peak area units/min/pmol UGT	V_{max}/K_m
UGT1A1	174 ± 27	2425 ± 265	3 ± 0.3	0.015
UGT1A3	266 ± 76	13354 ± 3004	89 ± 20	0.335
UGT1A7	51 ± 17	1157 ± 168	0.3 ± 0.1	0.006
UGT1A8	36 ± 7	1441 ± 104	3 ± 0.2	0.093
UGT1A9	18 ± 3	1774 ± 81	0.2 ± 0.1	0.011
HIM	69 ± 14	16822 ± 1818	N/A	N/A
HLM	95 ± 58	11978 ± 4165	N/A	N/A

Table 3-4. Kinetic parameters for the formation of the glucuronide metabolite of 4-oxo 13-cis RA by a panel of UGT enzymes, HIM and HLM.

The major UGTs found to metabolize 4-oxo 13-cis RA (1A1, 1A3, 1A7, 1A8 and 1A9 as well as HIM and HLM) were incubated with 0-100μM 4-oxo 13-cis RA for 1h. Metabolite formation was determined by HPLC analysis. Results are expressed as mean ± SD from n≥3 experiments. (N/A = not applicable as data on the individual UGT activities of HIM and HLM were not available).

Metabolism to 4'-oxo 4-HPR glucuronide was markedly different to glucuronidation of 4-HPR. Although metabolism was observed for both substrates when incubated with UGTs 1A1 and 1A3, HIM and HLM, no metabolism was seen with UGT1A6 in the case of 4'-oxo 4-HPR. However, the 4'-oxo 4-HPR glucuronide metabolite was produced by UGTs 1A8 and 1A9, whereas neither of these UGTs were able to metabolise 4-HPR itself.

3.3.4 Kinetic parameters for 4-HPR glucuronide and 4'-oxo 4-HPR glucuronide formation

4-HPR (0-2,000µM) or 4'-oxo 4-HPR (0-500µM) were incubated with HLM, HIM or individual UGT enzymes (0.5mg/ml) for 3h to determine enzyme kinetic parameters. UGTs 1A1, 1A3 and 1A6 were incubated with 4-HPR, and UGTs 1A1, 1A3, 1A8 and 1A9 were incubated with 4'-oxo 4-HPR, as these had been shown to metabolize 4-HPR and 4'-oxo 4-HPR respectively to their glucuronide metabolites in previous experiments (as shown in Figure 3-4).

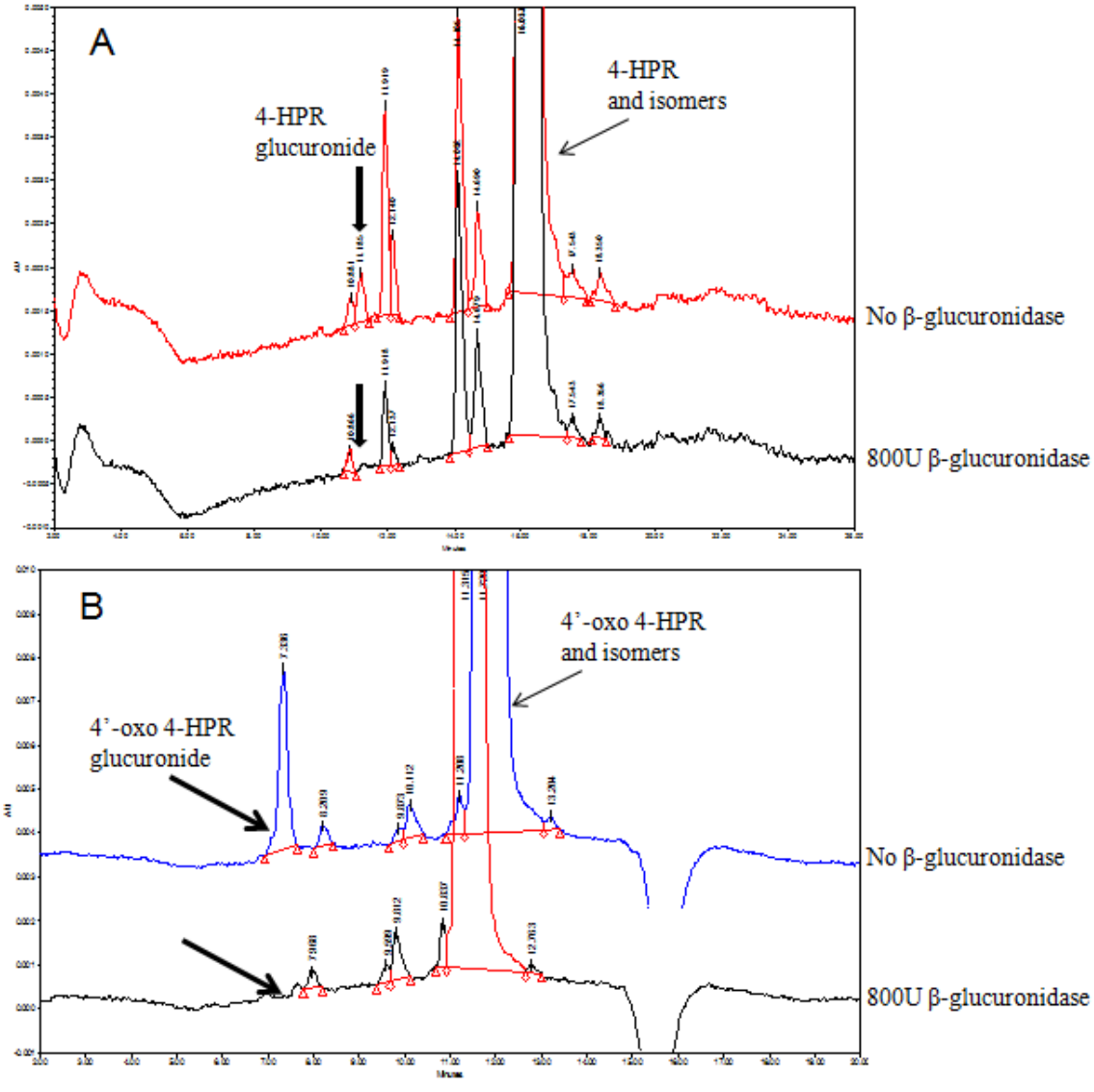

Figure 3-3. Representative chromatograms showing separation of A) 4-HPR and glucuronide metabolites and B) 4'-oxo 4-HPR and glucuronide metabolites.

The lower trace in each panel shows additional incubation with β-glucuronidase, resulting in breakdown of the glucuronide metabolite (as indicated by the arrow). Metabolites were generated following a 3.5h incubation of 4-HPR or 4'-oxo 4-HPR (200µM) with HLM (0.5mg/ml) ± β-glucuronidase (800U).

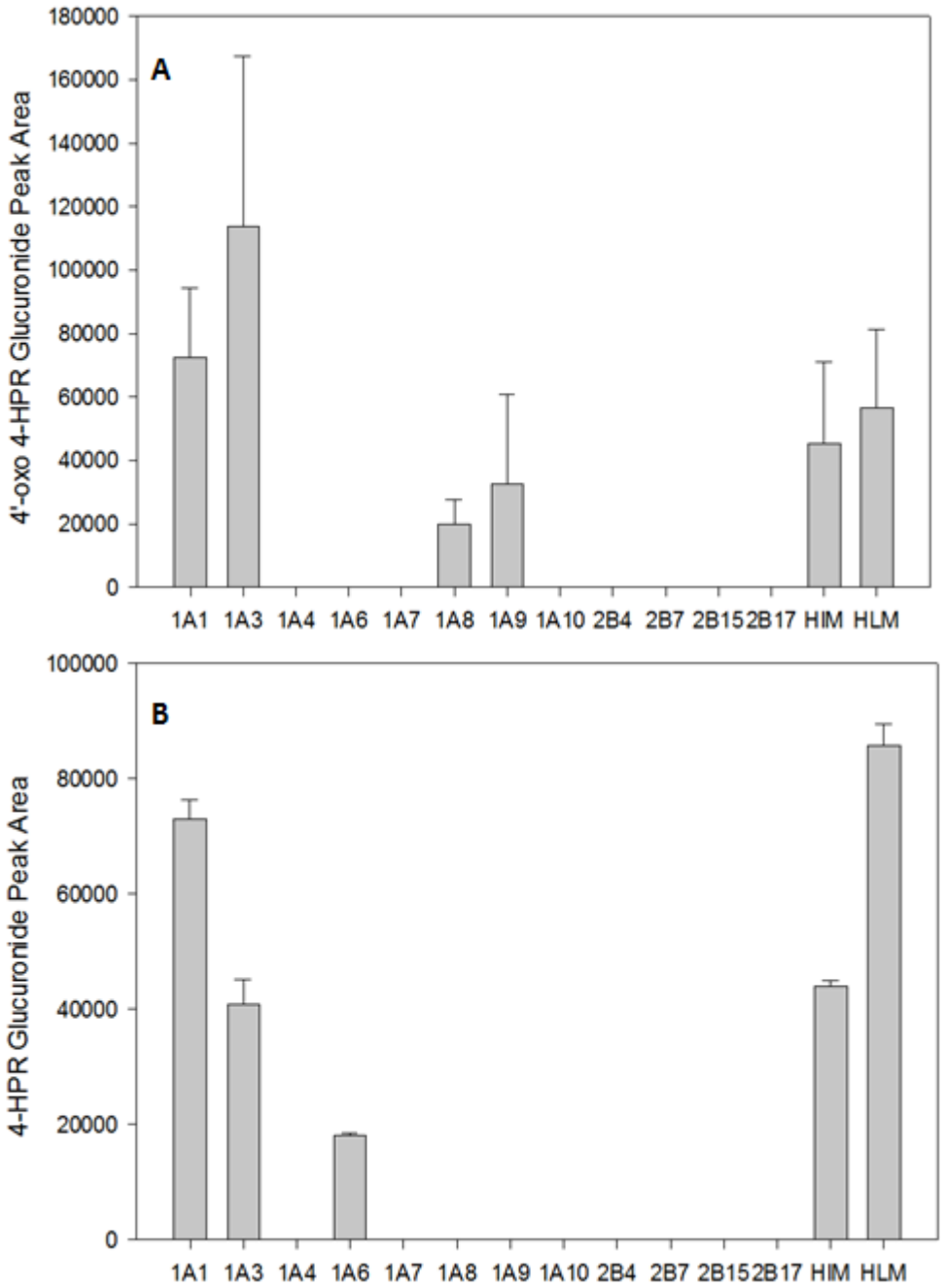

Figure 3-4. Formation of glucuronide metabolites of A) 4'-oxo 4-HPR and B) 4-HPR by a panel of Supersomes over-expressing individual human UGTs.

Metabolite formation was determined by HPLC analysis. Metabolites were generated following a 3h incubation of 4-HPR or 4'-oxo 4-HPR (200µM) and HIM, HLM or UGT Supersomes (0.5mg/ml). Results are the mean of 3 independent determinations (error bars are standard deviation).

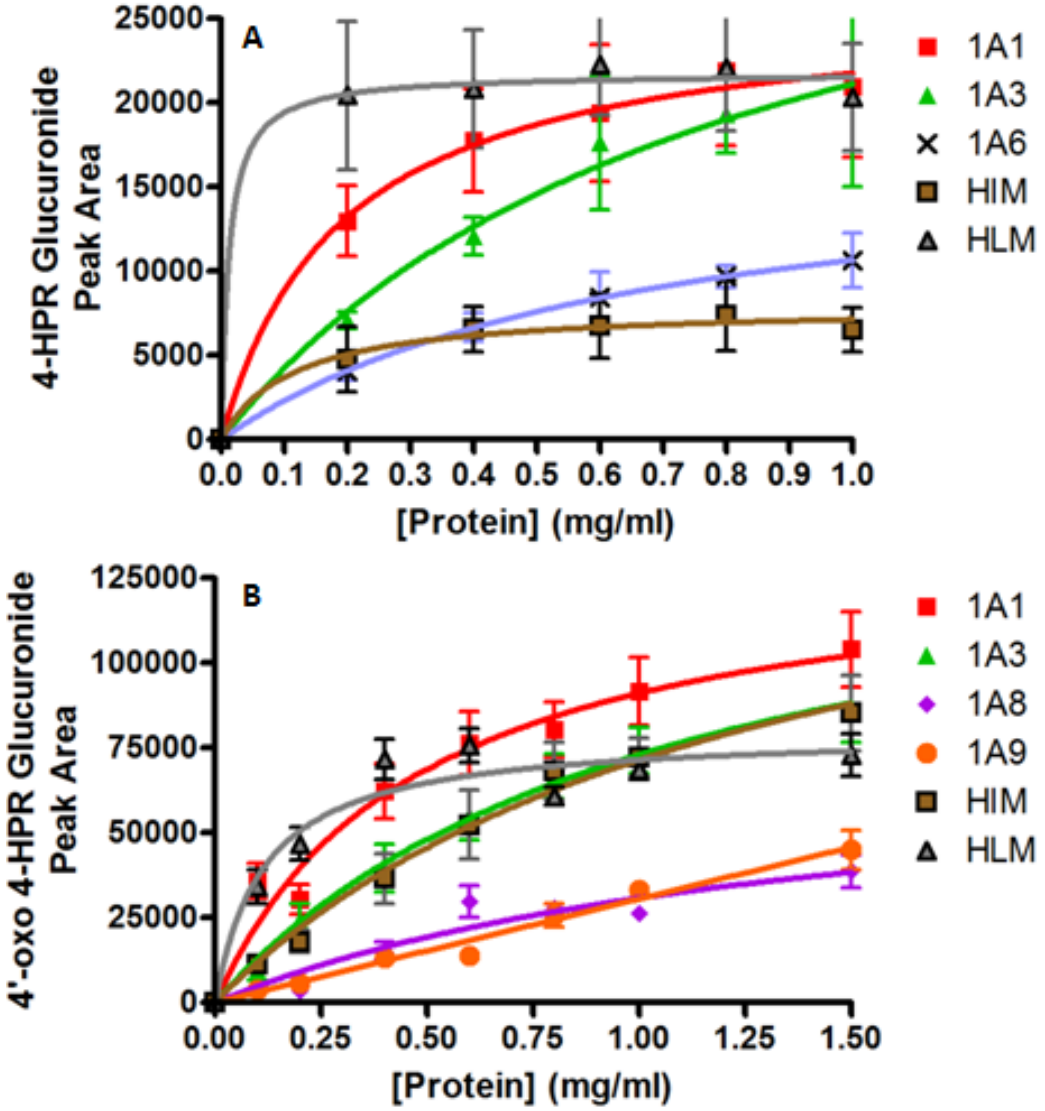

Figure 3-5. Effect of increasing protein concentration on the formation of A) 4-HPR glucuronide and B) 4'-oxo 4-HPR glucuronide by a panel of Supersomes over-expressing individual human UGTs.

The UGTs found to metabolise 4-HPR and 4'-oxo 4-HPR, as well as HIM and HLM (0-1.5mg/ml), were incubated with 4-HPR or 4'-oxo 4-HPR (200µM) for 3h. Metabolite formation was determined by HPLC analysis. Results are mean ± SD from 3 independent experiments.

Glucuronide production was related to protein concentration (Figure 3-5), incubation time (Figure 3-6) and substrate concentration (Figure 3-7) with kinetic parameters for 4-HPR glucuronide and 4'-oxo 4-HPR glucuronide formation provided in Table 3-5 and Table 3-6. V_{max} values for formation of 4'-oxo 4-HPR glucuronide of 0.6, 22, 0.7 and 0.07 (peak area units min/pmol UGT) were determined for UGTs 1A1, 1A3, 1A8 and 1A9 respectively and 456 and 870 peak area units/min for HIM and HLM. K_m values ranged from 230µM for UGT1A1 to 1151µM for UGT1A3. Metabolism to 4-HPR

glucuronide was markedly different to that for 4'-oxo 4-HPR, as not only was the glucuronide metabolite produced by UGT1A6 as well as 1A1 and 1A3 (V_{max} values of 0.2, 0.6 and 2.1 peak area units min/pmol UGT respectively), no metabolite was produced by UGTs 1A8 or 1A9. Again, K_m values were variable for all UGTs investigated, ranging from 389µM for UGT1A3 to 716µM for UGT1A1. Kinetic parameters for the glucuronidation of 4'-oxo 4-HPR were difficult to obtain due to limitations of substrate solubility. It was not possible to use concentrations of 4'-oxo 4-HPR greater than 500µM, however comparison of the slope of the plot with derived values for K_m/V_{max} suggest that the calculated V_{max} was accurately calculated.

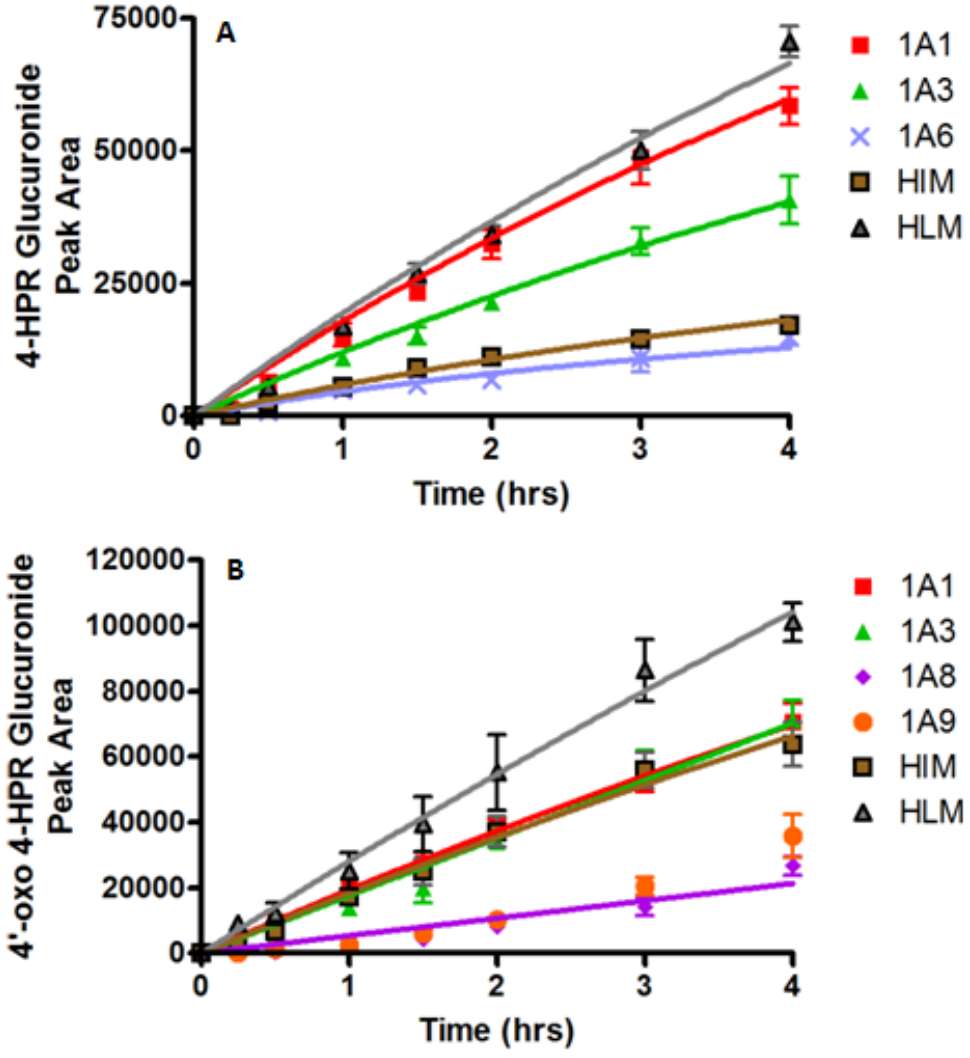

Figure 3-6. Formation of A) 4-HPR glucuronide and B) 4'-oxo 4-HPR glucuronide over time by a panel of Supersomes over-expressing individual human UGTs.

The UGTs found to metabolise 4-HPR and 4'-oxo 4-HPR, as well as HIM and HLM (0.5mg/ml), were incubated with 4-HPR (200µM) or 4'-oxo 4-HPR (200µM) for 0-4h. Metabolite formation was determined by HPLC analysis. Results are mean ± SD from 3 independent experiments.

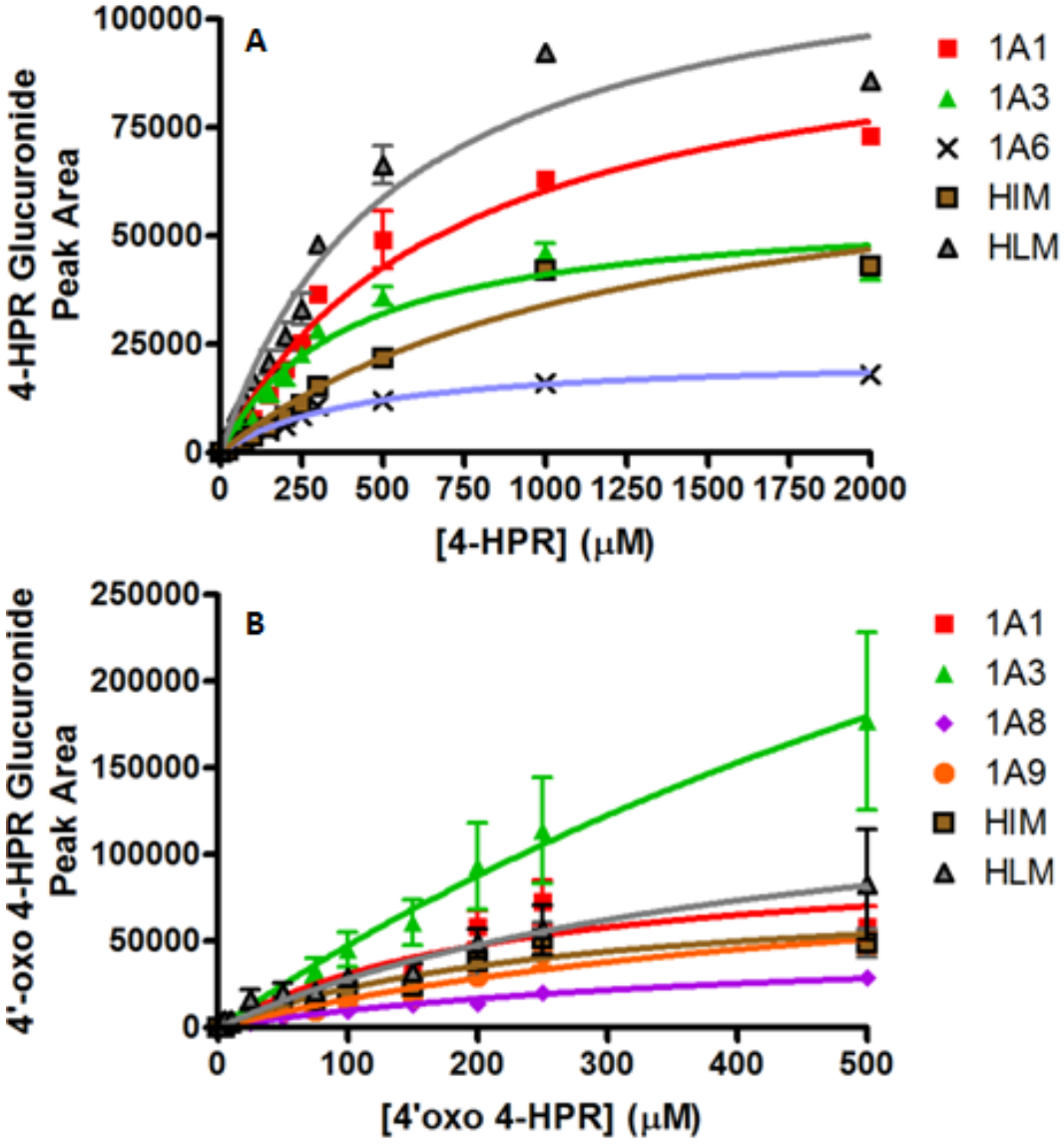

Figure 3-7. Effect of increasing substrate concentration on formation of A) 4-HPR glucuronide and B) 4'-oxo 4-HPR glucuronide by a panel of Supersomes over-expressing individual human UGTs.

The UGTs found to metabolise 4-HPR, as well as HIM and HLM (0.5mg/ml), were incubated with 4-HPR (0-2,000μM), or 4'-oxo 4-HPR (0-500μM) for 3h. Metabolite formation was determined by HPLC analysis. Results are mean ± SD from 3 independent experiments.

	K_m (µM)	V_{max}		
		(peak area units/min)	(peak area units/min/pmol UGT	V_{max}/K_m
UGT1A1	716 ± 87	577 ± 34	0.6 ± 0.1	0.001
UGT1A3	389 ± 53	317 ± 18	2 ± 0.1	0.005
UGT1A6	422 ± 46	124 ± 6	0.2 ± 0.1	0.0005
HIM	1212 ± 202	418 ± 38	N/A	N/A
HLM	540 ± 69	679 ± 39	N/A	N/A

Table 3-5. Kinetic parameters for the formation of the glucuronide metabolites of 4-HPR by a panel of UGT enzymes, HIM and HLM.

The UGTs found to metabolize 4-HPR as well as HIM and HLM (0.5mg/ml) were incubated with 4-HPR (0-2,000µM) for 3h. Metabolite formation was determined by HPLC analysis. Results are expressed as mean ± SD from n≥3 experiments. (N/A = not applicable as data on the individual UGT activities of HIM and HLM were not available).

Maximum rates of metabolism to 4-HPR glucuronide and 4'-oxo 4-HPR glucuronide per pmol of each UGT were compared by ANOVA followed by Bonferroni's post test, with $P \leq 0.05$ used to determine significance. Statistically significant differences were seen in metabolism to 4-HPR glucuronide and 4'-oxo 4-HPR glucuronide ($P < 0.0001$ and $P=0.0001$ respectively).

	K_m (μM)	V_{max}		
		(peak area units/min)	(peak area units/min/pmol UGT	V_{max}/K_m
UGT1A1	230 ± 95	569 ± 119	0.6 ± 0.1	0.0026
UGT1A3	1151 ± 96	3295 ± 2126	22 ± 14	0.0191
UGT1A8	437 ± 160	294 ± 66	0.7 ± 0.2	0.0016
UGT1A9	551 ± 224	596 ± 159	0.1 ± 0.1	0.0001
HIM	261 ± 97	456 ± 327	N/A	N/A
HLM	454 ± 273	870 ± 327	N/A	N/A

Table 3-6. Kinetic parameters for the formation of the glucuronide metabolites of 4'-oxo 4-HPR by a panel of UGT enzymes, HIM and HLM.

The UGTs found to metabolize 4'-oxo 4-HPR as well as HIM and HLM (0.5mg/ml) were incubated with 4'-oxo 4-HPR (0-500μM) for 3h. Metabolite formation was determined by HPLC analysis. Results are expressed as mean ± SD from n≥3 experiments. (N/A = not applicable as data on the individual UGT activities of HIM and HLM were not available).

3.4 Discussion

The metabolism of 13-cis RA, 4-oxo 13-cis RA, 4-HPR and 4'-oxo 4-HPR by UGTs was investigated in order to assess the potential role played by these enzymes *in vivo* and the likely impact of phase II detoxification on drug efficacy.

Both 13-cis RA and 4-HPR have been used to treat neuroblastoma, with 13-cis RA currently included in the standard treatment protocol for high risk patients. There is therefore considerable interest in comparing metabolism of both parent retinoid and 4-oxo metabolite for both 13-cis RA and 4-HPR. Although several studies have been carried out to assess the contribution of CYP metabolism to 13-cis RA and its efficacy, there are currently no data on metabolism by glucuronidation of either 13-cis RA or its 4-oxo metabolite. As both 13-cis RA and 4-HPR are administered orally for the treatment of neuroblastoma, enzyme kinetic studies for the glucuronidation of 13-cis RA and 4-oxo 13-cis RA were performed with microsomes from human liver and intestine (HLM and HIM), as the majority of UGTs are primarily expressed in the liver, with extra-hepatic expression mainly occurring in the intestinal epithelium (Bock, 2010). There were considerable differences in the kinetic parameters observed for 13-cis RA and its oxidative metabolite, 4-oxo 13-cis RA. Although both substrates were extensively glucuronidated by HIM, they had remarkably different metabolism profiles, for example a K_m of 5μM was observed for 13-cis RA compared to 69μM for 4-oxo 13-cis RA. Comparable data were also observed for HLM. Similarly, although the V_{max} for glucuronidation of 13-cis RA by HLM was much lower than that for 4-oxo 13-cis RA (335 peak area units/min and 11,978 peak area units/min respectively), a markedly lower K_m value was observed for 13-cis RA (8μM compared to 95μM for 4-oxo 13-cis RA). This would suggest that glucuronidation of 13-cis RA by HLM and HIM is more likely to be clinically relevant than glucuronidation of its 4-oxo metabolite. Maximum plasma concentrations achieved in a clinical trial in neuroblastoma patients were 2.8μM for 13-cis RA and 4.7μM for 4-oxo 13-cis RA on day 14 following two courses of 80mg/m^2/day of 13-cis RA (Veal et al., 2007).

Enzyme kinetic studies for the glucuronidation of 13-cis RA and 4-oxo 13-cis RA were also performed in Supersomes over-expressing human UGTs 1A1, 1A3, 1A7, 1A8 and 1A9. These were the UGTs found to generate the glucuronide metabolite of both substrates and therefore were utilised further to elucidate the individual UGTs likely to

be responsible for the metabolism by HIM and HLM. UGT1A3 clearly had the highest rate of activity for the glucuronidation of both 13-cis RA and 4-oxo 13-cis RA (25.7 and 89.0 peak area units/min/pmol UGT respectively). It is again, however, doubtful that glucuronidation by UGT1A3 has significant clinical relevance as, despite the high rate of the reaction, the K_m values observed were at least 20-fold higher than peak plasma concentrations reported *in vivo* (Veal et al., 2007, Villablanca et al., 1995). Based on these criteria, the only UGT that may be of clinical relevance is UGT1A9. Although this UGT had a low rate of reaction for both substrates (V_{max} values of 0.04 and 0.2 peak area units/min/pmol UGT for 13-cis RA and 4-oxo 13-cis RA respectively), the K_m value of 3μM for 13-cis RA is well within clinically achievable plasma concentrations. The K_m value of UGT1A9 for 4-oxo 13-cis RA (18μM) was approximately 4-fold higher than clinically relevant plasma concentrations, however this was still the lowest K_m value for any of the UGTs tested. As UGT1A9 is highly expressed in the liver and gastro-intestinal tract (Ohno and Nakajin, 2009), it is likely to be the UGT enzyme of most clinical interest when investigating the glucuronidation of both 13-cis RA and 4-oxo 13-cis RA. It is therefore possible that polymorphisms in UGT1A9 may therefore be a factor in determining the efficacy of 13-cis RA.

There are several known polymorphisms of UGT1A9, some of which have already been associated with affecting drug exposure. For example, significantly lower exposure to mycophenolic acid (an immunosuppressive drug) occurs in patients with UGT1A9-275/-2152 polymorphisms, whereas patients expressing UGT1A9*3 had significantly higher exposure to the drug. (Levesque et al., 2007, Miura et al., 2008). In addition, although dose reduction of irinotecan is advised for patients homozygous for UGT1A1*28 in order to reduce toxicity due to altered clearance of SN-38 (the active metabolite of irinotecan) (United States Food and Drug Administration, 2010), there is also evidence that isoforms of UGT1A9 may also play a role in determining drug disposition. Studies involving recombinant UGT enzymes have shown that glucuronidation of SN-38 is significantly lower for UGT1A9*3 than for the wild-type allele, UGT1A9*1. This may therefore result in lower clearance of SN-38 and a corresponding increase in risk of acute toxicity (Villeneuve et al., 2003). As UGT1A9 polymorphisms are found in approximately 5% of Caucasians, the impact on glucuronidation and therefore clearance of any drug metabolised by UGT1A9 could be significant, and may be a factor in the high inter-patient variability seen in 13-cis RA plasma concentrations in clinical trials (Veal et al., 2007). Currently, there is a lack of

evidence for the detection of glucuronide metabolites of 13-cis RA and its metabolites, or 4-HPR and its metabolites, although 13-cis retinoyl-beta-glucuronide and all-trans retinoyl-beta-glucuronide have been identified as major metabolites of 13-cis RA and ATRA in monkeys (Kraft et al., 1991).

Significant inter-patient pharmacokinetic variability is also observed in clinical trials of neuroblastoma patients treated with 4-HPR (Garaventa et al., 2003, Formelli et al., 2008). If glucuronides of 4-HPR are extensively produced, it could be of particular clinical interest, as 4-HPR glucuronide has been found to have cytotoxic properties, and is in fact more potent at inducing cell death in a breast cancer cell line than 4-HPR itself (Bhatnagar et al., 1991). Enzyme kinetic studies for the glucuronidation of 4-HPR and 4'-oxo 4-HPR were consequently performed with microsomes from human liver and intestine (HLM and HIM), as well as a panel of Supersomes over-expressing individual human UGT enzymes.

As predicted, both HLM and HIM were able to glucuronidate 4-HPR and 4'-oxo 4-HPR, with the metabolite produced confirmed as a glucuronide by its breakdown by β-glucuronidase. Metabolism of 4-HPR and 4'-oxo 4-HPR by HLM was similar for both substrates, with K_m values of 540 and 454μM and V_{max} values of 679 and 870 peak area units/min respectively. However, the glucuronidation reaction observed in HIM differed substantially between 4'-oxo 4-HPR and 4-HPR. The K_m for glucuronidation of 4-HPR by HIM was 1212μM compared to 261μM for 4'-oxo 4-HPR, with comparable V_{max} values of 418 peak area units/min for 4-HPR and 456 peak area units/min for 4'-oxo 4-HPR.

In order to ascertain the position of glucuronidation on 4-HPR, incubations were also carried out with 4-MPR and 4-EPR. No glucuronide metabolite was produced with either of these metabolites, indicating that the presence of the methoxy or ethoxy group was able to prevent 4-HPR glucuronidation. This means that the expected position of the glucuronosyl is on the 4^{th} carbon of the amide ring, as shown in Figure 3-8. It is predicted that glucuronidation of 4'-oxo 4-HPR would also occur at the same position.

Enzyme kinetic studies for the glucuronidation of 4-HPR and 4'-oxo 4-HPR were also performed in Supersomes over-expressing human UGTs in order to elucidate the individual UGTs likely to be responsible for the metabolism by HIM and HLM.

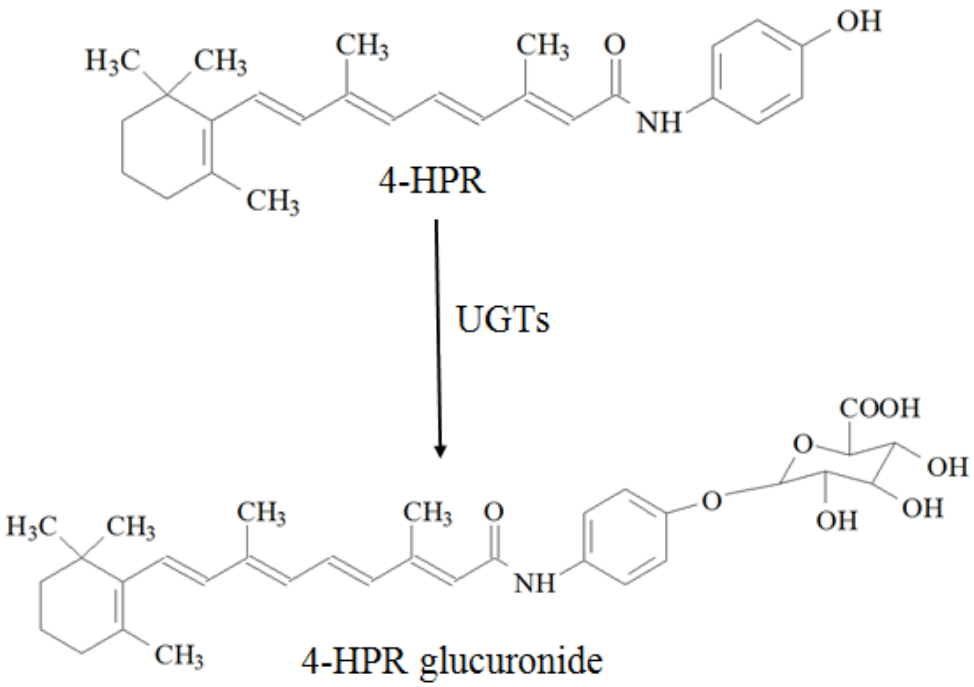

Figure 3-8. Structure of 4-HPR and proposed structure of 4-HPR glucuronide, demonstrating the likely position of glucuronidation.

Enzyme kinetics of 4-HPR glucuronidation were investigated with UGTs 1A1, 1A3 and 1A6, as these were the UGTs found to produce the glucuronide metabolite of 4-HPR. Similarly glucuronidation of 4'-oxo 4-HPR was investigated with UGTs 1A1, 1A3, 1A8 and 1A9, as these were the UGTs found to produce the glucuronide metabolite of 4'-oxo 4-HPR. This represents a key difference in the pattern of glucuronidation seen with 4-HPR and 4'-oxo 4-HPR as compared to 13-cis RA and 4-oxo 13-cis RA, where the same panel of UGTs was able to glucuronidate both 13-cis RA and 4-oxo 13-cis RA. Glucuronidation by any of the UGTs tested represented a relatively slow reaction, yielding relatively low concentrations of glucuronide metabolites. The highest concentrations of glucuronides were generated with UGT1A3, with V_{max} values of 22.0 peak area units/min/pmol UGT for 4'-oxo 4-HPR, and 2.11 peak area units/min/pmol UGT for 4-HPR. V_{max} values for all other UGTs were at least 30-fold lower for glucuronidation of 4'-oxo 4-HPR than observed for UGT1A3, and at least 3-fold lower for glucuronidation of 4-HPR. K_m values for all UGTs were relatively high, with the lowest K_m value for glucuronidation of 4-HPR found with UGT1A3 (389μM) and for glucuronidation of 4'-oxo 4-HPR by UGT1A1 (230μM). As clinical trials involving 4-HPR administration have failed to result in consistent peak plasma concentrations of 4-HPR above 10μM (Formelli et al., 2003, Garaventa et al., 2003, Formelli et al., 2008), it

is unlikely that metabolism by glucuronidation will play a major role in the clearance of 4-HPR at clinically relevant levels, or that polymorphisms of UGT enzymes would have a major clinical impact. However, UGT polymorphisms have been found to significantly alter the metabolism of other chemotherapeutic compounds, despite C_{max} values in patients being much lower than the K_m determined *in vitro*. C_{max} values of SN-38, the active metabolite of irinotecan, observed in patients are less than 1μM (Chabot, 1997, Sasaki et al., 1995), with in vitro K_m values of greater than 10μM (Jinno et al., 2003, Hanioka et al., 2001). Despite this 10-fold or greater difference in K_m and C_{max} concentrations, irinotecan toxicity is associated with polymorphisms in UGT1A1 and 1A9 (Gagné et al., 2002, Villeneuve et al., 2003). It is possible therefore, that improvements in bioavailability of 4-HPR by novel formulations may result in an increased impact of glucuronidation and consequently of UGT polymorphisms.

Elucidation of the contribution of glucuronidation to the metabolism of 13-cis RA, 4-HPR and their respective oxidative metabolites suggests that clearance by glucuronidation may play a much greater role in the metabolism of 13-cis RA than that of 4-HPR, and that the contribution of glucuronidation to the clearance of 4-HPR and 4'-oxo 4-HPR is unlikely to be significant at currently clinically achievable concentrations of 4-HPR. The possible impact of clearance via glucuronidation for 13-cis RA and 4-oxo 13-cis RA is relatively high, and merits further investigation in a patient population, particularly in regard to polymorphisms of UGT1A9.

Chapter 4 *In Vitro* 4-HPR metabolism with Ewing's sarcoma and neuroblastoma cell lines

4.1 Introduction

Neuroblastoma and Ewing's sarcoma have relatively low five year survival rates, despite intensive, multimodal treatment (Cancer Research UK, 2005). Standard treatment of high risk neuroblastoma currently consists of high dose induction chemotherapy, followed by myeloablative therapy and autologous bone marrow transplantation. For the last 10 years, this has been followed by minimal residual disease treatment with 13-cis RA. A phase III clinical trial in neuroblastoma patients showed an increase in five-year survival from 29 to 46%, that was further increased to 59% when combined with autologous bone marrow transplantation (p=0.054) (Matthay et al., 1999, Matthay et al., 2009). Ewing's sarcoma treatment currently involves surgery, radiation and chemotherapy. Multidrug chemotherapy for high risk ESFT includes vincristine, doxorubicin, ifosfamide, and etoposide, with most protocols also including cyclophosphamide (Juergens et al., 2006).

Both neuroblastoma and, particularly, Ewing's sarcoma cell lines have been found to be sensitive to 4-HPR treatment *in vitro* (Lovat et al., 2000, Myatt and Burchill, 2008), as well as being sensitive to the 4'-oxo metabolite of 4-HPR (Villani et al., 2006). This active metabolite has also been found in plasma samples during phase I clinical trials of 4-HPR in neuroblastoma patients (Villablanca et al., 2006, Formelli et al., 2008).

As previously described in chapter 2, metabolism by CYPs plays a significant part in the metabolism of many drugs, including 4-HPR. A group of these enzymes, known as the CYP26 family, are induced by retinoic acid (White et al., 1997). *CYP26A1* is induced by ATRA and 13-cis RA, with inhibition of *CYP26A1* by retinoic acid metabolism blocking agents (RAMBAs) significantly increasing plasma concentrations of ATRA and 13-cis retinoic acid both *in vitro* and in a neuroblastoma mouse model (Armstrong et al., 2005, Armstrong et al., 2007b). Due to the structural similarities between 4-HPR and the other analogues of retinoic acid, metabolism by CYP26A1 may impact on 4-HPR oxidation.

Little is currently known about intracellular 4-HPR metabolism and its effects on tumour cell sensitivity. This study therefore investigated intracellular 4-HPR metabolism, the contribution of CYP26A1 to 4-HPR metabolism and the possible modulation of CYP26 metabolism with RAMBAs.

4.2 Materials and Methods

4.2.1 Chemicals

Roswell Park Memorial Institute (RPMI) 1640 medium, ATRA, L-glutamine and sodium pyruvate were purchased from Sigma-Aldrich (Poole, UK). Foetal calf serum was provided by Gibco (Paisley, Scotland). CellTiter 96® AQueous Non-Radioactive Cell Proliferation Assay (MTS assay) was supplied by Promega (Southampton, UK). Tissue culture plasticware was purchased from Nunc (Denmark). Bio-Rad Protein Assay Dye and Bovine Serum Albumin Standard were from Bio-Rad Labs Ltd (UK). The MicroAmpTM Fast Optical 96-well 0.1ml reaction plate, ABI 7500 Fast Real-Time PCR system, GeneAmp 2700 PCR system, SNP genotyping assay mix, TaqMan® Genotyping PCR master mix and cDNA reverse transcription kit with RNase inhibitor were supplied by Applied Biosystems (UK). The SpectraMax® 250 Microplate Spectrophotometer System was from Molecular Devices Corporation (Reading, UK). The NanoDrop™ 1000 spectrophotometer was purchased from Thermo Scientific (Hampshire, UK).

4.2.2 Culture of cell lines

The neuroblastoma cell line SH-SY5Y was obtained from Dr C. Redfern (NICR, Newcastle University). The Ewing's sarcoma cell lines RD-ES, TC-32, TCC-446 and SK-ES were provided by Prof. S. Burchill (Experimental Oncology, Leeds University, UK). Cell lines were grown in monolayer culture in complete RPMI 1640 medium containing 10% foetal bovine serum (FBS), 1% L-glutamine and 1% sodium pyruvate. Cells were incubated at 37°C in a humidified atmosphere of 5% CO_2 and were maintained in an exponential growth phase by passage every 3-4 days with addition of fresh medium as required. Cells were harvested by trypsinisation using 0.25% Trypsin-EDTA when 70-80% confluent, centrifuged at 1,000g for 5min at room temperature and resuspended in fresh medium at the appropriate dilution factor.

4.2.3 Incubation of 4-HPR with cell lines

Cells were seeded in 6-well plates (20,000 cells per well) in complete RPMI (2ml) and left to adhere for 24h. The medium was then removed and replaced with medium

containing 4-HPR (2 or 20μM) and incubated for a further 3, 6 or 24h (2μM 4-HPR was used for 24h incubations to avoid effects on cell viability; 20μM was used for 3h and 6h incubations). Medium was then discarded and the cells were rinsed with ice-cold PBS (1ml). Cells were harvested by addition of trypsin (1ml) for 3-5min at 37°C to allow detachment of cells from the wells. The cell/trypsin solution was transferred into centrifuge tubes and centrifuged at 15,000g for 5min. Supernatant was discarded and the cell pellet was vortexed to break up the cells. Cell pellets were stored at -20°C until required for analysis.

4.2.4 Determination of intracellular concentrations of 4-HPR and metabolites

Cell pellets were defrosted on ice and acetonitrile (100μl) added, cells were vortexed and then centrifuged at 15,000g for 5min. The supernatant obtained was used for analysis of 4-HPR and metabolite levels, and the cell pellet was retained for protein analysis and determination of *CYP26A1* expression. HPLC analysis of intracellular 4-HPR concentrations was achieved using a Waters 2690 Separations Module and 996 Photodiode array (PDA) detector (Waters Ltd., Elstree, UK), with Waters Millennium software for data acquisition. A Waters Symmetry C_{18} 3.5 μm (4.6 x 150 mm) column was used with mobile phases (A) 70% acetonitrile / 30% (0.2%) acetic acid and (B) acetonitrile / 0.2% acetic acid. A linear gradient ran at 1ml/min from 100% A at 0min to 100% B at 20min, returning to 100% A for 10min to re-equilibrate the column. A sample volume of 50μl was injected onto the column for analysis.

4.2.5 Pre-incubation of cell lines with ATRA

In order to investigate the effect of up-regulation of *CYP26A1* expression on 4-HPR metabolism, cells were pre-incubated with ATRA prior to incubation with 4-HPR (Armstrong et al., 2005, Armstrong et al., 2007b). Cells seeded in 6- or 96-well plates were allowed to establish growth for 24h, and then medium was replaced with fresh medium containing ATRA (10μM). Cells were incubated for 24h, before medium was removed and replaced with medium containing 4-HPR (20μM), as described in section 4.2.3. Control cells not pre-treated with ATRA had their medium replaced with medium containing an equivalent concentration of ethanol as that used for ATRA pre-

treated cells. Cell pellets from 6-well plates were retained for protein analysis and determination of *CYP26A1* expression.

4.2.6 Cell viability assay

Cell viability was determined using the CellTiter 96® AQueous Non-Radioactive Cell Proliferation Assay (MTS assay). Cells were seeded in 96-well plates at a density of 5,000 cells per well in RPMI (200µl). The cells were left to adhere for 24h, then the medium was removed and replaced with medium (200µl) containing 4-HPR (0-50µM). Cells were incubated with drug for 96h, and then medium was removed and replaced with medium containing MTS reagent (12µl per 200µl of medium). Cells were incubated with MTS for 1-4h and the absorbance at 490nm was measured using a SpectraMax® 250 Microplate Spectrophotometer. Absorbance values in wells containing 4-HPR were compared to absorbance values in untreated wells and used to determine the effect of drug concentration on cell proliferation. Experiments were carried out in triplicate, with 6 wells treated with each concentration of drug for each replicate.

4.2.7 Protein analysis

In order to adjust for different cell numbers for intracellular 4-HPR concentration assays, cell pellets were retained for protein analysis utilising the Bradford assay. Cell pellets were defrosted on ice and dH_2O (50µl) was added. Pellets were vortexed and vigorously mixed by pipetting to homogenise the sample. An aliquot of sample (10µl) was then added to 4 wells of a 96 well plate. Bradford reagent (190µl) was added to each well and samples were mixed by pipetting. Absorbance was measured at 595nm using a SpectraMax® 250 Microplate Spectrophotometer and compared to standards of known concentrations of BSA (bovine serum albumin).

4.2.8 Inhibition of HLM metabolism with R116010

HLM (0.5mg/ml) and the CYP26 inhibitor R116010 (0-100µM) were incubated with 4-HPR (50µM) in phosphate buffer (100mM, pH 7.4), containing $MgCl_2$ (1mM) and NADPH (2mM) in a final volume of 200µl at 37°C for 3h. The reaction was stopped by

addition of acetonitrile (200µl) and samples were centrifuged at 10,000g for 5min to remove all protein. Supernatant was then retained for HPLC analysis.

4.2.9 Determination of CYP26A1 expression in cell lines

CYP26A1 expression in cell lines was determined by real-time assay before and after incubation of cells with ATRA (10µM) for 24h, as previously described (Armstrong et al., 2005, Armstrong et al., 2007b) and in section 4.2.5. *CYP26A1* expression was measured by fold-increase, relative to cells treated with 0.01µM ATRA. This provides a base-line expression for comparison to expression before and after ATRA pre-treatment. Pre- and post-incubation *CYP26A1* expression was compared for each cell line with a Student's T-test. $P \leq 0.05$ used to determine significance. All calculations were performed with GraphPad Prism version 4.0 software.

4.2.9.1 RNA extraction from cell pellets

RNA was extracted from cell pellets using the RNeasy® mini kit (Qiagen, Crawley UK), according to the manufacturer's instructions. Buffer RLT with β-mercaptoethanol (350µl) was added to the cell pellet and vortexed. The sample was homogenised by passing the solution through a narrow gauge needle several times, prior to addition of 70% ethanol (350µl) and mixed by pipetting. The homogenate was then added to an RNeasy column and centrifuged at 8,000g for 15s. The flow through was discarded and RW1 buffer (350µl) was added to the column before it was again centrifuged at 18,000g for 15s. DNaseI (80µl) was added to the column and incubated for 15min. A further aliquot of RW1 buffer (350µl) was then added to the column and the flow through was discarded after centrifugation for 15s at 8,000g. Buffer RW1 (700µl) was added to the column and it was again centrifuged at 8,000g for 15s. The flow through was discarded, and a fresh collection tube used with the column. Buffer RPE (500µl) was added to the column and centrifuged at 8,000g for 15s. The flow through was discarded and buffer RPE (500µl) was added to the column for a second time, followed by centrifugation at 8,000g for 2min. The flow through and collection tube were then discarded. RNA was finally eluted from the column into a sterile 1.5ml collection tube by the addition of RNase-free water (35µl) and centrifugation at 8,000g for 1min. The quality and

concentration of RNA extracted was analysed on a NanoDrop™ 1000 spectrophotometer. RNA was stored at -80°C until required.

4.2.9.2 Reverse transcription of RNA

RNA extracted from cell pellets was reverse transcribed using the high capacity cDNA reverse transcription kit with RNase inhibitor according to the manufacturer's instructions. A master mix was made up containing 10 x RT buffer, dNTP (100mM), 10 x random hexamers and reverse transcriptase (20U/µl). The master mix was made up to the appropriate volume for the number of samples with nuclease free H_2O. Master mix (10µl) was added to 1µg of RNA and made up to a 20µl final volume with sterile H_2O. The solution was then mixed by pipetting and samples were incubated on the GeneAmp 2700 PCR system with the following conditions applied: 25°C for 10min, followed by 37°C for 2h, then 85°C for 5s and then a 4°C hold. cDNA was stored at -80°C until required.

4.2.9.3 CYP26A1 Real-Time assay

cDNA was diluted in sterile H_2O to give a final concentration of 20ng/µl. A master mix was then made up containing 2 x TaqMan® Genotyping PCR mastermix and 20 x SNP genotyping assay mix. The master mix was made up to the appropriate volume for the number of samples with nuclease free H_2O. An aliquot of mastermix (24µl) was added to each well of a Fast Optical 96-well plate. DNA samples (1µl of 20ng/µl) were added to each well (except for two no-template control wells), and mixed by pipetting. The plate was then covered with optical adhesive film and centrifuged at 1,500g for 1min before analysis on the ABI 7500 Fast Real-Time PCR system.

4.3 Results

4.3.1 Intracellular concentrations of 4-HPR and metabolites

Intracellular concentrations of 4-HPR and its metabolites were determined by HPLC analysis following a 6h incubation of 4-HPR (20μM) with neuroblastoma and Ewing's sarcoma cell lines. As shown in Figure 4-1, all five cell lines tested were able to metabolise 4-HPR to its inactive metabolite 4-MPR.

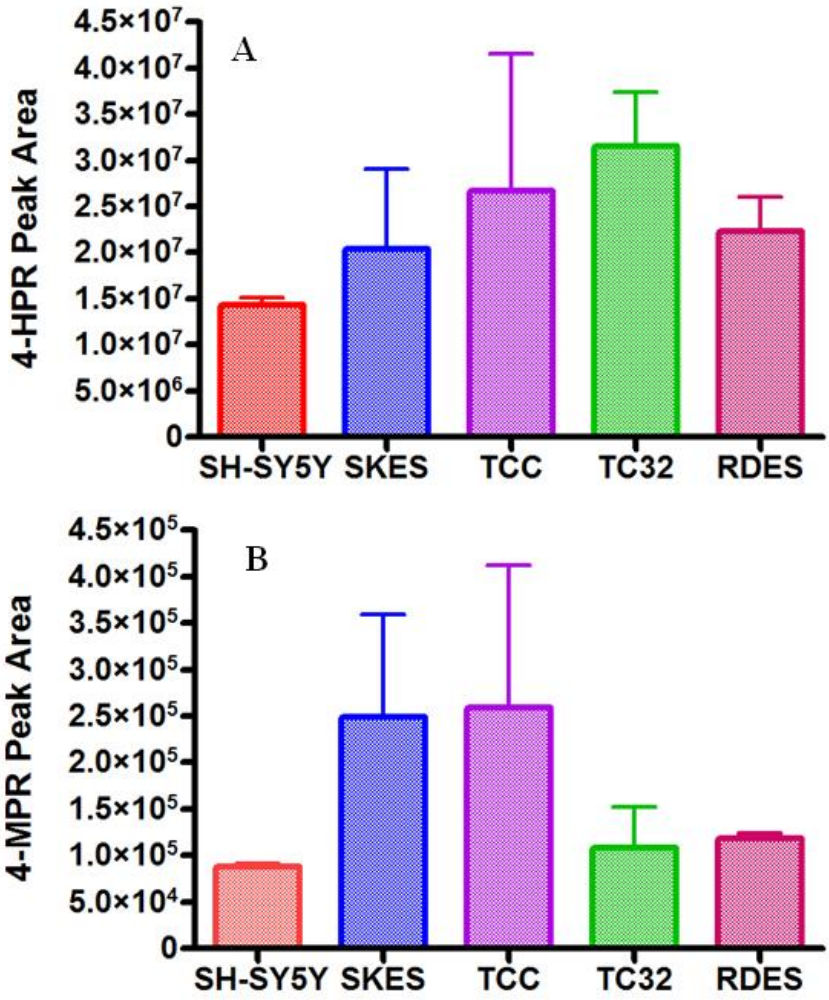

Figure 4-1. Intracellular concentrations of A) 4-HPR and B) 4-MPR following incubation of Ewing's sarcoma and neuroblastoma cell lines with 4-HPR.

Metabolite peak area was normalized to protein concentration (determined by Bradford assay). Metabolites were generated by incubation of 4-HPR (20μM) with each cell line for 6h. Results are the mean of 3 independent determinations (error bars are standard deviation).

Mean intracellular concentrations of 4-HPR varied, ranging from $1.4x10^7$ peak area units in SH-SY5Y cells to $3.1x10^7$ peak area units in TC-32 cells. Mean intracellular concentrations of 4-MPR also varied, ranging from $8.8x10^4$ peak area units in SH-SY5Y

cells to $2.6x10^5$ peak area units in TCC-446 cells. There was no correlation between peak area of 4-HPR and peak area of 4-MPR, with ratios of 4-HPR:4-MPR peak area units varying from 83 for SK-ES to 340 for TC-32. Other ratios were 107, 162 and 188 for TCC-446, SH-SY5Y and RD-ES respectively.

As shown in Figure 4-2, all four Ewing's sarcoma cell lines were able to metabolise 4-HPR to both 4'-OH 4-HPR and 4'-oxo 4-HPR, whereas no metabolism to these oxidative metabolites was observed in the neuroblastoma cell line SH-SY5Y.

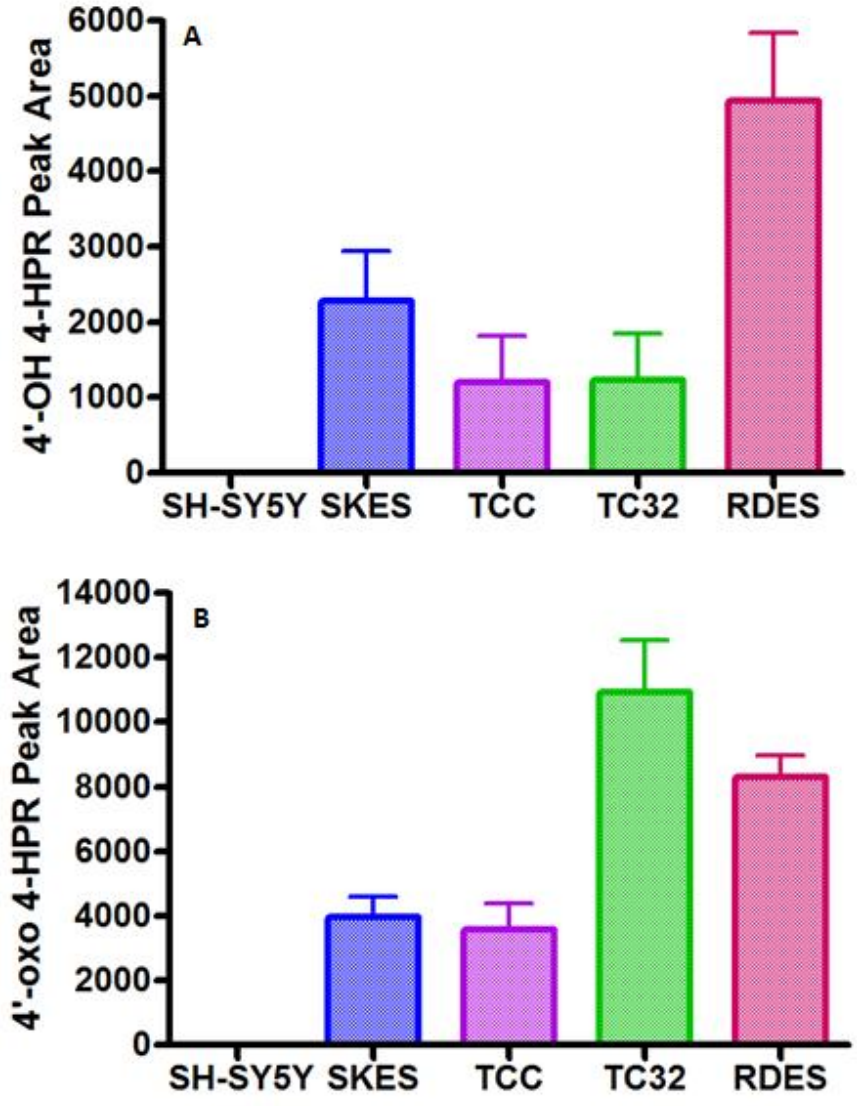

Figure 4-2. Intracellular concentrations of A) 4'-OH 4-HPR and B) 4'-oxo 4-HPR metabolites following incubation of Ewing's sarcoma and neuroblastoma cell lines with 4-HPR.

Metabolite peak area was normalized to protein concentration (determined by Bradford assay). Metabolites were generated by incubation of 4-HPR (20μM) with each cell line for 6h. Results are the mean of 3 independent determinations (error bars are standard deviation).

Intracellular concentrations of both oxidative metabolites varied between Ewing's sarcoma cell lines, although 4'-oxo 4-HPR was the major oxidative metabolite in all cases. 4'-OH 4-HPR concentrations ranged from 1,206 peak area units for TCC-446 cells, to 4,933 peak area units for RD-ES cells. Mean concentrations of the active metabolite, 4'-oxo 4-HPR were highest in TC-32 cells (10,942 peak area units). Mean 4'-oxo 4-HPR concentrations were lower in RD-ES cells (8,297 peak are units), although markedly higher than concentrations seen in TCC-446 and SK-ES cells (3,565 and 3,977 peak area units respectively). There was no correlation between peak area of 4-HPR and peak area of either 4'-OH 4-HPR or 4'-oxo 4-HPR.

4.3.2 Effect of ATRA on intracellular concentrations of 4-HPR and metabolites

In order to investigate the potential contribution of CYP26 to 4-HPR metabolism, cells were pre-treated with ATRA (10μM) for 24h to upregulate *CYP26A1* expression. As shown in Figure 4-3, pre-incubation of cell lines with ATRA had no marked effect on intracellular concentrations of 4-HPR or its inactive metabolite, 4-MPR.

However, as shown in Figure 4-4, intracellular concentrations of the oxidative metabolites were higher in all cell lines following pre-treatment with ATRA. Authentic standards for 4'-OH 4-HPR and 4'-oxo 4-HPR were not available, so it was assumed that there was a linear relationship between metabolite peak area and metabolite concentration, as there is for 4-HPR and 4-MPR. The greatest increase in extent of metabolism was seen in TC-32 cells, where metabolism to 4'-OH 4-HPR increased by 236% (from 1,226 peak area units to 4,126 peak area units), and metabolism to 4'-oxo 4-HPR increased by 90% (from 10,942 peak area units to 20,826 peak area units). For the neuroblastoma cell line, SH-SY5Y, both oxidative metabolites were only produced when cells were pre-treated with ATRA. The highest concentrations of the active metabolite 4'-oxo 4-HPR were found in the Ewing's sarcoma cell line TC-32 following pre-treatment with ATRA (20,754 peak area units). The increase in metabolism to 4'-OH 4-HPR was significant for SH-SY5Y cells ($p < 0.001$), TCC-446 cells ($p = 0.02$) and TC-32 cells ($p = 0.02$). Although there was a substantial increase in metabolism to 4'-OH 4-HPR in SK-ES cells, the increase did not reach significance ($p = 0.13$), and was also not significant in RD-ES cells ($p = 0.22$). Similar results were seen for the increase in metabolism to 4'-oxo 4-HPR, with significant increases seen in SH-SY5Y, TCC-446 and TC-32 cells ($p <0.001$, $p = 0.03$ and $p = 0.004$ respectively). Again, the

increase in metabolism by SK-ES cells did not reach significance (p = 0.15) and was also not significant for RD-ES cells (p = 0.15).

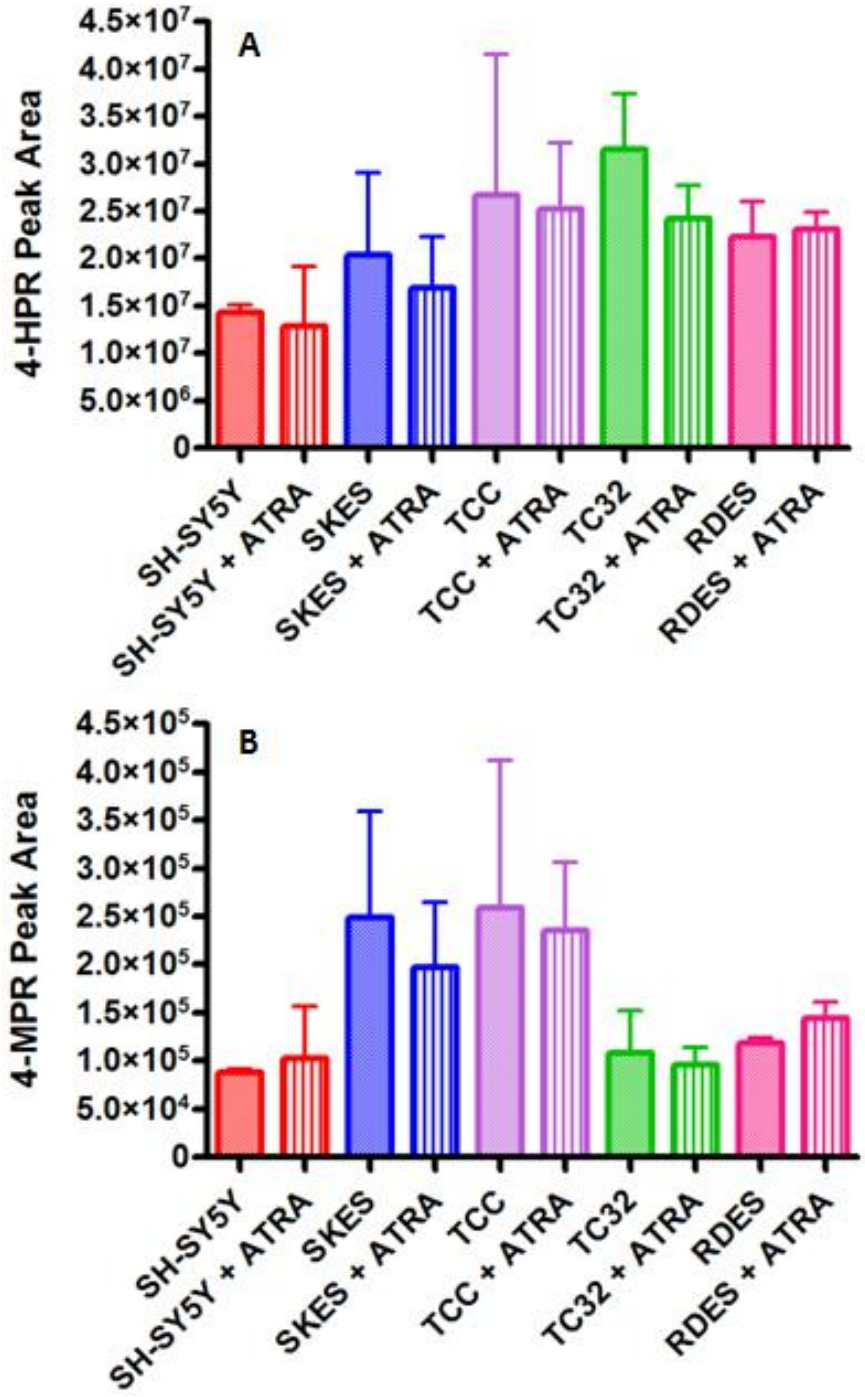

Figure 4-3. Intracellular concentrations of A) 4-HPR and B) 4-MPR by Ewing's sarcoma and neuroblastoma cell lines following pre-treatment with ATRA.

Peak areas were normalized to protein concentration (determined by Bradford assay). Metabolites were generated by incubation of 4-HPR (20μM) with each cell line for 6h, following pre-incubation with ATRA (10μM) for 24h. Results are the mean of 3 independent determinations (error bars are standard deviation).

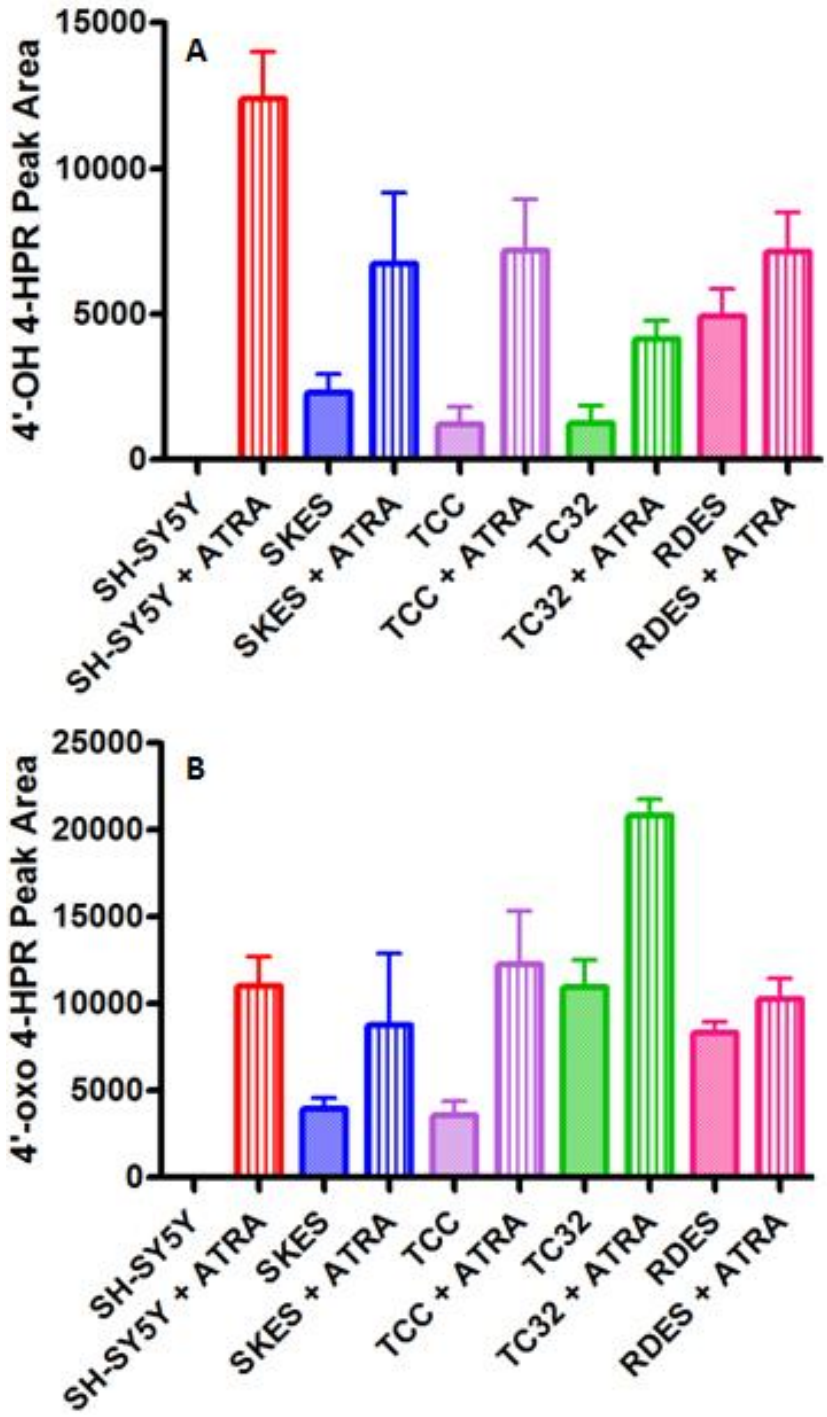

Figure 4-4. Intracellular concentrations of A) 4'-OH 4-HPR and B) 4'-oxo 4-HPR metabolites by Ewing's sarcoma and neuroblastoma cell lines following pre-treatment with ATRA.

Metabolite peak area was normalized to protein concentration (determined by Bradford assay). Metabolites were generated by incubation of 4-HPR (20μM) with each cell line for 6h, following incubation with ATRA (10μM) for 24h. Results are the mean of 3 independent determinations (error bars are standard deviation).

4.3.3 CYP26A1 expression in cell lines

CYP26A1 expression was determined by Real-Time PCR in cell lines, as shown in Figure 4-5. Expression was calculated by fold-increase relative to a base line expression determined by incubation of cells with 0.01µM ATRA for 24h. This enabled calculations of the relative increase in *CYP26A1* expression following incubations with ATRA in cell lines not expressing endogenous *CYP26A1*. *CYP26A1* was endogenously expressed at relatively low levels in SH-SY5Y, SK-ES and TC-32 cells, (0.3-, 0.02- and 0.1-fold respectively) and was not expressed at all in RD-ES cells. TCC-446 cells expressed the highest endogenous levels of *CYP26A1* (1.1-fold). After pre-treatment of cells with ATRA, *CYP26A1* expression significantly increased in all cell lines ($p=0.0065$, $p=0.0060$, $p=0.0222$ and $p=0.0047$ for SH-SY5Y, SK-ES, TC-32 and RDES, respectively, by one-way ANOVA followed by Bonferroni's post test) except TCC-446 ($p=0.5569$), which retained similar expression levels regardless of the addition of ATRA (1.5-fold with ATRA pre-treatment compared to 1.1-fold without).

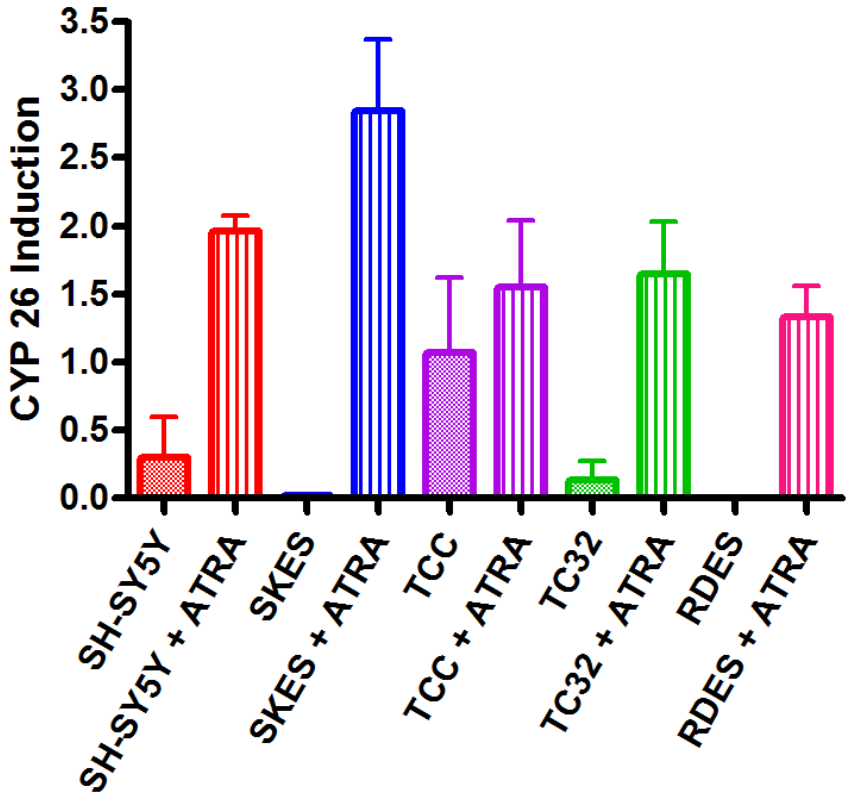

Figure 4-5. Induction of *CYP26A1* in Ewing's sarcoma and neuroblastoma cell lines.
Cell lines were incubated with ATRA (10µM) or an equivalent concentration of ethanol for 24h. RNA was extracted from cell pellets and reverse transcribed, then *CYP26A1* expression was analysed by Real-Time PCR. Results are the mean of 3 independent determinations and are expressed as fold-increase relative to induction by 0.01µM ATRA (error bars are standard deviation).

There was no correlation between the fold-increase in *CYP26A1* expression following incubation with ATRA and the increase in production of oxidative metabolites of 4-HPR (as shown in Figure 4-6).

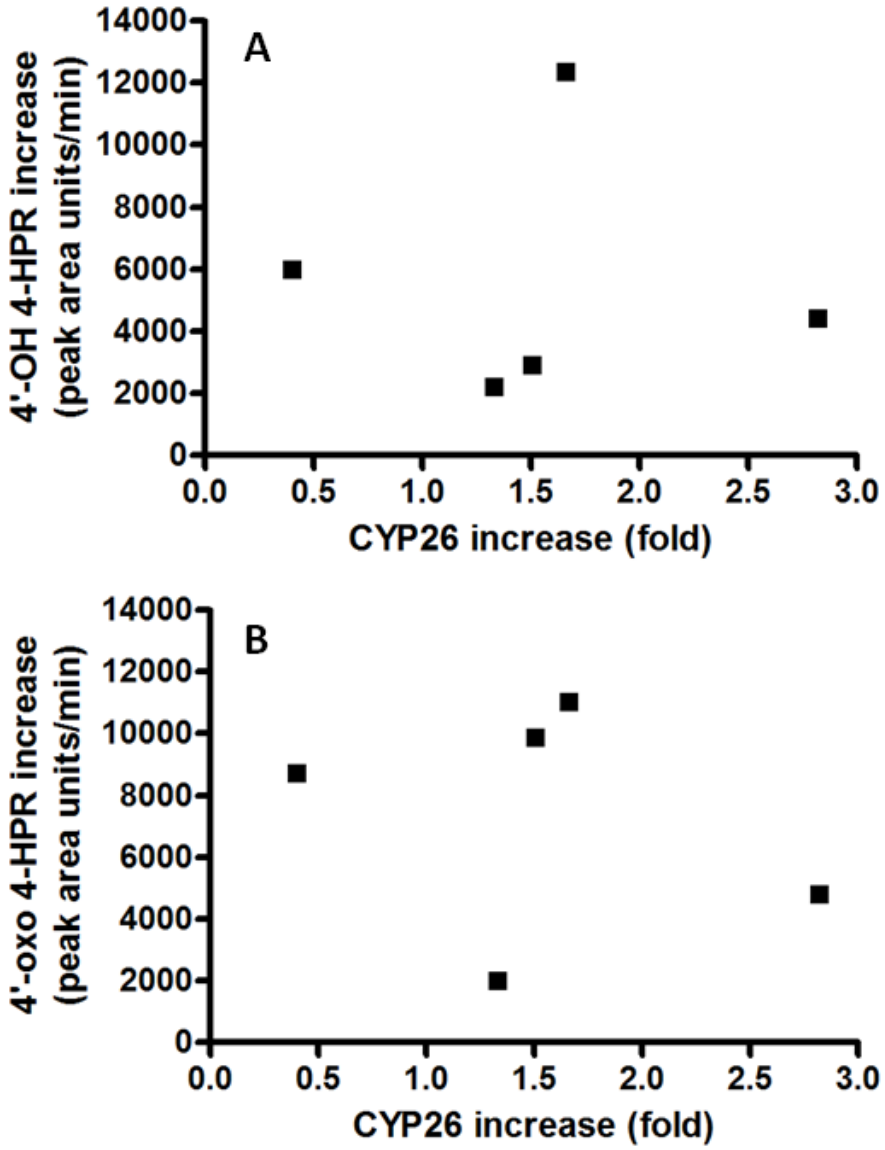

Figure 4-6. Correlation between increase in *CYP26A1* expression and increase in production of A) 4'-OH 4-HPR and B) 4'-oxo 4-HPR.

Cell lines were incubated with ATRA (10μM). Metabolite peak area was normalized to protein concentration (determined by Bradford assay). Metabolites were generated by incubation of 4-HPR (20μM) with each cell line for 6h. RNA was extracted from cell pellets and reverse transcribed, then *CYP26A1* expression was analysed by Real-Time PCR. R^2 for A) is <0.001, R^2 for B) is 0.064. Results are the mean of 3 independent determinations (error bars are standard deviation).

4.3.4 Effect of intracellular metabolite concentrations and CYP26A1 expression on sensitivity of cell lines to 4-HPR

Cell sensitivity to 4-HPR was determined by MTS assay, as shown in Figure 4-7. Cells were pre-treated with ATRA (10μM), or an equivalent concentration of ethanol prior to incubation with 4-HPR (0-50μM) for 96h.

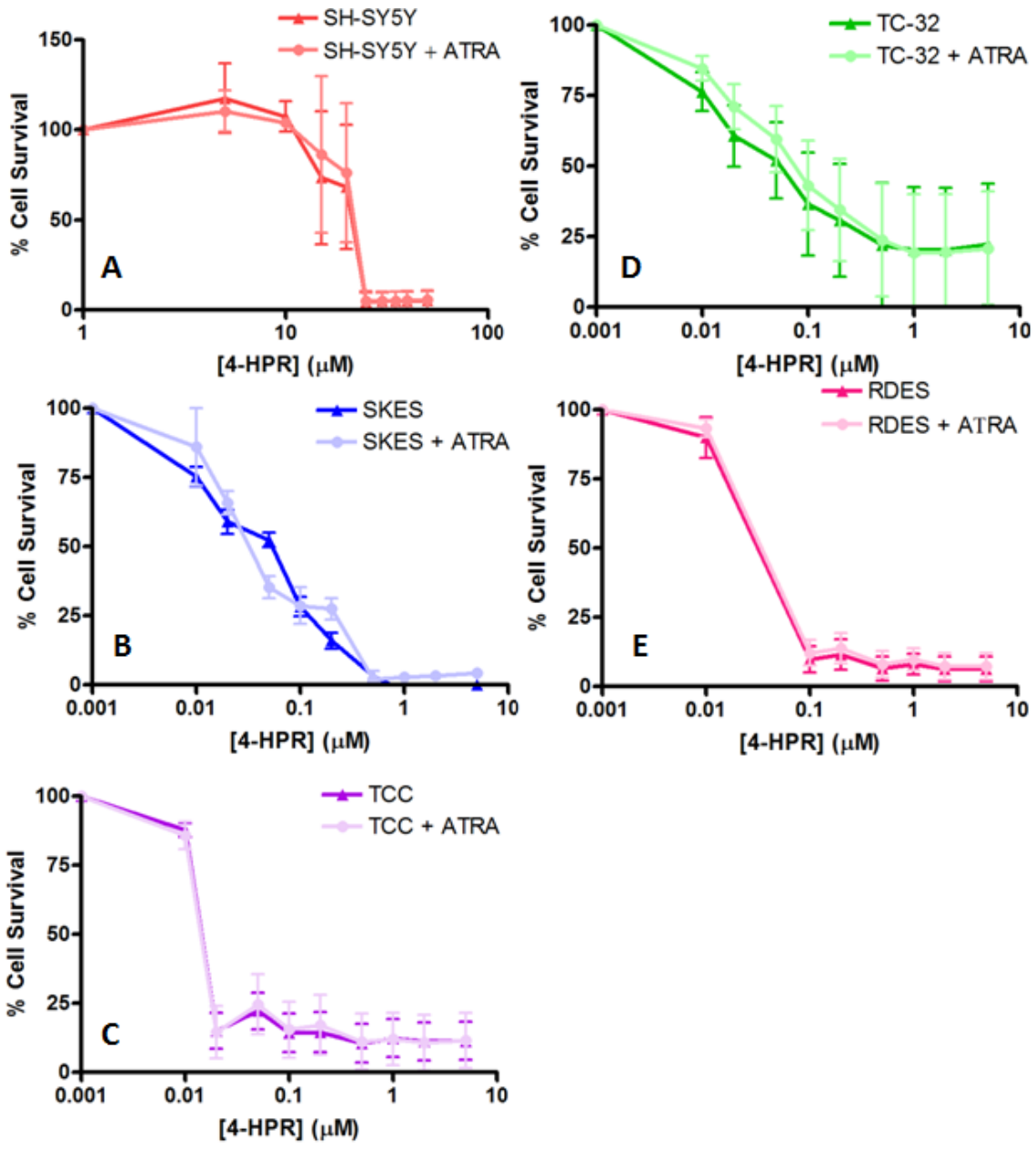

Figure 4-7. Sensitivity of neuroblastoma A) SH-SY5Y, and Ewing's sarcoma cell lines B) SK-ES, C) TCC-446, D) TC-32 or E) RD-ES, to 4-HPR with and without ATRA pre-treatment.

Cell viability was determined by MTS assay following incubations with 4-HPR (0-100μM) for 96h with or without ATRA (10μM) for 24h prior to addition of 4-HPR. Results are the mean of 3 independent determinations (error bars are standard deviation).

As shown in Table 4-1, 4-HPR IC_{50} values varied considerably between cell lines, ranging from 0.01µM for TCC-446 cells, to 16µM for SH-SY5Y cells. 4-HPR IC_{50} was several-fold higher in the neuroblastoma cell line tested, SH-SY5Y (16µM), than in any of the Ewing's sarcoma cell lines, with IC_{50} values ranging from 0.01µM in TCC-446 cells to 1µM in TC-32 cells. SH-SY5Y was also the only cell line where metabolism of 4-HPR to its oxiditative metabolites was not observed, as shown in Figure 4-2. However, induction of *CYP26A1* and the resulting increase in metabolism by SH-SY5Y cells to both oxidative metabolites (as shown in Figure 4-4) had no significant effect on 4-HPR IC_{50} (16µM without ATRA pre-treatment compared to 17µM following ATRA pre-treatment).

Cell Line	IC_{50} (µM) (- ATRA)	IC_{50} (µM) (+ ATRA)
SH-SY5Y	16 ± 5	17 ± 6
SK-ES	0.05 ± 0.01	0.03 ± 0.01
TCC-446	0.01 ± 0.01	0.01 ± 0.01
TC-32	1 ± 0.2	1 ± 0.2
RD-ES	0.02 ± 0.01	0.01 ± 0.01

Table 4-1. Effect of ATRA pre-treatment on sensitivity to 4-HPR in Ewing's sarcoma and neuroblastoma cell lines.

Cell sensitivity was determined by MTS assay. Cells were incubated with ATRA (10µM) for 24h prior to incubation with 4-HPR (0-50µM) for 96h. Results are the mean of 3 independent determinations (± standard deviation).

4.3.5 Inhibition of HLM metabolism with R116010

HLM were incubated with 4-HPR and the *CYP26A1* inhibitor R116010 (0-100µM). Figure 4-8 shows that concentrations of 4'-OH 4-HPR did not appear to be affected by the addition of inhibitor. Concentrations of the active oxidative metabolite (4'-oxo 4-HPR) decreased, but only when incubated with R116010 at concentrations above 40µM. At these concentrations it is likely that R116010 will have non-specific inhibitory effects on other CYP enzymes.

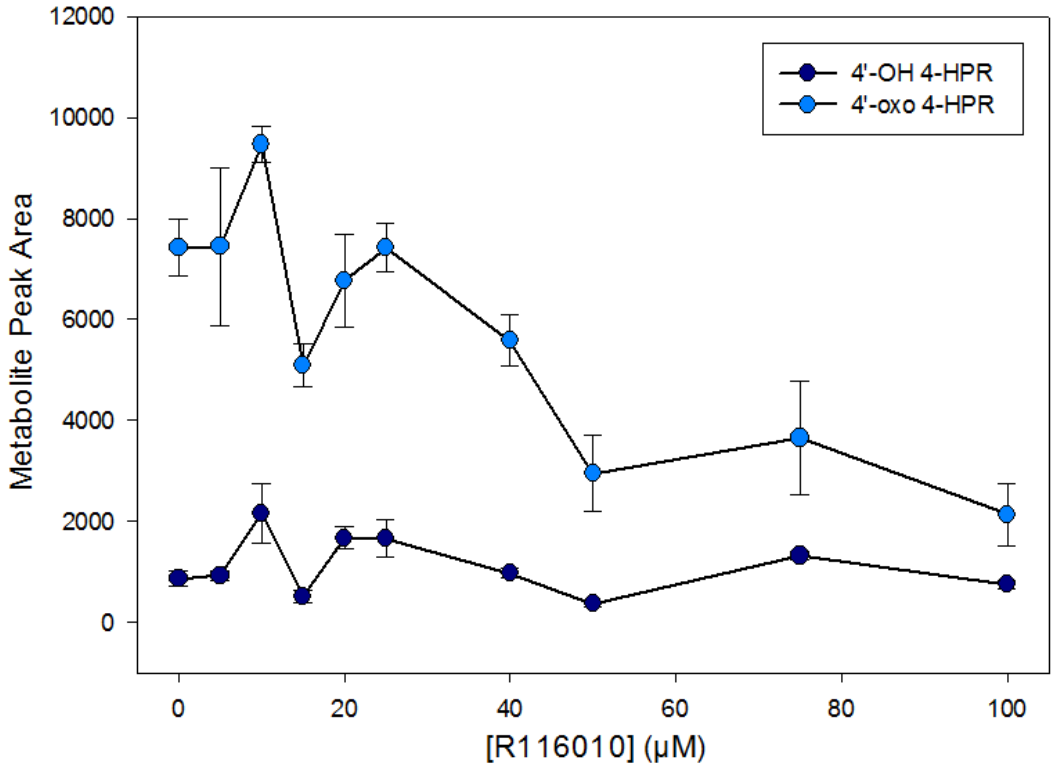

Figure 4-8. Inhibition of 4-HPR metabolism in HLM by the CYP26A1 inhibitor R116010. Metabolites were generated by incubation of 4-HPR (20µM) with HLM (0.5mg/ml) and R116010 (0-100µM) for 3h. Results are the mean of 3 independent determinations (error bars are standard deviation).

4.4 Discussion

4-HPR is extensively metabolised in patient samples to both an active metabolite (4'-oxo 4-HPR) and an inactive metabolite (4-MPR) (Formelli et al., 1993, Garaventa et al., 2003, Villani et al., 2004, Formelli et al., 2008). In addition, 4-HPR has also been found to be metabolised to a second oxidative metabolite, 4'-OH 4-HPR, as described in chapter 2. In order to further understand the mechanisms of 4-HPR metabolism and possible benefits of modulation of metabolism, cell lines derived from neuroblastoma and Ewing's sarcoma tumours were incubated with 4-HPR and the intracellular metabolism of 4-HPR investigated.

It is important to characterise metabolism in appropriate tumour cell lines in addition to characterisation of the contribution of individual metabolising enzymes, such as CYPs and UGTs, due to differences in cellular metabolism that have been seen with other retinoic acid analogues. Previous studies with ATRA and 13-cis RA have shown that isomerisation can have a significant impact on drug uptake and cell sensitivity, and that saturation of retinoid receptors can result in a lack of correlation between intracellular retinoid concentrations and growth inhibitory effects (Veal et al., 2002). In addition, 4-HPR has been shown to cause cell differentiation when present at low concentrations (<1μM) in a prostate cancer cell line, but can trigger apoptosis when present at higher concentrations (>5μM) (Sabichi et al., 2003). As 4-HPR is also metabolised to an active metabolite, 4'-oxo 4-HPR, it is particularly important to gain an understanding of the intracellular concentrations of 4-HPR and its metabolites that are achieved *in vitro*, and the effect that drug metabolism may have on growth inhibition.

4-HPR is a synthetic analogue of retinoic acid, and as such has significant structural homology with the retinoic acid derivative ATRA. There have been several studies carried out on the metabolism of ATRA and its isomeric form 13-cis RA. These studies have demonstrated that ATRA and 13-cis RA are able to induce their own metabolism, via induction of *CYP26* (White et al., 1997, Yamamoto et al., 2000, McSorley and Daly, 2000). There is some evidence that continuous treatment of an ovarian carcinoma cell line with 4-HPR is also able to up-regulate *CYP26*, and that increased expression of *CYP26* results in increased metabolism of 4-HPR to its active 4'-oxo 4-HPR metabolite (Villani et al., 2004). The effect of up-regulation of *CYP26A1* on 4-HPR metabolism

and cell sensitivity to 4-HPR treatment was therefore investigated by pre-treatment of neuroblastoma and Ewing's sarcoma cell lines with ATRA.

Incubation of 4-HPR with neuroblastoma and Ewing's sarcoma cells resulted in metabolism of 4-HPR to its inactive metabolite 4-MPR in all cell lines tested. Metabolism to the oxidative metabolites of 4-HPR varied considerably between cell lines, with no oxidative metabolites produced by SH-SY5Y cells. In comparison, the Ewing's sarcoma cell lines investigated all produced both 4'-oxo 4-HPR and 4'-OH 4-HPR. The lack of oxidative metabolism in SH-SY5Y cells is probably due to a lower expression of CYPs compared to the other cell lines tested, as up-regulation of *CYP26A1* by pre-treatment of cell lines with ATRA resulted in the formation of both 4'-oxo 4-HPR and 4'-OH 4-HPR at similar levels to those seen in the Ewing's sarcoma cell lines. This hypothesis is supported by data generated from a study of *CYP26A1* expression in a panel of neuroblastoma cell lines, that found no endogenous *CYP26A1* expression in any of the cell lines tested (Armstrong et al., 2007b).

The lack of oxidative metabolism of 4-HPR by SH-SY5Y cells did not appear to have a corresponding effect on growth inhibition, as formation of the oxidative metabolites following pre-incubation with ATRA had no effect on the 4-HPR IC_{50} value in this cell line. In fact ATRA pre-treatment had no effect on 4-HPR IC_{50} in any cell line tested, suggesting that up-regulation of *CYP26A1* and the corresponding up-regulation in oxidative metabolism is not an important factor in determining 4-HPR sensitivity. In addition, there was no correlation between constitutive *CYP26A1* expression and metabolite production or between *CYP26A1* expression and 4-HPR IC_{50} value. This may be due to the relatively small amount of overall metabolism that occurred, with metabolite peak areas varying from 0.01% to 2% of the parent peak area. Even a significant increase in concentration of the active metabolite 4'-oxo 4-HPR is therefore unlikely to have a significant effect on growth inhibition, as the vast majority of any cytotoxic effect is likely to be provided by the parent compound, 4-HPR. However, as 4'-oxo 4-HPR has been shown to be cytotoxic in cell lines resistant to 4-HPR itself (Villani et al., 2006), the contribution of metabolism to 4'-oxo 4-HPR could be a factor in determining IC_{50} in 4-HPR resistant cell lines. Metabolism to both 4'-oxo 4-HPR and 4-MPR is also significantly higher in patients and in mice treated with 4-HPR than observed in the current study, with plasma concentrations of 4'-oxo 4-HPR and 4-MPR accounting for up to 20% of 4-HPR concentrations (Cooper et al., 2011, Formelli et al.,

2003, Formelli et al., 2008, Formelli et al., 1993). This is closer to the amount of metabolism seen in human liver and intestinal microsomes, and indicates that the majority of 4-HPR metabolism occurs during first pass metabolism, and that metabolism within tumours may have less of an impact on drug efficacy. In addition, *CYP26A1* expression and intracellular metabolite concentrations were analysed following a 6h incubation with 4-HPR, whereas cell sensitivity was determined following a 96h incubation with 4-HPR. It is likely that the up-regulation of *CYP26A1* expression observed would have returned to baseline levels within the 96h incubation time, and this may therefore have limited any effect from an initial increase in metabolism to the active metabolite 4'-oxo 4-HPR.

There have been several studies investigating the metabolism of ATRA and 13-cis RA and the potential benefits of modulation of metabolism. These studies have demonstrated that different factors need to be taken into account when considering the benefits of blocking the metabolism of ATRA or 13-cis RA, as compared to those that need to be considered for 4-HPR. As none of the known metabolites of ATRA or 13-cis RA are active metabolites, any reduction in metabolism and corresponding increase in parent compound is likely to increase growth inhibition. Also, ATRA and 13-cis RA are able to up-regulate *CYP26A1*, a major retinoic acid metabolising enzyme, leading to extensive metabolism (Pavez Lorie et al., 2009b, White et al., 1997, Yamamoto et al., 2000). Increasing doses of these retinoids will result in an increase in metabolism, and may limit maximum plasma concentrations that can be achieved. Extensive metabolism of 13-cis RA has been observed in neuroblastoma patients (Veal et al., 2007). Similar results were observed in ATRA treatment of APL patients, with the subsequent progressive reduction in plasma concentrations of ATRA associated with relapse (Muindi et al., 1992). Studies have therefore been carried out to block metabolism by CYP26, using RAMBAs (Njar et al., 2006).

Incubation of neuroblastoma cell lines with 13-cis RA or ATRA and the RAMBA R116010 have been shown to result in decreased expression of *CYP26A1* and a corresponding increase in intracellular concentrations of ATRA (Armstrong et al., 2005), with a similar effect seen in a mouse model of neuroblastoma (Armstrong et al., 2007b). Reductions in *CYP26* expression and ATRA metabolism have also been shown in smooth muscle cells (Ocaya et al., 2007), epidermal cells (Pavez Lorie et al., 2009a) and in a prostate cancer cell line (Huynh et al., 2006). In the current study, 4-HPR was

incubated with human liver microsomes and the RAMBA R116010, resulting in a decrease in concentrations of 4'-oxo 4-HPR. However, this effect was only seen at high concentrations of R116010 (above 40μM) and no effect was seen on 4'-OH 4-HPR. At these concentrations it is probable that R116010 will also be inhibiting other CYPs, as it has been shown to inhibit CYP3A4 metabolism at concentrations above 10μM (Van heusden et al., 2002). In addition it is questionable whether inhibition of metabolism of 4-HPR by CYP26 would be advantageous. Not only is 4'-oxo 4-HPR an active metabolite of 4-HPR, it has also been shown to act synergistically with 4-HPR and to have activity in cell lines resistant to 4-HPR (Villani et al., 2006). In contrast to metabolism of ATRA and 13-cis RA, metabolism of 4-HPR to 4'-oxo 4-HPR therefore has the potential to be beneficial.

Although 4-HPR has also been shown to up-regulate *CYP26* in an ovarian carcinoma cell line (Villani et al., 2004), this was only following continuous incubation of 5μM 4-HPR, whereas a single incubation of 5μM 4-HPR for 6h only resulted in a modest increase in *CYP26* expression. Inhibition of *CYP26* is therefore unlikely to have a significant effect on the efficacy of 4-HPR, as the majority of its metabolism to 4'-oxo 4-HPR seems to be via other CYPs. This is supported by experiments showing that up-regulation of *CYP26A1* expression and increased metabolism to 4'-oxo 4-HPR had no effect on sensitivity to 4-HPR in the cell lines investigated.

Modulation of metabolism of 4-HPR to the inactive metabolite 4-MPR may be of more interest in terms of potentially increasing the efficacy of 4-HPR. 4-MPR was produced in all cell lines tested and peak areas were at least 10-fold higher than those seen for 4'-oxo 4-HPR. 4-MPR is also the major metabolite observed in patients (Hultin et al., 1990, Formelli et al., 2008, Marachelian et al., 2009), indicating that methylation is a major pathway of metabolism for 4-HPR. Inhibition of methylation of 4-HPR should subsequently increase concentrations of 4-HPR, and may well additionally increase concentrations of the active metabolite, as concentrations of 4'-oxo 4-HPR have been shown to increase with 4-HPR concentrations (as shown in chapter 2).

Characterisation of 4-HPR metabolism in neuroblastoma and Ewing's sarcoma cell lines suggests that metabolism within tumour cells to the active metabolite 4'-oxo 4-HPR has little effect on the efficacy of 4-HPR. This is most likely due to the minimal amount of metabolism that occurs. Although significantly more metabolism is seen *in*

vivo, a more effective strategy to improve 4-HPR efficacy may be to investigate modulation of metabolism to the inactive metabolite 4-MPR.

Chapter 5 Drug Transport

5.1 Introduction

The mammalian ATP-binding cassette (ABC) transporters are a family of proteins responsible for the efflux of many xenobiotic drugs and metabolites. They are transmembrane proteins that utilise the hydrolysis of ATP to transport substrates across the cell membrane (Higgins, 1992). The expression of these transporters has been shown to be responsible for drug resistance in many cancers, due to decreased intracellular drug concentrations in tumour cells (Gottesman et al., 2002), generally as a result of increased drug efflux, as is seen in resistance to vincristine, doxorubicin and paclitaxel (Ambudkar et al., 1999). In addition, the expression of drug transporters in other tissues can also affect drug disposition, for example by altering uptake into the liver and kidneys, and subsequently altering either drug metabolism or excretion (Yamazaki et al., 1996). Forty-eight ABC transporter genes have so far been identified in humans, with MDR1 (also known as ABCB1 or p-glycoprotein), MRP2 (ABCC2) and BCRP (ABCG2) being among the best characterised (Fletcher et al., 2010).

Methods for investigating multidrug resistance involving the ABC transporters generally include culturing cells with a constant low level of drug in order to select for resistant cells, or transfection of cells with the relevant transcripts, resulting in over-expression of a particular transporter (Evers et al., 1998). The second method has the advantage of allowing research into the effects of each individual ABC transporter in the same cell line, as well as allowing comparison to a 'wild-type' cell line transfected with an empty plasmid. Intracellular accumulation of drugs can then be investigated in the presence or absence of inhibitors of ABC transporters.

It is important to determine whether 4-HPR is a substrate for these drug transporters, and whether this is likely to have any effect on sensitivity to 4-HPR. This may be particularly important as resistance to histone deacetylase inhibitors (HDACIs), linked to ABC transporter expression, has previously been reported in Ewing's sarcoma cells (Okada et al., 2006), as has up-regulation of MDR1 in neuroblastoma tumour samples (Bates et al., 1991). Additionally, 4-HPR also has relatively low bioavailability (Reynolds et al., 2003) and it is possible this may be related to exclusion by MDR1 in the intestine.

The aim of the current study was therefore to investigate intracellular and extracellular concentrations of 4-HPR and its metabolites using cells transfected to over-express MDR1, MRP2 or BCRP as compared to WT cells. In addition, the effect of over-expression of individual ABC transporters on 4-HPR sensitivity was investigated.

5.2 Materials and Methods

5.2.1 Chemicals

Roswell Park Memorial Institute (RPMI) 1640 media, L-glutamine and sodium pyruvate were purchased from Sigma-Aldrich (Poole, UK). Foetal calf serum was provided by Gibco (Paisley, Scotland). CellTiter 96® AQueous Non-Radioactive Cell Proliferation Assay (MTS assay) was supplied by Promega (Southampton, UK). Tissue culture plasticware was purchased from Nunc (Denmark). Bio-Rad Protein Assay Dye reagent Concentrate and Bovine Serum Albumin Standard were from Bio-Rad Labs Ltd (UK). The SpectraMax® 250 Microplate Spectrophotometer System was from Molecular Devices Corporation (Reading, UK).

5.2.2 Culture of cell lines

MDCK-II (Madin-Darby Canine Kidney) cells transfected to over-express human ABC transporters MDR1, MRP2, BCRP or a blank plasmid (referred to as wild-type (WT)) were provided by Dr. Alfred Schinkel (The Netherlands Cancer Institute). Cell lines were grown in monolayer culture in complete RPMI 1640 medium containing 10% foetal bovine serum (FBS), 1% L-glutamine and 1% sodium pyruvate. Cells were incubated at 37°C in a humidified atmosphere of 5% CO_2 and were maintained in an exponential growth phase by passage every 3-4 days, with addition of fresh medium as required. Cells were harvested by trypsinisation using 0.25% Trypsin-EDTA when 70-80% confluent, centrifuged at 1,000g for 5min at room temperature and resuspended in fresh medium at the appropriate dilution factor.

5.2.3 Incubation of 4-HPR with cell lines

Cells were seeded in 6-well plates (20,000 cells per well) in complete RPMI (2ml) and left to adhere for 24h. The medium was then removed and replaced with medium containing 4-HPR (20μM) and incubated for a further 6h. Medium was retained for extracellular 4-HPR analysis and the cells rinsed with ice-cold PBS (1ml). Cells were harvested by addition of trypsin (1ml) for 3-5min at 37°C to allow detachment of cells from the wells. The cell/trypsin solution was transferred into centrifuge tubes and centrifuged at 15,000g for 5min. Supernatant was discarded and the cell pellet was

vortexed to break up the cells. Cell pellets were stored at -20°C until required for analysis.

5.2.4 Inhibition of cell transport

Cells were seeded in 6-well plates (20,000 cells per well) in complete RPMI (2ml) and left to adhere for 24h. The medium was then removed and replaced with medium containing 4-HPR (20μM) and an ABC transport inhibitor, and incubated for a further 6h. Each cell line was incubated with a concentration of inhibitor known to be acceptable for use on cells for 96h without causing toxicity, as well a concentration 10-fold higher. MDR1 over-expressing cells were incubated with verapamil (5μM and 50μM); MRP2 over-expressing cells were incubated with MK571 (2μM and 20μM); and BCRP over-expressing cells were incubated with KO143 (10μM and 100μM). Cells were incubated with 4-HPR (20μM) and experiments were also carried out using WT cells. Following incubation with 4-HPR and transport inhibitors, medium was discarded and the cells rinsed with ice-cold PBS (1ml). Cells were then harvested by addition of trypsin (1ml) for 3-5min at 37°C to allow detachment of cells from the wells. The cell/trypsin solution was transferred into centrifuge tubes and centrifuged at 15,000g for 5min. Supernatant was discarded and the cell pellet vortexed to break up the cells. Cell pellets were stored at -20°C until required for analysis.

5.2.5 Cell viability assay

Cell viability was determined using the CellTiter 96® AQueous Non-Radioactive Cell Proliferation Assay (MTS assay). Cells were seeded in 96-well plates at a density of 5,000 cells per well in RPMI (200μl). The cells were left to establish growth for 24h, then the medium was removed and replaced with fresh medium (200μl) containing 4-HPR (0-100μM) and an inhibitor of ABC transport. MDR1 over-expressing cells were incubated with verapamil (5μM); MRP2 over-expressing cells were incubated with MK571 (2μM); and BCRP over-expressing cells were incubated with KO143 (10μM). Each inhibitor was also incubated with 4-HPR (20μM) and WT cells. Cells were incubated with drug for 96h then medium was removed and replaced with medium containing MTS reagent (12μl per 200μl of medium). Cells were incubated with MTS for 1-4h and then absorbance at 490nm was measured using a SpectraMax® 250

Microplate Spectrophotometer. Absorbance values determined in wells containing 4-HPR in the presence or absence of inhibitors were compared to absorbance values determined in untreated wells to establish the effect on cell proliferation. Experiments were carried out in triplicate, with 6 wells treated with each concentration of drug within each replicate.

5.2.6 Protein analysis

In order to adjust for different levels of cell recovery from intracellular 4-HPR concentration assays, cell pellets were retained for protein analysis utilizing the Bradford assay. Cell pellets were defrosted on ice and dH_2O (50µl) was added. Pellets were vortexed and vigorously mixed by pipetting to homogenise the sample. Samples were then added to 4 wells of a 96-well plate (10µl per well). Bradford reagent (190µl) was added to each well, and samples were mixed by pipetting. Absorbance was then measured at 595nm using a SpectraMax® 250 Microplate Spectrophotometer and compared to standards of known concentrations of BSA (bovine serum albumin).

5.2.7 Determination of intracellular and extracellular concentrations of 4-HPR and metabolites

For the determination of intracellular 4-HPR concentrations, cell pellets were defrosted on ice, acetonitrile (100µl) was added and cells were vortexed and centrifuged at 15,000g for 5min. The supernatant obtained was used for analysis of 4-HPR and metabolite concentrations, and the cell pellet was retained for protein analysis. Extracellular 4-HPR concentrations were determined by addition of acetonitrile (400µl) to medium (200µl) collected from cell incubations. Medium was vortexed and then centrifuged at 15,000g for 5min. The supernatant obtained was used for analysis of 4-HPR and metabolite concentrations. HPLC analysis of 4-HPR concentrations was achieved using a Waters 2690 Separations Module and 996 Photodiode array (PDA) detector (Waters Ltd., Elstree, UK), with Waters Millennium software for data acquisition. A Waters Symmetry C_{18} 3.5µm (4.6 x 150mm) column was used with mobile phases (A) 70% acetonitrile / 30% (0.2%) acetic acid and (B) acetonitrile / 0.2% acetic acid. A linear gradient ran at 1ml/min from 100% A at 0min to 100% B at 20min, returning to 100% A for 10min to re-equilibrate the column. A sample volume

of 50µl was injected onto the column for analysis. Intracellular and extracellular concentrations of 4-HPR in cell lines over-expressing transporters were compared to concentrations in WT cells. One-way ANOVA followed by Bonferroni's post test was used to compare intracellular and extracellular 4-HPR concentrations in cell lines over-expressing transporters to intracellular and extracellular concentrations in WT cells, with $P<0.05$ used to determine significance. All calculations were performed with GraphPad Prism version 4.0 software.

5.3 Results

5.3.1 Intracellular and extracellular concentrations of 4-HPR and metabolites

Cells over-expressing ABC transporters (MDR1, MRP2 or BCRP) were incubated with 4-HPR (20μM) for 6h to determine intracellular and extracellular 4-HPR and 4-MPR concentrations compared to WT cells.

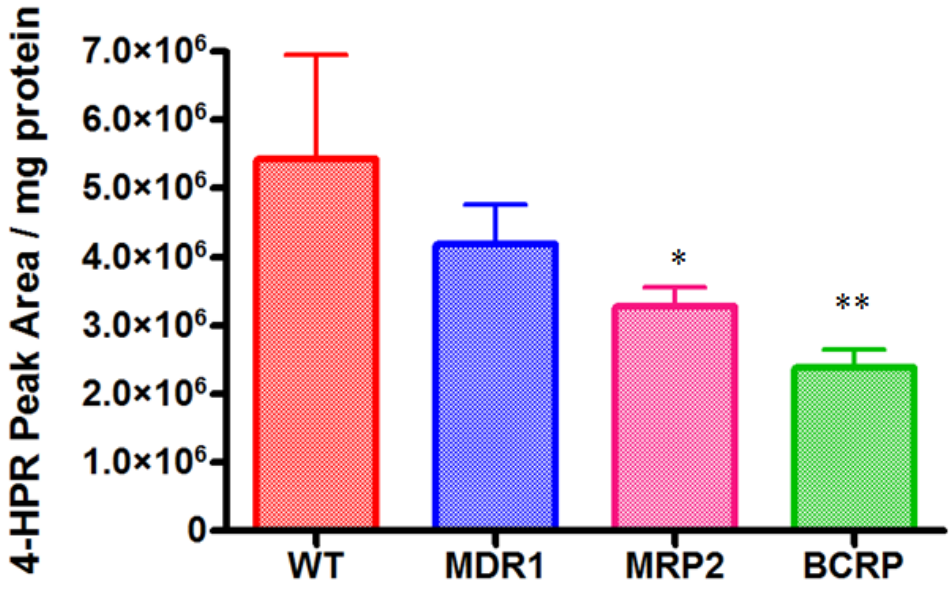

Figure 5-1. Intracellular 4-HPR concentrations in MDCK-II cells over-expressing ABC transporters.

4-HPR peak areas were normalized to protein concentration (determined by Bradford assay). Each cell line was incubated with 4-HPR (20μM) for 6h. Results are the mean of 3 independent determinations (error bars are standard deviation). * means significantly different to WT cells, P <0.05, (** P <0.001.)

Lower concentrations of 4-HPR were seen in all cell lines over-expressing ABC transporters as compared to wild-type cells, as shown in Figure 5-1. Concentrations of 4-HPR were significantly lower in cells over-expressing MRP2 (68% of WT, P = 0.0061) and in cells over-expressing BCRP (51% of WT, P < 0.0001) versus WT cells. 4-HPR concentrations were also lower in MDR1 (84% of WT), however the decrease was not statistically significant (p = 0.0988). Results for 4-MPR, the inactive metabolite of 4-HPR, were comparable to results for 4-HPR (as shown in Figure 5-2), with significantly lower concentrations of 4-MPR seen in all cell lines over-expressing ABC transporters than in WT cells. Intracellular 4-MPR concentrations were 46% of

WT in MDR1 over-expressing cells (p = 0.045), 34% of WT in MRP2 over-expressing cells (p = 0.012) and 17% of WT in BCRP over-expressing cells (p = 0.0013). The oxidative metabolites 4'-oxo 4-HPR and 4'-OH 4-HPR were not seen in any incubations with MDCK-II cells.

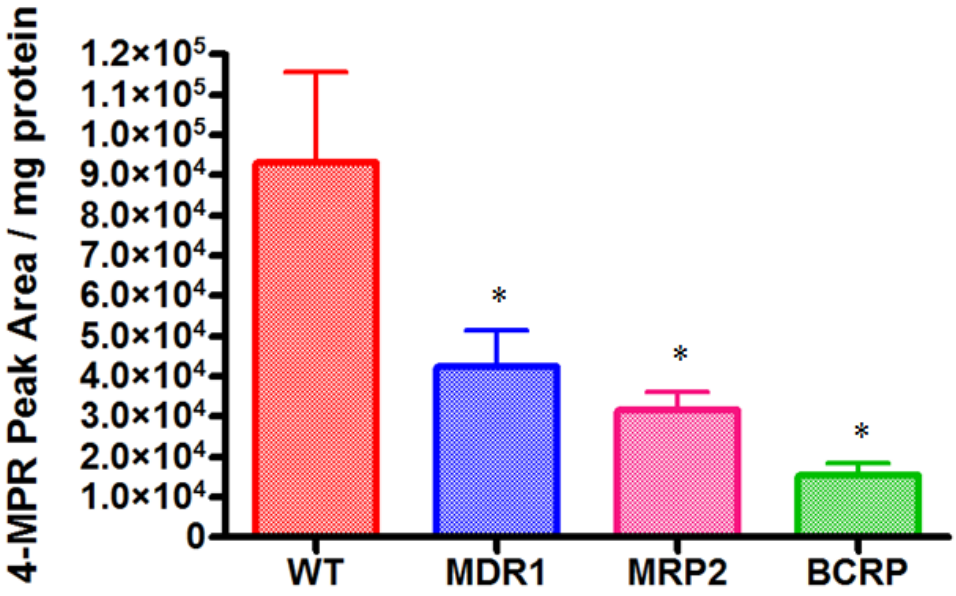

Figure 5-2. Intracellular 4-MPR concentrations in MDCK-II cells over-expressing ABC transporters.

4-MPR peak areas were normalized to protein concentration (determined by Bradford assay). Each cell line was incubated with 4-HPR (20µM) for 6h. Results are the mean of 3 independent determinations (error bars are standard deviation). * means significantly different to WT cells, P <0.05.

Cells over-expressing ABC transporters (MDR1, MRP2 or BCRP) were incubated with 4-HPR (20µM) for 6h to determine extracellular 4-HPR and 4-MPR concentrations compared to WT cells. There was no significant difference seen between extracellular 4-HPR concentrations in the cell lines over-expressing ABC transporters compared to the wild-type cells (as shown in Figure 5-3). However, as shown in Figure 5-4, significantly lower extracellular concentrations of 4-MPR were determined in all cell lines over-expressing ABC transporters as compared to WT cells. Extracellular 4-MPR concentrations were 67% of WT in MDR1 over-expressing cells (p = 0.0009), 71% of WT in MRP2 over-expressing cells (p = <0.0001) and 29% of WT in BCRP over-expressing cells (p = <0.0001).

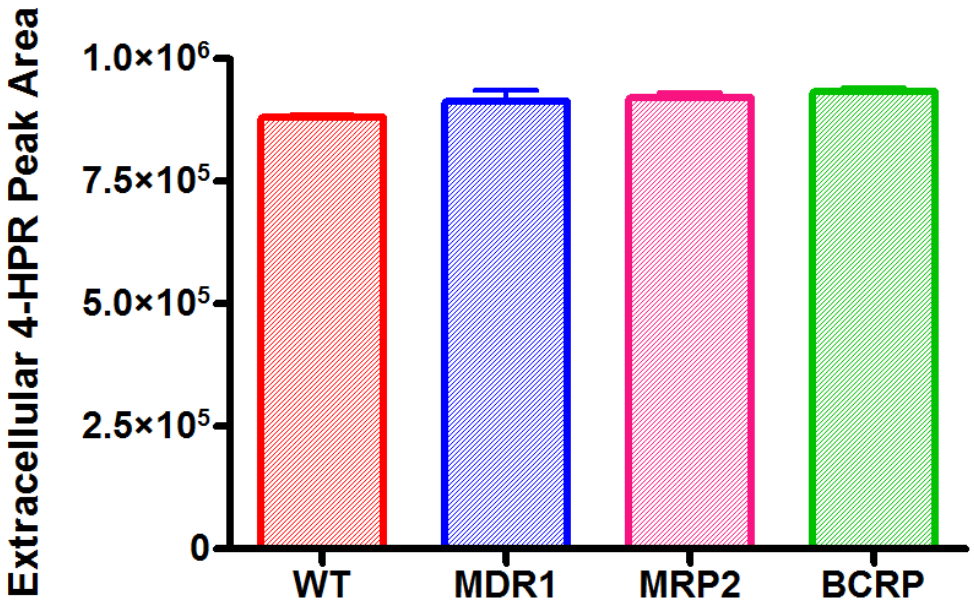

Figure 5-3. Extracellular 4-HPR concentrations in MDCK-II cells over-expressing ABC transporters.

Each cell line was incubated with 4-HPR (20μM) for 6h. Results are the mean of 3 independent determinations (error bars are standard deviation).

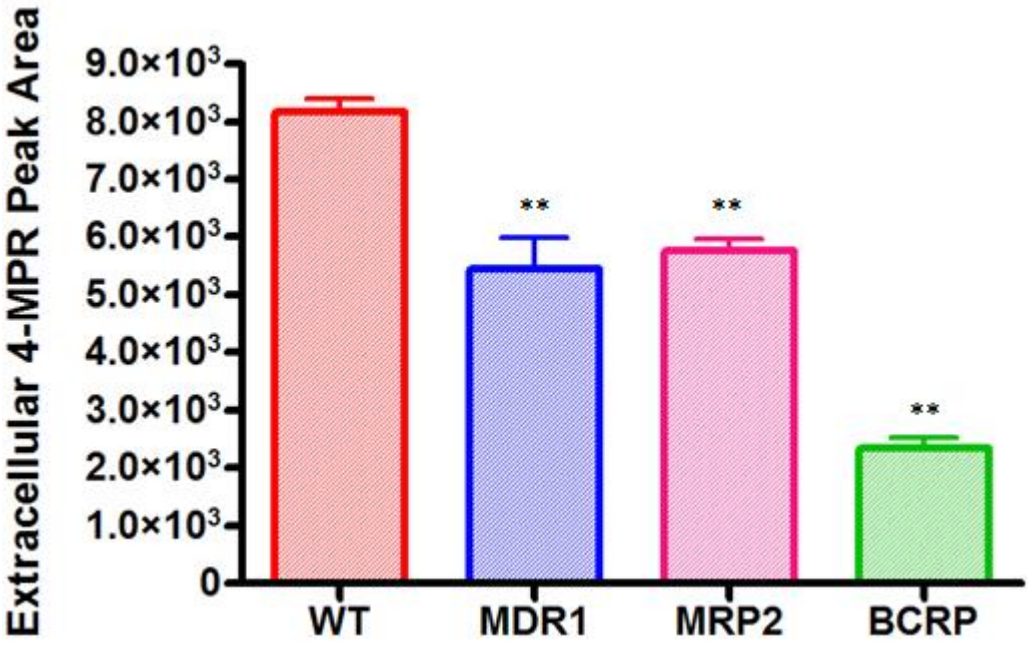

Figure 5-4. Extracellular 4-MPR concentrations in MDCK-II cells over-expressing ABC transporters.

Each cell line was incubated with 4-HPR (20μM) for 6h. Results are the mean of 3 independent determinations (error bars are standard deviation). ** means significantly different to WT cells, P <0.001.

Incubation of cell lines over-expressing ABC transporters and 4-HPR (20μM) for 3h was carried out in the presence and absence of inhibitors of ABC transport. Intracellular concentrations of 4-HPR generally increased in the presence of the inhibitors, with greater increases observed with higher concentrations of inhibitor.

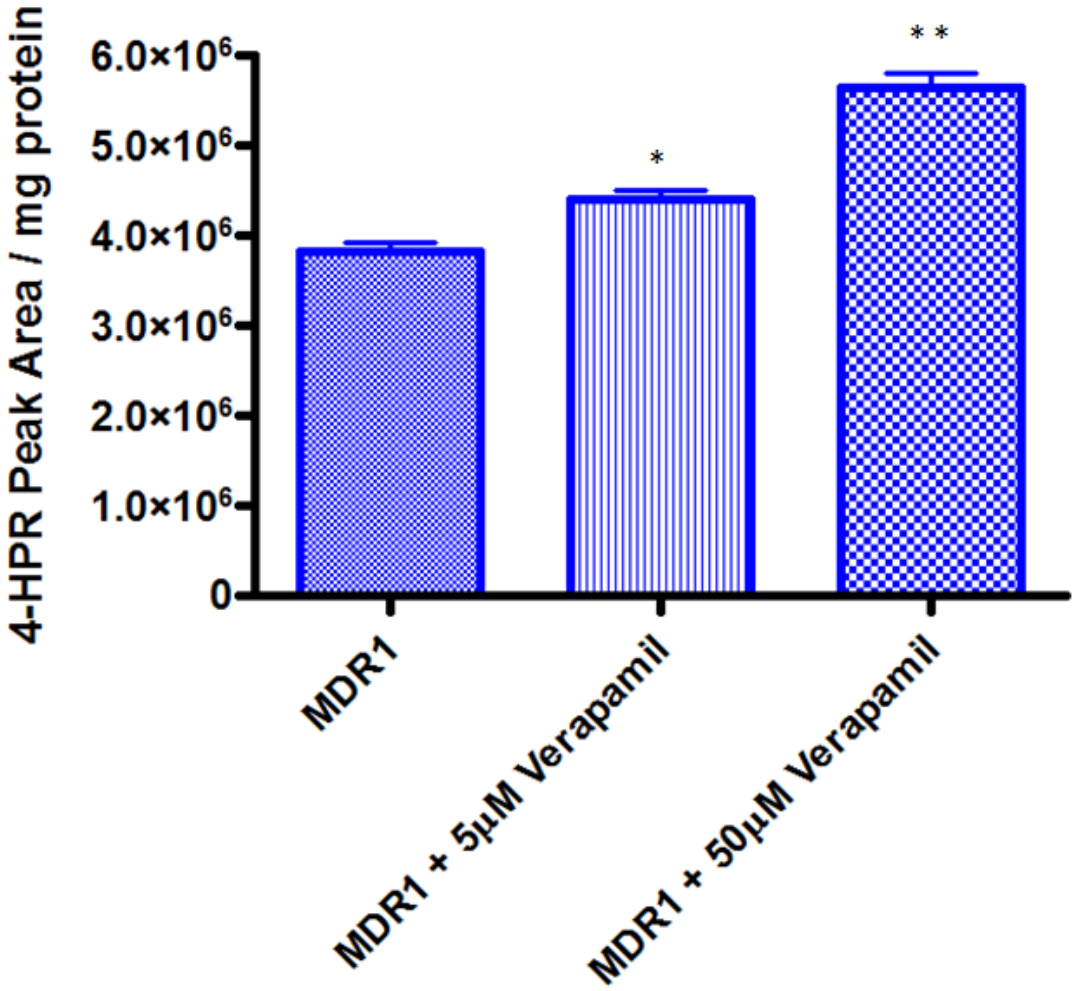

Figure 5-5. Intracellular 4-HPR concentrations in MDCK-II cells over-expressing MDR1 in the presence or absence of the MDR1 inhibitor verapamil.

4-HPR peak areas were normalized to protein concentration (determined by Bradford assay). A cell line over-expressing MDR1 was incubated with 4-HPR (20μM) and 0, 5 or 50μM verapamil (an inhibitor of MDR1) for 3h. Results are the mean of 3 independent determinations (error bars are standard deviation). * means significantly different to MDR1 over-expressing cells in the absence of inhibitor, $P < 0.05$, (** $P < 0.001$).

In the cell line over-expressing MDR1, as shown in Figure 5-5, intracellular 4-HPR peak area increased by 15% when incubated with 5μM verapamil ($p = 0.015$) and by 48% ($p = 0.0007$) in the presence of 50μM verapamil. In the MRP2 over-expressing

cell line (Figure 5-6), increases in 4-HPR intracellular peak areas were not significant, increasing by 6% with 10µM MK571 and 11% with 100µM MK571 ($p = 0.31$ and 0.09 respectively). In the cell line over-expressing BCRP, intracellular 4-HPR peak area increased significantly when incubated with the higher concentration of the inhibitor K0143 (100µM), with a 34% increase in peak area observed ($p = 0.019$). However the increase in intracellular 4-HPR was not significant at the lower concentration of K0143 (10µM), with a 13% increase in peak area observed ($p = 0.11$), as shown in Figure 5-7.

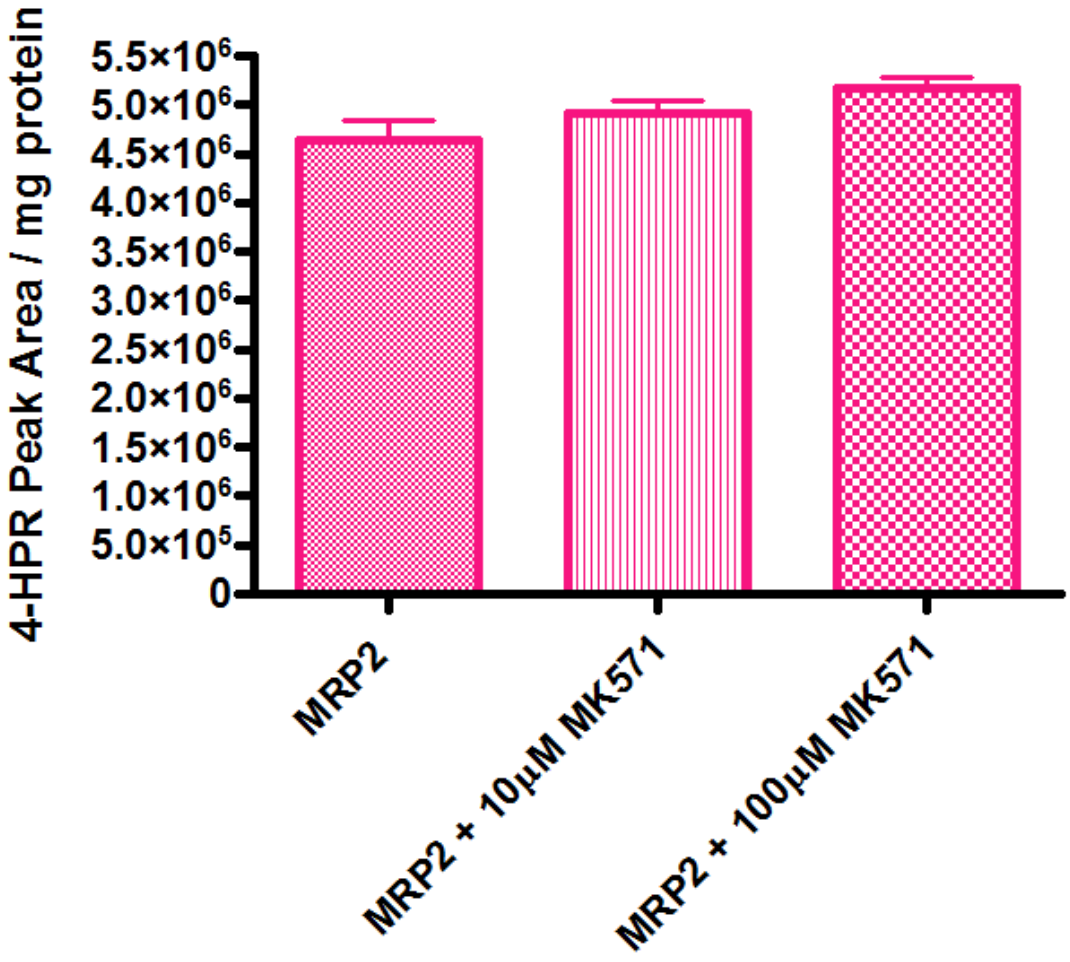

Figure 5-6. Intracellular 4-HPR concentrations in MDCK-II cells over-expressing MRP2 in the presence or absence of the MRP2 inhibitor MK571.

4-HPR peak areas were normalized to protein concentration (determined by Bradford assay). A cell line over-expressing MRP2 was incubated with 4-HPR (20µM) and 0, 10 or 100µM MK571 (an inhibitor of MRP2) for 3h. Results are the mean of 3 independent determinations (error bars are standard deviation).

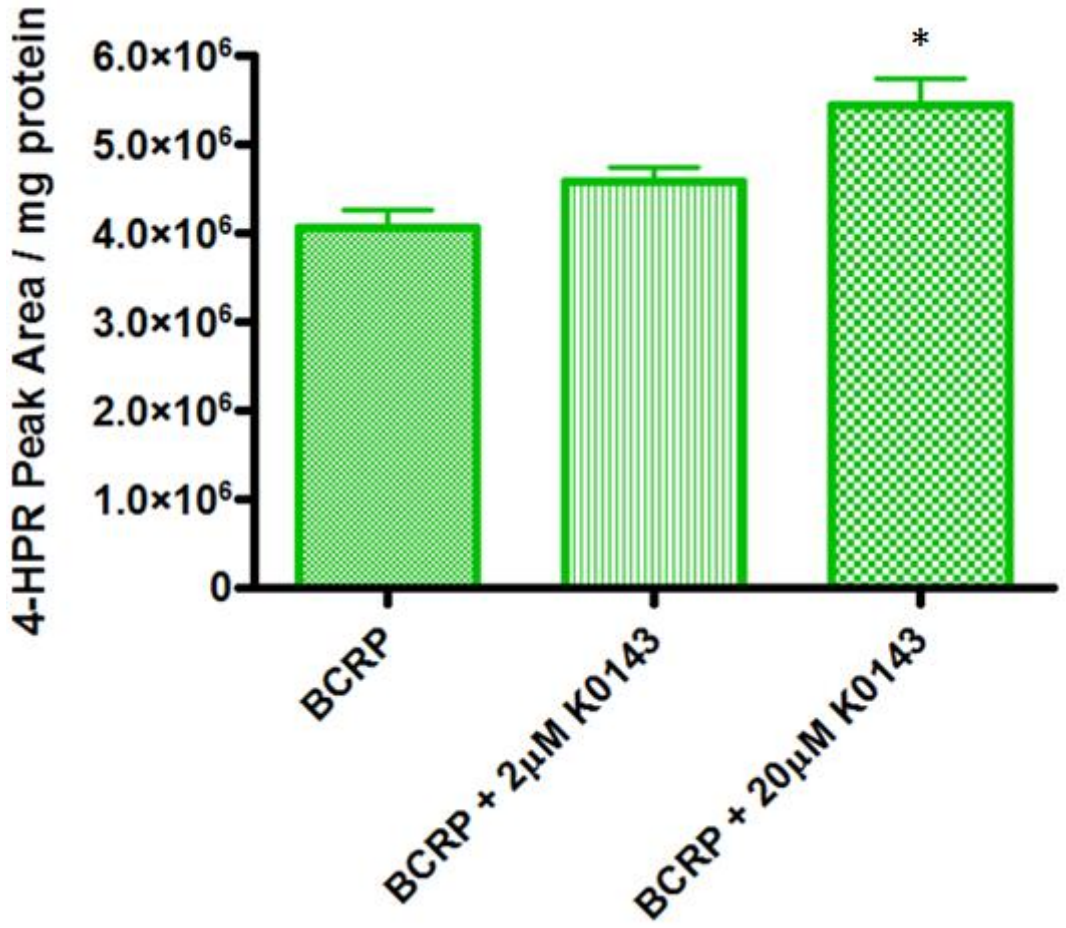

Figure 5-7. Intracellular 4-HPR concentrations in MDCK-II cells over-expressing BCRP in the presence or absence of the BCRP inhibitor K0143.

4-HPR peak areas were normalized to protein concentration (determined by Bradford assay). A cell line over-expressing BCRP was incubated with 4-HPR (20μM) and 0, 2 or 20μM K0143 (an inhibitor of BCRP) for 3h. Results are the mean of 3 independent determinations (error bars are standard deviation). * means significantly different to MDR1 over-expressing cells in the absence of inhibitor, $P < 0.05$.

5.3.2 Effect of drug transporters on cell sensitivity

Cell sensitivity was determined using the MTS cell proliferation assay. Cells were incubated with 4-HPR (0-100μM) for 96h in the presence or absence of inhibitors of ABC transporters. As shown in Figure 5-8, there was little variation in 4-HPR IC_{50} values between cell lines. The BCRP over-expressing cells were the most sensitive to 4-HPR treatment, with the MRP2 over-expressing cells the most resistant. The cell line over-expressing MDR1 and the WT cell line had intermediate IC_{50} values.

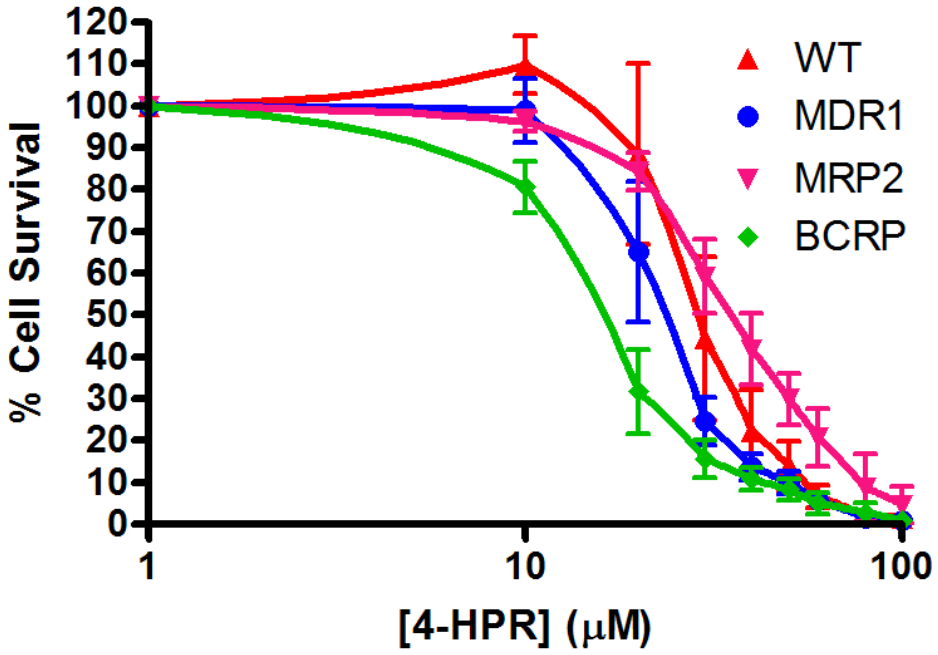

Figure 5-8. Sensitivity to 4-HPR in MDCK-II cells over-expressing ABC transporters.
Cell viability was determined by MTS assay following incubations with 4-HPR (0-100μM) with each cell line for 96h. Results are the mean of 3 independent determinations (error bars are standard deviation).

As shown in Table 5-1 and Figure 5-9, 4-HPR IC_{50} values ranged from 14.7μM for BCRP over-expressing cells to 30.5μM for MRP2 over-expressing cells. For cell lines over-expressing any of the transporters studied, there was less than a 2-fold change in 4-HPR IC_{50} compared to WT cells. No marked differences in 4-HPR IC_{50} were observed in any of the cell lines over-expressing transporters in the presence of inhibitors.

Cell Line	IC_{50} (μM) (- inhibitor)	IC_{50} (μM) (+ inhibitor)
WT	24 ± 2	n/a
MDR1	19 ± 2	22 ± 2
MRP2	31 ± 1	34 ± 1
BCRP	15 ± 1	16 ± 0.3

Table 5-1. 4-HPR IC_{50} values in MDCK-II cells over-expressing ABC transporters, relative to WT cells in the presence or absence of inhibitors of ABC transporters.
Cell viability was determined by MTS assay following incubations with 4-HPR (0-100μM) and either 0 or 5μM verapamil (an inhibitor of MDR1), 0 or 10μM MK571 (an inhibitor of MRP2) or 0 or 2μM K0143 (an inhibitor of BCRP) with each cell line for 96h. Results are the mean of 3 independent determinations (error bars are standard deviation).

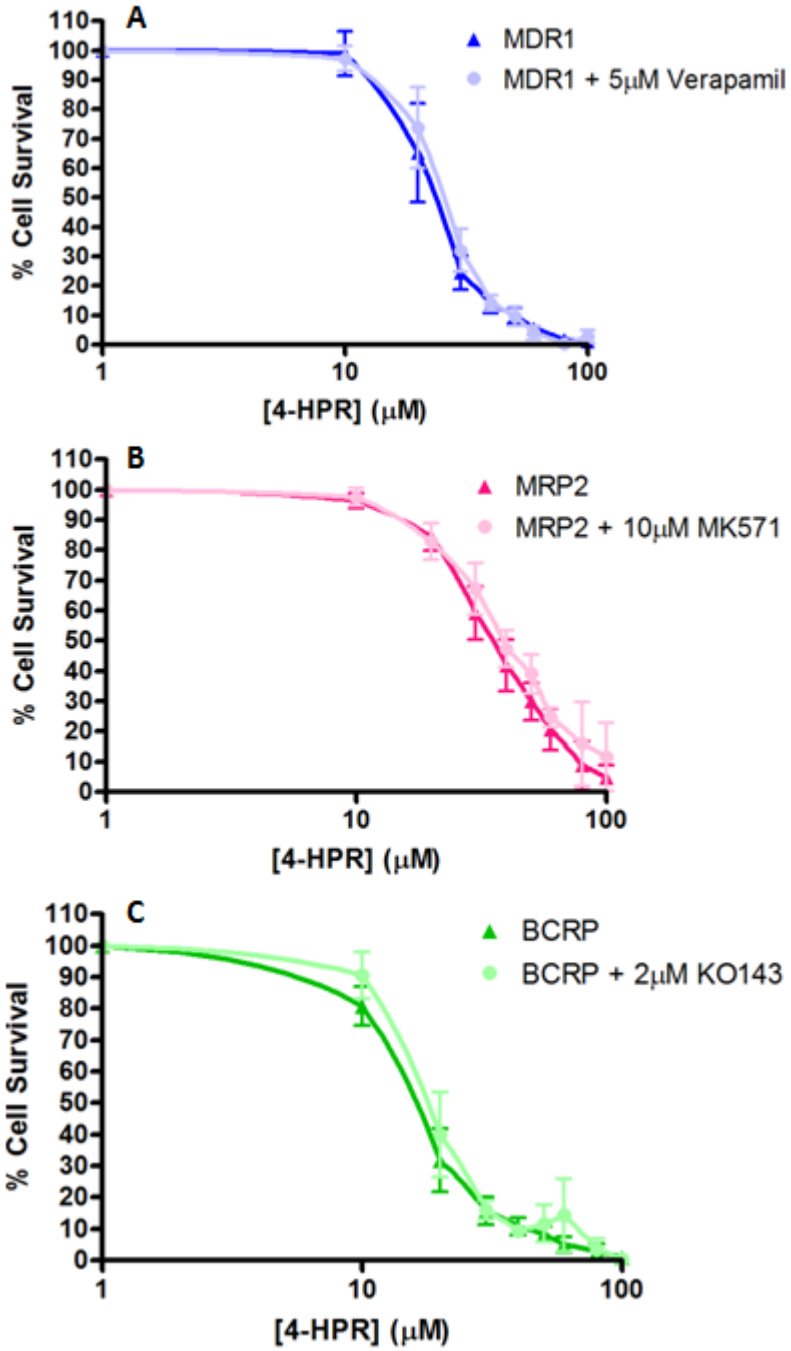

Figure 5-9. Sensitivity to 4-HPR in MDCK-II cells over-expressing ABC transporters, in the presence or absence of inhibitors of ABC transporters.

Cell viability was determined by MTS assay following incubations with 4-HPR (0-100μM) and either A) 0 or 5μM verapamil in MDR1 over-expressing cells, B) 0 or 10μM MK571 in MRP2 over-expressing cells or C) 0 or 2μM K0143 in BCRP over-expressing cells. All drug incubations were carried out for 96h. Results are the mean of 3 independent determinations (error bars are standard deviation).

5.4 Discussion

The ABC family of transport proteins is responsible for the cellular efflux or influx of many xenobiotic compounds. This includes transport of drugs out of tumour cells, with over-expression of these transporters shown to be responsible for drug resistance in many cancers, due to decreased intracellular drug concentrations in tumour cells (Gottesman et al., 2002). Increased drug efflux is a major problem for many chemotherapeutic drugs, including actinomycin D, vincristine, doxorubicin and paclitaxel (Ambudkar et al., 1999). Modulation of p-glycoprotein (MDR1) has been reported in some studies of leukeamic cell lines treated with ATRA (Tokura et al., 2002, Tabe et al., 2006), though other studies have found that ATRA had no effect on MDR1 expression in leukeamic murine cell lines (Sulová et al., 2008). The latter of these studies also determined that ATRA is not a substrate for MDR1, as co-incubation of the MDR1 substrate verapamil with ATRA had no effect on cell sensitivity.

Multidrug resistance is a significant cause of relapse in many cancers, including neuroblastoma (Munoz et al., 2007), where resistance has been associated with expression of MDR1 (Goldstein et al., 1990). One of the major prognostic factors for neuroblastoma patients is the expression of *MYCN* (Look et al., 1991, Seeger et al., 1985, Tang et al., 2006), and expression of this protein has also been associated with expression of multidrug resistance-associated protein (MRP), with both of these genes being down-regulated in cell lines following treatment with ATRA (Bordow et al., 1994). The same study found that neither N-myc nor MRP expression was associated with MDR1 expression. MRP expression has also been associated with neuroblastoma resistance to irinotecan *in vitro* (Norris et al., 2005). An additional study found that MDR1, MRP and BCRP (breast cancer resistance protein) were all expressed in neuroblastoma cell lines, although only BCRP expression was associated with a phenotype resistant to cisplatin (Iwasaki et al., 2002). In neuroblastoma tumour samples, no association was found between expression of multidrug resistance proteins and response, relapse or survival in patients treated with combinations of vincristine, cyclophosphamide, doxorubicin, etoposide, cisplatin, and carboplatin (de Cremoux et al., 2007).

Several studies have also been carried out to examine the expression of multidrug resistance proteins in Ewing's sarcoma. These studies have had mixed results, with

some demonstrating increased expression of MDR1 in Ewing's sarcoma tumour samples and cell lines (Noonan et al., 1990, Stein et al., 1993), whereas others have shown that there is a greater MRP expression (Oda et al., 1997). No association was found between MDR1 expression and relapse-free survival in Ewing's sarcoma and pPNET tumours (Hijazi et al., 1994).

Expression of drug transporters can also affect drug disposition, for example by altering uptake into the liver and kidneys, and subsequently altering either drug metabolism or excretion (Yamazaki et al., 1996). As 4-HPR is highly metabolised to both active and inactive metabolites *in vivo* (Villani et al., 2004, Villablanca et al., 2006, Formelli et al., 2008), altered uptake of either 4-HPR or its metabolites could have a significant effect on its efficacy.

No studies have so far investigated whether 4-HPR is a substrate for multidrug resistance proteins, or investigated the potential impact of altered uptake and altered metabolism in the liver. Due to the known expression of MDR1, MRP and BCRP in neuroblastoma and Ewing's sarcoma tumours, the aim of the current study was to investigate intracellular and extracellular concentrations of 4-HPR and its metabolites using cells stably transfected to over-express MDR1, MRP2 or BCRP.

Initial experiments incubating 4-HPR with cells over-expressing MDR1, MRP2 and BCRP suggested that 4-HPR is a substrate for ABC transporters. There were significantly lower intracellular concentrations of 4-HPR in cells over-expressing MRP2 and BCRP than in a wild-type cell line transfected with an empty vector. Lower intracellular concentrations of 4-HPR were also observed in a cell line over-expressing MDR1, although the decrease did not reach significance. There was no effect on extracellular 4-HPR, probably due to the high concentration of 4-HPR present in the medium. In order to observe efflux from cells, the medium containing the drug would need to be removed, the cells washed in PBS and then replaced with fresh medium. However, it is likely that concentrations of 4-HPR in medium would then be below the sensitivity limits of the HPLC assay.

The inactive metabolite 4-MPR was also seen in both intracellular and extracellular samples. Concentrations of 4-MPR were significantly lower in all three cell lines over-expressing transporter proteins, both intracellularly and extracellularly, than

concentrations observed with WT cells. This may mean that there is either decreased methylation of 4-HPR in these cell lines, or that 4-MPR is less stable in the transfected cell lines. No metabolism was seen to 4'-oxo 4-HPR or 4'-OH 4-HPR and consequently the effect of expression of MDR1, MRP2 and BCRP on the oxidative metabolites of 4-HPR could not be investigated.

In order to confirm that decreased intracellular concentrations of 4-HPR were due to increased drug efflux, rather than differences in metabolism or drug uptake, 4-HPR was incubated with cells over-expressing ABC transporters, as well as inhibitors of those transporters. Cells over expressing MDR1 were incubated with verapamil, a known substrate of MDR1 (Cornwell et al., 1987). Verapamil should compete with 4-HPR for binding to MDR1 and reduce drug efflux caused by the transporter, although verapamil has also been shown to reduce MDR1 gene transcription (Muller et al., 1995). Cells over-expressing MRP2 were incubated with MK571, which inhibits efflux by binding to the ATP catalytic site. This less specific mechanism of action means MK571 also shows some affinity for MDR1 and BCRP (Matsson et al., 2009). Cells over-expressing BCRP were incubated with a potent, specific inhibitor, K0143 (Matsson et al., 2009). Initial experiments were carried out at two different inhibitor concentrations, using a lower concentration known to be non-toxic to the cells, which would be acceptable for future cell viability studies, and a concentration 10-fold higher to look for concentration-dependent effects. Incubation of MDR1 over-expressing cells with verapamil resulted in significantly higher inhibitor concentration-dependent intracellular concentrations of 4-HPR. Incubations of MRP2 over-expressing cells with MK571 resulted in marginally higher intracellular concentrations of 4-HPR, that increased in a concentration-dependent way; however the increases observed were small and did not reach significance. Incubations of BCRP over-expressing cells with K0143 resulted in significantly higher intracellular concentrations of 4-HPR with the highest concentration of K0143 tested. An increase in intracellular 4-HPR was also seen at the lower concentration of K0143, although this did not reach significance. The increases in intracellular 4-HPR observed were all inhibitor-concentration dependent, thereby supporting the evidence that 4-HPR is a substrate for ABC transporters MDR1, MRP2 and BCRP.

Experiments to determine the impact of over-expression of ABC transporters on cell sensitivity to 4-HPR demonstrated an approximate 2-fold variability to IC_{50} value.

Surprisingly, the cell line with the lowest IC_{50} value (BCRP over-expressing cells) also had the lowest intracellular concentrations of 4-HPR, and only one of the ABC transporter over-expressing cell lines (MRP2) had a higher IC_{50} value than the wild-type, meaning there was no correlation between intracellular concentrations of 4-HPR and IC_{50} value. The apparent disparity between intracellular 4-HPR concentrations and IC_{50} values may well be explained by the fact that cell sensitivity experiments were carried out over 96h, whereas the intracellular and extracellular concentrations of 4-HPR and 4-MPR were carried out following 6h incubations. This may also be due to differences in metabolism, as significantly less metabolism to 4-MPR was seen in cell lines over-expressing transporters, that over time could result in a higher proportion of 4-HPR within these cells.

4-HPR causes apoptosis by the generation of reactive oxygen species, that results in oxidative stress triggering programmed cell death (Lovat et al., 2000). Several studies have shown that high levels of reactive species act to down-regulate MDR1 expression (Wartenberg et al., 2003, Comerford et al., 2002). It is possible that over a longer time course a reduction in 4-HPR metabolism will result in increased generation of reactive oxygen species and a corresponding decrease in MDR1 expression. The only ABC transporter over-expressing cell line that was more resistant to 4-HPR than the wild-type cells were the MRP2 over-expressing cells. MRP has been associated with the regulation of glutathione, with increased MRP expression resulting in increased glutathione release within cells (Hirrlinger et al., 2001). As glutathione is known to protect against oxidative stress caused by reactive oxygen species (Akerboom et al., 1982, Sies and Akerboom, 1984, Ishikawa and Sies, 1989), any increase in glutathione would protect against 4-HPR induced apoptosis and would result in cells more resistant to 4-HPR treatment. BCRP expression is also modulated by reactive oxygen species, due to the presence of an anti-oxidant response element (Singh et al., 2010). It is unclear why attenuation of BCRP expression would result in cells being more sensitive to 4-HPR treatment than wild-type cells, however significantly reduced metabolism to 4-MPR was also observed in BCRP over-expressing cells, that could again have increased 4-HPR exposure over time.

Incubation of ABC over-expressing cell lines with specific inhibitors of ABC transport did not increase sensitivity to 4-HPR in any of the cell lines tested. This could be because at the concentration of inhibitors used for the cell sensitivity experiments, there

was only a relatively small increase in intracellular 4-HPR concentrations (a maximum of 15%). As the ABC over-expressing cells were all relatively resistant to 4-HPR (IC_{50} values ranged from 14.7μM to 30.5μM), this relatively small increase in 4-HPR may have little effect. In addition, if generation of reactive oxygen species from treatment with 4-HPR resulted in down-regulation of ABC transporter expression, or an increase in production of glutathione, inhibition of ABC transport would subsequently have little effect on cell sensitivity.

This study was able to identify that 4-HPR is likely to be a substrate for ABC transport by MRP2 and BCRP, but not by MDR1. However, due to the complications of possible down-regulation of exporter expression and upregulation of glutathione in response to 4-HPR treatment, in addition to altered 4-HPR metabolism, it is not possible to determine the full effects of ABC transport over-expression on the efficacy of 4-HPR. This would require investigation into intracellular 4-HPR concentrations over a longer time period (96h), at varying concentrations of 4-HPR. It would also be beneficial to investigate the effect of transporter over-expression in cell lines more sensitive to 4-HPR than MDCK-II, and particularly in a cell line able to metabolise 4-HPR to its active metabolite, 4'-oxo 4-HPR, as this may also be a substrate for ABC transporter efflux. This study has not investigated the possible impact of expression of influx transporters, such as the organic anion-transporting polypeptides (OATPs). These are expressed in the liver and intestine (amongst other tissues) and are able to mediate the uptake of drugs into these organs. Similarly to ABC transporters, OATPs are subject to genetic polymorphisms that can effect drug uptake and subsequently drug metabolism (Kim, 2003). Therefore, the combined impact of uptake and efflux must be taken into consideration to fully characterise the disposition of xenobiotic compounds.

Chapter 6 Conclusion

Retinoids were first recognized for their role in cell differentiation almost 100 years ago (Wolbach and Howe, 1925), and since then the use of retinoid derivatives as chemopreventative and chemotherapeutic agents had been widely explored. Two retinoid analogues in particular, ATRA and its stereoisomeric form, 13-cis RA, have significantly increased life expectancy for patients suffering from acute promyelocytic leukaemia (APL) and high-risk neuroblastoma respectively. Nevertheless, despite the successes seen with retinoid-based chemotherapy, there are still several aspects of retinoid therapy that need to be improved. For example, 13-cis RA and ATRA work by causing differentiation of cancerous cells rather than apoptosis, and many patients suffer a relapse upon cessation of treatment when used as single agent therapy (Sanz et al., 2009). In addition, both compounds are able to induce their own metabolism via up-regulation of CYP26. This limits achievable peak plasma concentrations, particularly following multiple courses of treatment (Muindi et al., 1992, Smith et al., 1992), though this is less of a problem for 13-cis RA, where plasma concentrations have been found to be relatively consistent over multiple courses, (Veal et al., 2007). Both of these retinoid derivatives are also reliant on normal expression of retinoid receptors, the expression of that is aberrant in many cancers (Sun and Lotan, 2002).

4-HPR is a synthetic analogue of retinoic acid, and a more recent addition to the chemotherapeutic retinoid family, that overcomes several of the limitations described above. 4-HPR is able to cause apoptosis rather than differentiation of cells (Kitareewan et al., 1999, Lovat et al., 2000, Vene et al., 2007), and is also effective at treating cell lines expressing either aberrant or wild-type retinoid receptors, suggesting its mechanism of action is independent of retinoid receptor status (Dmitrovsky, 2004). In clinical trials in neuroblastoma patients, 4-HPR has been better tolerated than 13-cis RA, with one trial using doses of 4,000mg/m^2/day without reaching an MTD, and another trial determining an MTD of 2,475mg/m^2/day (Villablanca et al., 2006, Garaventa et al., 2003). Both of these trials reported 4-HPR peak plasma concentrations of a similar magnitude to those found to be effective *in vitro*. 4-HPR was investigated as a chemotherapeutic agent for the treatment of neuroblastoma and Ewing's sarcoma after cell lines derived from these tumours were shown to be sensitive to 4-HPR *in vitro*, and 4-HPR was shown to reduce tumour growth in mouse models (Di Vinci et al.,

1994, Myatt et al., 2005). Both Ewing's sarcoma and neuroblastoma represent cancer types where improved treatments are needed as high risk patients or those who relapse currently have a five year survival of less than 50% (Damron et al., 2007, Laverdière et al., 2009).

In clinical trials in neuroblastoma patients the major limitation in the use of 4-HPR has been the ability to achieve and maintain consistent plasma concentrations following oral administration (Villablanca et al., 2006). This is in part due to the relatively low bioavailability of 4-HPR, an issue currently being addressed by the use of novel formulations of 4-HPR, such as liposomal delivery methods (Raffaghello et al., 2003, Maurer et al., 2007, Orienti et al., 2009). However, the metabolism of 4-HPR is also likely to have a significant impact on clinically achievable maximum plasma concentrations, as 4-HPR is metabolised *in vivo* to two major metabolites, 4'-oxo 4-HPR and 4-MPR (Mehta et al., 1991, Mehta et al., 1998, Garaventa et al., 2003, Villablanca et al., 2006). The former of these metabolites is active, even in some cell lines resistant to 4-HPR, and is able to work synergistically with 4-HPR itself (Villani et al., 2006), whilst the latter is an inactive metabolite (Sabichi et al., 2003, Mehta et al., 1998). The work described in this thesis therefore investigated the enzymes involved in 4-HPR metabolism and the impact of metabolism on efficacy in neuroblastoma and Ewing's sarcoma cell lines, as well as assessing the potential for 4-HPR to act as a substrate for common drug transporters.

As predicted, several members of the CYP family of enzymes were able to metabolise 4-HPR to its active metabolite, 4'-oxo 4-HPR, in addition to the previously unidentified metabolite 4'-OH 4-HPR. The activity of this newly identified metabolite is not yet known, however it appears to be a precursor for 4'oxo 4-HPR. Therefore, factors affecting metabolism to 4'-OH 4-HPR may have an effect on the efficacy of 4-HPR regardless of whether 4'-OH 4-HPR itself proves to be an active or inactive metabolite. Oxidative metabolism was predominantly carried out by CYPs 3A4, 3A5 and 2C8. These CYPs are all expressed at relatively high levels in HIM and HLM, and are likely to be responsible for the majority of oxidative metabolism observed. In addition, oxidative metabolism in cell lines was increased following upregulation of *CYP26A1*, suggesting that 4-HPR is also a substrate for metabolism by CYP26. These findings are consistent with those for metabolism of 13-cis RA and ATRA (Perlmann, 2002).

Several CYPs are known to be highly polymorphic, including CYP2C8, with polymorphisms *2 and *3, both resulting in significantly lower clearance of paclitaxel and arachidonic acid, with consequential clinical implications for patients homozygous for these alleles (Bahadur et al., 2002, Dai et al., 2001, Daly et al., 2007). Although the different CYP2C8 isoforms have been shown to have similar activity for 13-cis RA metabolism (Rowbotham et al., 2010a), oxidative metabolism of 4-HPR is of particular interest due to production of the active metabolite 4'-oxo 4-HPR and therefore the impact of CYP2C8 polymorphisms was investigated. Incubation of 4-HPR with microsomes prepared from *E. coli* cells transfected to over-express individual human CYP2C8 variants *1 (wild-type), *3 or *4 resulted in significant differences in metabolism. The CYP2C8*4 variant had significantly higher K_m and V_{max} values for production of 4'-oxo 4'-HPR, and lower K_m and V_{max} values for production of 4'-OH 4-HPR. As CYP2C8*4 alleles are found in just over 2% of Caucasians (Henningsson et al., 2005), slower metabolism to the active metabolite 4'-oxo 4-HPR may be of clinical relevance and would justify further examination in a patient population.

In investigating the metabolism of 4-HPR to its inactive metabolite, 4-MPR, it was found that methylation is likely to be carried out by an amine-N-methyltransferase, and methylation was not the result of metabolism by catechol-O-methyltransferases or phenol methyltransferases. Due to the lack of a specific inhibitor of amine-N-methyltransferase, inhibition of 4-HPR methylation could only be investigated with imidazole, a competitive substrate (Ansher and Jakoby, 1986) meaning it was not possible to definitively identify the enzyme involved in this important pathway of 4-HPR metabolism. Inhibition of methylation was seen only at high concentrations of imidazole, that limited investigations into the effect of inhibition of methylation on cell sensitivity and on 4-HPR and 4'-oxo 4-HPR concentrations; however it would be useful to explore this further.

Following characterisation of the enzymes involved in phase I metabolism, the contribution of phase II metabolising enzymes was also investigated. Glucuronidation is one of the major phase II detoxification pathways occurring in the liver and intestine, and several studies have investigated the major UGTs responsible for the glucuronidation of retinoid-based drugs, including ATRA (Czernik et al., 2000, Samokyszyn et al., 2000), phase II metabolism of 13-cis RA has not been fully characterised. It is particularly important to identify whether glucuronidation plays a

major part in the metabolism of 4-HPR as polymorphisms of UGT enzymes can have a significant effect on drug toxicity, in much the same way as for CYPs. For example, patients with a variant allele for UGT1A1 have significantly lower glucuronidation of SN-38, the active metabolite of irinotecan. This can result in a higher risk of treatment related toxicity and has lead to dose-reduction advice for patients homozygous for the risk-allele being included on the product label (Ando et al., 2000, O'Dwyer and Catalano, 2006, United States Food and Drug Administration, 2010, Gagné et al., 2002). Due to the wide inter-patient variation in peak plasma concentrations seen *in vivo* for 4-HPR in clinical trials, this study characterised the glucuronidation of 4-HPR and 4'-oxo 4-HPR. Parallel investigations of the glucuronidation of 13cis RA and its 4-oxo metabolite were performed, as this pathway of metabolism had not been previously characterised.

Glucuronidation of 13-cis RA and 4-oxo 13-cis RA was carried out by UGTs 1A1, 1A3, 1A7, 1A8 and 1A9, and it is expected that these UGTs are also responsible for glucuronidation by HIM and HLM. As maximum plasma concentrations achieved in a clinical trial in neuroblastoma patients were 2.8μM for 13-cis RA and 4.7μM for 4-oxo 13-cis RA (Veal et al., 2007), UGT1A9 was the only UGT investigated that is likely to metabolise 13-cis RA and 4-oxo 13-cis RA at clinically relevant concentrations, with K_m values of 3μM and 18μM respectively. However, metabolism by this UGT exhibited relatively low maximum rates of reaction with V_{max} values of 0.04 and 0.2 peak area units/min/pmol UGT for 13-cis RA and 4-oxo 13-cis RA respectively. Glucuronidation by UGT1A9 may be of clinical relevance, as polymorphisms in UGT1A9 occur in approximately 5% of Caucasians, and have previously been shown to influence exposure to SN-38 and mycophenolic acid (Villeneuve et al., 2003, Levesque et al., 2007, Miura et al., 2008).

The glucuronidation of 4-HPR was carried out by UGTs 1A1, 1A3 and 1A6, whereas glucuronidation of 4'-oxo 4-HPR was due to UGTs 1A1, 1A3, 1A8 and 1A9. It is consequently likely that these UGTs are responsible for glucuronidation by HIM and HLM of each substrate. One of the major differences in glucuronidation seen with 4-HPR and 4'-oxo 4-HPR compared to 13-cis RA and 4-oxo 13-cis RA was that the same panel of UGTs were able to glucuronidate both 13-cis RA and 4-oxo 13-cis RA, whereas different UGTs were responsible for the glucuronidation of 4-HPR than those responsible for the glucuronidation of 4'-oxo 4-HPR. 4-MPR and 4-EPR were not

glucuronidated by HIM, HLM or any of the individual UGT enzymes tested. This indicated that the likely position of the glucuronidation is at the hydroxyl group on the 4th carbon of the amide ring. It is probable that 4'-oxo 4-HPR will be glucuronidated in the same position. The fundamental difference between glucuronidation of 13-cis RA and of 4-HPR is that the former is metabolised to an acyl glucuronide, while the latter would form an ether glucuronide.

Glucuronidation by any of the UGTs tested was a relatively slow reaction, yielding low concentrations of glucuronide metabolites. K_m values for all UGTs were high, with the lowest K_m value for glucuronidation of 4-HPR found with UGT1A3 (389μM) and for glucuronidation of 4'-oxo 4-HPR with UGT1A1 (230μM). As clinical trials involving 4-HPR administration have struggled to obtain peak plasma concentrations of 4-HPR above 10μM (Formelli et al., 2003, Garaventa et al., 2003, Formelli et al., 2008), is it highly unlikely that metabolism by glucuronidation will play a major part in the clearance of 4-HPR at clinically relevant levels, and it is doubtful that polymorphisms of UGT enzymes would have a major impact on the clinical pharmacology of the drug. However, as glucuronidation has a significant impact on exposure to SN-38 (Gagné et al., 2002), despite comparatively high in vitro K_m values (Jinno et al., 2003) and low clinical C_{max} concentrations (Chabot, 1997), it is possible that 4-HPR glucuronidation could play a role in determining efficacy. In particular, glucuronidation of 4-HPR and its metabolites may be of greater interest where 4-HPR is administered in combination with compounds affecting the metabolism of 4-HPR by CYPs. In a Ewing's sarcoma mouse model, co-administration of 4-HPR and ketoconazole (an inhibitor of CYP3A4) resulted in increased concentrations of both 4-HPR and, surprisingly, 4'-oxo 4-HPR (Cooper et al., 2011). Metabolism of 4-HPR to 4'-oxo 4-HPR is carried out by CYPs 3A4 and 2C8. As CYP3A4 is expressed in both the liver and the intestine, whereas CYP2C8 is only expressed in the intestine, co-administration of ketoconazole should significantly reduce oxidative metabolism of 4-HPR in the intestine. However, significant metabolism by CYP2C8 should still occur in the liver. As the rate of glucuronidation of 4'-oxo 4-HPR is significantly higher in HIM than in HLM, it is likely that 4'-oxo 4-HPR produced in the intestine will undergo significant glucuronidation, whereas if 4'-oxo 4-HPR is produced only in the liver it will largely remain intact. This would therefore explain the unexpected increase in 4'-oxo 4-HPR resulting from inhibition of CYP3A4 by ketoconazole. Understanding the clinical impact of inhibition of CYP metabolism of 4-HPR may be of particular relevance, as a

clinical trial in Ewing's sarcoma patients in currently underway investigating the effect of co-administration of 4-HPR and ketoconazole (US National Institutes of Health, 2010a).

Neuroblastoma and Ewing's sarcoma cell lines have both been found to be sensitive to 4-HPR treatment *in vitro* (Lovat et al., 2000, Myatt and Burchill, 2008), as well as being sensitive to the 4'-oxo metabolite of 4-HPR (Villani et al., 2006). However, little is currently known about intracellular 4-HPR metabolism and the effect that this has on determining sensitivity to 4-HPR. The CYP26 family of enzymes is induced by ATRA and 13-cis RA (White et al., 1997), and inhibition of *CYP26A1* by RAMBAs significantly increases plasma concentrations of ATRA and 13-cis RA both *in vitro* and in a neuroblastoma mouse model (Armstrong et al., 2007b). CYP26 is induced by retinoid treatment in several tumours (White et al., 1997), and although there is relatively low expression of CYP26 in the liver and intestine, the enzyme may be responsible for the majority of retinoid metabolism within tumour cells. This study therefore investigated intracellular 4-HPR metabolism, the contribution of CYP26A1 to 4-HPR metabolism and the possible modulation of CYP26A1 metabolism with RAMBAs.

Incubation of 4-HPR with neuroblastoma and Ewing's sarcoma cell lines resulted in metabolism of 4-HPR to its inactive metabolite 4-MPR in all cell lines tested. Conversely, metabolism to the oxidative metabolites of 4-HPR varied considerably between cell lines, although the differences in extent of oxidative metabolism did not appear to have a corresponding effect on growth inhibition. In addition, upregulation of *CYP26A1* expression following pre-incubation of cell lines with ATRA had no effect on 4-HPR IC_{50} values, despite a corresponding up-regulation in oxidative metabolism. This may be due in part to the relatively small amount of overall metabolism that occurred, with metabolite peak areas varying from 0.01 – 2.0% of the parent peak area. Metabolism to both 4'-oxo 4-HPR and 4-MPR is significantly higher in patients and mice treated with 4-HPR, with plasma concentrations of 4'-oxo 4-HPR and 4-MPR of up to 20% of 4-HPR concentrations (Cooper et al., 2011, Formelli et al., 2003, Formelli et al., 2008, Formelli et al., 1993). This is closer to the amount of metabolism seen in human liver and intestinal microsomes, and indicates that the majority of 4-HPR metabolism occurs during first pass metabolism, and that metabolism within tumours is likely to have less of an impact on drug efficacy.

The final factor considered that may contribute to drug efficacy is the impact of the ABC family of transport proteins. These cellular transmembrane proteins are responsible for the efflux of many xenobiotic compounds, including transport out of tumour cells. The over-expression of these transporters has been linked with drug resistance in many cancers, due to decreased intracellular drug concentrations in tumour cells (Gottesman et al., 2002), and has been associated with relapse in neuroblastoma (Munoz et al., 2007). In addition, expression of drug transporters can also affect drug disposition, for example by altering uptake into the liver and kidneys, and subsequently altering either drug metabolism or excretion (Yamazaki et al., 1996). As 4-HPR is substantially metabolised by human liver and intestinal microsomes, and no studies have so far investigated whether 4-HPR is a substrate for multidrug resistance proteins, this study investigated intracellular and extracellular concentrations of 4-HPR and its metabolites using cells transfected to over-express the common transporters MDR1, MRP2 and BCRP.

Initial experiments incubating 4-HPR with cells over-expressing MDR1, MRP2 and BCRP suggested that 4-HPR is a substrate for these ABC transporters, as cells over-expressing MRP2 and BCRP had significantly lower intracellular concentrations of 4-HPR than wild-type cells transfected with a blank plasmid. In addition, an increase in intracellular 4-HPR concentrations was seen when inhibitors of MDR1 and BCRP were co-incubated with 4-HPR. However, despite the differences seen in intracellular 4-HPR concentrations, there was no correlation with growth inhibition, with some cell lines over-expressing transporters appearing to be more sensitive to 4-HPR treatment than wild-type cells, whilst others were more resistant. In addition the use of inhibitors of ABC transporters had little effect on sensitivity to 4-HPR. Elucidation of the effect of ABC transporters on cell sensitivity to 4-HPR was further complicated by possible differences in metabolism, as lower concentrations of both intracellular and extracellular 4-MPR were observed in incubations with cells over-expressing transporters than with wild-type cells. These contradictory results may be partly explained by different experimental methods used for cell sensitivity and intracellular 4-HPR concentration experiments, however the overall evidence for 4-HPR being a substrate of ABC transporters is relatively weak.

The major metabolites and metabolising enzymes of 4-HPR have been identified and characterised. CYP2C8 isoform has been identified as having potential clinical relevance and may help to explain the wide variation seen in patient plasma concentrations of 4-HPR. The data suggest that neither glucuronidation, auto up-regulation of CYP26 nor the over-expression of ABC transporters are expected to have a significant impact on 4-HPR efficacy *in vivo*. However, polymorphisms of UGT1A9 may have an impact on metabolism of another retinoic acid analogue, 13-cis RA, and the effect of UGT polymorphisms on 13-cis RA efficacy should be explored further. As novel formulations of 4-HPR address the limitations of low bioavailability and the resulting difficulties in achieving higher plasma concentrations of 4-HPR, the role of 4-HPR metabolism is likely to have a greater impact on efficacy. This may provide the potential for optimisation of the clinical utility of 4-HPR through modulation of drug metabolism.

Chapter 7 References

ABDEL-RAZZAK, Z., LOYER, P., FAUTREL, A., GAUTIER, J. C., CORCOS, L., TURLIN, B., BEAUNE, P. & GUILLOUZO, A. 1993. Cytokines down-regulate expression of major cytochrome P-450 enzymes in adult human hepatocytes in primary culture. *Molecular Pharmacology,* 44**,** 707-715.

AITHAL, G. P., DAY, C. P., KESTEVEN, P. J. L. & DALY, A. K. 1999. Association of polymorphisms in the cytochrome P450 CYP2C9 with warfarin dose requirement and risk of bleeding complications. *The Lancet,* 353**,** 717-719.

AKERBOOM, T., BILZER, M. & SIES, H. 1982. The relationship of biliary glutathione disulfide efflux and intracellular glutathione disulfide content in perfused rat liver. *J Biol Chem,* 257**,** 4248-4252.

ALLENBY, G., BOCQUEL, M. T., SAUNDERS, M., KAZMER, S., SPECK, J., ROSENBERGER, M., LOVEY, A., KASTNER, P., GRIPPO, J. F. & CHAMBON, P. 1993. Retinoic acid receptors and retinoid X receptors: interactions with endogenous retinoic acids. *Proceedings of the National Academy of Sciences,* 90**,** 30-34.

AMBUDKAR, S. V., DEY, S., HRYCYNA, C. A., RAMACHANDRA, M., PASTAN, I. & GOTTESMAN, M. M. 1999. Biochemical, cellular and pharmacological aspects of the multidrug transporter. *Annual Review of Pharmacology and Toxicology,* 39**,** 361-398.

ANAND, P., KUNNUMAKARA, A. B., SUNDARAM, C., HARIKUMAR, K. B., THARAKAN, S. T., LAI, O. S., SUNG, B. & AGGARWAL, B. B. 2008. Cancer is a Preventable Disease that Requires Major Lifestyle Changes. *Pharmaceutical Research,* 25**,** 2097 - 2116.

ANDO, Y., SAKA, H., ANDO, M., SAWA, T., MURO, K., UEOKA, H., YOKOYAMA, A., SAITOH, S., SHIMOKATA, K. & HASEGAWA, Y. 2000. Polymorphisms of UDP-Glucuronosyltransferase Gene and Irinotecan Toxicity: A Pharmacogenetic Analysis. *Cancer Research,* 60**,** 6921-6926.

ANSHER, S. S. & JAKOBY, W. B. 1986. Amine N-methyltransferases from rabbit liver. *Journal of Biological Chemistry,* 261**,** 3996-4001.

ANZENBACHER, P. & ANZENBACHEROVÁ, E. 2001. Cytochromes P450 and metabolism of xenobiotics. *Cellular and Molecular Life Sciences,* 58**,** 737-747.

APPIERTO, V., CAVADINI, E., PERGOLIZZI, R., CLERIS, L., LOTAN, R., CANEVARI, S. & FORMELLI, F. 2001. Decrease in drug accumulation and in tumour aggressiveness marker expression in a fenretinide-induced resistant ovariantumour cell line. *British Journal of Cancer,* 84**,** 1528-1534.

ARMSTRONG, J., VEAL, G., REDFERN, C. & LOVAT, P. 2007a. Role of Noxa in p53-independent fenretinide-induced apoptosis of neuroectodermal tumours. *Apoptosis,* 12**,** 613-622.

ARMSTRONG, J. L., RUIZ, M., BODDY, A. V., REDFERN, C. P. F., PEARSON, A. D. J. & VEAL, G. J. 2005. Increasing the intracellular availability of all-trans retinoic acid in neuroblastoma cells. *British Journal of Cancer,* 92**,** 696-704.

ARMSTRONG, J. L., TAYLOR, G. A., THOMAS, H. D., BODDY, A. V., REDFERN, C. P. F. & VEAL, G. J. 2007b. Molecular targeting of retinoic acid metabolism in neuroblastoma: the role of the CYP26 inhibitor R116010 in vitro and in vivo. *British Journal of Cancer,* 96**,** 1675-83.

ARVAND, A. & DENNY, C. T. 2001. Biology of EWS/ETS fusions in Ewing'sfamily tumours. *Oncogene,* 20**,** 5747-5754.

AURIAS, A., RIMBAUT, C., BUFFE, D., ZUCKER, J.-M. & MAZABRAUD, A. 1984. Translocation involving chromosome 22 in Ewing's Sarcoma. A cytogenetic study of four fresh tumors. *Cancer Genetics and Cytogenetics,* 12**,** 21-25.

BACCI, G., TONI, A. & AVELLA, M. 1989. Long-term results in 144 localized Ewing's sarcoma patients treated with combined therapy. *J Clin Oncol,* 63**,** 1477-1486.

BACK, D. J. & ROGERS, S. M. 1987. Review: first-pass metabolism by the gastrointestinal mucosa. *Alimentary Pharmacology & Therapeutics,* 1**,** 339-357.

BAHADUR, N., LEATHART, J. B. S., MUTCH, E., STEIMEL-CRESPI, D., DUNN, S. A., GILISSEN, R., HOUDT, J. V., HENDRICKX, J., MANNENS, G., BOHETS, H., WILLIAMS, F. M., ARMSTRONG, M., CRESPI, C. L. & DALY, A. K. 2002. CYP2C8 polymorphisms in Caucasians and their relationship with paclitaxel 6alpha-hydroxylase activity in human liver microsomes. *Biochemical Pharmacology,* 64**,** 1579-89.

BATES, S. E., SHIEH , C. Y. & TSOKOS, M. 1991. Expression of mdr-1/P-glycoprotein in human neuroblastoma. *Am J Pathol,* 139**,** 305-315.

BEAUNE, P., DANSETTE, P., FLINOIS, J. P., COLUMELLI, S., MANSUY, D. & LEROUX, J. P. 1979. Partial purification of human liver cytochrome P 450. *Biochemical and Biophysical Research Communications,* 88**,** 826-832.

BENNER, S. E., PAJAK, T. F., LIPPMAN, S. M., EARLEY, C. & HONG, W. K. 1994. Prevention of Second Primary Tumors With Isotretinoin in Patients With Squamous Cell Carcinoma of the Head and Neck: Long-term Follow-up. *Journal of the National Cancer Institute,* 86**,** 140-141.

BERTHOLD, F., HERO, B., BREU, H., CHRISTIANSEN, H., ERTTMANN, R., GNEKOW, A., HERRMANN, F., KLINGEBIEL, T., LAMPERT, F., MIILLER-WEIHRICH, S. & WEINEL, P. 1996. The recurrence patterns of stages I, II and III neuroblastoma: Experience with 77 relapsing patients. *Annals of Oncology,* 7**,** 183-187.

BHATNAGAR, R., ABOU-ISSA, H., CURLEY JR, R. W., KOOLEMANS-BEYNEN, A., MOESCHBERGER, M. L. & WEBB, T. E. 1991. Growth suppression of human breast carcinoma cells in culture by N-(4-hydroxyphenyl)retinamide and its glucuronide and through synergism with glucarate. *Biochemical Pharmacology,* 41**,** 1471-1477.

BJORGE, T., ENGELAND, A., TRETLI, S. & HEUCH, I. 2008. Birth and parental characteristics and risk of neuroblastoma in a population-based Norwegian cohort study. *British Journal of Cancer,* 99**,** 1165-9.

BLOMHOFF, R. & BLOMHOFF, H. K. 2006. Overview of retinoid metabolism and function. *Journal of Neurobiology,* 66**,** 606-630.

BLUHM, E., MCNEIL, D. E., CNATTINGIUS, S., GRIDLEY, G., EL GHORMLI, L. & FRAUMENI, J. F., JR. 2008. Prenatal and perinatal risk factors for neuroblastoma. *International Journal of Cancer,* 123**,** 2885-90.

BOCK, K. W. 2010. Functions and transcriptional regulation of adult human hepatic UDP-glucuronosyl-transferases (UGTs): mechanisms responsible for interindividual variation of UGT levels. *Biochemical Pharmacology,* 80**,** 771-7.

BORDOW, S. B., HABER, M., MADAFIGLIO, J., CHEUNG, B., MARSHALL, G. M. & NORRIS, M. D. 1994. Expression of the Multidrug Resistance-associated Protein (MRP) Gene Correlates with Amplification and Overexpression of the N-myc Oncogene in Childhood Neuroblastoma. *Cancer Research,* 54**,** 5036-5040.

BOSCH, T. M., MEIJERMAN, I., BEIJNEN, J. H. & SCHELLENS, J. H. M. 2006. Genetic polymorphisms of drug-metabolising enzymes and drug transporters in

the chemotherapeutic treatment of cancer. *Clinical Pharmacokinetics,* 45**,** 253-85.
BRINKMANN, U. & EICHELBAUM, M. 2001. Polymorphisms in the ABC drug transporter gene MDR1. *Pharmacogenomics J,* 1**,** 59-64.
BUCKLEY, J. D., PENDERGRASS, T. W., BUCKLEY, C. M., PRITCHARD, D. J., NESBIT, M. E., PROVISOR, A. J. & ROBISON, L. L. 1998. Epidemiology of osteosarcoma and Ewing's sarcoma in childhood. *Cancer,* 83**,** 1440-1448.
CAMERINI, T., MARIANI, L., DE PALO, G., MARUBINI, E., DI MAURO, M. G., DECENSI, A., COSTA, A. & VERONESI, U. 2001. Safety of the Synthetic Retinoid Fenretinide: Long-Term Results From a Controlled Clinical Trial for the Prevention of Contralateral Breast Cancer. *J Clin Oncol,* 19**,** 1664-1670.
CANCER RESEARCH UK. 2005. *Childhood Cancer Statistics* [Online]. Available: http://info.cancerresearchuk.org/cancerstats/childhoodcancer/survival/ [Accessed 2011].
CANCER RESEARCH UK. 2010. *Survival Statistics* [Online]. Available: http://info.cancerresearchuk.org/cancerstats/survival/latestrates/#source2 [Accessed 15th April 2011].
CANCERINDEX. 1999. *About James Ewing, 1866 - 1943* [Online]. Available: http://www.cancerindex.org/bone/ewing.htm [Accessed 2008].
CANCERINDEX. 2003. *Ewing's Sarcoma* [Online]. Available: http://www.cancerindex.org/ccw/faq/ewings.htm [Accessed 2008].
CHABOT, G. G. 1997. Clinical pharmacokinetics of irinotecan. *Clinical Pharmacokinetics,* 33**,** 245 - 259.
CHAMBON, P. 1996. A decade of molecular biology of retinoic acid receptors. *The FASEB Journal,* 10**,** 940-954.
CHOLERTON, S., DALY, A. K. & IDLE, J. R. 1992. The role of individual human cytochromes P450 in drug metabolism and clinical response. *Trends in Pharmacological Sciences,* 13**,** 434-9.
CHOUDHARY, D., JANSSON, I., STOILOV, I., SARFARAZI, M. & SCHENKMAN, J. 2005. Expression patterns of mouse and human CYP orthologs
(families 1–4) during development and in diVerent adult tissues. *Archives of Biochemistry and Biophysics,* 436**,** 50-61.
CHUNG, J.-Y., CHO, J.-Y., YU, K.-S., KIM, J.-R., JUNG, H.-R., LIM, K.-S., JANG, I.-J. & SHIN, S.-G. 2005. Effect of the UGT2B15 Genotype on the Pharmacokinetics, Pharmacodynamics, and Drug Interactions of Intravenous Lorazepam in Healthy Volunteers[ast]. *Clin Pharmacol Ther,* 77**,** 486-494.
COBLEIGH, M. A., VOGEL, C. L., TRIPATHY, D., ROBERT, N. J., SCHOLL, S., FEHRENBACHER, L., WOLTER, J. M., PATON, V., SHAK, S., LIEBERMAN, G. & SLAMON, D. J. 1999. Multinational Study of the Efficacy and Safety of Humanized Anti-HER2 Monoclonal Antibody in Women Who Have HER2-Overexpressing Metastatic Breast Cancer That Has Progressed After Chemotherapy for Metastatic Disease. *Journal of Clinical Oncology,* 17**,** 2639.
COMERFORD, K. M., WALLACE, T. J., KARHAUSEN, J., LOUIS, N. A., MONTALTO, M. C. & COLGAN, S. P. 2002. Hypoxia-inducible factor-1-dependent regulation of the multidrug resistance (MDR1) gene. *Cancer Research,* 62**,** 3387-3394.
COOK, M. N., OLSHAN, A. F., GUESS, H. A., SAVITZ, D. A., POOLE, C., BLATT, J., BONDY, M. L. & POLLOCK, B. H. 2004. Maternal medication use and neuroblastoma in offspring. *American Journal of Epidemiology,* 159**,** 721-31.
COOPER, J., HWANG, K., SINGH, H., WANG, D., REYNOLDS, C. P., CURLEY, R. W., JR., WILLIAMS, S., MAURER, B. J. & KANG, M. H. 2011. Fenretinide

Metabolism in Humans and Mice: Utilizing Pharmacologic Modulation of its Metabolic Pathway to Increase Systemic Exposure. *British Journal of Pharmacology,* In Press.

CORAZZARI, M., LOVAT, P. E., OLIVERIO, S., DI SANO, F., DONNORSO, R. P., REDFERN, C. P. F. & PIACENTINI, M. 2005. Fenretinide: a p53-independent way to kill cancer cells. *Biochemical & Biophysical Research Communications,* 331**,** 810-5.

CORNWELL, M. M., PASTAN, I. & GOTTESMAN, M. M. 1987. Certain calcium channel blockers bind specifically to multidrug-resistant human KB carcinoma membrane vesicles and inhibit drug binding to P-glycoprotein. *Journal of Biological Chemistry,* 262**,** 2166-2170.

COTTERILL, S. J., AHRENS, S., PAULUSSEN, M., JURGENS, H. F., VOUTE, P. A., GADNER, H. & CRAFT, A. W. 2000. Prognostic Factors in Ewing's Tumor of Bone: Analysis of 975 Patients From the European Intergroup Cooperative Ewing's Sarcoma Study Group. *J Clin Oncol,* 18**,** 3108-3114.

CZERNIK, P. J., LITTLE, J. M., BARONE, G. W., RAUFMAN, J.-P. & RADOMINSKA-PANDYA, A. 2000. Glucuronidation of Estrogens and Retinoic Acid and Expression of UDP-Glucuronosyltransferase 2B7 in Human Intestinal Mucosa. *Drug Metabolism and Disposition,* 28**,** 1210-1216.

DAI, D., ZELDIN, D. C., BLAISDELL, J. A., CHANAS, B., COULTER, S. J., GHANAYEM, B. I. & GOLDSTEIN, J. A. 2001. Polymorphisms in human CYP2C8 decrease metabolism of the anticancer drug paclitaxel and arachidonic acid. *Pharmacogenetics,* 11**,** 597-607.

DALY, A. K., AITHAL, G. P., LEATHART, J. B. S., SWAINSBURY, R. A., DANG, T. S. & DAY, C. P. 2007. Genetic susceptibility to diclofenac-induced hepatotoxicity: contribution of UGT2B7, CYP2C8, and ABCC2 genotypes. *Gastroenterology,* 132**,** 272-81.

DALY, A. K., MONKMAN, S. C., SMART, J., STEWARD, A. & CHOLERTON, S. 1998. Analysis of cytochrome P450 polymorphisms. *Methods in Molecular Biology,* 107**,** 405-22.

DAMRON, T. A., WARD, W. G. & STEWART, A. 2007. Osteosarcoma, chondrosarcoma, and Ewing's sarcoma: National Cancer Data Base Report. *Clin Orthop Relat Res,* 459**,** 40 - 47.

DAVIS, S., ROGERS, M. & PENDERGRASS, T. 1987. THE INCIDENCE AND EPIDEMIOLOGIC CHARACTERISTICS OF NEUROBLASTOMA IN THE UNITED STATES. *American Journal of Epidemiology,* 126**,** 1063-1074.

DE ALAVA, E. & GERALD, W. L. 2000. Molecular Biology of the Ewing's Sarcoma/Primitive Neuroectodermal Tumor Family. *J Clin Oncol,* 18**,** 204-.

DE CREMOUX, P., JOURDAN-DA-SILVA, N., COUTURIER, J., TRAN-PERENNOU, C., SCHLEIERMACHER, G., FEHLBAUM, P., DOZ, F., MOSSERI, V., DELATTRE, O., KLIJANIENKO, J., VIELH, P. & MICHON, J. 2007. Role of chemotherapy resistance genes in outcome of neuroblastoma. *Pediatric Blood & Cancer,* 48**,** 311-317.

DELIA, D., AIELLO, A., MERONI, L., NICOLINI, M., REED, J. C. & PIEROTTI, M. A. 1997. Role of antioxidants and intracellular free radicals in retinamide-induced cell death. *Carcinogenesis,* 18**,** 943-948.

DELVA, L., CORNIC, M., BALITRAND, N., GUIDEZ, F., MICLEA, J., DELMER, A., TEILLET, F., FENAUX, P., CASTAIGNE, S. & DEGOS, L. 1993. Resistance to all-trans retinoic acid (ATRA) therapy in relapsing acute promyelocytic leukemia: study of in vitro ATRA sensitivity and cellular retinoic acid binding protein levels in leukemic cells [see comments]. *Blood,* 82**,** 2175-2181.

DEVITA, V. T. & CHU, E. 2008. A History of Cancer Chemotherapy. *Cancer Research,* 68**,** 8643-8653.

DI VINCI, A., GEIDO, E., INFUSINI, E. & GIARETTI, W. 1994. Neuroblastoma cell apoptosis induced by the synthetic retinoid N-(4-hydroxyphenyl)retinamide. *International Journal of Cancer,* 59**,** 422-6.

DMITROVSKY, E. 2004. Fenretinide Activates a Distinct Apoptotic Pathway. *J. Natl. Cancer Inst.,* 96**,** 1264-1265.

DOSTALEK, M., COURT, M. H., YAN, B. & AKHLAGHI, F. 2011. Significantly reduced cytochrome P450 3A4 expression and activity in liver from humans with diabetes mellitus. *British Journal of Pharmacology***,** no-no.

DUNST, J., SAUER, R., BURGERS, J. M. V., HAWLICZEK, R., KÜRTEN, R., WINKELMANN, W., SALZER-KUNTSCHIK, M., MÜSCHENICH, M. & GROUP, H. J. C. E. S. S. S. 1991. Radiation therapy as local treatment in ewing's sarcoma. Results of the cooperative ewing's sarcoma studies cess 81 and cess 86. *Cancer,* 67**,** 2818-2825.

EFFERTH, T. & VOLM, M. 2005. Pharmacogenetics for individualized cancer chemotherapy. *Pharmacology & Therapeutics,* 107**,** 155-176.

EKHART, C., DOODEMAN, V. D., RODENHUIS, S., SMITS, P. H., BEIJNEN, J. H. & HUITEMA, A. D. 2008. Influence of polymorphisms of drug metabolizing enzymes (CYP2B6, CYP2C9, CYP2C19, CYP3A4, CYP3A5, GSTA1, GSTP1, ALDH1A1 and ALDH3A1) on the pharmacokinetics of cyclophosphamide and 4-hydroxycyclophosphamide. *Pharmacogenet Genomics,* 18**,** 515 - 523.

ELIAZER, S., SPENCER, J., YE, D., OLSON, E. & ILARIA, R. L., JR. 2003. Alteration of Mesodermal Cell Differentiation by EWS/FLI-1, the Oncogene Implicated in Ewing's Sarcoma. *Mol. Cell. Biol.,* 23**,** 482-492.

ERDREICH-EPSTEIN, A., TRAN, L. B., BOWMAN, N. N., WANG, H., CABOT, M. C., DURDEN, D. L., VLCKOVA, J., REYNOLDS, C. P., STINS, M. F., GROSHEN, S. & MILLARD, M. 2002. Ceramide Signaling in Fenretinide-induced Endothelial Cell Apoptosis. *J. Biol. Chem.,* 277**,** 49531-49537.

EVANS, T. B. & KAYE, S. B. 1999. Retinoids: Present role and future potential. *Br J Cancer,* 80**,** 1 - 8.

EVERS, R., KOOL, M., VAN DEEMTER, L., JANSSEN, H., CALAFAT, J., OOMEN, L. C., PAULUSMA, C. C., OUDE ELFERINK, R. P., BAAS, F., SCHINKEL, A. H. & BORST, P. 1998. Drug export activity of the human canalicular multispecific organic anion transporter in polarized kidney MDCK cells expressing cMOAT (MRP2) cDNA. *The Journal of Clinical Investigation,* 101**,** 1310-1319.

EWING, J. 1984. Diffuse Endothelioma of Bone. *Clinical Orthopaedics and Related Research,* 185**,** 2-5.

FANJUL, A. N., DELIA, D., PIEROTTI, M. A., RIDEOUT, D., QIU, J. & PFAHL, M. 1996. 4-Hydroxyphenyl Retinamide Is a Highly Selective Activator of Retinoid Receptors. *J. Biol. Chem.,* 271**,** 22441-22446.

FARBER, S., DIAMOND, L. K., MERCER, R. D., SYLVESTER, R. F. & WOLFF, J. A. 1948. Temporary Remissions in Acute Leukemia in Children Produced by Folic Acid Antagonist, 4-Aminopteroyl-Glutamic Acid (Aminopterin). *New England Journal of Medicine,* 238**,** 787-793.

FLETCHER, J. I., HABER, M., HENDERSON, M. J. & NORRIS, M. D. 2010. ABC transporters in cancer: more than just drug efflux pumps. *Nat Rev Cancer,* 10**,** 147-156.

FORMELLI, F., CAMERINI, T., CAVADINI, E., APPIERTO, V., VILLANI, M. G., COSTA, A., DE PALO, G., DI MAURO, M. G. & VERONESI, U. 2003. Fenretinide breast cancer prevention trial: drug and retinol plasma levels in

relation to age and disease outcome. *Cancer Epidemiology, Biomarkers & Prevention,* 12**,** 34-41.

FORMELLI, F., CARSANA, R., COSTA, A., BURANELLI, F., CAMPA, T., DOSSENA, G., MAGNI, A. & PIZZICHETTA, M. 1989. Plasma retinol level reduction by the synthetic retinoid fenretinide: a one year follow-up study of breast cancer patients. *Cancer Research,* 49**,** 6149-52.

FORMELLI, F., CAVADINI, E., LUKSCH, R., GARAVENTA, A., VILLANI, M. G., APPIERTO, V. & PERSIANI, S. 2008. Pharmacokinetics of oral fenretinide in neuroblastoma patients: indications for optimal dose and dosing schedule also with respect to the active metabolite 4-oxo-fenretinide. *Cancer Chemotherapy & Pharmacology,* 62**,** 655-65.

FORMELLI, F., CLERICI, M., CAMPA, T., DI MAURO, M. G., MAGNI, A., MASCOTTI, G., MOGLIA, D., DE PALO, G., COSTA, A. & VERONESI, U. 1993. Five-year administration of fenretinide: pharmacokinetics and effects on plasma retinol concentrations. *Journal of Clinical Oncology,* 11**,** 2036-42.

GAGNÉ, J.-F., MONTMINY, V., BELANGER, P., JOURNAULT, K., GAUCHER, G. & GUILLEMETTE, C. 2002. Common Human UGT1A Polymorphisms and the Altered Metabolism of Irinotecan Active Metabolite 7-Ethyl-10-hydroxycamptothecin (SN-38). *Molecular Pharmacology,* 62**,** 608-617.

GARAVENTA, A., LUKSCH, R., PICCOLO, M. S. L., CAVADINI, E., MONTALDO, P. G., PIZZITOLA, M. R., BONI, L., PONZONI, M., DECENSI, A., BERNARDI, B. D., BELLANI, F. F. & FORMELLI, F. 2003. Phase I Trial and Pharmacokinetics of Fenretinide in Children with Neuroblastoma. *Clin Cancer Res,* 9**,** 2032-2039.

GIGUERE, V., ONG, E. S., SEGUI, P. & EVANS, R. M. 1987. Identification of a receptor for the morphogen retinoic acid. *Nature,* 330**,** 624-629.

GOH, Y. I., BOLLANO, E., EINARSON, T. R. & KOREN, G. 2007. Prenatal multivitamin supplementation and rates of pediatric cancers: a meta-analysis. *Clinical Pharmacology & Therapeutics,* 81**,** 685-91.

GOLDSTEIN, L. J., FOJO, A. T., UEDA, K., CRIST, W., GREEN, A., BRODEUR, G., PASTAN, I. & GOTTESMAN, M. M. 1990. Expression of the multidrug resistance, MDR1, gene in neuroblastomas. *Journal of Clinical Oncology,* 8**,** 128-36.

GOTTESMAN, M. M., FOJO, T. & BATES, S. E. 2002. Multidrug resistance in cancer: role of ATP-dependent transporters. *Nat Rev Cancer,* 2**,** 48-58.

GREENWOOD, C. 1963. A partial purification and some properties of the cytochrome oxidase from pig-heart muscle. *Biochem J,* 86**,** 535 - 540.

GRIER, H., KRAILO, M. & LINK, M. 1994. Improved outcome in non-metastatic Ewing's sarcoma (EWS) and PNET of bone with the addition of ifosfamide (I) and etoposide (E) to vincristine (V), adriamycin (Ad), cyclophosphamide (C), and actinomycin (A): A Childrens Cancer Group (CCG) and Pediatric Oncology Group (POG) report. *Proceedings of the American Society of Clinical Oncology,* 13**,** 421.

GRIER, H. E., KRAILO, M. D., TARBELL, N. J., LINK, M. P., FRYER, C. J. H., PRITCHARD, D. J., GEBHARDT, M. C., DICKMAN, P. S., PERLMAN, E. J., MEYERS, P. A., DONALDSON, S. S., MOORE, S., RAUSEN, A. R., VIETTI, T. J. & MISER, J. S. 2003. Addition of ifosfamide and etoposide to standard chemotherapy for Ewing's sarcoma and primitive neuroectodermal tumor of bone. *New England Journal of Medicine,* 348**,** 694-701.

HAINING, R. L., HUNTER, A. P., VERONESE, M. E., TRAGER, W. F. & RETTIE, A. E. 1996. Allelic variants of human cytochrome P450 2C9: Baculovirus-mediated expression, purification, structural characterization, substrate

stereoselectivity, and prochiral selectivity of the wild-type and 1359L mutant forms. *Archives of Biochemistry and Biophysics,* 333**,** 447-458.
HAN, J. 1993. Highlights of the Cancer Chemoprevention Studies in China. *Preventive Medicine,* 22**,** 712-722.
HANAHAN, D. & WEINBERG, ROBERT A. 2011. Hallmarks of Cancer: The Next Generation. *Cell,* 144**,** 646-674.
HANIOKA, N., OZAWA, S., JINNO, H., ANDO, M., SAITO, Y. & SAWADA, J. 2001. Human liver UDP-glucuronosyltransferase isoforms involved in the glucuronidation of 7-ethyl-10-hydroxycamptothecin. *Xenobiotica,* 31**,** 687-699.
HATTINGER, C. M., RUMPLER, S., STREHL, S., AMBROS, I. M., ZOUBEK, A., POTSCHGER, U., GADNER, H. & AMBROSE, P. F. 1999. Prognostic impact of deletions at 1p36 and numerical aberrations in Ewing tumors. *Genes, Chromosomes and Cancer,* 24**,** 243-254.
HE, F. 2005. Human Liver Proteome Project. *Molecular & Cellular Proteomics,* 4**,** 1841-1848.
HEIDELBERGER, C., CHAUDHURI, N. K., DANNEBERG, P., MOOREN, D., GRIESBACH, L., DUSCHINSKY, R., SCHNITZER, R. J., PLEVEN, E. & SCHEINER, J. 1957. Fluorinated Pyrimidines, A New Class of Tumour-Inhibitory Compounds. *Nature,* 179**,** 663-666.
HENNINGSSON, A., MARSH, S., LOOS, W. J., KARLSSON, M. O., GARSA, A., MROSS, K., MIELKE, S., VIGANÒ, L., LOCATELLI, A., VERWEIJ, J., SPARREBOOM, A. & MCLEOD, H. L. 2005. Association of CYP2C8, CYP3A4, CYP3A5, and ABCB1 Polymorphisms with the Pharmacokinetics of Paclitaxel. *Clinical Cancer Research,* 11**,** 8097-8104.
HIGGINS, C. F. 1992. ABC transporters: from microorganisms to man. *Annu Rev Cell Biol,* 8**,** 67-113.
HIJAZI, Y., AXIOTIS, C., NAVARRO, S., STEINBERG, S., HOROWITZ, M. & TSOKOS, M. 1994. Immunohistochemical detection of P-glycoprotein in Ewing's sarcoma and peripheral primitive neuroectodermal tumors before and after chemotherapy. *Am J Clin Pathol,* 102**,** 61-67.
HILDEBRANDT, T. & TRAUNECKER, H. 2005. Neuroblastoma: A tumour with many faces. *Current Paediatrics,* 15**,** 412-420.
HIRRLINGER, J., KÖNIG, J., KEPPLER, D., LINDENAU, J., SCHULZ, J. B. & DRINGEN, R. 2001. The multidrug resistance protein MRP1 mediates the release of glutathione disulfide from rat astrocytes during oxidative stress. *Journal of Neurochemistry,* 76**,** 627-636.
HITCHINGS, G. H. & ELION, G. B. 1954. THE CHEMISTRY AND BIOCHEMISTRY OF PURINE ANALOGS. *Annals of the New York Academy of Sciences,* 60**,** 195-199.
HIYAMA, E., IEHARA, T., SUGIMOTO, T., FUKUZAWA, M., HAYASHI, Y., SASAKI, F., SUGIYAMA, M., KONDO, S., YONEDA, A., YAMAOKA, H., TAJIRI, T., AKAZAWA, K. & OHTAKI, M. 2008. Effectiveness of screening for neuroblastoma at 6 months of age: a retrospective population-based cohort study. *Lancet,* 371**,** 1173-80.
HOEHNER, J. C., GESTBLOM, C., HEDBORG, F., SANDSTEDT, B., OLSEN, L. & PAHLMAN, S. 1996. A developmental model of neuroblastoma: differentiating stroma-poor tumors' progress along an extra-adrenal chromaffin lineage. *Lab Invest,* 75**,** 659-675.
HONG, W. K., ENDICOTT, J., ITRI, L. M., DOOS, W., BATSAKIS, J. G., BELL, R., FOFONOFF, S., BYERS, R., ATKINSON, E. N., VAUGHAN, C., TOTH, B. B., KRAMER, A., DIMERY, I. W., SKIPPER, P. & STRONG, S. 1986. 13-Cis-

Retinoic Acid in the Treatment of Oral Leukoplakia. *New England Journal of Medicine,* 315**,** 1501-1505.

HONG, W. K., LIPPMAN, S. M., ITRI, L. M., KARP, D. D., LEE, J. S., BYERS, R. M., SCHANTZ, S. P., KRAMER, A. M., LOTAN, R., PETERS, L. J., DIMERY, I. W., BROWN, B. W. & GOEPFERT, H. 1990. Prevention of Second Primary Tumors with Isotretinoin in Squamous-Cell Carcinoma of the Head and Neck. *New England Journal of Medicine,* 323**,** 795-801.

HU-LIESKOVAN, S., ZHANG, J., WU, L., SHIMADA, H., SCHOFIELD, D. E. & TRICHE, T. J. 2005. EWS-FLI1 Fusion Protein Up-regulates Critical Genes in Neural Crest Development and Is Responsible for the Observed Phenotype of Ewing's Family of Tumors. *Cancer Res,* 65**,** 4633-4644.

HULTIN, T. A., FILLA, M. S. & MCCORMICK, D. L. 1990. Distribution and metabolism of the retinoid, N-(4-methoxyphenyl)-all-trans-retinamide, the major metabolite of N-(4-hydroxyphenyl)-all-trans-retinamide, in female mice. *Drug Metabolism and Disposition,* 18**,** 175-179.

HULTIN, T. A., MAY, C. M. & MOON, R. C. 1986. N-(4-hydroxyphenyl)-all-trans-retinamide pharmacokinetics in female rats and mice. *Drug Metab Dispos,* 14**,** 714-717.

HUYNH, C. K., BRODIE, A. M. H. & NJAR, V. C. O. 2006. Inhibitory effects of retinoic acid metabolism blocking agents (RAMBAs) on the growth of human prostate cancer cells and LNCaP prostate tumour xenografts in SCID mice. *Br J Cancer,* 94**,** 513-523.

IDRES, N., MARILL, J., FLEXOR, M. A. & CHABOT, G. G. 2002. Activation of Retinoic Acid Receptor-dependent Transcription by All-trans-retinoic Acid Metabolites and Isomers. *Journal of Biological Chemistry,* 277**,** 31491-31498.

ILLINGWORTH, N. A., BODDY, A. V., DALY, A. K. & VEAL, G. J. 2011. Characterization of the metabolism of fenretinide by human liver microsomes, cytochrome P450 enzymes and UDP-glucuronosyltransferases. *British Journal of Pharmacology,* 162**,** 989-999.

ILLMER, T., SCHULER, U. S., THIEDE, C., SCHWARZ, U. I., KIM, R. B., GOTTHARD, S., FREUND, D., SCHÄKEL, U., EHNINGER, G. & SCHAICH, M. 2002. MDR1 gene polymorphisms affect therapy outcome in acute myeloid leukemia patients. *Cancer Research,* 62**,** 4955-4962.

ISHIKAWA, T. & SIES, H. 1989. *Glutathione: Chemical, Biochemical, and Medical Aspects.*, Wiley.

ISHOLA, T. A. & CHUNG, D. H. 2007. Neuroblastoma. *Surgical Oncology,* 16**,** 149-156.

IWASAKI, I., SUGIYAMA, H., KANAZAWA, S. & HEMMI, H. 2002. Establishment of cisplatin-resistant variants of human neuroblastoma cell lines, TGW and GOTO, and their drug cross-resistance profiles. *Cancer Chemotherapy and Pharmacology,* 49**,** 438-444.

IZUKAWA, T., NAKAJIMA, M., FUJIWARA, R., YAMANAKA, H., FUKAMI, T., TAKAMIYA, M., AOKI, Y., IKUSHIRO, S.-I., SAKAKI, T. & YOKOI, T. 2009. Quantitative Analysis of UDP-Glucuronosyltransferase (UGT) 1A and UGT2B Expression Levels in Human Livers. *Drug Metabolism and Disposition,* 37**,** 1759-1768.

JEMAL, A., SIEGEL, R., WARD, E., MURRAY, T., XU, J. & THUN, M. J. 2007. Cancer Statistics, 2007. *CA Cancer J Clin,* 57**,** 43-66.

JINNO, H., TANAKA-KAGAWA, T., HANIOKA, N., SAEKI, M., ISHIDA, S., NISHIMURA, T., ANDO, M., SAITO, Y., OZAWA, S. & SAWADA, J.-I. 2003. Glucuronidation of 7-Ethyl-10-hydroxycamptothecin (SN-38), an Active

Metabolite of Irinotecan (CPT-11), by Human UGT1A1 Variants, G71R, P229Q, and Y486D. *Drug Metabolism and Disposition,* 31**,** 108-113.

JUERGENS, C., WESTON, C., LEWIS, I., WHELAN, J., PAULUSSEN, M., OBERLIN, O., MICHON, J., ZOUBEK, A., JUERGENS, H. & CRAFT, A. 2006. Safety assessment of intensive induction with vincristine, ifosfamide, doxorubicin, and etoposide (VIDE) in the treatment of Ewing tumors in the EURO-E.W.I.N.G. 99 clinical trial. *Pediatric Blood & Cancer,* 47**,** 22-29.

KERR, D. J., GRAHAM, J., CUMMINGS, J., MORRISON, J. G., THOMPSON, G. G., BRODIE, M. J. & KAYE, S. B. 1986. The effect of verapamil on the pharmacokinetics of adriamycin. *Cancer Chemotherapy and Pharmacology,* 18**,** 239-242.

KESHAVA, C., MCCANLIES, E. C. & WESTON, A. 2004. CYP3A4 Polymorphisms—Potential Risk Factors for Breast and Prostate Cancer: A HuGE Review. *American Journal of Epidemiology,* 160**,** 825-841.

KHAN, A. A., VILLABLANCA, J. G., REYNOLDS, C. P. & AVRAMIS, V. I. 1996. Pharmacokinetic studies of 13-cis-retinoic acid in pediatric patients with neuroblastoma following bone marrow transplantation. *Cancer Chemotherapy & Pharmacology,* 39**,** 34-41.

KIM, R. B. 2003. Organic anion-transporting polypeptide (OATP) transporter family and drug disposition. *European Journal of Clinical Investigation,* 33**,** 1-5.

KITAREEWAN, S., SPINELLA, M. J., ALLOPENNA, J., RECZEK, P. R. & DMITROVSKY, E. 1999. 4HPR triggers apoptosis but not differentiation in retinoid sensitive and resistant human embryonal carcinoma cells through an RARgamma independent pathway. *Oncogene,* 18**,** 5747-55.

KRAFT, J. C., SLIKKER, W., BAILEY, J. R., ROBERTS, L. G., FISCHER, B., WITTFOHT, W. & NAU, H. 1991. Plasma pharmacokinetics and metabolism of 13-cis- and all-trans-retinoic acid in the cynomolgus monkey and the identification of 13-cis- and all-trans-retinoyl-beta-glucuronides. A comparison to one human case study with isotretinoin. *Drug Metabolism and Disposition,* 19**,** 317-324.

KUSHNER, B. H. 2004. Neuroblastoma: A Disease Requiring a Multitude of Imaging Studies. *The Journal of Nuclear Medicine,* 45**,** 1172-1118.

LA, T. H., MEYERS, P. A., WEXLER, L. H., ALEKTIAR, K. M., HEALEY, J. H., LAQUAGLIA, M. P., BOLAND, P. J. & WOLDEN, S. L. 2006. Radiation therapy for Ewing's sarcoma: Results from Memorial Sloan-Kettering in the modern era. *International Journal of Radiation Oncology*Biology*Physics,* 64**,** 544-550.

LADENSTEIN, R., POTSCHGER, U., LE DELEY, M. C., WHELAN, J., PAULUSSEN, M., OBERLIN, O., VAN DEN BERG, H., DIRKSEN, U., HJORTH, L., MICHON, J., LEWIS, I., CRAFT, A. & JURGENS, H. 2010. Primary disseminated multifocal Ewing sarcoma: results of the Euro-EWING 99 trial. *Journal of Clinical Oncology,* 28**,** 3284-91.

LAVERDIÈRE, C., LIU, Q., YASUI, Y., NATHAN, P. C., GURNEY, J. G., STOVALL, M., DILLER, L. R., CHEUNG, N.-K., WOLDEN, S., ROBISON, L. L. & SKLAR, C. A. 2009. Long-term Outcomes in Survivors of Neuroblastoma: A Report From the Childhood Cancer Survivor Study. *Journal of the National Cancer Institute,* 101**,** 1131-1140.

LEE, J., HOANG, B. H., ZIOGAS, A. & ZELL, J. A. 2010. Analysis of prognostic factors in Ewing sarcoma using a population-based cancer registry. *Cancer,* 116**,** 1964-73.

LEVESQUE, E., DELAGE, R., BENOIT-BIANCAMANO, M. O., CARON, P., BERNARD, O., COUTURE, F. & GUILLEMETTE, C. 2007. The Impact of

UGT1A8, UGT1A9, and UGT2B7 Genetic Polymorphisms on the Pharmacokinetic Profile of Mycophenolic Acid After a Single Oral Dose in Healthy Volunteers. *Clin Pharmacol Ther,* 81**,** 392-400.

LEVIN, W., LU, A. Y. H., RYAN, D., WEST, S., KUNTZMAN, R. & CONNEY, A. H. 1972. Partial purification and properties of cytochromes P-450 and P-448 from rat liver microsomes. *Archives of Biochemistry and Biophysics,* 153**,** 543-553.

LEWIS, D. 2003. Human Cytochromes P450 Associated with the Phase 1 Metabolism of Drugs and other Xenobiotics: A Compilation of Substrates and Inhibitors of the CYP1, CYP2 and CYP3 Families. *Current Medicinal Chemistry,* 10**,** 1955-1972.

LI, X.-Q., ANDERSSON, T. B., AHLSTRÖM, M. & WEIDOLF, L. 2004. Comparison of inhibitory effects of the proton pump-inhibiting drugs omeprazole, esomeprazole, lansoprazole, pantoprazole and rabeprazole on human cytochrome P450 activities. *Drug Metabolism and Disposition,* 32**,** 821-827.

LIMDI, N. A., ARNETT, D. K., GOLDSTEIN, J. A., BEASLEY, T. M., MCGWIN, G., ADLER, B. K. & ACTON, R. T. 2008. Influence of CYP2C9 and VKORC1 on warfarin dose, anticoagulation attainment and maintenance among European–Americans and African–Americans. *Pharmacogenomics,* 9**,** 511-526.

LITTLE, J. M., LEHMAN, P. A., NOWELL, S., SAMOKYSZYN, V. & RADOMINSKA, A. 1997. Glucuronidation of all-trans-Retinoic Acid and 5,6-Epoxy-all-trans-retinoic Acid. *Drug Metabolism and Disposition,* 25**,** 5-11.

LOOK, A., HAYES, F., SHUSTER, J., DOUGLASS, E., CASTLEBERRY, R., BOWMAN, L., SMITH, E. & BRODEUR, G. 1991. Clinical relevance of tumor cell ploidy and N-myc gene amplification in childhood neuroblastoma: a Pediatric Oncology Group study. *Journal of Clinical Oncology,* 9**,** 581-591.

LOVAT, P. E., CORAZZARI, M., SANO, F. D., PIACENTINI, M. & REDFERN, C. P. F. 2005. The role of gangliosides in fenretinide-induced apoptosis of neuroblastoma. *Cancer Letters,* 228**,** 105-110.

LOVAT, P. E., OLIVERIO, S., CORAZZARI, M., RANALLI, M., PEARSON, A. D. J., MELINO, G., PIACENTINI, M. & REDFERN, C. P. F. 2003a. Induction of GADD153 and Bak: novel molecular targets of fenretinide-induced apoptosis of neuroblastoma. *Cancer Letters,* 197**,** 157-63.

LOVAT, P. E., OLIVERIO, S., CORAZZARI, M., RODOLFO, C., RANALLI, M., GORANOV, B., MELINO, G., REDFERN, C. P. F. & PIACENTINI, M. 2003b. Bak: A Downstream Mediator of Fenretinide-Induced Apoptosis of SH-SY5Y Neuroblastoma Cells. *Cancer Res,* 63**,** 7310-7313.

LOVAT, P. E., RANALLI, M., ANNICHIARRICO-PETRUZZELLI, M., BERNASSOLA, F., PIACENTINI, M., MALCOLM, A. J., PEARSON, A. D. J., MELINO, G. & REDFERN, C. P. F. 2000. Effector Mechanisms of Fenretinide-Induced Apoptosis in Neuroblastoma. *Experimental Cell Research,* 260**,** 50-60.

LOVAT, P. E., RANALLI, M., CORAZZARI, M., RAFFAGHELLO, L., PEARSON, A. D. J., PONZONI, M., PIACENTINI, M., MELINO, G. & REDFERN, C. P. F. 2003c. Mechanisms of free-radical induction in relation to fenretinide-induced apoptosis of neuroblastoma. *Journal of Cellular Biochemistry,* 89**,** 698-708.

MACKALL, C. L., MELTZER, P. S. & HELMAN, L. J. 2002. Focus on sarcomas. *Cancer Cell,* 2**,** 175-178.

MARACHELIAN, A., KANG, M. H., HWANG, K., VILLABLANCA, J. G., GROSHEN, S., MATTHAY, K. K., MARIS, J., DESANTES, K. B., REYNOLDS, C. P. & MAURER, B. J. 2009. Phase I study of fenretinide (4-

HPR) oral powder in patients with recurrent or resistant neuroblastoma: New Approaches to Neuroblastoma Therapy (NANT) Consortium trial. *J Clin Oncol* suppl; abstr 10009**,** 27 - 15s.

MARILL, J., CAPRON, C. C., IDRES, N. & CHABOT, G. G. 2002. Human cytochrome P450s involved in the metabolism of 9-cis- and 13-cis-retinoic acids. *Biochemical Pharmacology,* 63**,** 933-43.

MARILL, J., CRESTEIL, T., LANOTTE, M. & CHABOT, G. G. 2000. Identification of human cytochrome P450s involved in the formation of all-trans-retinoic acid principal metabolites. *Molecular Pharmacology,* 58**,** 1341-8.

MARIS, J. M., HOGARTY, M. D., BAGATELL, R. & COHN, S. L. 2007. Neuroblastoma. *The Lancet,* 369**,** 2106-2120.

MARIS, J. M. & MATTHAY, K. K. 1999. Molecular Biology of Neuroblastoma. *Journal of Clinical Oncology,* 17**,** 2264.

MATSSON, P., PEDERSEN, J., NORINDER, U., BERGSTRÖM, C. & ARTURSSON, P. 2009. Identification of Novel Specific and General Inhibitors of the Three Major Human ATP-Binding Cassette Transporters P-gp, BCRP and MRP2 Among Registered Drugs. *Pharmaceutical Research,* 26**,** 1816-1831.

MATTHAY, K. K., REYNOLDS, C. P., SEEGER, R. C., SHIMADA, H., ADKINS, E. S., HAAS-KOGAN, D., GERBING, R. B., LONDON, W. B. & VILLABLANCA, J. G. 2009. Long-term results for children with high-risk neuroblastoma treated on a randomized trial of myeloablative therapy followed by 13-cis-retinoic acid: a children's oncology group study. *Journal of Clinical Oncology,* 27**,** 1007-13.

MATTHAY, K. K., VILLABLANCA, J. G., SEEGER, R. C., STRAM, D. O., HARRIS, R. E., RAMSAY, N. K., SWIFT, P., SHIMADA, H., BLACK, C. T., BRODEUR, G. M., GERBING, R. B., REYNOLDS, C. P. & THE CHILDREN'S CANCER, G. 1999. Treatment of High-Risk Neuroblastoma with Intensive Chemotherapy, Radiotherapy, Autologous Bone Marrow Transplantation, and 13-cis-Retinoic Acid. *N Engl J Med,* 341**,** 1165-1173.

MAURER, B. J., KALOUS, O., YESAIR, D. W., WU, X., JANEBA, J., MALDONADO, V., KHANKALDYYAN, V., FRGALA, T., SUN, B., MCKEE, R. T., BURGESS, S. W., SHAW, W. A. & REYNOLDS, C. P. 2007. Improved Oral Delivery of N-(4-Hydroxyphenyl)Retinamide with a Novel LYM-X-SORB Organized Lipid Complex. *Clinical Cancer Research,* 13**,** 3079-3086.

MAURER, B. J., METELITSA, L. S., SEEGER, R. C., CABOT, M. C. & REYNOLDS, C. P. 1999. Increase of Ceramide and Induction of Mixed Apoptosis/Necrosis by N-(4-Hydroxyphenyl)- retinamide in Neuroblastoma Cell Lines. *J. Natl. Cancer Inst.,* 91**,** 1138-1146.

MAURICI, D., PEREZ-ATAYDE, A., GRIER, H. E., BALDINI, N., SERRA, M. & FLETCHER, J. A. 1998. Frequency and Implications of Chromosome 8 and 12 Gains in Ewing Sarcoma. *Cancer Genetics and Cytogenetics,* 100**,** 106-110.

MCCAFFERY, P., EVANS, J., KOUL, O., VOLPERT, A., REID, K. & ULLMAN, M. D. 2002. Retinoid quantification by HPLC/MSn. *Journal of Lipid Research,* 43**,** 1143-1149.

MCLAUGHLIN, C. C., BAPTISTE, M. S., SCHYMURA, M. J., ZDEB, M. S. & NASCA, P. C. 2009. Perinatal risk factors for neuroblastoma. *Cancer Causes & Control,* 20**,** 289-301.

MCSORLEY, L. C. & DALY, A. K. 2000. Identification of human cytochrome P450 isoforms that contribute to all-trans-retinoic acid 4-hydroxylation. *Biochemical Pharmacology,* 60**,** 517-26.

MEHTA, R. G., MOON, R. C., HAWTHORNE, M., FORMELLI, F. & COSTA, A. 1991. Distribution of fenretinide in the mammary gland of breast cancer patients. *European Journal of Cancer,* 27**,** 138-141.

MEHTA, R. R., HAWTHORNE, M. E., GRAVES, J. M. & MEHTA, R. G. 1998. Metabolism of N-[4-hydroxyphenyl]retinamide (4-HPR) to N-[4-methoxyphenyl]retinamide (4-MPR) may serve as a biomarker for its efficacy against human breast cancer and melanoma cells. *European Journal of Cancer,* 34**,** 902-7.

MEYER, W. H., KUN, L., MARINA, N., ROBERSON, P., PARHAM, D., RAO, B., FLETCHER, B. & PRATT, C. B. 1992. Ifosfamide plus etoposide in newly diagnosed Ewing's sarcoma of bone. *J Clin Oncol,* 10**,** 1737-1742.

MEYSKENS, F. L., SURWIT, E., MOON, T. E., CHILDERS, J. M., DAVIS, J. R., DORR, R. T., JOHNSON, C. S. & ALBERTS, D. S. 1994. Enhancement of Regression of Cervical Intraepithelial Neoplasia II (Moderate Dysplasia) With Topically Applied All-trans-Retinoic Acid: a Randomized Trial. *Journal of the National Cancer Institute,* 86**,** 539-543.

MIURA, M., KAGAYA, H., SATOH, S., INOUE, K., SAITO, M., HABUCHI, T. & SUZUKI, T. 2008. Influence of Drug Transporters and UGT Polymorphisms on Pharmacokinetics of Phenolic glucuronide Metabolite of Mycophenolic Acid in Japanese Renal Transplant Recipients. *Therapeutic Drug Monitoring,* 30**,** 559-564 10.1097/FTD.0b013e3181838063.

MOON, T. E., LEVINE, N., CARTMEL, B. & BANGERT, J. L. 1997. Retinoids in prevention of skin cancer. *Cancer Letters,* 114**,** 203-205.

MUENTER, M. D., PERRY, H. O. & LUDWIG, J. 1971. Chronic vitamin A intoxication in adults : Hepatic, neurologic and dermatologic complications. *The American Journal of Medicine,* 50**,** 129-136.

MUINDI, J., FRANKEL, S., MILLER, W. J., JAKUBOWSKI, A., SCHEINBERG, D., YOUNG, C., DMITROVSKY, E. & WARRELL, R. J. 1992. Continuous treatment with all-trans retinoic acid causes a progressive reduction in plasma drug concentrations: implications for relapse and retinoid "resistance" in patients with acute promyelocytic leukemia [published erratum appears in Blood 1992 Aug 1;80(3):855]. *Blood,* 79**,** 299-303.

MULLER, C., GOUBIN, F., FERRANDIS, E., CORNIL-SCHARWTZ, I., BAILLY, J. D., BORDIER, C., BÉNARD, J., SIKIC, B. I. & LAURENT, G. 1995. Evidence for transcriptional control of human mdr1 gene expression by verapamil in multidrug-resistant leukemic cells. *Molecular Pharmacology,* 47**,** 51-56.

MUNOZ, M., HENDERSON, M., HABER, M. & NORRIS, M. 2007. Role of the MRP1/ABCC1 multidrug transporter protein in cancer. *IUBMB Life,* 59**,** 752-7.

MURDTER, T. E., SCHROTH, W., BACCHUS-GERYBADZE, L., WINTER, S., HEINKELE, G., SIMON, W., FASCHING, P. A., FEHM, T., EICHELBAUM, M., SCHWAB, M. & BRAUCH, H. 2011. Activity Levels of Tamoxifen Metabolites at the Estrogen Receptor and the Impact of Genetic Polymorphisms of Phase I and II Enzymes on Their Concentration Levels in Plasma. *Clin Pharmacol Ther,* 89**,** 708-717.

MYATT, S. S. & BURCHILL, S. A. 2008. The sensitivity of the Ewing's sarcoma family of tumours to fenretinide-induced cell death is increased by EWS-Fli1-dependent modulation of p38(MAPK) activity. *Oncogene,* 27**,** 985-96.

MYATT, S. S., REDFERN, C. P. F. & BURCHILL, S. A. 2005. p38MAPK-Dependent sensitivity of Ewing's sarcoma family of tumors to fenretinide-induced cell death. *Clinical Cancer Research,* 11**,** 3136-48.

NAGAR, S. & REMMEL, R. P. 2006. Uridine diphosphoglucuronosyltransferase pharmacogenetics and cancer. *Oncogene,* 25**,** 1659-1672.

NELSON, A. C., HUANG, W. & MOODY, D. E. 2001. Variables in Human Liver Microsome Preparation: Impact on the Kinetics of L-α-Acetylmethadol (LAAM)N-Demethylation and DextromethorphanO-Demethylation. *Drug Metabolism and Disposition,* 29**,** 319-325.

NELSON, D. R., KOYMANS, L., KAMATAKI, T., J.J., S., FEYEREISEN, R., WAXMAN, D. J., WATERMAN, M. R., GOTOH, O., COON, M. J., ESTABROOK, R. W., GUNSALUS, I. C. & NEBERT, D. W. 1996. P450 superfamily: update on new sequences, gene mapping, accession numbers and nomenclature. *Pharmacogenetics,* 6**,** 1 - 42.

NESBIT JR, M. E., GEHAN, E. A., BURGERT JR, E. O., VIETTI, T. J., CANGIR, A., TEFFT, M., EVANS, R., THOMAS, P., ASKIN, F. B., KISSANE, J. M., PRITCHARD, D. J., HERRMANN, J., NEFF, J., MAKLEY, J. T. & GILULA, L. 1990. Multimodal therapy for the management of primary, nonmetastatic Ewing's Sarcoma of bone: A long-term follow-up of the first intergroup study. *Journal of Clinical Oncology,* 8**,** 1664-1674.

NJAR, V. C. O., GEDIYA, L., PURUSHOTTAMACHAR, P., CHOPRA, P., VASAITIS, T. S., KHANDELWAL, A., MEHTA, J., HUYNH, C., BELOSAY, A. & PATEL, J. 2006. Retinoic acid metabolism blocking agents (RAMBAs) for treatment of cancer and dermatological diseases. *Bioorganic & Medicinal Chemistry,* 14**,** 4323-4340.

NOONAN, K. E., BECK, C., HOLZMAYER, T. A., CHIN, J. E., WUNDER, J. S., ANDRULIS, I. L., GAZDAR, A. F., WILLMAN, C. L., GRIFFITH, B. & VON HOFF, D. D. 1990. Quantitative analysis of MDR1 (multidrug resistance) gene expression in human tumors by polymerase chain reaction. *Proceedings of the National Academy of Sciences of the United States of America,* 87**,** 7160-7164.

NORRIS, M. D., SMITH, J., TANABE, K., TOBIN, P., FLEMMING, C., SCHEFFER, G. L., WIELINGA, P., COHN, S. L., LONDON, W. B., MARSHALL, G. M., ALLEN, J. D. & HABER, M. 2005. Expression of multidrug transporter MRP4/ABCC4 is a marker of poor prognosis in neuroblastoma and confers resistance to irinotecan in vitro. *Molecular Cancer Therapeutics,* 4**,** 547-553.

O'DWYER, P. & CATALANO, R. 2006. Uridine Diphosphate Glucuronosyltransferase (UGT) 1A1 and Irinotecan: Practical Pharmacogenomics Arrives in Cancer Therapy. *Journal of Clinical Oncology,* 24**,** 4534 - 4538.

OBERLIN, O., HABRAND, J. L., ZUCKER, J. M., BRUNAT-MENTIGNY, M., TERRIER-LACOMBE, M. J., DUBOUSSET, J., GENTET, J. C., SCHMITT, C., PONVERT, D. & CARRIE, C. 1992. No benefit of ifosfamide in Ewing's sarcoma: a nonrandomized study of the French Society of Pediatric Oncology. *J Clin Oncol,* 10**,** 1407-1412.

OCAYA, P., GIDLOF, A. C., OLOFSSON, P. S., TORMA, H. & SIRSJO, A. 2007. CYP26 inhibitor R115866 increases retinoid signaling in intimal smooth muscle cells. *Arteriosclerosis, Thrombosis & Vascular Biology,* 27**,** 1542-8.

ODA, Y., DOCKHORN-DWORNICZAK, B., JÜRGENS, H. & ROESSNER, A. 1997. Expression of multidrug resistance-associated protein gene in Ewing's sarcoma and malignant peripheral neuroectodermal tumor of bone. *Journal of Cancer Research and Clinical Oncology,* 123**,** 237-239.

OHNO, S. & NAKAJIN, S. 2009. Determination of mRNA Expression of Human UDP-Glucuronosyltransferases and Application for Localization in Various Human Tissues by Real-Time Reverse Transcriptase-Polymerase Chain Reaction. *Drug Metabolism and Disposition,* 37**,** 32-40.

OKADA, T., TANAKA, K., NAKATANI, F., SAKIMURA, R., MATSUNOBU, T., LI, X., HANADA, M., NAKAMURA, T., ODA, Y., TSUNEYOSHI, M. & IWAMOTO, Y. 2006. Involvement of P-glycoprotein and MRP1 in resistance to

cyclic tetrapeptide subfamily of histone deacetylase inhibitors in the drug-resistant osteosarcoma and Ewing's sarcoma cells. *International Journal of Cancer,* 118**,** 90-7.

OLSHAN, A. F., SMITH, J. C., BONDY, M. L., NEGLIA, J. P. & POLLOCK, B. H. 2002. Maternal vitamin use and reduced risk of neuroblastoma. *Epidemiology,* 13**,** 575-580.

ONG, C.-E., COULTER, S., BIRKETT, D. J., BHASKER, C. R. & MINERS, J. O. 2000. The xenobiotic inhibitor profile of cytochrome P4502C8. *British Journal of Clinical Pharmacology,* 50**,** 573-580.

ORIENTI, I., ZUCCARI, G., CAROSIO, R. & MONTALDO, P. G. 2009. Improvement of aqueous solubility of fenretinide and other hydrophobic anti-tumor drugs by complexation with amphiphilic dextrins. *Drug Delivery,* 16**,** 389-98.

ORTIZ DE MOTELLANO, P. R. 1995. *Cytochrome P450. Structure, Mechanism and Biochemistry,* New York, Plenum.

PASTORINO, U., INFANTE, M., MAIOLI, M., CHIESA, G., BUYSE, M., FIRKET, P., ROSMENTZ, N., CLERICI, M., SORESI, E. & VALENTE, M. 1993. Adjuvant treatment of stage I lung cancer with high-dose vitamin A. *Journal of Clinical Oncology,* 11**,** 1216-1222.

PAULUSSEN, M., CRAFT, A. W., LEWIS, I., HACKSHAW, A., DOUGLAS, C., DUNST, J., SCHUCK, A., WINKELMANN, W., KÖHLER, G., POREMBA, C., ZOUBEK, A., LADENSTEIN, R., VAN DEN BERG, H., HUNOLD, A., CASSONI, A., SPOONER, D., GRIMER, R., WHELAN, J., MCTIERNAN, A. & JÜRGENS, H. 2008. Results of the EICESS-92 Study: Two Randomized Trials of Ewing's Sarcoma Treatment—Cyclophosphamide Compared With Ifosfamide in Standard-Risk Patients and Assessment of Benefit of Etoposide Added to Standard Treatment in High-Risk Patients. *Journal of Clinical Oncology,* 26**,** 4385-4393.

PAVEZ LORIE, E., COOLS, M., BORGERS, M., WOUTERS, L., SHROOT, B., HAGFORSEN, E., TORMA, H. & VAHLQUIST, A. 2009a. Topical treatment with CYP26 inhibitor talarozole (R115866) dose dependently alters the expression of retinoid-regulated genes in normal human epidermis. *British Journal of Dermatology,* 160**,** 26-36.

PAVEZ LORIE, E., LI, H., VAHLQUIST, A. & TORMA, H. 2009b. The involvement of cytochrome p450 (CYP) 26 in the retinoic acid metabolism of human epidermal keratinocytes. *Biochimica et Biophysica Acta,* 1791**,** 220-8.

PEARCE, R. E., MCINTYRE, C. J., MADAN, A., SANZGIRI, U., DRAPER, A. J., BULLOCK, P. L., COOK, D. C., BURTON, L. A., LATHAM, J., NEVINS, C. & PARKINSON, A. 1996. Effects of Freezing, Thawing, and Storing Human Liver Microsomes on Cytochrome P450 Activity. *Archives of Biochemistry and Biophysics,* 331**,** 145-169.

PERLMANN, T. 2002. Retinoid metabolism: a balancing act. *Nature Genetics,* 31**,** 7 - 8.

PETKOVICH, M., BRAND, N. J., KRUST, A. & CHAMBON, P. 1987. A human retinoic acid receptor which belongs to the family of nuclear receptors. *Nature,* 330**,** 444-450.

PETROS, W. P., HOPKINS, P. J., SPRUILL, S., BROADWATER, G., VREDENBURGH, J. J., COLVIN, O. M., PETERS, W. P., JONES, R. B., HALL, J. & MARKS, J. R. 2005. Associations Between Drug Metabolism Genotype, Chemotherapy Pharmacokinetics, and Overall Survival in Patients With Breast Cancer. *Journal of Clinical Oncology,* 23**,** 6117-6125.

PINKEL, D. 1959. ACTINOMYCIN D IN CHILDHOOD CANCER: A Preliminary Report. *Pediatrics,* 23**,** 342-347.

RADOMINSKA-PANDYA, A., LITTLE, J. M., PANDYA, J. T., TEPHLY, T. R., KING, C. D., BARONE, G. W. & RAUFMAN, J.-P. 1998. UDP-glucuronosyltransferases in human intestinal mucosa. *Biochimica et Biophysica Acta (BBA) - Lipids and Lipid Metabolism,* 1394**,** 199-208.

RADOMINSKA, A., LITTLE, J. M., LEHMAN, P. A., SAMOKYSZYN, V., RIOS, G. R., KING, C. D., GREEN, M. D. & TEPHLY, T. R. 1997. Glucuronidation of Retinoids by Rat Recombinant UDP: Glucuronosyltransferase 1.1 (Bilirubin UGT). *Drug Metabolism and Disposition,* 25**,** 889-893.

RAFFAGHELLO, L., PAGNAN, G., PASTORINO, F., COSIMO, E., BRIGNOLE, C., MARIMPIETRI, D., BOGENMANN, E., PONZONI, M. & MONTALDO, P. G. 2003. Immunoliposomal fenretinide: a novel antitumoral drug for human neuroblastoma. *Cancer Letters,* 197**,** 151-5.

RAY, W. J., BAIN, G., YAO, M. & GOTTLIEB, D. I. 1997. CYP26, a Novel Mammalian Cytochrome P450, Is Induced by Retinoic Acid and Defines a New Family. *J. Biol. Chem.,* 272**,** 18702-18708.

RETTIE, A. E., WIENKERS, L. C., GONZALEZ, F. J., TRAGER, W. F. & KORZEKWA, K. R. 1994. Impaired (S)-warfarin metabolism catalysed by the R144C allelic variant of CYP2C9. *Pharmacogenetics,* 4**,** 39-42.

REYNOLDS, C. P., MATTHAY, K. K., VILLABLANCA, J. G. & MAURER, B. J. 2003. Retinoid therapy of high-risk neuroblastoma. *Cancer Letters,* 197**,** 185-92.

RIGGI, N. & STAMENKOVIC, I. 2007. The Biology of Ewing sarcoma. *Cancer Letters,* 254**,** 1-10.

RO, J., SAHIN, A., RO, J. Y., FRITSCHE, H., HORTOBAGYI, G. & BLICK, M. 1990. Immunohistochemical analysis of P-glycoprotein expression correlated with chemotherapy resistance in locally advanced breast cancer. *Human Pathology,* 21**,** 787-791.

RODRIGUEZ-GALINDO, C., SPUNT, S. L. & PAPPO, A. S. 2003. Treatment of Ewing sarcoma family of tumors: Current status and outlook for the future. *Medical and Pediatric Oncology,* 40**,** 276-287.

ROOS, T. C., JUGERT, F. K., MERK, H. F. & BICKERS, D. R. 1998. Retinoid Metabolism in the Skin. *Pharmacological Reviews,* 50**,** 315-333.

ROWBOTHAM, S. E., BODDY, A. V., REDFERN, C. P. F., VEAL, G. J. & DALY, A. K. 2010a. Relevance of nonsynonymous CYP2C8 polymorphisms to 13-cis retinoic acid and paclitaxel hydroxylation. *Drug Metabolism & Disposition,* 38**,** 1261-6.

ROWBOTHAM, S. E., ILLINGWORTH, N. A., DALY, A. K., VEAL, G. J. & BODDY, A. V. 2010b. Role of UDP-glucuronosyltransferase isoforms in 13-cis retinoic acid metabolism in humans. *Drug Metabolism & Disposition,* 38**,** 1211-7.

SABICHI, A. L., XU, H., FISCHER, S., ZOU, C., YANG, X., STEELE, V. E., KELLOFF, G. J., LOTAN, R. & CLIFFORD, J. L. 2003. Retinoid Receptor-Dependent and Independent Biological Activities of Novel Fenretinide Analogues and Metabolites. *Clin Cancer Res,* 9**,** 4606-4613.

SAMOKYSZYN, V. M., GALL, W. E., ZAWADA, G., FREYALDENHOVEN, M. A., CHEN, G., MACKENZIE, P. I., TEPHLY, T. R. & RADOMINSKA-PANDYA, A. 2000. 4-Hydroxyretinoic Acid, a Novel Substrate for Human Liver Microsomal UDP-glucuronosyltransferase(s) and Recombinant UGT2B7. *Journal of Biological Chemistry,* 275**,** 6908-6914.

SANDBERG, A. A. & BRIDGE, J. A. 2000. Updates on cytogenetics and molecular genetics of bone and soft tissue tumors:: Ewing sarcoma and peripheral primitive neuroectodermal tumors. *Cancer Genetics and Cytogenetics,* 123**,** 1-26.

SANZ, M. A., GRIMWADE, D., TALLMAN, M. S., LOWENBERG, B., FENAUX, P., ESTEY, E. H., NAOE, T., LENGFELDER, E., BUCHNER, T., DOHNER, H., BURNETT, A. K. & LO-COCO, F. 2009. Management of acute promyelocytic leukemia: recommendations from an expert panel on behalf of the European LeukemiaNet. *Blood,* 113**,** 1875-1891.

SASAKI, Y., HAKUSUI, H., MIZUNO, S., MORITA, M., MIYA, T., EGUCHI, K., SHINKAI, T., TAMURA, T., OHE, Y. & SAIJO, N. 1995. A Pharmacokinetic and Pharmacodynamic Analysis of CPT-11 and Its Active Metabolite SN-38. *Cancer Science,* 86**,** 101-110.

SCHILLING, F. H., SPIX, C., BERTHOLD, F., ERTTMANN, R., SANDER, J., TREUNER, J. & MICHAELIS, J. 2003. Children may not benefit from neuroblastoma screening at 1 year of age. Updated results of the population based controlled trial in Germany. *Cancer Letters,* 197**,** 19-28.

SCHLEIERMACHER, G., MICHON, J., HUON, I., D'ENGHIEN, C. D., KLIJANIENKO, J., BRISSE, H., RIBEIRO, A., MOSSERI, V., RUBIE, H., MUNZER, C., THOMAS, C., VALTEAU-COUANET, D., AUVRIGNON, A., PLANTAZ, D., DELATTRE, O. & COUTURIER, J. 2007. Chromosomal CGH identifies patients with a higher risk of relapse in neuroblastoma without MYCN amplification. *British Journal of Cancer,* 97**,** 238-246.

SCHMIEDLIN-REN, P., EDWARDS, D. J., FITZSIMMONS, M. E., HE, K., LOWN, K. S., WOSTER, P. M., RAHMAN, A., THUMMEL, K. E., FISHER, J. M., HOLLENBERG, P. F. & WATKINS, P. B. 1997. Mechanisms of Enhanced Oral Availability of CYP3A4 Substrates by Grapefruit Constituents. *Drug Metabolism and Disposition,* 25**,** 1228-1233.

SCHROEDER, H., WACHER, J., LARSSON, H., ROSTHOEJ, S., RECHNITZER, C., PETERSEN, B. L. & CARLSEN, N. L. T. 2009. Unchanged incidence and increased survival in children with neuroblastoma in Denmark 1981-2000: a population-based study.[Erratum appears in Br J Cancer. 2009 Apr 7;100(7):1212 Note: Pedersen, B L [corrected to Petersen, B L]]. *British Journal of Cancer,* 100**,** 853-7.

SCHWAB, M., ALITALO, K., KLEMPNAUER, K.-H., VARMUS, H. E., BISHOP, J. M., GILBERT, F., BRODEUR, G., GOLDSTEIN, M. & TRENT, J. 1983. Amplified DNA with limited homology to myc cellular oncogene is shared by human neuroblastoma cell lines and a neuroblastoma tumour. *Nature,* 305**,** 245-248.

SCHWAB, M., WESTERMANN, F., HERO, B. & BERTHOLD, F. 2003. Neuroblastoma: biology and molecular and chromosomal pathology. *The Lancet Oncology,* 4**,** 472-480.

SCHWARTZ, E. L., HALLAM, S., GALLAGHER, R. E. & WIERNIK, P. H. 1995. Inhibition of all-trans-retinoic acid metabolism by fluconazole in vitro and in patients with acute promyelocytic leukemia. *Biochemical Pharmacology,* 50**,** 923-928.

SEEGER, R. C., BRODEUR, G. M., SATHER, H., DALTON, A., SIEGEL, S. E., WONG, K. Y. & HAMMOND, D. 1985. Association of Multiple Copies of the N-myc Oncogene with Rapid Progression of Neuroblastomas. *New England Journal of Medicine,* 313**,** 1111-1116.

SHEN, D.-W., GOLDENBERG, S., PASTAN, I. & GOTTESMAN, M. M. 2000. Decreased accumulation of [14c]carboplatin in human cisplatin-resistant cells results from reduced energy-dependent uptake. *Journal of Cellular Physiology,* 183**,** 108-116.

SHEN, D.-W., PASTAN, I. & GOTTESMAN, M. M. 1998. Cross-Resistance to Methotrexate and Metals in Human Cisplatin-resistant Cell Lines Results from a

Pleiotropic Defect in Accumulation of These Compounds Associated with Reduced Plasma Membrane Binding Proteins. *Cancer Research,* 58**,** 268-275.

SIES, H. & AKERBOOM, T. 1984. Glutathione disulphide (GSSG) efflux from cells and tissues. *Methods in Enzymology,* 105**,** 445-451.

SINGH, A., WU, H., ZHANG, P., HAPPEL, C., MA, J. & BISWAL, S. 2010. Expression of ABCG2 (BCRP) Is Regulated by Nrf2 in Cancer Cells That Confers Side Population and Chemoresistance Phenotype. *Molecular Cancer Therapeutics,* 9**,** 2365-2376.

SMITH, H. E., JONES, J. P. I., KALHORN, T. F., FARIN, F. M., STAPLETON, P. L., DAVIS, C. L., PERKINS, J. D., BLOUGH, D. K., HEBERT, M. F., THUMMEL, K. E. & TOTAH, R. A. 2008. Role of cytochrome P450 2C8 and 2J2 genotypes in calcineurin inhibitor-induced chronic kidney disease. *Pharmacogenetics and Genomics,* 18**,** 943-953 10.1097/FPC.0b013e32830e1e16.

SMITH, M. A., ADAMSON, P. C., BALIS, F. M., FEUSNER, J., ARONSON, L., MURPHY, R. F., HOROWITZ, M. E., REAMAN, G., DENMAN HAMMOND, G., FENTON, R. M., CONNAGHAN, G. D., HITTELMAN, W. N. & POPLACK, D. G. 1992. Phase I and Pharmacokinetic Evaluation of All- Trans-Retinoic Acid in Pediatric Patients With Cancer. *J Clin Oncol,* 10**,** 1666 - 1673.

STEIN, U., WUNDERLICH, V., HAENSCH, W. & SCHMIDT-PETER, P. 1993. Expression of the mdr1 gene in bone and soft tissue sarcomas of adult patients. *European Journal of Cancer,* 29A**,** 1979-1981.

STRASSBURG, C. P., OLDHAFER, K., MANNS, M. P. & TUKEY, R. H. 1997. Differential Expression of the UGT1A Locus in Human Liver, Biliary, and Gastric Tissue: Identification ofUGT1A7 and UGT1A10 Transcripts in Extrahepatic Tissue. *Molecular Pharmacology,* 52**,** 212-220.

SULOVÁ, Z., MACEJOVÁ, D., SERES, M., SEDLÁK, J., BRTKO, J. & BREIER, A. 2008. Combined treatment of P-gp-positive L1210/VCR cells by verapamil and all-trans retinoic acid induces down-regulation of P-glycoprotein expression and transport activity. *Toxicology in Vitro,* 22**,** 96-105.

SUN, S.-Y. & LOTAN, R. 2002. Retinoids and their receptors in cancer development and chemoprevention. *Critical Reviews in Oncology/Hematology,* 41**,** 41-55.

SWANSON, B. N., NEWTON, D. L., ROLLER, P. P. & SPORN, M. B. 1981. Biotransformation and biological activity of N-(4- hydroxyphenyl)retinamide derivatives in rodents. *J Pharmacol Exp Ther,* 219**,** 632-637.

SWANSON, B. N., ZAHAREVITZ, D. W. & SPORN, M. B. 1980. Pharmacokinetics of N-(4-hydroxyphenyl)-all-trans-retinamide in rats. *Drug Metabolism and Disposition,* 8**,** 168-172.

TABE, Y., KONOPLEVA, M., CONTRACTOR, R., MUNSELL, M., SCHOBER, W. D., JIN, L., TSUTSUMI-ISHII, Y., NAGAOKA, I., IGARI, J. & ANDREEFF, M. 2006. Up-regulation of MDR1 and induction of doxorubicin resistance by histone deacetylase inhibitor depsipeptide (FK228) and ATRA in acute promyelocytic leukemia cells. *Blood,* 107**,** 1546-1554.

TAJIRI, T., SOUZAKI, R., KINOSHITA, Y., TANAKA, S., KOGA, Y., SUMINOE, A., MATSUZAKI, A., HARA, T. & TAGUCHI, T. 2009. Risks and benefits of ending of mass screening for neuroblastoma at 6 months of age in Japan. *Journal of Pediatric Surgery,* 44**,** 2253-7.

TANG, X. X., ZHAO, H., KUNG, B., KIM, D. Y., HICKS, S. L., COHN, S. L., CHEUNG, N.-K., SEEGER, R. C., EVANS, A. E. & IKEGAKI, N. 2006. The MYCN Enigma: Significance of MYCN Expression in Neuroblastoma. *Cancer Research,* 66**,** 2826-2833.

TERPE, K. 2006. Overview of bacterial expression systems for heterologous protein production: from molecular and biochemical fundamentals to commercial systems. *Applied Microbiology and Biotechnology,* 72**,** 211-222.

THEKEN, K. N., DENG, Y., KANNON, M. A., MILLER, T. M., POLOYAC, S. M. & LEE, C. R. 2011. Activation of the Acute Inflammatory Response Alters Cytochrome P450 Expression and Eicosanoid Metabolism. *Drug Metabolism and Disposition,* 39**,** 22-29.

TOKURA, Y., SHIKAMI, M., MIWA, H., WATARAI, M., SUGAMURA, K., WAKABAYASHI, M., SATOH, A., IMAMURA, A., MIHARA, H., KATOH, Y., KITA, K. & NITTA, M. 2002. Augmented expression of P-gp/multi-drug resistance gene by all-trans retinoic acid in monocytic leukemic cells. *Leukemia Research,* 26**,** 29-36.

UNITED STATES FOOD AND DRUG ADMINISTRATION. 2010. *Irinotecan label and approval history* [Online]. Available: http://www.accessdata.fda.gov/scripts/cder/drugsatfda/index.cfm?fuseaction=Search.Label_ApprovalHistory [Accessed 3rd March 2011].

URAYAMA, K. Y., VON BEHREN, J. & REYNOLDS, P. 2007. Birth characteristics and risk of neuroblastoma in young children. *American Journal of Epidemiology,* 165**,** 486-95.

US NATIONAL INSTITUTES OF HEALTH. 2009. *Study in Localized and Disseminated Ewing Sarcoma (EWING 2008)* [Online]. Available: http://clinicaltrials.gov/ct2/show/NCT00987636?term=fenretinide&rank=36 [Accessed 14th April 2011].

US NATIONAL INSTITUTES OF HEALTH. 2010a. *Fenretinide LXS in Treating Patients With Recurrent, Refractory, or Persistent Neuroblastoma* [Online]. Available: http://clinicaltrials.gov/ct2/show/NCT00295919?term=fenretinide&rank=3 [Accessed 14th April 2011].

US NATIONAL INSTITUTES OF HEALTH. 2010b. *Intravenous Fenretinide in Treating Young Patients With Recurrent or Resistant Neuroblastoma* [Online]. Available: http://clinicaltrials.gov/ct2/show/NCT00646230?term=fenretinide&rank=11 [Accessed 14th April 2011].

VAN HEUSDEN, J., VAN GINCKEL, R., BRUWIERE, H., MOELANS, P., JANSSEN, B., FLOREN, W., VAN DER LEEDE, B. J., VAN DUN, J., SANZ, G., VENET, M., DILLEN, L., VAN HOVE, C., WILLEMSENS, G., JANICOT, M. & WOUTERS, W. 2002. Inhibition of all-TRANS-retinoic acid metabolism by R116010 induces antitumour activity. *Br J Cancer,* 86**,** 605-611.

VANDESOMPELE, J., EDSJO, A., DE PRETER, K., AXELSON, H., SPELEMAN, F. & PAHLMAN, S. 2003. ID2 expression in neuroblastoma does not correlate to MYCN levels and lacks prognostic value. *Oncogene,* 22**,** 456-460.

VANE, F. M. & BUGGÉ, C. J. 1981. Identification of 4-oxo-13-cis-retinoic acid as the major metabolite of 13-cis-retinoic acid in human blood. *Drug Metabolism and Disposition,* 9**,** 515-520.

VEAL, G. J., COLE, M., ERRINGTON, J., PEARSON, A. D. J., FOOT, A. B. M., WHYMAN, G., BODDY, A. V. & GROUP, U. P. W. 2007. Pharmacokinetics and metabolism of 13-cis-retinoic acid (isotretinoin) in children with high-risk neuroblastoma - a study of the United Kingdom Children's Cancer Study Group. *British Journal of Cancer,* 96**,** 424-31.

VEAL, G. J., ERRINGTON, J., REDFERN, C. P. F., PEARSON, A. D. J. & BODDY, A. V. 2002. Influence of isomerisation on the growth inhibitory effects and

cellular activity of 13-cis and all-trans retinoic acid in neuroblastoma cells. *Biochemical Pharmacology,* 63**,** 207-15.

VENE, R., ARENA, G., POGGI, A., D'ARRIGO, C., MORMINO, M., NOONAN, D. M., ALBINI, A. & TOSETTI, F. 2007. Novel cell death pathways induced by N-(4-hydroxyphenyl)retinamide: therapeutic implications. *Mol Cancer Ther,* 6**,** 286-298.

VILLABLANCA, J., KHAN, A., AVRAMIS, V., SEEGER, R., MATTHAY, K., RAMSAY, N. & REYNOLDS, C. 1995. Phase I trial of 13-cis-retinoic acid in children with neuroblastoma following bone marrow transplantation. *Journal of Clinical Oncology,* 13**,** 894-901.

VILLABLANCA, J. G., KRAILO, M. D., AMES, M. M., REID, J. M., REAMAN, G. H. & REYNOLDS, C. P. 2006. Phase I trial of oral fenretinide in children with high-risk solid tumors: a report from the Children's Oncology Group (CCG 09709). *J Clin Oncol,* 24**,** 3423-3430.

VILLANI, M. G., APPIERTO, V., CAVADINI, E., BETTIGA, A., PRINETTI, A., CLAGETT-DAME, M., CURLEY, R. W. & FORMELLI, F. 2006. 4-oxo-fenretinide, a recently identified fenretinide metabolite, induces marked G2-M cell cycle arrest and apoptosis in fenretinide-sensitive and fenretinide-resistant cell lines. *Cancer Research,* 66**,** 3238-47.

VILLANI, M. G., APPIERTO, V., CAVADINI, E., VALSECCHI, M., SONNINO, S., CURLEY, R. W. & FORMELLI, F. 2004. Identification of the fenretinide metabolite 4-oxo-fenretinide present in human plasma and formed in human ovarian carcinoma cells through induction of cytochrome P450 26A1. *Clinical Cancer Research,* 10**,** 6265-75.

VILLENEUVE, L., GIRARD, H., FORTIER, L.-C., GAGNÉ, J.-F. & GUILLEMETTE, C. 2003. Novel Functional Polymorphisms in the UGT1A7 and UGT1A9 Glucuronidating Enzymes in Caucasian and African-American Subjects and Their Impact on the Metabolism of 7-Ethyl-10-hydroxycamptothecin and Flavopiridol Anticancer Drugs. *Journal of Pharmacology and Experimental Therapeutics,* 307**,** 117-128.

VRATILOVA, J., FRGALA, T., MAURER, B. J. & PATRICK REYNOLDS, C. 2004. Liquid chromatography method for quantifying N-(4-hydroxyphenyl)retinamide and N-(4-methoxyphenyl)retinamide in tissues. *Journal of Chromatography B: Analytical Technologies in the Biomedical & Life Sciences,* 808**,** 125-30.

WARTENBERG, M., LING, F. C., MÜSCHEN, M., KLEIN, F., ACKER, H., GASSMANN, M., PETRAT, K., PÜTZ, V., HESCHELER, J. & SAUER, H. 2003. Regulation of the multidrug resistance transporter P-glycoprotein in multicellular tumor spheroids by hypoxia-inducible factor (HIF-1) and reactive oxygen species. *The FASEB journal : official publication of the Federation of American Societies for Experimental Biology,* 17**,** 503-505.

WHITE, J. A., BECKETT-JONES, B., GUO, Y.-D., DILWORTH, F. J., BONASORO, J., JONES, G. & PETKOVICH, M. 1997. cDNA Cloning of Human Retinoic Acid-metabolizing Enzyme (hP450RAI) Identifies a Novel Family of Cytochromes P450 (CYP26). *Journal of Biological Chemistry,* 272**,** 18538-18541.

WOLBACH, S. & HOWE, P. 1925. Tissue changes following deprivation of fat soluble A vitamin. *J Exp Med,* 42**,** 753 - 777.

WORCH, J., MATTHAY, K. K., NEUHAUS, J., GOLDSBY, R. & DUBOIS, S. G. 2010. Ethnic and racial differences in patients with Ewing sarcoma. *Cancer,* 116**,** 983-8.

WORLD HEALTH ORGANIZATION. 2011. *Micronutrient deficiencies* [Online]. Available: http://www.who.int/nutrition/topics/vad/en/ [Accessed 15.03.11 2011].

XU, C., LI, C. & KONG, A.-N. 2005. Induction of phase I, II and III drug metabolism/transport by xenobiotics. *Archives of Pharmacal Research,* 28**,** 249-268.

YAMAMOTO, Y., ZOLFAGHARI, R. & ROSS, A. C. 2000. Regulation of CYP26 (cytochrome P450RAI) mRNA expression and retinoic acid metabolism by retinoids and dietary vitamin A in liver of mice and rats. *FASEB Journal,* 14**,** 2119-27.

YAMAZAKI, M., SUZUKI, H. & SUGIYAMA, Y. 1996. Recent Advances in Carrier-mediated Hepatic Uptake and Biliary Excretion of Xenobiotics. *Pharmaceutical Research,* 13**,** 497-513.

ZHANG, Q.-Y., DUNBAR, D. & KAMINSKY, L. 2000. Human Cytochrome P-450 Metabolism of Retinals to Retinoic Acids. *Drug Metabolism and Disposition,* 28**,** 292-297.

ZHOU, S. F. 2008. Drugs behave as substrates, inhibitors and inducers of human cytochrome P450 3A4. *Current Drug Metabolism,* 9**,** 310-22.

Appendix 1: Published Papers

ILLINGWORTH, N. A., BODDY, A. V., DALY, A. K. & VEAL, G. J. 2011. Characterization of the metabolism of fenretinide by human liver microsomes, cytochrome P450 enzymes and UDP-glucuronosyltransferases. *British Journal of Pharmacology,* 162**,** 989-999.

ROWBOTHAM, S. E., ILLINGWORTH, N. A., DALY, A. K., VEAL, G. J. & BODDY, A. V. 2010. Role of UDP-glucuronosyltransferase isoforms in 13-cis retinoic acid metabolism in humans. *Drug Metabolism & Disposition,* 38**,** 1211-7.

Appendix 2: Conference Abstracts

Poster Presentation
PAMM conference
Toulouse, France 27th – 30th January 2010

Pre-clinical metabolism studies with fenretinide in paediatric tumours
N.A.Harris, A.V. Boddy, J.L. Armstrong, G.J. Veal

Background:
Fenretinide (4HPR) is a synthetic analogue of retinoic acid, currently used in clinical trials in children for the treatment of neuroblastoma and Ewing's sarcoma. The metabolism of 4HPR is of particular interest due to production of the active metabolite 4'-oxo fenretinide (4'-oxo 4HPR), that has been reported to act synergistically with 4HPR and is also active against some 4HPR resistant cell lines. The aim of this study was to characterise 4HPR metabolism by cytochrome P450 enzymes (CYPs) and to investigate the effect of CYP 2C8 variants
Methods:
4HPR metabolism was investigated in human liver microsomes (HLM) and Supersomes over-expressing individual human CYPs, as well as in variants of CYP 2C8, generated from co-expression of CYP 2C8 variant plasmids (*1, *3, *3A, *3B and *4) and a P450 reductase plasmid. 3 hour incubations were carried out with 50µM 4HPR. Samples

were extracted and analysed by HPLC and LCMS assays developed to separate 4HPR and individual metabolites. Kinetic parameters for the formation of 4'-OH 4-HPR and 4'-oxo 4-HPR were determined following incubations of 0-1mg/ml protein of CYP 2C8 isoform membrane fractions with or 0-100μM 4-HPR and 0.25mg/ml protein.

Results:

HLM were found to predominantly produce 4'-oxo 4HPR, with 4'-hydroxy 4HPR predominantly produced by individual CYPs. 3 CYPs from a panel of 8 tested were found to metabolise 4HPR (2C8 >3A4 >3A5). There was a wide range of Vmax values observed between the variants, with a 4-fold difference between *4 and the wild-type (*1). Km values were similar for *1, *3 and *3A (5.2, 5,0 and 5.4μM respectively), and lower for *3B (2.4μM) and *4 (3.9μM). The metabolism profile for 4'-oxo 4-HPR was very different to that for 4'-OH 4-HPR. Vmax results were very similar for all variants except *1, that was nearly 10-fold higher than any of the other variants. Considerable variation in Km values was observed, with values ranging from 7.7 – 176.8μM.

Conclusion

The major metabolites of 4HPR have been identified, and work is ongoing to fully characterise the enzymes responsible. This will enable further research into the modulation of 4HPR metabolism and potential optimisation of drug efficacy.

Poster Presentation

NCRI conference

Birmingham, UK 4th – 7th October 2009

Characterisation of the metabolism of fenretinide in paediatric tumour types

N.A.Harris, A.V. Boddy, J.L. Armstrong, G.J. Veal

Background:

Fenretinide (4HPR) is a synthetic analogue of retinoic acid, currently used in clinical trials in children for the treatment of neuroblastoma and Ewing's sarcoma. The metabolism of 4HPR is of particular interest due to production of the active metabolite 4'-oxo fenretinide (4'-oxo 4HPR), which is able to act synergistically with 4HPR and is also active against some 4HPR resistant cell lines. The aim of this study was to characterise the *in vitro* metabolism of fenretinide in a microsomal assay and in neuroblastoma and Ewing's sarcoma cell lines.

Methods:

4HPR metabolism was investigated in human liver microsomes (HLM), Supersomes over-expressing individual human cytochrome P450s (CYPs) and Ewing's sarcoma and neuroblastoma cell lines. Incubations were carried out for up to 3h with 20µM or 50µM 4HPR. In additional experiments cell lines were pre-incubated with ATRA (10µM) to induce CYP 26. Samples were extracted and analysed by HPLC / LCMS assays developed to separate 4HPR and metabolites.

Results:

HLM were found to predominantly produce 4'-oxo 4HPR, with 4'-hydroxy 4HPR generated as a minor metabolite. 3 CYPs from a panel of 8 tested were found to metabolise 4HPR (2C8 >3A4 >3A5). With CYP incubations, 4'-hydroxy 4HPR was produced as a major metabolite and 4'-oxo 4HPR produced as a minor metabolite.

Cell lines produced an additional metabolite, 4-methoxy PR (4MPR). 4MPR could also be produced by HLM with the addition of the methylation co-factor S-Adenosyl methionine, a reaction not blocked by inhibitors of catechol-O-methyltransferases (COMT). Pre-treatment with ATRA increased metabolism in all cell lines, with some cell lines only producing the active metabolite after ATRA pre-treatment.

Conclusion

The major metabolites of fenretinide have been identified and work is ongoing to fully characterise the enzymes responsible. These investigations will enable further research into the modulation of fenretinide metabolism with a view to optimising drug efficacy.

Poster Presentation

AACR conference

Denver, CO, USA 18th – 22nd April 2009

Characterisation of the metabolism of fenretinide in paediatric tumour types

N.A.Harris, A.V. Boddy, J.L. Armstrong, G.J. Veal

Fenretinide (4HPR) is a synthetic analogue of retinoic acid, currently used in clinical trials in children for the treatment of neuroblastoma and Ewing's sarcoma. It has been shown to be better tolerated than other retinoid derivatives currently in clinical use, such as all-trans retinoic acid (ATRA) and 13-*cis* retinoic acid. Metabolism of 4HPR is generally by methylation or oxidation. Factors affecting metabolism of 4HPR are of

particular interest due to production of the active metabolite 4-oxo fenretinide (4'-oxo 4HPR), which has been shown to act synergistically with 4HPR and have activity against some 4HPR resistant cell lines. The current study was aimed to characterise 4HPR metabolism in a microsomal assay and in neuroblastoma and Ewing's sarcoma cell lines *in vitro*.

4HPR metabolism was investigated in human liver microsomes (HLM) and Supersomes over-expressing individual human cytochrome P450's (CYPs), as well as in Ewing's sarcoma and neuroblastoma cell lines (TC-32, RD-ES, SKES-1, SH-SY5Y, NGP). Incubations were carried out for up to 3 hours, with 20µM 4HPR used for cell line experiments and 50µM 4HPR used for HLM and supersome experiments. 4HPR metabolism was also investigated in cell line experiments following pre-incubation of cells with ATRA (10µM). Samples were extracted and analysed by HPLC and LCMS assays developed to separate 4HPR and individual metabolites. HLM were found to predominantly produce 4'-oxo 4HPR, with 4'-hydroxy 4HPR being generated as a minor metabolite. A panel of 8 CYPs were used, including those known to be commonly involved in metabolism and those reported to be involved in retinoid metabolism. Only 3 CYPs were found to metabolise 4HPR by varying amounts (3A4 > 2C8 > 3A5). With CYP incubations, 4'-hydroxy 4HPR was produced as a major metabolite and 4'-oxo 4HPR produced as a minor metabolite.

Cell lines were found to produce an additional metabolite, 4-methoxy PR (4MPR). 4MPR could also be produced by HLM, but only with the addition of the methylation co-factor S-Adenosyl methionine. This reaction was not blocked by inhibitors of catechol-O-methyltransferases (COMT).

As CYP 26 is known to mediate the oxidation of retinoids and its expression is known to be induced by ATRA, cell lines were also pre-incubated with ATRA to ascertain whether this would alter the metabolic profile of 4HPR. Metabolism to 4'-oxo 4HPR and 4'-hydroxy 4HPR varied considerably among cell lines, but was increased in all cell lines when pre-treated with ATRA, with some cell lines only producing these metabolites after ATRA pre-treatment. All cell lines tested produced 4MPR and ATRA pre-treatment had little effect on the formation of this metabolite.

The major metabolites of fenretinide have been identified, and work is ongoing to fully characterise the enzymes responsible. These investigations will enable further research into the modulation of fenretinide metabolism with a view to optimising drug efficacy.

Appendix 3: Awards

EACR/BACR Symposium July 2009 – 2nd prize in poster competition

Max Perutz Science Writing Prize August 2009 – Highly commended essay

North East Postgraduate Research Conference January 2010 – 2nd prize for best oral presentation

Winner of the 2010 Max Perutz Science Writing Prize:

Wanted: Dead or Alive

My palms are sweaty and my mouth is dry, but it's more excitement than nerves, though of course the nerves are there too. I've got my cells out of the incubator and now I just can't resist having a quick glance at them down the microscope – will I see more dead cells floating in one set than the other? I know I can't tell properly till I add some staining solution and analyse them accurately, but that will take hours and I just can't wait that long to find out: has it worked or not?

If you've ever held that envelope of exam results and been desperate to tear them open and find out how you did, but also terrified to look in case you didn't get what you were hoping for, then you'll know exactly the sort of feelings I'm talking about.

I'm working on tumour cells from 2 childhood cancers, called neuroblastoma and Ewing's sarcoma. These are both very hard to treat, with less than half the children surviving for 5 years after their diagnosis. That's the problem with treating cancer, some patients do brilliantly on a particular drug, but for others it'll have little effect. At the moment it's often a case of trial and error working out which drug is going work – and some people simply run out of time before we can find the right one. So what I'm trying to find out is what causes the differences in responses and how can we use that to our advantage.

The drug I'm using is called fenretinide, and it's similar to vitamin A (the vitamin found in carrots). It's able to kill cancer cells, whilst normal cells remain healthy. It works by causing a build-up of oxidants in the cells (you'll all probably have seen the adverts for

beauty creams offering anti-oxidant properties to get glowing skin – that's because oxidants are bad news for cells!) Normal, healthy cells should be able to cope with the presence of a few oxidants, but cancer cells will already be exposed to high levels as they're produced when cells divide, and so they can't cope with the extra oxidants produced from fenretinide treatment.

Due to its similarity to vitamin A, fenretinide can get into receptors meant for that vitamin and so the main side effect with fenretinide treatment is that the patients get what's called night-blindness; basically, you can't see very well in the dark. This makes it particularly suitable for treating childhood cancers as it's a much easier side effect to deal with than many other treatments – it's easier to give a 5 year old a night light than to comfort them as they're losing their hair. The problem is that fenretinide seems to work really well for some neuroblastoma and Ewing's sarcoma tumours, but not others. And I want to know why!

I've found that some of the tumours have more of an enzyme called CYP26 than others, and this enzyme helps to metabolise fenretinide in the body. Usually, you'd expect the patients to do worse if their body is breaking down the drug, but fenretinide is a little different. As well as the drug itself being able to kill cancer cells (what we call an 'active' compound), one of the metabolites of fenretinide is also active. This means there could be an extra hit from this second compound to those cancer cells where there is metabolism going on. This is the reason I'm desperately hoping to see more dead cells in some of my flasks than others – these should hopefully be the cells with more CYP26.

So what would it mean if I'm right about the link between CYP26 and how many cancer cells die? There are a few options actually – we could be selective and only give the drug to those whose cancer has been tested and shown to have CYP26, or there are other drugs which have been shown to increase concentrations of CYP26 in the body, so alternatively these could be used in combination with fenretinide. The important point is that we could decide on which drug or combination of drugs to use based on what should work for each particular patient, and that's what this is all about – taking the guess work out of cancer treatment.

I’ve already analysed these cells to see how much CYP26 they have, and then I’ve added the drug to them and left them to grow for a few days (having a quick peek everyday to see how they’re getting on!) Now it’s the moment of truth, as I look down the microscope and bring the cells into focus.....